©2018

Amy Marie Kuzminov

ALL RIGHTS RESERVED

SOUTHERN OCEAN GLACIAL-INTERGLACIAL VARIATIONS IN DELTA-^{238}U: TOWARDS UNDERSTANDING THE CONTROL OF SEDIMENTARY ^{238}U/^{235}U FRACTIONATION

By

AMY MARIE KUZMINOV

A thesis submitted to the

School of Graduate Studies

Rutgers, The State University of New Jersey

In partial fulfillment of the requirements

For the degree of

Master of Science

Graduate Program in Oceanography

Written under the direction of

Silke Severmann

And approved by

_____

_____

_____

_____

New Brunswick, New Jersey

October, 2018

ABSTRACT OF THE THESIS

Southern Ocean glacial-interglacial variations in delta-^{238}U:

Towards understanding the control of sedimentary ^{238}U/^{235}U fractionation

by AMY MARIE KUZMINOV

Thesis Director:

Silke Severmann

Sedimentary uranium (U) abundance peaks have been aligned with changes in glacial-interglacial cycles in the Southern Ocean sediment record. These peaks have been interpreted to reflect changes in the biological pump efficiency, with high U abundance associated with high carbon burial. Uranium isotopic composition (^{238}U/^{235}U; δ^{238}U) may provide additional information about the depositional conditions and biogeochemical cycling. In this study, I measured δ^{238}U from samples spanning glacial-interglacial cycles at RC13-254 (48.57^{o}S, 5.127^{o}E, 3636 mbss), an Atlantic sector Southern Ocean core, which has previously documented pronounced U peaks. Uranium-isotope composition showed a broad range, with a positive excursion (0.07 to 0.31 ‰) in the glacial period and a seawater-like signal in the interglacials (-0.67 to -0.30 ‰). The glacial positive excursion coincided with the elevated authigenic U concentrations. The magnitude of the δ^{238}U excursion is similar to published values for the Black Sea. Unlike the euxinic conditions in the Black Sea, studies from nearby locations show that the bottom water remained oxygenated during glacial periods. In previous studies, δ^{238}U has

been applied as a global redox proxy to reconstruct the extent of anoxia, owing to the conservative oceanic behavior of U. My results show that variability in $\delta^{238}U$ reflects local processes, including carbon burial rate. Therefore, rather than being a global ocean redox proxy, $\delta^{238}U$ should be treated as a localized signature of the carbon burial rate.

Acknowledgments

First and foremost, I'd like to thank my family. My husband, Fedor, for his love, patience, and support. Mum and Emily, thank you for regularly checking in on me. I could not have done this without their support.

To the amazing friends, Chris, Isabel, Joe, Nicole, Christien, Mike, and all the GPO students, thank you for being supportive and there to listen.

To Linda Godfrey, thank you for being a wonderful mentor. I am grateful for all of the many technical lessons and discussions we had. I would not have been able to master the Neptune without her help.

To my committee, Yair Rosenthal, Rob Sherrell, and Jim McManus, thank you for your support, advice, and guidance. I would not have been able to do this without their assistance.

To my advisor, Silke Severmann, thank you.

This work was supported by Rutgers School of Environmental and Biological Sciences, Rutgers Department of Marine Sciences, grant to Severmann and McManus (NSF OCE 1657690), and during my final year by the USSSP-IODP Schlanger fellowship (NSF OCE 1450528).

Table of Contents

Abstract of the thesis ii
Acknowledgments iv
Table of Contents v
List of Figures vi
List of Tables vii
List of Appendices viii
Introduction 1
Uranium background 6
Study Region 11
Methods Overview 13
Sample Preparation *13*
U spiking and separation *14*
MC-ICP-MS analysis *15*
Authigenic uranium and $\delta^{238}U$ calculation *16*
Analytical precision and accuracy *17*
Results 18
Discussion 19
Summary 24
References 25
Figures 38
Tables 45
Appendices 51
Appendix 1: Overview *51*
Appendix 2: Southern Ocean ODP 1094 ..... *53*
Appendix 3: Proto-North Atlantic during Ocean Anoxic Event 2 ..... *62*
Appendix 4: Modern day comparison – Black Sea *92*
Appendix 5: Modern day comparison – Baltic Sea *141*
Appendix 6: Additional Methods *215*

List of Figures

Figure 1: Mass balance model of U isotopes in the modern ocean. …….. 38

Figure 2: Histograms of the $\delta^{238}U$ of six reservoirs collected up till 2010. ….. 39

Figure 3: Updated histograms of all published data of $\delta^{238}U$ from several different environments. …….……..…….… 40

Figure 4: Distribution of published $\delta^{238}U$ in marine sediments based on bottom water redox conditions and organic carbon burial rates. …….. 41

Figure 5: Records from RC13-254 in the Southern Ocean spanning glacial-interglacial cycles from 2-140 kya. …….…….. 42

Figure 6: Plots of the $\delta^{238}U$ versus the U concentration within the sediments for bulk $\delta^{238}U$ and authigenic $\delta^{238}U$. ……43

Figure 7: Schematic representation of application of $\delta^{238}U$ proxy as previously used and my new interpretation. ……... 44

List of Tables

Table 1: RC13-254 Sample information. …….. 45

Table 2: RC13-254 auxiliary data. …… 46

Table 3: Authigenic uranium calculations at RC13-254……..…. 47

Table 4: Uranium isotope data at RC13-254 …… 48

Table 5: iCap concentration accuracy…… 49

Table 6: Neptune isotopic accuracy……... 50

List of Appendices

Appendix 1: Overview. …….. 51

Appendix 2: Southern Ocean ODP 1094. …… 53

Appendix 2-1: Overview of Southern Ocean ODP 1094. …….. 53

Appendix 2-2: Map of Southern Ocean sites. …… 57

Appendix 2-3: Sample information for ODP 1094. ……... 58

Appendix 2-4: ODP 1094 auxiliary data. …….. 59

Appendix 2-5: Authigenic uranium calculations at ODP 1094. …… 60

Appendix 2-6: Uranium isotope data at ODP 1094. …….. 61

Appendix 3: Proto-North Atlantic during Ocean Anoxic Event 2. …….. 62

Appendix 3-1: Overview of proto-North Atlantic during OAE 2. ……..... 62

Appendix 3-2: Map of proto-North Atlantic sites during OAE 2. …… 67

Appendix 3-3: ODP 174AX (Bass River). …….. 68

Appendix 3-3-1: Sample information for OAE 2 samples ODP 174AX (Bass River). …… 68

Appendix 3-3-2: ODP 174AX (Bass River) auxiliary data. …….. 69

Appendix 3-3-3: Uranium isotope data at ODP 174AX (Bass River). ……. 71

Appendix 3-4: DSDP 603B (Continental Rise). …… 72

Appendix 3-4-1: Sample information for OAE 2 samples DSDP 603B (Continental Rise). …….. 72

Appendix 3-4-2: DSDP 603B (Continental Rise) auxiliary data. ……. 73

Appendix 3-4-3: Uranium isotope data at DSDP 603B (Continental Rise). 75

Appendix 3-5: ODP 1276 (Newfoundland). …….. 76

Appendix 3-5-1: Sample information for OAE 2 samples ODP 1276 (Newfoundland). …… 76

Appendix 3-5-2: ODP 1276 (Newfoundland) auxiliary data. …….. 77

Appendix 3-5-3: Uranium isotope data at ODP 1276 (Newfoundland). ….. 79

Appendix 3-6: Shell S75 (Tarfaya). …….. 80

Appendix 3-6-1: Sample information for OAE 2 samples S75 (Tarfaya). .. 80

Appendix 3-6-2: S75 (Tarfaya) auxiliary data. ……. 81
Appendix 3-6-3: Uranium isotope data at S75 (Tarfaya). …… 83
Appendix 3-7: DSDP 367 (Cape Verde). …….. 84
Appendix 3-7-1: Sample information for OAE 2 samples DSDP 367 (Cape Verde). …… 84
Appendix 3-7-2: DSDP 367 (Cape Verde) auxiliary data. …… 85
Appendix 3-7-3: Uranium isotope data at DSDP 367 (Cape Verde). ……... 87
Appendix 3-8: ODP 1258 (Demerara Rise). …… 88
Appendix 3-8-1: Sample information for OAE 2 samples ODP 1258 (Demerara Rise). ……. 88
Appendix 3-8-2: ODP 1258 (Demerara Rise) auxiliary data. …….. 89
Appendix 3-8-3: Uranium isotope data at ODP 1258 (Demerara Rise). ….. 91

Appendix 4: Modern day comparison – Black Sea. …….. 92
Appendix 4-1: Overview of modern day comparison – Black Sea. ……. 92
Appendix 4-2: Map of Black Sea sites. …… 97
Appendix 4-3: Black Sea site descriptions by region. ……. 98
Appendix 4-4: Black Sea coastal shelf sites (St. 9 & 13). ……... 99
Appendix 4-4-1: Sedimentary Black Shelf (St. 13) auxiliary data. ……. 99
Appendix 4-4-2: 0.2 μm filtered sea water concentration data at Black Sea Shelf (St. 9). …… 101
Appendix 4-4-3: Pore water concentration data at Black Sea Shelf (St. 13 – core 1). …… 102
Appendix 4-4-4: Pore water concentration data at Black Sea Shelf (St. 13 – core 2). …… 104
Appendix 4-4-5: Pore water concentration data at Black Sea Shelf (St. 9). . 106
Appendix 4-4-6: Sedimentary uranium isotope data at Black Sea Shelf (St. 13). ……. 108
Appendix 4-4-7: Uranium isotope data for water column samples from Black Sea shelf (St. 9). ……... 108
Appendix 4-5: Black Sea shelf break sites (St. 4 & 5). …… 109

Appendix 4-5-1: Sedimentary Black Shelf Break (St. 5) auxiliary data. ….. 109
Appendix 4-5-2: 0.2 μm filtered sea water concentration data at Black Sea Shelf Break (St. 4). …….. 111
Appendix 4-5-3: Pore water concentration data at Black Sea Shelf Break (St. 5). ……. 113
Appendix 4-5-4: Pore water concentration data at Black Sea Shelf Break (St. 4). ……. 115
Appendix 4-5-5: Sedimentary uranium isotope data at Black Sea Shelf Break (St. 5). …… 117
Appendix 4-5-6: Uranium isotope data for water column samples from Black Sea shelf break (St. 4). ……... 117
Appendix 4-6: Black Sea deep site (St. 2). …….. 118
Appendix 4-6-1: Sedimentary Black Deep (St. 2) auxiliary data. …….. 118
Appendix 4-6-2: 0.2 μm filtered sea water concentration data at Black Sea Deep (St. 2). ……. 120
Appendix 4-6-3: Pore water concentration data at Black Sea Deep (St. 2 – cores 1-2). …… 122
Appendix 4-6-4: Pore water concentration data at Black Sea Deep (St. 2 – cores 2-3). ……... 124
Appendix 4-6-5: Particulate matter concentration data at Black Sea Deep per L (St. 2). …… 126
Appendix 4-6-6: Particulate matter concentration data at Black Sea Deep per square cm (St. 2). ……... 127
Appendix 4-6-7: Sedimentary uranium isotope data at Black Sea Deep (St. 2). ……. 128
Appendix 4-6-8: Uranium isotope data for water column samples from Black Sea Deep (St. 2). …… 129
Appendix 4-7: Black Sea additional sites. …… 130
Appendix 4-7-1: Black Sea mid-shelf sites (St. 8 & 7). …….. 130
Appendix 4-7-1-1: 0.2 μm filtered sea water concentration data at Black Sea (St. 8). …….. 130

Appendix 4-7-1-2: Pore water concentration data at Black Sea (St. 8). 132
Appendix 4-7-1-3: Pore water concentration data at Black Sea (St. 7). 134
Appendix 4-7-2: Black Sea shelf edge site (St. 6). ……. 135
Appendix 4-7-2-1: 0.2 μm filtered sea water concentration data at Black Sea Shelf Break site (St. 6). …… 135
Appendix 4-7-3: Black Sea deep site (St. 3). …….. 137
Appendix 4-7-3-1: Pore water concentration data at Black Sea (St. 3 – cores 1-2). ……. 137
Appendix 4-7-3-2: Pore water concentration data at Black Sea (St. 3 – cores 2-3). ……. 139

Appendix 5: Modern day comparison – Baltic Sea. …….…. 141
Appendix 5-1: Overview of modern day comparison – Baltic Sea. …….…….. 141
Appendix 5-2: Map of Baltic Sea sites. …….…. 145
Appendix 5-3: Baltic Sea site descriptions by region. …… 146
Appendix 5-4: North Gotland, Baltic Sea (St. 17). ……147
Appendix 5-4-1: Sedimentary Baltic North Gotland (St. 17) auxiliary data. 147
Appendix 5-4-2: 0.2 μm filtered sea water concentration data at North Gotland, Baltic Sea (St. 17). ……. 149
Appendix 5-4-3: Pore water concentration data at North Gotland, Baltic Sea (St. 17 – Core A & >18cm). …….. 151
Appendix 5-4-4: Pore water concentration data at North Gotland, Baltic Sea (St. 17 – cores B&C). …… 153
Appendix 5-4-5: Sedimentary uranium isotope data at Baltic North Gotland (St. 17). …… 155
Appendix 5-4-6: Uranium isotope data for water column samples from North Gotland, Baltic Sea (St. 17). …….. 155
Appendix 5-5: Faro Deep, Baltic Sea (St. 18). ……. 156
Appendix 5-5-1: Sedimentary Baltic Faro Deep (St. 18) auxiliary data. ….. 156
Appendix 5-5-2: 0.2 μm filtered sea water concentration data at Faro Deep, Baltic Sea (St. 18). …… 158

Appendix 5-5-3: Pore water concentration data at Faro Deep, Baltic Sea (St. 18). …… 160
Appendix 5-5-4: Particulate matter concentration data at Faro Deep, Baltic Sea per L (St. 18). …….. 162
Appendix 5-5-5: Particulate matter concentration data at Faro Deep, Baltic Sea per square cm (St. 18). ……. 163
Appendix 5-5-6: Uranium isotope data for water column samples from Faro Deep, Baltic Sea (St. 18). ……. 164
Appendix 5-6: East Gotland, Baltic Sea (St. 14 & 19). …….. 165
Appendix 5-6-1: Sedimentary Baltic East Gotland (St. 14) auxiliary data. … 165
Appendix 5-6-2: 0.2 μm filtered sea water concentration data at East Gotland, Baltic Sea (St. 19). …….. 167
Appendix 5-6-3: Pore water concentration data at East Gotland, Baltic Sea (St. 14). ……. 169
Appendix 5-6-4: Sedimentary uranium isotope data at Baltic East Gotland (St. 14). …… 171
Appendix 5-6-5: Uranium isotope data for water column samples from East Gotland, Baltic Sea (St. 19). …….. 171
Appendix 5-7: Bornholm Basin, Baltic Sea (St. 22). …… 172
Appendix 5-7-1: Sedimentary Baltic Bornholm Basin (St. 22) auxiliary data. 172
Appendix 5-7-2: 0.2 μm filtered sea water concentration data at Bornholm Basin, Baltic Sea (St. 22). ……. 174
Appendix 5-7-3: Pore water concentration data at Bornholm Basin, Baltic Sea (St. 22). ……. 175
Appendix 5-7-4: Particulate matter concentration data at Bornholm Basin, Baltic Sea per L (St. 22). …….. 176
Appendix 5-7-5: Particulate matter concentration data at Bornholm Basin, Baltic Sea per square cm (St. 22). …… 177
Appendix 5-7-6: Sedimentary uranium isotope data at Baltic Bornholm Basin (St. 22). …… 178

Appendix 5-7-7: Uranium isotope data for water column samples from Bornholm Basin, Baltic Sea (St. 22). ……. 178

Appendix 5-8: Baltic Sea additional sites. …… 179

Appendix 5-8-1: Aland-Bothnian exchange, Baltic Sea (St. 4). …….. 179

Appendix 5-8-1-1: 0.2 μm filtered sea water concentration data at Aland-Bothnian exchange, Baltic Sea (St. 4). …… 179

Appendix 5-8-1-2: Pore water concentration data at Aland-Bothnian exchange, Baltic Sea (St. 4). …… 180

Appendix 5-8-2: North Gotland, Baltic Sea (St. 12). …….181

Appendix 5-8-2-1: 0.2 μm filtered sea water concentration data at North Gotland, Baltic Sea (St. 12). ……. 181

Appendix 5-8-3: Gulf of Finland, Baltic Sea (St. 7, 9, 10, 15). ……182

Appendix 5-8-3-1: 0.2 μm filtered sea water concentration data at Gulf of Finland, Baltic Sea (St. 7, 9, 10). ……. 182

Appendix 5-8-3-2: Pore water concentration data at Gulf of Finland, Baltic Sea (St. 9). …… 183

Appendix 5-8-3-3: Pore water concentration data at Gulf of Finland, Baltic Sea (St. 10). ……. 185

Appendix 5-8-3-4: Pore water concentration data at Gulf of Finland, Baltic Sea (St. 15). ……. 187

Appendix 5-8-4: Stockholm Archipelago, Baltic Sea (St. 1, 3). ……. 189

Appendix 5-8-4-1: 0.2 μm filtered sea water concentration data at Baggensfjarden, Stockholm Archipelago, Baltic Sea (St. 1). …….. 189

Appendix 5-8-4-2: Pore water concentration data at Stockholm Archipelago, Baltic Sea (St. 3). ……190

Appendix 5-8-5: East Gotland, Baltic Sea (St. 13, 16). ……192

Appendix 5-8-5-1: 0.2 μm filtered sea water concentration data at East Gotland, Baltic Sea (St. 16). ……192

Appendix 5-8-5-2: Pore water concentration data at East Gotland, Baltic Sea (St. 16 – core A). ……. 193

Appendix 5-8-5-3: Pore water concentration data at East Gotland, Baltic Sea (St. 16 – core B). ……... 195
Appendix 5-8-5-4: Pore water concentration data at East Gotland, Baltic Sea (St. 16 – core C). ……... 197
Appendix 5-8-5-5: Pore water concentration data at East Gotland, Baltic Sea (St. 16 – core D). ……... 199
Appendix 5-8-5-6: Pore water concentration data at East Gotland, Baltic Sea (St. 16 – core E). ……... 201
Appendix 5-8-5-7: Pore water concentration data at East Gotland, Baltic Sea (St. 13 – cores A&B). …… 203
Appendix 5-8-5-8: Pore water concentration data at East Gotland, Baltic Sea (St. 13 – cores C&D). …… 205
Appendix 5-8-6: Arkona Basin, Baltic Sea (St. 21). …… 207
Appendix 5-8-6-1: Pore water concentration data at Arkona Basin, Baltic Sea (St. 21 – core A). ……... 207
Appendix 5-8-6-2: Pore water concentration data at Arkona Basin, Baltic Sea (St. 21 – core B). ……... 209
Appendix 5-8-6-3: Pore water concentration data at Arkona Basin, Baltic Sea (St. 21 – core C). ……... 211
Appendix 5-8-6-4: Pore water concentration data at Arkona Basin, Baltic Sea (St. 21 – core D). ……... 213

Appendix 6: Additional Methods. …… 215

Introduction

Changes in climate directly impact nutrient cycles, primary productivity, ocean circulation, and extent of anoxia (Meyer and Kump, 2008; Stramma et al., 2008; Deutsch et al., 2011). The global climate is unstable and had abrupt changes in the past (Dansgaard et al., 1993; Broecker, 2000); the modern warming of climate is leading to interruptions of natural biogeochemical cycles (Keeling and Garcia, 2002; Keeling et al., 2010; Deutsch et al., 2015). Nutrient cycles of phosphorus and nitrogen, two key macronutrients, are directly impacted as climate affects their supply to, removal from, and recycling in the ocean (Tyrrell, 1999; Galbraith et al., 2004; Mort et al., 2007b; Canfield et al., 2010). Changes in nutrient availability impact primary productivity; one well-studied example of these changes is glacial and interglacial cycles. (Kumar et al., 1995; von Rad et al., 1995; Anderson et al., 1998; Anderson et al., 2002; Jaccard et al., 2013). Further, an increase in productivity can lead to expansions of anoxia within the bottom waters, especially in shallow, coastal, local environments where conditions stagnate (Hotinski et al., 2001; Zillén et al., 2008; Middleburg and Levin, 2009). Widespread ocean anoxia can be seen in periods throughout history during the Proterozoic (Canfield, 1998), end-Permian extinction, (Brennecka et al., 2011a) and periodically during the Cretaceous (Sarmiento et al., 1988). These multiple lines of evidence suggest that changes in areal extent of anoxia and primary productivity occur in response to shifts in climate.

Preservation of chemical signatures in marine sediments depends on many factors, including water depth, productivity rates, dilution by terrigenous detrital, along with dissolution and decomposition of organic material (Tyson, 1995; Arthur and Dean,

1998; Tyson, 2001). An increase in the percent of organic material can represent expansion of bottom water anoxia, enhanced surface productivity, or a combination of both in addition to potential changes in the sedimentation rate driven by terrigenous inputs (Muller and Suess, 1979; Pedersen and Calvert, 1990; Canfield, 1994; Hedges and Keil, 1995; Arthur and Dean, 1998; Piper and Calvert, 2009). Discriminating between these processes for organic-rich sediments requires using paleoproxies. Paleoproxies provide a tool to differentiate between different processes as each proxy responds to distinct environmental conditions. Chemical proxies provide a tool to unravel the past, as the chemical signatures preserved in the sediments have an established relationship to a transient signal (e.g. redox state) that cannot be retained (Calvert and Pedersen, 1993; Nameroff et al., 2004). By combining the information from multiple proxies, we can increase the complexity of paleoenvironment reconstruction to understand the mechanisms that are driving these changes (Arthur et al., 1988; Brumsack, 2006). For example, the reconstruction of Ocean Anoxic Event 2 (OAE 2, 93.5 million years ago) shows that there was high productivity in the southern proto-North Atlantic due to upwelling, while redox conditions throughout the basin were variable (Schlanger and Jenkyns, 1976; Arthur et al., 1987; Schlanger et al., 1987; Mort et al., 2007a; Jenkyns, 2010; Arnold et al., 2012; Owens et al., 2013).

Studies have explored the relationship of a variety of elements to productivity or redox state within the water column and sediments. Tools utilized to study environmental processes, include concentration data, ratios of two elements, and isotope ratios (Henderson, 2002; Tribovillard et al., 2006; Algeo and Maynard, 2008). Developed paleoproductivity proxies include barium (Ba), protactinium to thorium ratios

(Pa/Th), phosphorus (P), and uranium (U) concentration (Mo et al., 1973; Veeh et al., 1974; Anderson et al., 1989a; Anderson et al., 1989b; Mortlock et al., 1991; Dymond et al., 1992; Kumar et al., 1993; Rosenthal et al., 1995; Latimer and Filippelli, 2001). Some of the redox sensitive proxies used to study anoxic conditions are rhenium (Re), molybdenum (Mo), iron (Fe), chromium (Cr), and iodine to calcium ratios (I/Ca) (Crusius et al., 1996; Morford and Emerson, 1999; Arnold et al., 2004; Lyons and Severmann, 2006; Lyons et al., 2009; Lu et al., 2010; Muratli et al., 2010; Morford et al., 2012; Reinhard et al., 2013; Zhou et al., 2014). By combining multiple proxies, a more complete picture of paleoproductivity and paleoredox can be deduced.

The use of isotope ratios provides a tool that can expand on information gained from concentration data. Natural variations in isotope ratios in seawater and sediments result from fractionation based on environmental conditions and an element's geochemistry (Anbar and Rouxel, 2007; Lyons et al., 2009). For example, dissolved Mo in the presence of at least 11 μmol/L hydrogen sulfide (H_2S) precipitates Mo quantitatively (Nagler et al., 2005; Neubert et al., 2008), as observed in elevated concentrations and Mo/TOC ratios (Nagler et al., 2005; Algeo and Lyons, 2006; McManus et al., 2006). Measurements of Mo isotopes in euxinic sediments provided a method to quantify the areal extent of euxinia by using an isotope mass budget (Arnold et al., 2004; Neubert et al., 2008; Arnold et al., 2012). Recently, a similar isotope mass budget has been proposed for U isotopes responding to anoxic conditions (Stirling et al., 2007; Weyer et al., 2008; Montoya-Pino et al., 2010; Andersen et al., 2014). The application of U isotopes as a proxy for anoxia resulted from a simplistic comparison of two locations with different environmental conditions, whereas the traditional application

of U abundance as a proxy for paleoproductivity was based on detailed studies of opposing geochemical records from north and south of the Antarctic Polar Front Zone (APFZ) (Anderson et al., 1989a; Anderson et al., 1989b; Rosenthal et al., 1995). These applications have been tested in different locations (evidence for both will be expanded upon within the following section *Uranium Background*), with the isotopic interpretation providing questionable results (Noordmann et al., 2015; Hinojosa et al., 2016). My work will explore the discrepancy between U abundance and U isotope ratios.

Based on the observed inconsistency in uranium usage, my research examines uranium isotopes application. I will investigate the link between known productivity changes and uranium isotope compositions at an oxygenated site. The Southern Ocean has been shown to be affected by productivity changes over glacial-interglacial cycles (Kumar et al., 1995; Anderson et al., 1998) while the region never experienced bottom water anoxia (Keir, 1988). Additionally, I worked on some other projects that also approach these questions. In Appendix 2, is an additional Southern Ocean study that focused on a glacial-interglacial transition. Appendix 3 includes data on six sites around the proto-North Atlantic before, during, and after the Ocean Anoxic Event 2, in order to explore the productivity and extent of anoxia during that period. The final two appendices contain data that were collected, to clarify how the uranium isotope proxy works by using samples from the Black (Appendix 4) and Baltic (Appendix 5) Seas, two basins containing euxinic waters but differing in productivity (Calvert et al., 1991; Winogradow and Pempkowiak, 2014). These basins provide two modern analogues to understand the U removal mechanisms in relation to environmental variables. Water

column, suspended particulates, sediments, and porewaters were collected to show where fractionation of the isotopes occurs.

The motivation for this work is to better understand the controls of $\delta^{238}U$ and how it is influenced by variations in carbon burial rates and redox conditions. Data presented within the thesis and in the four regional sections in the appendix provide a variety of different spatial and temporal scales to consider $\delta^{238}U$ fractionation. Together, these projects should provide a more comprehensive view of the uranium isotope fractionation and clarify the criteria involved. The specific goal of the project discussed within the thesis is to study a site with oxygenated bottom water conditions. Throughout glacial-interglacial cycles the productivity at this site changed, and as will be discussed the $\delta^{238}U$ responded to this. In summary, this work is intended to clarify the factors influencing uranium isotope fractionation.

Uranium background

In the ocean, U shows a conservative distribution, in addition to a long residence time of 400 kyr (Ku et al., 1977; Mangini et al., 1979; Dunk et al., 2002). In the global ocean, U behaves conservatively with a concentration of 3.3 µg/L or 13.96 nM at salinity of 35 (Ku et al., 1977; Mangini et al., 1979; Chen et al., 1986). Uranium is typically found in U(VI) species and is often in a variety of complexes, predominantly carbonate complexes composed of the uranyl ion complexed with carbonate ions ($UO_2(CO_3)_x$ [where x could be 1, 2, or 3]) in oxic seawaters (Langmuir, 1978). Even in reducing environments with hydrogen sulfide (H_2S) present, the oxidized U(VI) species dominates (Anderson, 1984). Sources of U to the ocean include rivers groundwater and trace amounts of atmospheric dust (Figure 1) (Dunk et al., 2002; Tissot and Dauphas, 2015). The major sinks of U are removal into carbonates, oceanic crusts during hydrothermal alteration, Fe-Mn nodules and crusts, suboxic/oxic sediments, and anoxic/euxinic sediments (Mo et al., 1973; Sackett et al., 1973; Veeh et al., 1974; Anderson, 1987; Anderson et al., 1989a; Anderson et al., 1989b; Barnes and Cochran, 1990; Klinkhammer and Palmer, 1991; Morford and Emerson, 1999; Morford et al., 2009).

The long-term removal of uranium into sediments is not driven by water column reactions. Water column studies in the Black and Baltic Seas observed salinity-normalized U concentration to decrease by 40% in the deepest waters (Anderson et al., 1989a; Colodner et al., 1995; Andersen et al., 2014). The sulfidic, deep waters in the Black Sea have a residence time of between 500-2000 years (Deuser, 1971; Buesseler et al., 1991) while in the Baltic Sea the residence time is significantly shorter, only 11 years at Landsort Deep (Meier, 2005). If removal of U occurred in the water column, there

should be observed differences in the water column concentrations for the two basins; furthermore if sulfide was involved in the reaction, there should be no dissolved U left in the deep basin. Additionally for U, the presence of H_2S is inconsequential for U geochemical reactions (Anderson et al., 1989a). The trend of partial removal of U from the bottom water column has been observed in other silled basins, including Cariaco basin (Anderson, 1987), and Saanich Inlet (Todd et al., 1988; Anderson et al., 1989b). The major process driving the removal of U(VI) is bacterial reduction to U(IV) during early diagenesis within the sediments (Cochran et al., 1986; Shaw et al., 1990; Barnes and Cochran, 1991, 1993; McManus et al., 2005; Morford et al., 2005; Wall and Krumholz, 2006; Morford et al., 2009). Due to the porewater depletion of U during early diagenesis, U in the overlying bottom water diffuses into the sediments to allow the bacterial U removal to continue. Diffusion into the sediments and diagenesis drive the concentration patterns observed for the U within the porewaters and water column (Klinkhammer and Palmer, 1991; McManus et al., 2005).

In the sediments, U reduction removal is tightly linked to organic carbon. Organic carbon was first hypothesized to play an important role in U removal into sediments by Frederickson (1948). This hypothesis was supported by Swanson (1961), who observed that organic rich sediments, shales, were enriched in U. Subsequent studies in the 1980s by Robert Anderson established the use of uranium concentration as a proxy for organic carbon burial by studying both sediments and the particle flux in the water column via sediment traps (Anderson, 1982, 1987; Anderson et al., 1989a). Anderson found a tight correlation between the carbon burial flux and uranium concentration in sediments and proposed that U can be used as a proxy for carbon burial.

In the years following, several other publications have confirmed this trend in a variety of sedimentary environments, including the Southern Ocean (Kumar et al., 1995; Rosenthal et al., 1995; Chase et al., 2001), fjords and other restricted basins (Anderson et al., 1989b; Shaw et al., 1994), and continental margins (Prakash Babu et al., 2002; McManus et al., 2005; Morford et al., 2009).

Uranium isotopes have traditionally been used for dating due to their radioactivity; recently they have been treated as quasi-stable isotopes. Uranium has multiple isotopes, with ^{238}U being the most abundant (Weyer et al., 2008), while ^{235}U and ^{234}U occur naturally in small abundances (0.72% and 0.005% respectively), also trace amounts of ^{236}U and ^{233}U exist (Christl et al., 2012). Isotopes ^{238}U and ^{235}U, the primordial isotopes from Earth's formation, begin two distinct U-Pb decay series, which have been used extensively for dating (Edwards et al., 1987; Bard et al., 1990). One dating mechanism, ^{234}U/^{238}U can be used to determine ages for sediments between 0.1 to 1.1 million years (Ku, 1965; Ku et al., 1977). The ^{234}U/^{238}U ratio also provides information about weathering rates and river discharge (Andersson et al., 1995; Chen et al., 2016a). Both applications rely on ^{238}U-^{234}U not being in secular equilibrium in seawater due to alpha recoil of ^{234}U during weathering of crustal materials (Chen et al., 1986). Recent analytical advancements allowed measurements of the ^{238}U/^{235}U ratio, which can be used as a quasi-stable isotope system. ^{238}U/^{235}U fractionation is driven by nuclear volume effects rather than mass-dependent fractionation; meaning that due to the smaller atomic volume of ^{238}U as the additional 3 neutrons provide for a tighter nucleus configuration, ^{238}U will be incorporated into biological materials or minerals more easily

than ^{235}U (Schauble, 2007). Stirling et al. (2007) and Weyer et al. (2008) were the first studies to confirm that significant variation in ratios occurs naturally.

The earliest data sets of $\delta^{238}U$ looked at a limited number of sites covering nominally suboxic and anoxic/euxinic redox conditions. A mass balance was developed based on the redox state of the environment (Figure 2) (Montoya-Pino et al., 2010). Additional studies observed the fractionation occurring during U incorporation and removal into solid phase from an aqueous source. The typical ranges of fractionation of $\delta^{238}U$ from the source material for different removal mechanisms include adsorption to manganese oxides and crusts (Brennecka et al., 2011b; Goto et al., 2014), bacteria reduction (Basu et al., 2014), and carbonate incorporation of U (Chen et al., 2016b). The degree of fractionations and the size of the source/sink influence the overall isotope budget (Figure 1).

For marine sediments, the current interpretation of the $\delta^{238}U$ ratio shows discrepancies with the known understanding of elemental U chemistry. The current $\delta^{238}U$ interpretation suggests that U isotope composition responds most directly to bottom water oxygen and the presence of sulfide, with suboxic sediments having a signature similar to seawater and anoxic sediments enriched in ^{238}U (Montoya-Pino et al., 2010). This interpretation relied on a limited data set of two sites, the Peru Margin and Black Sea (Weyer et al., 2008; Montoya-Pino et al., 2010), which are extreme scenarios of their respective redox conditions and productivity (Figure 2). Issues emerged when subsequent studies applied this interpretation to other modern sites and recognized discrepancies not aligning with the model (Noordmann et al., 2015; Hinojosa et al., 2016). By considering all published data in modern sites, $\delta^{238}U$ is not likely being

controlled solely by the redox state of the environment (Figure 3), and other factors need to be considered, such as carbon burial (Figure 4).

Study Region

The biogeochemistry of the Southern Ocean responds to glacial-interglacial cycles and ocean ventilation, impacting global biogeochemical cycles including the carbon cycle (Charles et al., 1991; Mortlock et al., 1991; Kumar et al., 1993; Kumar et al., 1995; Rosenthal et al., 1995; Anderson et al., 1998). In these works, productivity was shown to be an important factor influencing the uranium concentrations in sediments of the Southern Ocean, including at site RC13-254. According to Kumar et al. (1995), increased export production occurred at this Subantarctic site during the glacial periods and U concentration also increased during that time. These measurements of sedimentary U have been applied to identify the potential mechanism that could have caused lowering of atmospheric CO_2 during multiple glacial-interglacial cycles. Elevated authigenic U in the Southern Ocean suggests that conditions in these sediments experienced higher export production leading to an increased C_{org} burial rate (Kumar et al. 1995), and this may have depleted some of the bottom water O_2. Lowering the O_2 in the ocean interior would result from an intensification of the biological pump. To my best knowledge, no evidence from this region shows that bottom water oxygen levels were suboxic or anoxic during glacial-interglacial transitions (Keir, 1988; Francois et al., 1997; Galbraith and Jaccard, 2015).

Here I investigate authigenic U enrichments in Southern Ocean sediments to test if their U-isotope composition changes over glacial-interglacial timescale. The long residence time of U implies that the U-isotope composition of global seawater should remain constant over these timescales, unless if the sedimentary U removal significantly altered the oceanic isotope budget which would require several orders of magnitude

increase in the removal to result in an oceanic 0.01‰ change. (Based on the modern day oceanic reservoir size (Figure 1), the amount of uranium that would need to be removed to achieve -0.40 ‰ [compared to -0.39 ‰] in the ocean using the observed +0.2 ‰ in anoxic sediments as the only removal mechanism [due to its large isotopic fractionation] would be 950 000 Mmol/yr. For comparison: the modern day flux to anoxic sediments is 11.6 Mmol/yr and for all sinks together the flux is ~40 Mmol/yr, which is 4-5 orders of magnitude less).

This study discusses results from sediments recovered from 3636 mbss at RC13-254 (48.57^{o}S, 5.127^{o}E) in the Atlantic sector of the northern Southern Ocean on the USNS *Robert D. Conrad*. The samples were requested from the Lamont-Doherty core repository. The site, RC13-254, was used in early studies correlating U concentration to productivity (Kumar et al., 1995; Anderson et al., 1998).

Methods Overview

Samples were digested using a bulk digest and concentration measurements were analyzed on an inductively coupled plasma-mass spectrometer (ICP-MS, iCap, ThermoScientific). Uranium was separated from matrix with column chromatography using Uteva ion exchange resin (Potter et al., 2005). Uranium isotope ratios were measured by multi-collector-ICP-MS (MC-ICP-MS; NeptunePlus, ThermoScientific) using CRM112a for a bracketing standard. *See below more details.*

Sample Preparation

An aliquot of dried sediments (~1 g) was ashed at 450°C for 0.5 hours to burn off the organic materials and then the temperature ramped up to 850°C for 6 hours to burn off sulfides. Based on the concentration data from Kumar et al. (1995), this provided an estimate of the amount of sediment needed to achieve at least 70 ng U. The mass of sediment ranged from 0.030 g in the glacial stages to 0.350 g in the interglacial stages. This initial subsample of ashed sediment sample was then measured into a Savillix® 8 ml Teflon jar and 2 ml of 20% HCl was added and the solution was placed on a shaker table overnight. The aqueous portion was then removed into a 15 ml Teflon jar and the residual sediments were rinsed three times with MilliQ® water which was then added to the 20% HCl leach fraction; these steps removed the calcium to avoid Ca-fluoride formation during subsequent HF treatment. The remaining residue was then digested using a combination of HF and NHO_3. The fully dissolved samples were then dried down at 100°C to remove residual HF, and then the aqueous Ca-portions were mixed with the dissolved solid phase solutions in order to achieve a total digest of the original sample. Dilute samples were then analyzed on the iCap ICP-MS (ThermoFisher) to

determine U concentrations as well as other major and minor elements. Based on the concentrations measured it was determined that either enough sample was digested, or an additional digestion was completed to ensure that least 70 ng U was available for U isotope analysis.

U spiking and separation

From the sample total digest solutions, aliquots were subsampled to have~ 70 ng U for isotope work. These subsamples were spiked with IRMM3636a, a certified $^{233}U/^{236}U$ spike, before U was separated from the matrix. The spiking ratio was set to have the $^{236}U:^{235}U$ to be ~ 3:2. The samples were then refluxed for some time and then dried down before bringing back up in 0.25 ml in 3N HNO_3.

To separate the uranium from the other matrix elements, the 3N HNO_3 solutions were processed using a modified procedure with UTEVA®(Eichrom) U-specific ion exchange resin (Potter et al., 2005; Stirling et al., 2007). The procedure utilized a 200 μl resin column of UTEVA, which was cleaned with 5 ml of 0.1N HCl. The column was buffered with 5 ml of 3N HNO_3 and the samples were loaded onto the preconditioned column. Matrix solutes were rinsed off the column using 2 ml of 3N HNO_3. To remove thorium, 2 ml of 3N HNO_3 with trace HF was added to the column. To recondition the column, 1 ml of 5N HCl prepared the column for the final elution. The uranium was removed and collected from the column using 0.1N HCl using 2 ml. Afterwards, the samples were dried down at 60°C and were then redissolved in 2% HNO_3 in 1 ml. Small aliquots of the purified U samples were analyzed on the iCap to quantify the concentration of the sample and estimate the U recovery prior to being analyzed on the

Neptune for U isotope ratios. Prior to Neptune analysis, solutions were microcentrifuged for 10 minutes and then were diluted to ~18ppb.

MC-ICP-MS analysis

All solutions (standards and samples) were prepared to have the same isotopic ratio and aimed to have the same concentration ~18 ppb. When the Neptune was completely tuned up for ^{238}U, the signal of the volts for all isotopes was assessed while in the standard solution (CRM112a). Usually, ^{238}U signal was in the range of 12-15 volts (when ^{238}U signal was ~12 V, ^{235}U signal was ~90 mV, and ^{233}U and ^{236}U signals were ~100 mV. A minimum threshold of 50 mV for ^{235}U signal was used (^{238}U signal ~8 V): all data with ^{235}U signal below this threshold was removed post-measurement. A note of comparison, our measurements of ^{238}U are performed on solutions with a lower concentration of U (compared to 50-100 ppb solutions used in other labs) and also a lower spiking ratio (other labs are using ^{235}U:^{236}U at 1:4). The reason I have used a lower U concentration solution and less spike was so that no signal memory would be retained within the Neptune as Rick Mortlock uses the instrument for U-Th dating in the static mode.

Measurements of the ^{238}U/^{235}U ratios on the purified U samples were completed on a ThermoScientific NeptunePlus multi-collector ICP-MS (MC-ICP-MS), following a modified measuring protocol from Weyer et al. (2008). Abundance sensitivity was measured without the retarding potential quadrople (RPQ) filter to determine tailing from ^{238}U on the minor U isotopes (Hiess et al., 2012), and was found to have only reached 0.7 ppm after 3 years of analysis. Isotope spike was added to samples and standards at the same sample to spike ratio. Instrumental mass bias was corrected using the exponential

law with the reported $^{233}U/^{236}U$ for IRMM 3636a. For each sample analysis, a defocussed background measured while the sample was taken up, and then the instrument conducted 100 sweeps with 4-second integrations. A 5-minute rinse (2% nitric acid with ~0.1% HF) was conducted between each sample. An Aridus II (Cetac Technologies) desolvating nebulizer system was used to increase sensitivity and reduce interferences from water vapor (an Apex sample introduction was considered but not used since the membrane clogs more easily). Standard sample and x-skimmer cones were used for the analysis.

At the beginning of an analysis run, a blank acid was analyzed followed by CRM112a as bracketing standard (New Brunswick Laboratory, US DOE) and CRM 129, as a certified uranium oxide isotope standard (New Brunswick Laboratory, US DOE). After this, samples and in-house standard materials (BCR-2 Hawaii basalt, BATS Bermuda seawater, East Pacific Rise seawater) were analyzed with three sample measurements in between the bracketing CRM 112a. In a standard block, 9 samples/reference materials with bracketing were analyzed and then a CRM 112a, and a blank finished the block. Throughout the analysis, drift in the CRM 112a was accommodated by using a linear, weighted bracket approach to calculate the delta values for the samples (~15% signal loss occurred over 16 hours).

$$\delta^{238}U = \left(\frac{{}^{238}U/{}^{235}U_{sample}}{{}^{238}U/{}^{235}U_{CRM112a}} - 1 \right) * 1000$$

Authigenic uranium and $\delta^{238}U$ calculation

To determine the detrital and authigenic portions of U and $\delta^{238}U$, mathematical calculations were completed (Table 3 & 4). The detrital U was determined by using the

continental crust concentrations given in Rudnick & Gao (2003), [Al] = 81.50 mg/g and [U] = 2.7 μg/g. The authigenic fraction is the total uranium minus the detrital fraction.

$$[U]_T = [U]_{auth} + [U]_{detrital}$$

$$[U]_{auth} = [U]_T - \left({[U]_{crust}}/{[Al]_{crust}} \times [Al]_T \right)$$

The fraction authigenic U is the concentration authigenic U divided by the total U concentration. The isotopic compositions of the authigenic uranium fraction was calculated based on the following equation where the value of the $\delta^{238}U_{bulk}$ was the value measured and the $\delta^{238}U_{detrital}$ was -0.30 based on Tissot & Dauphas (2015) average continental crust composition.

$$\delta\ ^{238}U_{auth} = (\delta\ ^{238}U_{bulk\ meas.} \times [U]_T - \delta\ ^{238}U_{detrital} \times [U]_{detrital}) \div [U]_{auth}$$

Analytical precision and accuracy

The analytical precision and accuracy were assessed for both the concentration and isotopic measurements. Concentration was assessed by using reference materials with certified concentrations along with replicate sample digestions (Table 5). For isotopic measurements, BCR-2, seawater from the East Pacific, and CRM129 (a uranium ore) were used to determine the precision of the Neptune (Table 6).

Results

My results from the Southern Ocean show that significant isotopic variations occur over glacial-interglacial cycles (Figure 5, Table 2-4). During glacial stages, the increase in $\delta^{238}U$ was concurrent with the peaks in U concentration reflecting periods of higher productivity.

The interglacial sediments have a signal that is similar to modern seawater ($\delta^{238}U$ = -0.4 ± 0.09, average 2SD) with only a few exceptions being more depleted in ^{238}U (Figure 5C, Figure 6). These negative deviations from seawater could be related to adsorption processes. Previous studies have looked at the influence of MnO_2 on U isotope adsorption in oxic conditions and found a negative excursion of 0.2 – 0.3 away from the source material (Brennecka et al., 2011b; Goto et al., 2014). The negative excursion observed for the interglacial samples are not due to instrumental mass bias or analytical issues, but have a significant detrital component that, when calculating the authigenic component the $\delta^{238}U$, is based on a very small amount of uranium present within the sample. I acknowledge the negative excursion in the interglacial periods and that I cannot offer a satisfactory explanation for this occurrence at this time without doing more extensive observations of the mineralogy.

The glacial sediments have a signal with a positive excursion (0.07 to 0.31 ‰). Majority of the uranium present in these sediments is authigenic (Table 3). I think that there is more value in data obtained for the glacial periods as it could improve our understanding of $\delta^{238}U$ proxy use. Thus, in the following paragraphs, I will focus my attention on the context and depositional conditions that lead to the positive enrichment during the glacial stages.

Discussion

Previous studies of semi-enclosed basins (Weyer et al., 2008; Montoya-Pino et al., 2010; Andersen et al., 2014; Rolison et al., 2017) show similar range of $\delta^{238}U$ variability to what I have observed in this study of RC13-254 site from the Southern Ocean (Figure 6). Glacial sediments are enriched in ^{238}U, resulting in $\delta^{238}U$ values significantly more positive than the modern seawater. The majority of the glacial data spans a narrow range (+0.07 to +0.31) (Figure 6). The few outliers are associated with the glacial-interglacial transition events (Figure 6, outlined in a black circle). Out of all published data on isotope ratios, the glacial values that I measured were most similar to what has been previously observed in the Black Sea (Weyer et al., 2008; Montoya-Pino et al., 2010; Andersen et al., 2014; Rolison et al., 2017). The Black Sea is the classic euxinic system that has been used in part to define the $\delta^{238}U$ redox proxy (Weyer et al., 2008; Montoya-Pino et al., 2010) (Figure 7A). The schematic presented in 7A simplifies the original $\delta^{238}U$ model, even though it had two modern day sites calibrating it, the paleo-application utilized the $\delta^{238}U$ to determine the areal coverage of anoxic conditions. For my site, if the bottom water redox based $\delta^{238}U$ proxy is to be used at face value, it implies the global ocean can become euxinic on glacial-interglacial timescales. In the following paragraphs, I examine lines of evidence showing that it is not the case, and that bottom waters in the Southern ocean remained oxygenated.

The depositional conditions of the Southern Ocean suggest that the bottom waters remained fully oxygenated (Keir, 1988; Francois et al., 1997; Galbraith and Jaccard, 2015) despite productivity increases over glacial-interglacial cycles, which would lead to substantial drawdown of oxygen in waters below the mixed layer. The first line of

evidence comes from modeling studies of bottom water for this region, which suggested that during glacial periods, oxygen levels were depleted, down to 70 μmol/L compared to ~225 μmol/L in the modern deep ocean (Keir, 1988; Francois et al., 1997; Galbraith and Jaccard, 2015). Foraminifera data from the Portuguese margin support the drawdown of oxygen within the bottom waters for a range of 45-65 μmol/L; this site was located at 3146 mbss and provides a perspective of the relative depletion of source bottom waters (Hoogakker et al., 2015). Contrasting the Portuguese study, Lu et al. (2016) measured I/Ca within foraminifera at a site in the Pacific sector of the Southern Ocean (71°S, 119°W, 2096 mbss) showing that dissolved oxygen concentrations in intermediary waters before becoming Antarctic Bottom Water (AABW) was 70 μmol/L (Lu et al., 2016). The second area of evidence is related to trace metal abundances, where in sediments from RC13-254 there is a lack of enrichment in other redox sensitive metals (such as iron and molybdenum enrichments) that is typical for reducing basins (Table 2). Glacial sediments from along the Western Antarctic Peninsula have shown that rhenium (Re) enrichment occurred, suggesting that suboxic conditions occurred along the continental slope (Wagner et al., 2015). In both Southern Ocean and Black Sea sediments, the amount of $\delta^{238}U$ fractionation from the seawater source is comparable, which fits with incomplete removal of source material to the sediments, signifying that Rayleigh fractionation did not go to completion. The fact that the bottom waters of these two sites (euxinic in the Black Sea and oxygenated in the Southern Ocean) provide similar $\delta^{238}U$ raises a key question: what is the acting control on U isotope fractionation if different oxygen conditions give similar isotopic ranges?

My $\delta^{238}U$ data suggests that the signals captured in these sediments are a local signal driven by organic carbon burial rate. Carbon respiration could be responsible for the removal of U through U(VI) to U(IV) bacterial reduction during early diagenesis (Barnes and Cochran, 1991; Lovley et al., 1991; McManus et al., 2005; Morford et al., 2005). Due to the porewater depletion of U during this process, U in the overlying bottom water diffuses into the sediments allowing further reduction of U by bacteria. This removal from porewater does not require the presence of free sulfide (a marker of euxinic conditions) (Anderson, 1987; Lovley et al., 1993). Rather, bacteria completing U reduction show metabolic versatility, using NO_3, Mn, Fe, SO^{4-}, and As- as electron acceptors, and thus can operate at a variety of redox potentials (examples of such species include denitrifier *Pseudomonas putida* (Barton et al., 1996) and iron-reducer *Shewanella oneidenis MR-1* (Lovley et al., 1991), see Wall & Krumholz, 2006 and references therein for a review of known bacteria undergoing U reduction). Locally, the extent and style of sedimentary diagenesis depends on the amount of carbon buried. Carbon burial responds to water column conditions, since bottom water oxygen concentration impacts the degree of decomposition and therefore the amount of organic carbon delivered to the sediments (but it is not the only factor controlling the carbon burial) (Muller and Suess, 1979; Hartnett et al., 1998; Tyson, 2001). Therefore, carbon burial could serve as the primary control of the $\delta^{238}U$ signal preserved in the sediments and is impacted by the amount of bacterial degradation in the local water column (Figure 4). If carbon burial is controlling $\delta^{238}U$, how does my site fit into this interpretation?

Based on the conditions at RC13-254, productivity was greater during the glacial stages than in interglacial stages (Figure 5); however, the argument presented in Figure 4

of $\delta^{238}U$ shows that low carbon has an isotopic signature enriched in ^{238}U. This mismatch of a 'high productivity' site with a 'low carbon' isotopic signature needs a bit more clarification to show that carbon is the driving factor. I'll address this concern with two arguments, first by the whole record and then how the glacial stages fit into Figure 4. The authigenic data may provide a more complete picture of the carbon story of the site (Tables 3 and 4). In Figure 6, the two plots show the bulk and authigenic $\delta^{238}U$ for these samples. During the glacial stages, authigenic U composed greater than 80% of the bulk U, and that the U concentration was greater than 2 ppm. Contrastingly, interglacial U was variable in in concentration and in the fraction of authigenic, but overall there was less U and even less authigenic U present. The $\delta^{238}U$ observed in the interglacials could be driven more by the low amount of U and the choice of detrital correction parameters. Detrital correction has minimal impacts on the glacial stages since the authigenic U dominated the sample. Therefore, the authigenic $\delta^{238}U$ (and fraction authigenic) provide a more complete picture of which processes are dominant. In addressing the glacial stage authigenic data and how it fits into Figure 4's main statement, the conditions present would allow for my data to be classified as a low carbon environment. In a comprehensive compilation of carbon burial rates, Cartapanis et al. (2016) presented a global perspective of how burial rates changed over glacial and interglacial cycles. In their re-calculations of data from Mackensen et al. (2001), they showed for a comparable site to RC13-254 (PS2499-5, 46.51^{o}S, 15.33^{o}W, 3175 mbss) that during the glacials the productivity was > 0.03 gC/m^2/yr, while the interglacial values was < 0.01 gC/m^2/yr. These levels of carbon burial levels are very low, especially compared to coastal regions. Therefore, my data support the carbon burial rate hypothesis, and that authigenic signal

provides a solid a view of when data should be considered for carbon burial reconstructions.

Seeing as $\delta^{238}U$ is a record of local conditions specifically carbon burial rates, measurements of $\delta^{238}U$ at a single site should not be universally applied to infer change in the global conditions (Figure 7B). Although other studies have noted conflicting results for the $\delta^{238}U$ as they attempted to interpret it in relation to bottom water redox only (Noordmann et al., 2015; Hinojosa et al., 2016). Carbon burial, and not redox, is the key factor controlling $\delta^{238}U$; therefore classifications of depositional environments should be denoted in terms of carbon instead of oxygen (even though they are closely linked) (Figure 4). The collective understanding of the U isotope mass balance model needs to be revised.

Summary

My $\delta^{238}U$ results from the Southern Ocean showed a significant amount of variation over glacial-interglacial cycles. I focused on understanding the glacial signals, which had a $\delta^{238}U$ range similar to the Black Sea. As opposed to Black Sea, the Southern Ocean remained oxygenated in the bottom waters throughout glacial periods, and redox conditions alone can therefore not explain the $\delta^{238}U$ signal observed. Rather, a local signal that reflects carbon burial is likely to be the key factor influencing $\delta^{238}U$. Thus, my data show that $\delta^{238}U$ measurements are highly influenced by local conditions and single-site $\delta^{238}U$ should not be used as a global redox proxy. As seen in this study, the role of carbon burial is the primary control on local and global U isotope compositions. Overall my analysis indicates a need to rethink the oxygen based U isotopic mass balance.

References

Algeo, T.J., and Lyons, T.W., 2006, Mo-total organic carbon covariation in modern anoxic marine environments: Implications for analysis of paleoredox and paleohydrographic conditions: Paleoceanography, v. 21, Artn Pa1016, doi: 10.1029/2004pa001112.

Algeo, T.J., and Maynard, J.B., 2008, Trace-metal covariation as a guide to water-mass conditions in ancient anoxic marine environments: Geosphere, v. 4, p. 872-887, doi: 10.1130/Ges00174.1.

Amelin, Y., Kaltenbach, A., Iizuka, T., Stirling, C.H., Ireland, T.R., Petaev, M., and Jacobsen, S.B., 2010, U–Pb chronology of the Solar System's oldest solids with variable $^{238}U/^{235}U$: Earth and Planetary Science Letters, v. 300, p. 343-350, doi: 10.1016/j.epsl.2010.10.015.

Anbar, A.D., and Rouxel, O., 2007, Metal stable isotopes in paleoceanography: Annual Review of Earth and Planetary Sciences, v. 35, p. 717-746, doi: 10.1146/annurev.earth.34.031405.125029.

Andersen, M.B., Elliott, T., Freymuth, H., Sims, K.W.W., Niu, Y., and Kelley, K.A., 2015, The terrestrial uranium isotope cycle: Nature, v. 517, p. 356-359, doi: 10.1038/nature14062.

Andersen, M.B., Romaniello, S., Vance, D., Little, S.H., Herdman, R., and Lyons, T.W., 2014, A modern framework for the interpretation of $^{238}U/^{235}U$ in studies of ancient ocean redox: Earth and Planetary Science Letters, v. 400, p. 184-194, doi: 10.1016/j.epsl.2014.05.051.

Andersen, M.B., Vance, D., Morford, J.L., Bura-Nakić, E., Breitenbach, S.F.M., and Och, L., 2016, Closing in on the marine $^{238}U/^{235}U$ budget: Chemical Geology, v. 420, p. 11-22, doi: 10.1016/j.chemgeo.2015.10.041.

Anderson, R.F., 1982, Concentration, Vertical Flux, and Remineralization of Particulate Uranium in Sea-Water: Geochimica Et Cosmochimica Acta, v. 46, p. 1293-1299, doi: 10.1016/0016-7037(82)90013-8.

Anderson, R.F., 1984, A Method for Determining the Oxidation-State of Uranium in Natural-Waters: Nuclear Instruments & Methods in Physics Research Section a-Accelerators Spectrometers Detectors and Associated Equipment, v. 223, p. 213-217, doi: 10.1016/0167-5087(84)90650-1.

Anderson, R.F., 1987, Redox Behavior of Uranium in an Anoxic Marine Basin: Uranium, v. 3, p. 145-164.

Anderson, R.F., Chase, Z., Fleisher, M.Q., and Sachs, J., 2002, The Southern Ocean's biological pump during the Last Glacial Maximum: Deep-Sea Research Part II-Topical Studies in Oceanography, v. 49, p. 1909-1938, Pii S0967-0645(02)00018-8, doi: 10.1016/S0967-0645(02)00018-8.

Anderson, R.F., Fleisher, M.Q., and Lehuray, A.P., 1989a, Concentration, Oxidation-State, and Particulate Flux of Uranium in the Black-Sea: Geochimica Et Cosmochimica Acta, v. 53, p. 2215-2224, doi: 10.1016/0016-7037(89)90345-1.

Anderson, R.F., Kumar, N., Mortlock, R.A., Froelich, P.N., Kubik, P., Dittrich-Hannen, B., and Suter, M., 1998, Late-Quarternary changes in productivity of the Southern Ocean: Journal of Marine Systems, v. 17, p. 497-514, doi: 10.1016/S0924-7963(98)00060-8.

Anderson, R.F., Lehuray, A.P., Fleisher, M.Q., and Murray, J.W., 1989b, Uranium deposition in Saanich Inlet sediments, Vancouver Island: Geochimica et Cosmochimica Acta, v. 53, p. 2205-2213, doi: 10.1016/0016-7037(89)90344-X.

Andersson, P.S., Wasserburg, G.J., Chen, J.H., Papanastassiou, D.A., and Ingri, J., 1995, ^{238}U-^{234}U and ^{232}Th-^{230}Th in the Baltic Sea and in River Water: Earth and Planetary Science Letters, v. 130, p. 217-234, doi: 10.1016/0012-821x(94)00262-W.

Arnold, G.L., Anbar, A.D., Barling, J., and Lyons, T.W., 2004, Molybdenum isotope evidence for widespread anoxia in mid-Proterozoic oceans: Science, v. 304, p. 87-90, doi: 10.1126/science.1091785.

Arnold, G.L., Lyons, T.W., Gordon, G.W., and Anbar, A.D., 2012, Extreme change in sulfide concentrations in the Black Sea during the Little Ice Age reconstructed using molybdenum isotopes: Geology, v. 40, p. 595-598, doi: 10.1130/G32932.1.

Arthur, M.A., and Dean, W.E., 1998, Organic-matter production and preservation and evolution of anoxia in the Holocene Black Sea: Paleoceanography, v. 13, p. 395-411, doi: 10.1029/98pa01161.

Arthur, M.A., Dean, W.E., and Pratt, L.M., 1988, Geochemical and climatic effects of increased marine organic carbon burial at the Cenomanian/Turonian boundary: Nature, v. 335, p. 714-717.

Arthur, M.A., Schlanger, S.O., and Jenkyns, H.C., 1987, The Cenomanian-Turonian Oceanic Anoxic Event, II. Palaeoceanographic controls on organic-matter production and preservation: Geological Society, London, Special Publications, v. 26, p. 401-420, doi: 10.1144/gsl.sp.1987.026.01.25.

Asael, D., Tissot, F.L.H., Reinhard, C.T., Rouxel, O., Dauphas, N., Lyons, T.W., Ponzevera, E., Liorzou, C., and Cheron, S., 2013, Coupled molybdenum, iron and uranium stable isotopes as oceanic paleoredox proxies during the Paleoproterozoic Shunga Event: Chemical Geology, v. 362, p. 193-210, doi: 10.1016/j.chemgeo.2013.08.003.

Bard, E., Hamelin, B., Fairbanks, R.G., and Zindler, A., 1990, Calibration of the ^{14}C timescale over the past 30,000 years using mass spectrometric U-Th ages from Barbados corals: Nature, v. 345, p. 405-410, doi: 10.1038/345405a0.

Barnes, C.E., and Cochran, J.K., 1990, Uranium Removal in Oceanic Sediments and the Oceanic-U Balance: Earth and Planetary Science Letters, v. 97, p. 94-101, doi: 10.1016/0012-821x(90)90101-3.

Barnes, C.E., and Cochran, J.K., 1991, Geochemistry of Uranium in Black-Sea Sediments: Deep-Sea Research Part a-Oceanographic Research Papers, v. 38, p. S1237-S1254, doi: 10.1016/S0198-0149(10)80032-9.

Barnes, C.E., and Cochran, J.K., 1993, Uranium Geochemistry in Estuarine Sediments - Controls on Removal and Release Processes: Geochimica Et Cosmochimica Acta, v. 57, p. 555-569, doi: 10.1016/0016-7037(93)90367-6.

Barton, L.L., Choudhury, K., Thomson, B.M., Steenhoudt, K., and Groffman, A.R., 1996, Bacterial reduction of soluble uranium: the first step of in situ immobilization of uranium: Radioactive Waste Management and Environmental Restoration, v. 20, p. 141-151.

Basu, A., Sanford, R.A., Johnson, T.M., Lundstrom, C.C., and Loffler, F.E., 2014, Uranium isotopic fractionation factors during U(VI) reduction by bacterial isolates: Geochimica Et Cosmochimica Acta, v. 136, p. 100-113, doi: 10.1016/j.gca.2014.02.041.

Bopp, C.J., Lundstrom, C.C., Johnson, T.M., and Glessner, J.J.G., 2009, Variations in $^{238}U/^{235}U$ in uranium ore deposits: Isotopic signatures of the U reduction process?: Geology, v. 37, p. 611-614, doi: 10.1130/G25550a.1.

Bouvier, A., Spivak-Birndorf, L.J., Brennecka, G.A., and Wadhwa, M., 2011, New constraints on early Solar System chronology from Al–Mg and U–Pb isotope systematics in the unique basaltic achondrite Northwest Africa 2976: Geochimica et Cosmochimica Acta, v. 75, p. 5310-5323, doi: 10.1016/j.gca.2011.06.033.

Brennecka, G.A., Borg, L.E., Hutcheon, I.D., Sharp, M.A., and Anbar, A.D., 2010a, Natural variations in uranium isotope ratios of uranium ore concentrates: Understanding the $^{238}U/^{235}U$ fractionation mechanism: Earth and Planetary Science Letters, v. 291, p. 228-233, doi: 10.1016/j.epsl.2010.01.023.

Brennecka, G.A., Herrmann, A.D., Algeo, T.J., and Anbar, A.D., 2011a, Rapid expansion of oceanic anoxia immediately before the end-Permian mass extinction: Proceedings of the National Academy of Sciences of the United States of America, v. 108, p. 17631-17634, doi: 10.1073/pnas.1106039108.

Brennecka, G.A., and Wadhwa, M., 2012, Uranium isotope compositions of the basaltic angrite meteorites and the chronological implications for the early Solar System: Proc Natl Acad Sci U S A, v. 109, p. 9299-9303, doi: 10.1073/pnas.1114043109.

Brennecka, G.A., Wasylenki, L.E., Bargar, J.R., Weyer, S., and Anbar, A.D., 2011b, Uranium isotope fractionation during adsorption to Mn-oxyhydroxides: Environ Sci Technol, v. 45, p. 1370-1375, doi: 10.1021/es103061v.

Brennecka, G.A., Weyer, S., Wadhwa, M., Janney, P.E., Zipfel, J., and Anbar, A.D., 2010b, $^{238}U/^{235}U$ variations in meteorites: extant ^{247}Cm and implications for Pb-Pb dating: Science, v. 327, p. 449-451, doi: 10.1126/science.1180871.

Broecker, W.S., 2000, Abrupt climate change: causal constraints provided by the paleoclimate record: Earth-Science Reviews, v. 51, p. 137-154, doi: 10.1016/S0012-8252(00)00019-2.

Brumsack, H.J., 2006, The trace metal content of recent organic carbon-rich sediments: Implications for Cretaceous black shale formation: Palaeogeography Palaeoclimatology Palaeoecology, v. 232, p. 344-361, doi: 10.1016/j.palaeo.2005.05.011.

Buesseler, K.O., Livingston, H.D., and Casso, S.A., 1991, Mixing between Oxic and Anoxic Waters of the Black-Sea as Traced by Chernobyl Cesium Isotopes: Deep-Sea Research Part a-Oceanographic Research Papers, v. 38, p. S725-S745, doi: 10.1016/S0198-0149(10)80006-8.

Calvert, S.E., Karlin, R.E., Toolin, L.J., Donahue, D.J., Southon, J.R., and Vogel, J.S., 1991, Low Organic-Carbon Accumulation Rates in Black-Sea Sediments: Nature, v. 350, p. 692-695, doi: 10.1038/350692a0.

Calvert, S.E., and Pedersen, T.F., 1993, Geochemistry of Recent Oxic and Anoxic Marine-Sediments - Implications for the Geological Record: Marine Geology, v. 113, p. 67-88, doi: 10.1016/0025-3227(93)90150-T.

Canfield, D.E., 1994, Factors influencing organic carbon preservation in marine sediments: Chem Geol, v. 114, p. 315-329.

Canfield, D.E., 1998, A new model for Proterozoic ocean chemistry: Nature, v. 396, p. 450-453, Doi 10.1038/24839.

Canfield, D.E., Glazer, A.N., and Falkowski, P.G., 2010, The evolution and future of Earth's nitrogen cycle: Science, v. 330, p. 192-196, doi: 10.1126/science.1186120.

Cartapanis, O., Bianchi, D., Jaccard, S.L., and Galbraith, E.D., 2016, Global pulses of organic carbon burial in deep-sea sediments during glacial maxima: Nature Communications, v. 7, p. 10796, doi: 10.1038/ncomms10796.

Charles, C.D., Froelich, P.N., Zibello, M.A., Mortlock, R.A., and Morley, J.J., 1991, Biogenic opal in Southern Ocean sediments over the last 450,000 years: Implications for surface water chemistry and circulation: Paleoceanography, v. 6, p. 697-728, doi: 10.1029/91PA02477.

Chase, Z., Anderson, R.F., and Fleisher, M.Q., 2001, Evidence from authigenic uranium for increased productivity of the glacial Subantarctic Ocean: Paleoceanography, v. 16, p. 468-478, doi: 10.1029/2000pa000542.

Chen, J.H., Edwards, R.L., and Wasserburg, G.J., 1986, ^{238}U, ^{234}U and ^{232}Th in seawater: Earth and Planetary Science Letters, v. 80, p. 241-251.

Chen, T., Robinson, L.F., Beasley, M.P., Claxton, L.M., Andersen, M.B., Gregoire, L.J., Wadham, J., Fornari, D.J., and Harpp, K.S., 2016a, Ocean mixing and ice-sheet control of seawater ^{234}U/^{238}U during the last deglaciation: Science, doi: 10.1126/science.aag1015.

Chen, X., Romaniello, S.J., Herrmann, A.D., Wasylenki, L.E., and Anbar, A.D., 2016b, Uranium isotope fractionation during coprecipitation with aragonite and calcite: Geochimica et Cosmochimica Acta, v. 188, p. 189-207, doi: 10.1016/j.gca.2016.05.022.

Christl, M., Lachner, J., Vockenhuber, C., Lechtenfeld, O., Stimac, I., van der Loeff, M.R., and Synal, H.-A., 2012, A depth profile of uranium-236 in the Atlantic Ocean: Geochimica et Cosmochimica Acta, v. 77, p. 98-107, doi: 10.1016/j.gca.2011.11.009.

Cochran, J.K., Carey, A.E., Sholkovitz, E.R., and Surprenant, L.D., 1986, The Geochemistry of Uranium and Thorium in Coastal Marine-Sediments and Sediment Pore Waters: Geochimica Et Cosmochimica Acta, v. 50, p. 663-680, doi: 10.1016/0016-7037(86)90344-3.

Colodner, D., Edmond, J., and Boyle, E., 1995, Rhenium in the Black-Sea - Comparison with Molybdenum and Uranium: Earth and Planetary Science Letters, v. 131, p. 1-15, doi: 10.1016/0012-821x(95)00010-A.

Connelly, J.N., Bizzarro, M., Krot, A.N., Nordlund, Å., Wielandt, D., and Ivanova, M.A., 2012, The Absolute Chronology and Thermal Processing of Solids in the Solar Protoplanetary Disk: Science, v. 338, p. 651-655, doi: 10.1126/science.1226919.

Crusius, J., Calvert, S., Pedersen, T., and Sage, D., 1996, Rhenium and molybdenum enrichments in sediments as indicators of oxic, suboxic and sulfidic conditions of deposition: Earth and Planetary Science Letters, v. 145, p. 65-78, doi: 10.1016/S0012-821x(96)00204-X.

Dahl, T.W., Boyle, R.A., Canfield, D.E., Connelly, J.N., Gill, B.C., Lenton, T.M., and Bizzarro, M., 2014, Uranium isotopes distinguish two geochemically distinct

stages during the later Cambrian SPICE event: Earth and Planetary Science Letters, v. 401, p. 313-326, doi: 10.1016/j.epsl.2014.05.043.

Dansgaard, W., Johnsen, S., Clausen, H., Dahl-Jensen, D., Gundestrup, N., Hammer, C., Hvidberg, C., Steffensen, J., Sveinbjörnsdottir, A., and Jouzel, J., 1993, Evidence for general instability of past climate from a 250-kyr ice-core record: Nature, v. 364, p. 218-220.

Deuser, W.G., Organic-carbon budget of the Black Sea, *in* Proceedings Deep Sea Research and Oceanographic Abstracts1971, Volume 18, Elsevier, p. 995-1004.

Deutsch, C., Brix, H., Ito, T., Frenzel, H., and Thompson, L., 2011, Climate-forced variability of ocean hypoxia: Science, v. 333, p. 336-339, doi: 10.1126/science.1202422.

Deutsch, C., Ferrel, A., Seibel, B., Portner, H.O., and Huey, R.B., 2015, Ecophysiology. Climate change tightens a metabolic constraint on marine habitats: Science, v. 348, p. 1132-1135, doi: 10.1126/science.aaa1605.

Dunk, R.M., Mills, R.A., and Jenkins, W.J., 2002, A reevaluation of the oceanic uranium budget for the Holocene: Chemical Geology, v. 190, p. 45-67, Pii S0009-2541(02)00110-9, doi: 10.1016/S0009-2541(02)00110-9.

Dymond, J., Suess, E., and Lyle, M., 1992, Barium in deep-sea sediment: A geochemical proxy for paleoproductivity: Paleoceanography, v. 7, p. 163-181.

Edwards, R.L., Chen, J.H., and Wasserburg, G.J., 1987, ^{238}U-^{234}U-^{230}Th-^{232}Th systematics and the precise measurement of time over the past 500,000 years: Earth and Planetary Science Letters, v. 81, p. 175-192, doi: 10.1016/0012-821X(87)90154-3.

Elrick, M., Polyak, V., Algeo, T.J., Romaniello, S., Asmerom, Y., Herrmann, A.D., Anbar, A.D., Zhao, L., and Chen, Z.-Q., 2017, Global-ocean redox variation during the middle-late Permian through Early Triassic based on uranium isotope and Th/U trends of marine carbonates: Geology, v. 45, p. 163-166, doi: 10.1130/g38585.1.

Francois, R., Altabet, M.A., Yu, E.-F., Sigman, D.M., Bacon, M.P., Frank, M., Bohrmann, G., Bareille, G., and Labeyrie, L.D., 1997, Contribution of Southern Ocean surface-water stratification to low atmospheric CO_2 concentrations during the last glacial period: Nature, v. 389, p. 929-935, doi: 10.1038/40073.

Frederickson, A.F., 1948, Some Mechanisms for the Fixation of Uranium in Certain Sediments: Science, v. 108, p. 184-185.

Galbraith, E.D., and Jaccard, S.L., 2015, Deglacial weakening of the oceanic soft tissue pump: global constraints from sedimentary nitrogen isotopes and oxygenation proxies: Quaternary Science Reviews, v. 109, p. 38-48, doi: 10.1016/j.quascirev.2014.11.012.

Galbraith, E.D., Kienast, M., Pedersen, T.F., and Calvert, S.E., 2004, Glacial-interglacial modulation of the marine nitrogen cycle by high-latitude O_2 supply to the global thermocline: Paleoceanography, v. 19, doi: 10.1029/2003PA001000.

Goldmann, A., Brennecka, G., Noordmann, J., Weyer, S., and Wadhwa, M., 2015, The uranium isotopic composition of the Earth and the Solar System: Geochimica et Cosmochimica Acta, v. 148, p. 145-158, doi: 10.1016/j.gca.2014.09.008.

Goto, K.T., Anbar, A.D., Gordon, G.W., Romaniello, S.J., Shimoda, G., Takaya, Y., Tokumaru, A., Nozaki, T., Suzuki, K., Machida, S., Hanyu, T., and Usui, A.,

2014, Uranium isotope systematics of ferromanganese crusts in the Pacific Ocean: Implications for the marine $^{238}U/^{235}U$ isotope system: Geochimica et Cosmochimica Acta, v. 146, p. 43-58, doi: 10.1016/j.gca.2014.10.003.

Hartnett, H.E., Keil, R.G., Hedges, J.I., and Devol, A.H., 1998, Influence of oxygen exposure time on organic carbon preservation in continental margin sediments: Nature, v. 391, p. 572-575.

Hedges, J.I., and Keil, R.G., 1995, Sedimentary organic matter preservation: an assessment and speculative synthesis: Marine Chemistry, v. 49, p. 81-115.

Henderson, G.M., 2002, New oceanic proxies for paleoclimate: Earth and Planetary Science Letters, v. 203, p. 1-13, Pii S0012-821x(02)00809-9, doi: 10.1016/S0012-821x(02)00809-9.

Hiess, J., Condon, D.J., McLean, N., and Noble, S.R., 2012, $^{238}U/^{235}U$ systematics in terrestrial uranium-bearing minerals: Science, v. 335, p. 1610-1614, doi: 10.1126/science.1215507.

Hinojosa, J.L., Stirling, C.H., Reid, M.R., Moy, C.M., and Wilson, G.S., 2016, Trace metal cycling and $^{238}U/^{235}U$ in New Zealand's fjords: Implications for reconstructing global paleoredox conditions in organic-rich sediments: Geochimica et Cosmochimica Acta, v. 179, p. 89-109, doi: 10.1016/j.gca.2016.02.006.

Holmden, C., Amini, M., and Francois, R., 2015, Uranium isotope fractionation in Saanich Inlet: A modern analog study of a paleoredox tracer: Geochimica et Cosmochimica Acta, v. 153, p. 202-215, doi: 10.1016/j.gca.2014.11.012.

Hood, A.v.S., Planavsky, N.J., Wallace, M.W., Wang, X., Bellefroid, E.J., Gueguen, B., and Cole, D.B., 2016, Integrated geochemical-petrographic insights from component-selective $\delta^{238}U$ of Cryogenian marine carbonates: Geology, v. 44, p. 935-938, doi: 10.1130/g38533.1.

Hoogakker, B.A.A., Elderfield, H., Schmiedl, G., McCave, I.N., and Rickaby, R.E.M., 2015, Glacial-interglacial changes in bottom-water oxygen content on the Portuguese margin: Nature Geosci, v. 8, p. 40-43, 10.1038/ngeo2317.

Hotinski, R.M., Bice, K.L., Kump, L.R., Najjar, R.G., and Arthur, M.A., 2001, Ocean stagnation and end-Permian anoxia: Geology, v. 29, p. 7-10, doi: 10.1130/0091-7613(2001)029<0007:Osaepa>2.0.Co;2.

Iizuka, T., Amelin, Y., Kaltenbach, A., Koefoed, P., and Stirling, C.H., 2014, U–Pb systematics of the unique achondrite Ibitira: Precise age determination and petrogenetic implications: Geochimica et Cosmochimica Acta, v. 132, p. 259-273, doi: 10.1016/j.gca.2014.02.017.

Jaccard, S.L., Hayes, C.T., Martínez-García, A., Hodell, D.A., Anderson, R.F., Sigman, D.M., and Haug, G.H., 2013, Two Modes of Change in Southern Ocean Productivity Over the Past Million Years: Science, v. 339, p. 1419-1423, doi: 10.1126/science.1227545.

Jenkyns, H.C., 2010, Geochemistry of oceanic anoxic events: Geochemistry Geophysics Geosystems, v. 11, Artn Q03004, doi: 10.1029/2009gc002788.

Kaltenbach, A., 2012, Uranium isotopic analysis of terrestrial and extraterrestrial samples [Doctor of Philosophy: University of Otago].

Keeling, R.F., and Garcia, H.E., 2002, The change in oceanic O_2 inventory associated with recent global warming: Proc Natl Acad Sci U S A, v. 99, p. 7848-7853, doi: 10.1073/pnas.122154899.

Keeling, R.F., Kortzinger, A., and Gruber, N., 2010, Ocean Deoxygenation in a Warming World: Annual Review of Marine Science, v. 2, p. 199-229, doi: 10.1146/annurev.marine.010908.163855.

Keir, R.S., 1988, On the late Pleistocene ocean geochemistry and circulation: Paleoceanography, v. 3, p. 413-445, doi: 10.1029/PA003i004p00413.

Kendall, B., Brennecka, G.A., Weyer, S., and Anbar, A.D., 2013, Uranium isotope fractionation suggests oxidative uranium mobilization at 2.50 Ga: Chemical Geology, v. 362, p. 105-114, doi: 10.1016/j.chemgeo.2013.08.010.

Kendall, B., Komiya, T., Lyons, T.W., Bates, S.M., Gordon, G.W., Romaniello, S.J., Jiang, G., Creaser, R.A., Xiao, S., McFadden, K., Sawaki, Y., Tahata, M., Shu, D., Han, J., Li, Y., Chu, X., and Anbar, A.D., 2015, Uranium and molybdenum isotope evidence for an episode of widespread ocean oxygenation during the late Ediacaran Period: Geochimica et Cosmochimica Acta, v. 156, p. 173-193, doi: 10.1016/j.gca.2015.02.025.

Kirchenbaur, M., Maas, R., Ehrig, K., Kamenetsky, V.S., Strub, E., Ballhaus, C., and Münker, C., 2016, Uranium and Sm isotope studies of the supergiant Olympic Dam Cu–Au–U–Ag deposit, South Australia: Geochimica et Cosmochimica Acta, v. 180, p. 15-32, doi: 10.1016/j.gca.2016.01.035.

Klinkhammer, G.P., and Palmer, M.R., 1991, Uranium in the Oceans - Where It Goes and Why: Geochimica Et Cosmochimica Acta, v. 55, p. 1799-1806, doi: 10.1016/0016-7037(91)90024-Y.

Ku, T.L., 1965, An evaluation of the $^{234}U/^{238}U$ method as a tool for dating pelagic sediments: Journal of Geophysical Research, v. 70, p. 3457-3474.

Ku, T.L., Knauss, K.G., and Mathieu, G.G., 1977, Uranium in open ocean: concentration and isotopic composition: Deep-Sea Research v. 24, p. 1005-1017, doi: 10.1016/0146-6291(77)90571-9.

Kumar, N., Anderson, R.F., Mortlock, R.A., Froelich, P.N., Kubik, P., Dittrichhannen, B., and Suter, M., 1995, Increased Biological Productivity and Export Production in the Glacial Southern-Ocean: Nature, v. 378, p. 675-680, doi: 10.1038/378675a0.

Kumar, N., Gwiazda, R., Anderson, R., and Froelich, P., 1993, $^{231}Pa/^{230}Th$ ratios in sediments as a proxy for past changes in Southern Ocean productivity: Nature, v. 362, p. 45-48, doi: 10.1038/362045a0.

Langmuir, D., 1978, Uranium solution-mineral equilibria at low temperatures with applications to sedimentary ore deposits: Geochimica et Cosmochimica Acta, v. 42, p. 547-569.

Larsen, K.K., Trinquier, A., Paton, C., Schiller, M., Wielandt, D., Ivanova, M.A., Connelly, J.N., Nordlund, Å., Krot, A.N., and Bizzarro, M., 2011, Evidence for magnesium isotope heterogeneity in the solar protoplanetary disk: The Astrophysical Journal Letters, v. 735, p. L37.

Latimer, J.C., and Filippelli, G.M., 2001, Terrigenous input and paleoproductivity in the Southern Ocean: Paleoceanography, v. 16, p. 627-643, doi: 10.1029/2000PA000586.

Lau, K.V., Macdonald, F.A., Maher, K., and Payne, J.L., 2017, Uranium isotope evidence for temporary ocean oxygenation in the aftermath of the Sturtian Snowball Earth: Earth and Planetary Science Letters, v. 458, p. 282-292, doi: 10.1016/j.epsl.2016.10.043.

Lau, K.V., Maher, K., Altiner, D., Kelley, B.M., Kump, L.R., Lehrmann, D.J., Silva-Tamayo, J.C., Weaver, K.L., Yu, M., and Payne, J.L., 2016, Marine anoxia and delayed Earth system recovery after the end-Permian extinction: Proc Natl Acad Sci U S A, v. 113, p. 2360-2365, doi: 10.1073/pnas.1515080113.

Lisiecki, L.E., and Raymo, M.E., 2005, A Pliocene-Pleistocene stack of 57 globally distributed benthic $\delta^{18}O$ records: Paleoceanography, v. 20.

Lovley, D.R., Phillips, E.J.P., Gorby, Y.A., and Landa, E.R., 1991, Microbial reduction of uranium: Nature, v. 350, p. 413-416, doi: 10.1038/350413a0.

Lovley, D.R., Roden, E.E., Phillips, E.J.P., and Woodward, J.C., 1993, Enzymatic iron and uranium reduction by sulfate-reducing bacteria: Marine Geology, v. 113, p. 41-53.

Lu, Z., Hoogakker, B.A.A., Hillenbrand, C.-D., Zhou, X., Thomas, E., Gutchess, K.M., Lu, W., Jones, L., and Rickaby, R.E.M., 2016, Oxygen depletion recorded in upper waters of the glacial Southern Ocean: Nat Commun, v. 7, 10.1038/ncomms11146.

Lu, Z., Jenkyns, H.C., and Rickaby, R.E.M., 2010, Iodine to calcium ratios in marine carbonate as a paleo-redox proxy during oceanic anoxic events: Geology, v. 38, p. 1107-1110, doi: 10.1130/g31145.1.

Lyons, T.W., Anbar, A.D., Severmann, S., Scott, C., and Gill, B.C., 2009, Tracking Euxinia in the Ancient Ocean: A Multiproxy Perspective and Proterozoic Case Study: Annual Review of Earth and Planetary Sciences, v. 37, p. 507-534, doi: 10.1146/annurev.earth.36.031207.124233.

Lyons, T.W., and Severmann, S., 2006, A critical look at iron paleoredox proxies: New insights from modern euxinic marine basins: Geochimica Et Cosmochimica Acta, v. 70, p. 5698-5722, doi: 10.1016/j.gca.2006.08.021.

Mackensen, A., Rudolph, M., and Kuhn, G., 2001, Late Pleistocene deep-water circulation in the subantarctic eastern Atlantic: Global and Planetary Change, v. 30, p. 197-229, doi: 10.1016/S0921-8181(01)00102-3.

Mangini, A., Sonntag, C., Bertsch, G., and Muller, E., 1979, Evidence for a higher natural uranium content in world rivers: Nature, v. 278, p. 337-339.

McManus, J., Berelson, W.M., Klinkhammer, G.P., Hammond, D.E., and Holm, C., 2005, Authigenic uranium: relationship to oxygen penetration depth and organic carbon rain: Geochimica Et Cosmochimica Acta, v. 69, p. 95-108, doi: 10.1016/j.gca.2004.06.023.

McManus, J., Berelson, W.M., Severmann, S., Poulson, R.L., Hammond, D.E., Klinkhammer, G.P., and Holm, C., 2006, Molybdenum and uranium geochemistry in continental margin sediments: Paleoproxy potential: Geochimica Et Cosmochimica Acta, v. 70, p. 4643-4662, doi: 10.1016/j.gca.2006.06.1564.

Meier, H.E.M., 2005, Modeling the age of Baltic Seawater masses: Quantification and steady state sensitivity experiments: Journal of Geophysical Research: Oceans, v. 110, doi: 10.1029/2004JC002607.

Meyer, K.M., and Kump, L.R., 2008, Oceanic euxinia in Earth history: Causes and consequences: Annual Review of Earth and Planetary Sciences, v. 36, p. 251-288, doi: 10.1146/annurev.earth.36.031207.124256.

Middleburg, J.J., and Levin, L.A., 2009, Coastal hypoxia and sediment biogeochemistry: Biogeosciences, v. 6, p. 1273-1293.

Mo, T., Suttle, A.D., and Sackett, W.M., 1973, Uranium concentrations in marine sediments: Geochimica et Cosmochimica Acta, v. 37, p. 35-51, doi: 10.1016/0016-7037(73)90242-1.

Montoya-Pino, C., Weyer, S., Anbar, A.D., Pross, J., Oschmann, W., van de Schootbrugge, B., and Arz, H.W., 2010, Global enhancement of ocean anoxia during Oceanic Anoxic Event 2: A quantitative approach using U isotopes: Geology, v. 38, p. 315-318, doi: 10.1130/G30652.1.

Morford, J.L., and Emerson, S., 1999, The geochemistry of redox sensitive trace metals in sediments: Geochimica Et Cosmochimica Acta, v. 63, p. 1735-1750, doi: 10.1016/S0016-7037(99)00126-X.

Morford, J.L., Emerson, S.R., Breckel, E.J., and Kim, S.H., 2005, Diagenesis of oxyanions (V, U, Re, and Mo) in pore waters and sediments from a continental margin: Geochimica Et Cosmochimica Acta, v. 69, p. 5021-5032, doi: 10.1016/j.gca.2005.05.015.

Morford, J.L., Martin, W.R., and Carney, C.M., 2009, Uranium diagenesis in sediments underlying bottom waters with high oxygen content: Geochimica et Cosmochimica Acta, v. 73, p. 2920-2937.

Morford, J.L., Martin, W.R., and Carney, C.M., 2012, Rhenium geochemical cycling: Insights from continental margins: Chemical Geology, v. 324, p. 73-86, doi: 10.1016/j.chemgeo.2011.12.014.

Mort, H., Jacquat, O., Adatte, T., Steinmann, P., Föllmi, K., Matera, V., Berner, Z., and Stüben, D., 2007a, The Cenomanian/Turonian anoxic event at the Bonarelli Level in Italy and Spain: enhanced productivity and/or better preservation?: Cretaceous Research, v. 28, p. 597-612.

Mort, H.P., Adatte, T., Föllmi, K.B., Keller, G., Steinmann, P., Matera, V., Berner, Z., and Stüben, D., 2007b, Phosphorus and the roles of productivity and nutrient recycling during oceanic anoxic event 2: Geology, v. 35, p. 483-486.

Mortlock, R.A., Charles, C.D., Froelich, P.N., Zibello, M.A., Saltzman, J., Hays, J.D., and Burckle, L.H., 1991, Evidence for lower productivity in the Antarctic Ocean during the last glaciation: Nature, v. 351, p. 220-223, doi:10.1038/351220a0.

Muller, P.G., and Suess, E., 1979, Productivity, sedimentation rate, and sedimentary organic matter in the oceans-- I. Organic carbon preservation: Deep-Sea Research, v. 26, p. 1347-1362.

Muratli, J.M., Chase, Z., Mix, A.C., and McManus, J., 2010, Increased glacial-age ventilation of the Chilean margin by Antarctic Intermediate Water: Nature Geoscience, v. 3, p. 23-26, doi: 10.1038/Ngeo715.

Murphy, M.J., Stirling, C.H., Kaltenbach, A., Turner, S.P., and Schaefer, B.F., 2014, Fractionation of $^{238}U/^{235}U$ by reduction during low temperature uranium mineralisation processes: Earth and Planetary Science Letters, v. 388, p. 306-317, doi: 10.1016/j.epsl.2013.11.034.

Nagler, T.F., Siebert, C., Luschen, H., and Bottcher, M.E., 2005, Sedimentary Mo isotope record across the Holocene fresh-brackish water transition of the Black Sea: Chemical Geology, v. 219, p. 283-295, doi: 10.1016/j.chemgeo.2005.03.006.

Nameroff, T.J., Calvert, S.E., and Murray, J.W., 2004, Glacial-interglacial variability in the eastern tropical North Pacific oxygen minimum zone recorded by redox-sensitive trace metals: Paleoceanography, v. 19, doi: 10.1029/2003PA000912.

Neubert, N., Nagler, T.F., and Bottcher, M.E., 2008, Sulfidity controls molybdenum isotope fractionation into euxinic sediments: Evidence from the modern Black Sea: Geology, v. 36, p. 775-778, doi: 10.1130/G24959a.1.

Noordmann, J., Weyer, S., Georg, R.B., Jöns, S., and Sharma, M., 2015a, $^{238}U/^{235}U$ isotope ratios of crustal material, rivers and products of hydrothermal alteration: new insights on the oceanic U isotope mass balance: Isotopes in Environmental and Health Studies, p. 1-23, doi: 10.1080/10256016.2015.1047449.

Noordmann, J., Weyer, S., Montoya-Pino, C., Dellwig, O., Neubert, N., Eckert, S., Paetzel, M., and Böttcher, M.E., 2015b, Uranium and molybdenum isotope systematics in modern euxinic basins: Case studies from the central Baltic Sea and the Kyllaren fjord (Norway): Chemical Geology, v. 396, p. 182-195, doi: 10.1016/j.chemgeo.2014.12.012.

Owens, J.D., Gill, B.C., Jenkyns, H.C., Bates, S.M., Severmann, S., Kuypers, M.M., Woodfine, R.G., and Lyons, T.W., 2013, Sulfur isotopes track the global extent and dynamics of euxinia during Cretaceous Oceanic Anoxic Event 2: Proceedings of the National Academy of Sciences, v. 110, p. 18407-18412.

Pedersen, T.F., and Calvert, S.E., 1990, Anoxia Vs Productivity - What Controls the Formation of Organic-Carbon-Rich Sediments and Sedimentary-Rocks: Aapg Bulletin-American Association of Petroleum Geologists, v. 74, p. 454-466.

Piper, D.Z., and Calvert, S.E., 2009, A marine biogeochemical perspective on black shale deposition: Earth-Science Reviews, v. 95, p. 63-96, doi: 10.1016/j.earscirev.2009.03.001.

Potter, E.K., Stirling, C.H., Andersen, M.B., and Halliday, A.N., 2005, High precision Faraday collector MC-ICPMS thorium isotope ratio determination: International Journal of Mass Spectrometry, v. 247, p. 10-17, doi: 10.1016/j.ijms.2005.08.017.

Prakash Babu, C., Brumsack, H.J., Schnetger, B., and Böttcher, M.E., 2002, Barium as a productivity proxy in continental margin sediments: a study from the eastern Arabian Sea: Marine Geology, v. 184, p. 189-206, doi: 10.1016/S0025-3227(01)00286-9.

Reinhard, C.T., Planavsky, N.J., Robbins, L.J., Partin, C.A., Gill, B.C., Lalonde, S.V., Bekker, A., Konhauser, K.O., and Lyons, T.W., 2013, Proterozoic ocean redox and biogeochemical stasis: Proc Natl Acad Sci U S A, v. 110, p. 5357-5362, doi: 10.1073/pnas.1208622110.

Rolison, J.M., 2016, The biogeochemistry of trace metals and their isotopes in the Mediterranean and Black Seas [PhD: University of Otago].

Rolison, J.M., Stirling, C.H., Middag, R., and Rijkenberg, M.J.A., 2017, Uranium stable isotope fractionation in the Black Sea: Modern calibration of the $^{238}U/^{235}U$ paleo-redox proxy: Geochimica et Cosmochimica Acta, v. 203, p. 69-88, doi: 10.1016/j.gca.2016.12.014.

Romaniello, S.J., 2012, Incorporation and preservation of molybdenum and uranium isotope variations in modern marine sediments [Doctor of Philosophy: Arizona State University, 154 p].

Romaniello, S.J., Herrmann, A.D., and Anbar, A., 2013, Uranium concentrations and $^{238}U/^{235}U$ isotope ratios in modern carbonates from the Bahamas: Assessing a novel paleoredox proxy: Chemical Geology, v. 362, p. 305-316.

Rosenthal, Y., Boyle, E.A., Labeyrie, L., and Oppo, D., 1995, Glacial enrichments of authigenic Cd and U in Subantarctic sediments: A climatic control on the elements' oceanic budget?: Paleoceanography, v. 10, p. 395-413, doi: 10.1029/95PA00310.

Rudnick, R.L., and Gao, S., 2003, Composition of the continental crust: Treatise on geochemistry, v. 3, p. 659.

Sackett, W., Mo, T., Spalding, R., and Exner, M., A reevaluation of the marine geochemistry of uranium, *in* Proceedings Proc Int Symp Interaction of Radioactive Contaminants with the Constituents of the Marine Environment. IAEA, Wien/A1973, p. 757-769.

Sarmiento, J.L., Herbert, T.D., and Toggweiler, J., 1988, Causes of anoxia in the world ocean: Global Biogeochemical Cycles, v. 2, p. 115-128.

Schauble, E.A., 2007, Role of nuclear volume in driving equilibrium stable isotope fractionation of mercury, thallium, and other very heavy elements: Geochimica Et Cosmochimica Acta, v. 71, p. 2170-2189, doi: 10.1016/j.gca.2007.02.004.

Schlanger, S., and Jenkyns, H., 1976, Cretaceous oceanic anoxic events: causes and consequences: Geologie en Mijnbouw, v. 55, p. 179-184.

Schlanger, S.O., Arthur, M.A., Jenkyns, H.C., and Scholle, P.A., 1987, The Cenomanian-Turonian Oceanic Anoxic Event, I. Stratigraphy and distribution of organic carbon-rich beds and the marine δ13C excursion: Geological Society, London, Special Publications, v. 26, p. 371-399, doi: 10.1144/gsl.sp.1987.026.01.24.

Shaw, T.J., Gieskes, J.M., and Jahnke, R.A., 1990, Early Diagenesis in Differing Depositional-Environments - the Response of Transition-Metals in Pore Water: Geochimica Et Cosmochimica Acta, v. 54, p. 1233-1246, doi: 10.1016/0016-7037(90)90149-F.

Shaw, T.J., Sholkovitz, E.R., and Klinkhammer, G., 1994, Redox dynamics in the Chesapeake Bay: The effect on sediment/water uranium exchange: Geochimica et Cosmochimica Acta, v. 58, p. 2985-2995, doi: 10.1016/0016-7037(94)90173-2.

Stirling, C.H., Andersen, M.B., Potter, E.K., and Halliday, A.N., 2007, Low-temperature isotopic fractionation of uranium: Earth and Planetary Science Letters, v. 264, p. 208-225, doi: 10.1016/j.epsl.2007.09.019.

Stirling, C.H., Halliday, A.N., and Porcelli, D., 2005, In search of live ^{247}Cm in the early solar system: Geochimica et Cosmochimica Acta, v. 69, p. 1059-1071, doi: 10.1016/j.gca.2004.06.034.

Stramma, L., Johnson, G.C., Sprintall, J., and Mohrholz, V., 2008, Expanding oxygen-minimum zones in the tropical oceans: Science, v. 320, p. 655-658, doi: 10.1126/science.1153847.

Swanson, V.E., 1961, Geology and geochemistry of uranium in marine black shales a review, US Government Printing Office.

Telus, M., Dauphas, N., Moynier, F., Tissot, F.L.H., Teng, F.-Z., Nabelek, P.I., Craddock, P.R., and Groat, L.A., 2012, Iron, zinc, magnesium and uranium isotopic fractionation during continental crust differentiation: The tale from migmatites, granitoids, and pegmatites: Geochimica et Cosmochimica Acta, v. 97, p. 247-265, doi: 10.1016/j.gca.2012.08.024.

Tissot, F.L.H., and Dauphas, N., 2015, Uranium isotopic compositions of the crust and ocean: Age corrections, U budget and global extent of modern anoxia: Geochimica et Cosmochimica Acta, v. 167, p. 113-143, doi: 10.1016/j.gca.2015.06.034.

Todd, J.F., Elsinger, R.J., and Moore, W.S., 1988, The distribution of uranium, radium and thorium isotopes in two anoxic fjords: Framvaren Fjord (Norway) and Saanich Inlet (British Columbia): Marine Chemistry, v. 23, p. 393-415.

Tribovillard, N., Algeo, T.J., Lyons, T., and Riboulleau, A., 2006, Trace metals as paleoredox and paleoproductivity proxies: An update: Chemical Geology, v. 232, p. 12-32, Doi: 10.1016/j.chemgeo.2006.02.012.

Tyrrell, T., 1999, The relative influences of nitrogen and phosphorus on oceanic primary production: Nature, v. 400, p. 525-531, Doi: 10.1038/22941.

Tyson, R.V., 1995, Abundance of Organic Matter in Sediments: TOC, Hydrodynamic Equivalence, Dilution and Flux Effects, Sedimentary Organic Matter: Organic facies and palynofacies: Dordrecht, Springer Netherlands, p. 81-118.

Tyson, R.V., 2001, Sedimentation rate, dilution, preservation and total organic carbon: some results of a modelling study: Organic Geochemistry, v. 32, p. 333-339, doi: 10.1016/S0146-6380(00)00161-3.

Uvarova, Y.A., Kyser, T.K., Geagea, M.L., and Chipley, D., 2014, Variations in the uranium isotopic compositions of uranium ores from different types of uranium deposits: Geochimica et Cosmochimica Acta, v. 146, p. 1-17, doi: 10.1016/j.gca.2014.09.034.

Veeh, H.H., Calvert, S.E., and Price, N.B., 1974, Accumulation of uranium in sediments and phosphorites on the South West African shelf: Marine Chemistry, v. 2, p. 189-202, doi: 10.1016/0304-4203(74)90014-0.

von Rad, U., Schulz, H., Khan, A.A., Ansari, M., Berner, U., Čepek, P., Cowie, G., Dietrich, P., Erlenkeuser, H., Geyh, M., Jennerjahn, T., Lückge, A., Marchig, V., Riech, V., Rösch, H., Schäfer, P., Schulte, S., Sirocko, F., Tahir, M., and Weiss, W., 1995, Sampling the oxygen minimum zone off Pakistan: glacial-interglacial variations of anoxia and productivity (preliminary results, sonne 90 cruise): Marine Geology, v. 125, p. 7-19, doi: 10.1016/0025-3227(95)00051-Y.

Wagner, M., Hendy, I.L., McKay, J.L., and Pedersen, T.F., 2015, Redox chemistry of West Antarctic Peninsula margin surface sediments: Chemical Geology, v. 417, p. 102-114, doi:10.1016/j.chemgeo.2015.10.002.

Wall, J.D., and Krumholz, L.R., 2006, Uranium reduction: Annu Rev Microbiol, v. 60, p. 149-166, doi: 10.1146/annurev.micro.59.030804.121357.

Wang, X., Planavsky, N.J., Reinhard, C.T., Hein, J.R., and Johnson, T.M., 2016, A Cenozoic seawater redox record derived from $^{238}U/^{235}U$ in ferromanganese crusts: American Journal of Science, v. 316, p. 64-83, doi: 10.2475/01.2016.02.

Weyer, S., Anbar, A.D., Gerdes, A., Gordon, G.W., Algeo, T.J., and Boyle, E.A., 2008, Natural fractionation of $^{238}U/^{235}U$: Geochimica et Cosmochimica Acta, v. 72, p. 345-359, doi: 10.1016/j.gca.2007.11.012.

Winogradow, A., and Pempkowiak, J., 2014, Organic carbon burial rates in the Baltic Sea sediments: Estuarine Coastal and Shelf Science, v. 138, p. 27-36, doi: 10.1016/j.ecss.2013.12.001.

Zhou, X., Thomas, E., Rickaby, R.E.M., Winguth, A.M.E., and Lu, Z., 2014, I/Ca evidence for upper ocean deoxygenation during the PETM: Paleoceanography, v. 29, p. 964-975, doi: 10.1002/2014PA002702.

Zillén, L., Conley, D.J., Andrén, T., Andrén, E., and Björck, S., 2008, Past occurrences of hypoxia in the Baltic Sea and the role of climate variability, environmental change and human impact: Earth-Science Reviews, v. 91, p. 77-92, doi: 10.1016/j.earscirev.2008.10.001.

Figures

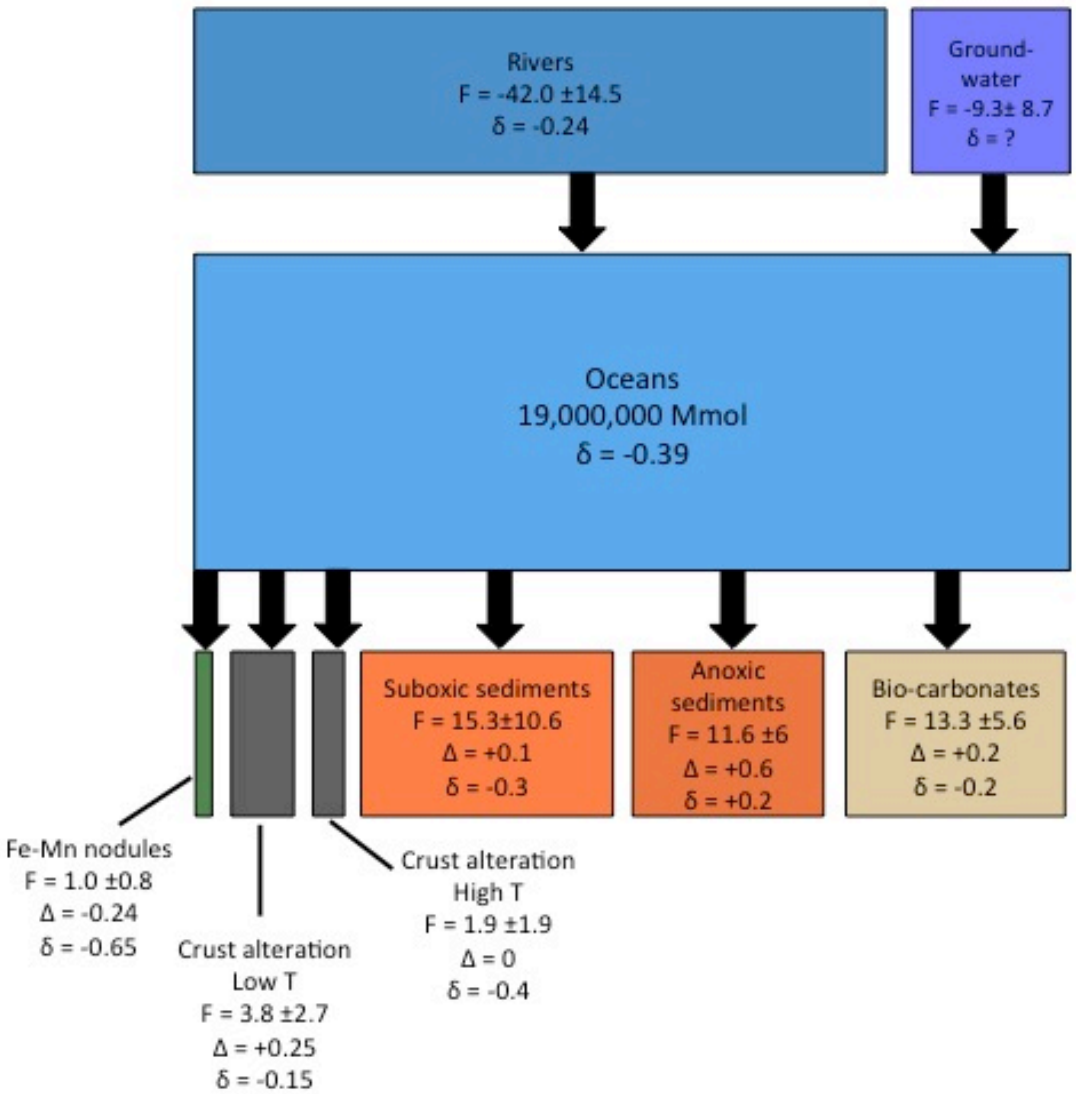

Figure 1: Mass balance model of U isotopes in the modern ocean with major source from the ocean and sinks into anoxic and suboxic/oxic reservoirs. The size of the fluxes (in Mmol/yr) moving into a sink or source is denoted by F and is drawn to scale. The Δ represents the isotopic difference of a sink to the seawater ratio. The δ is the value observed in marine environments. The relative sizes of the sinks have been determined based on the elemental mass balance. Over geologic time the relative sizes of the sinks have varied in size causing changes in the isotopic composition of seawater. Modified from Montoya-Pino et al., 2010, mass budget based on Dunk et al., 2002, and isotopes based on Tissot & Dauphas, 2015.

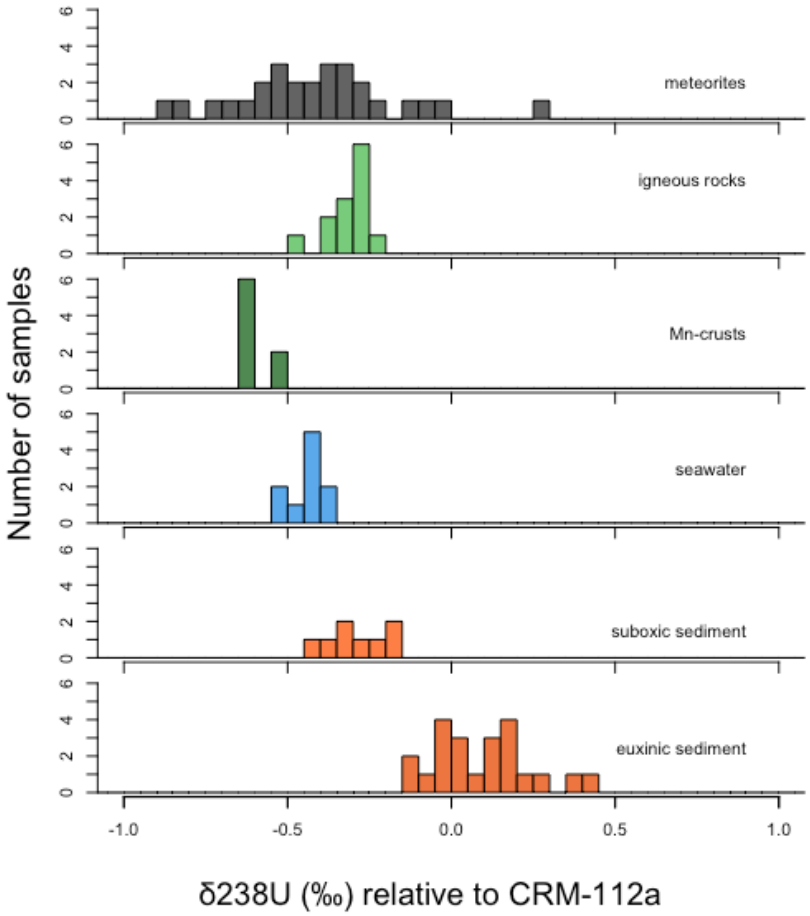

Figure 2: Histograms of the $\delta^{238}U$ of six reservoirs collected up till 2010. The distribution of the suboxic and euxinic sediments were applied to create the U redox model from Montoya-Pino et al., 2010. Data from Stirling et al, 2005; Stirling et al., 2007; Weyer et al., 2008; Amelin et al., 2010, Brennecka et al., 2010a; Montoya-Pino et al., 2010.

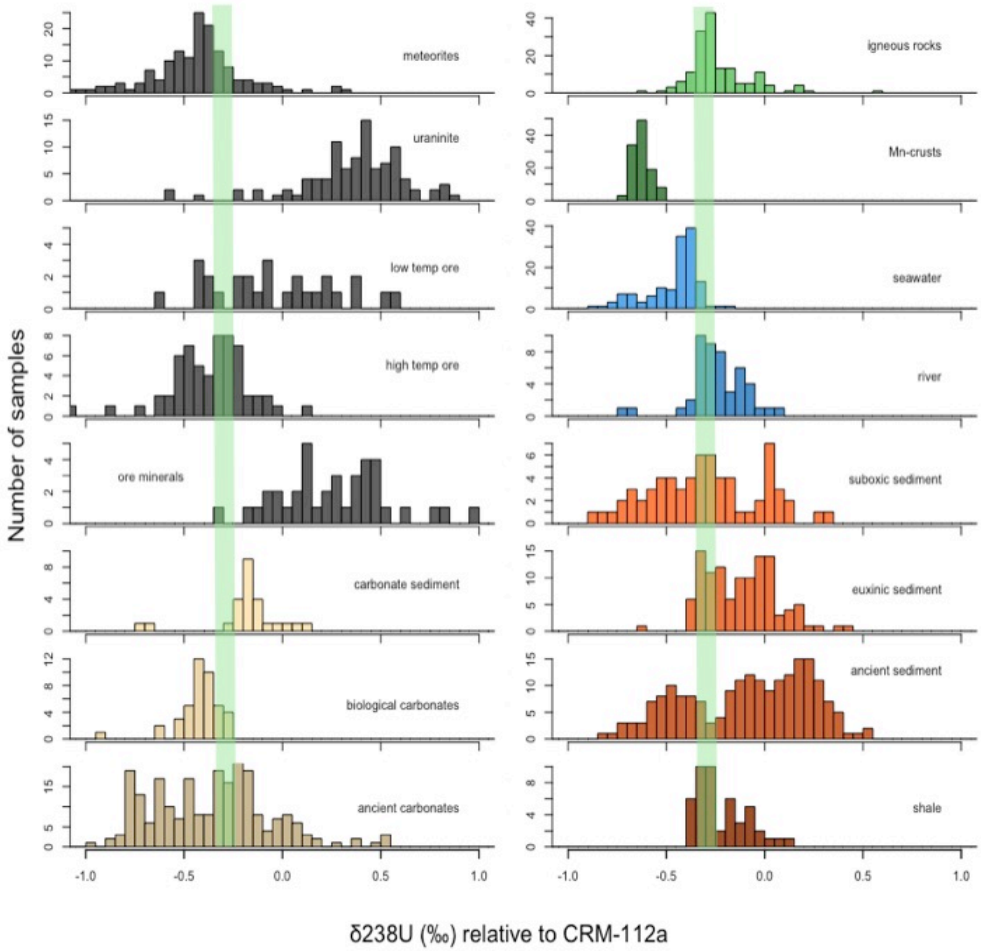

Figure 3: Updated histograms of all published data of $\delta^{238}U$ from several different depositional environments. A pale green bar shows the igneous rock composition. Left (top to bottom): meteorites, uraninite, low temp ore, high temp ore, ore minerals, carbonate sediment, biological carbonates, ancient carbonates. Right (top to bottom): igneous rocks, Mn-crusts, seawater, river, suboxic sediment, euxinic sediment, ancient sediment, shale. Data from (Stirling et al., 2005; Stirling et al., 2007; Weyer et al., 2008; Bopp et al., 2009; Amelin et al., 2010; Brennecka et al., 2010a; Brennecka et al., 2010b; Montoya-Pino et al., 2010; Bouvier et al., 2011; Brennecka et al., 2011a; Larsen et al., 2011; Brennecka and Wadhwa, 2012; Connelly et al., 2012; Hiess et al., 2012; Kaltenbach, 2012; Romaniello, 2012; Telus et al., 2012; Asael et al., 2013; Kendall et al., 2013; Romaniello et al., 2013; Andersen et al., 2014; Dahl et al., 2014; Goto et al., 2014; Iizuka et al., 2014; Murphy et al., 2014; Uvarova et al., 2014; Andersen et al., 2015; Goldmann et al., 2015; Holmden et al., 2015; Kendall et al., 2015; Noordmann et al., 2015a; Noordmann et al., 2015b; Tissot and Dauphas, 2015; Andersen et al., 2016; Elrick et al., 2016; Hinojosa et al., 2016; Hood et al., 2016; Kirchenbaur et al., 2016; Lau et al., 2016; Rolison, 2016; Wang et al., 2016; Lau et al., 2017; Rolison et al., 2017).

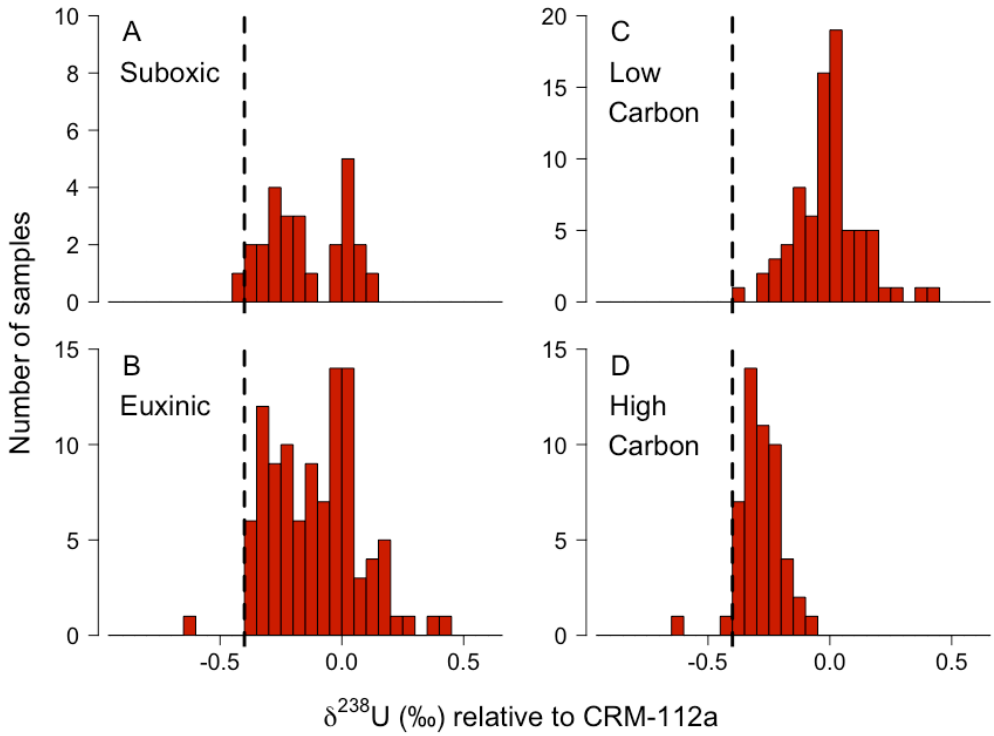

Figure 4: Distribution of published $\delta^{238}U$ in marine sediments. A: sediments under suboxic or oxic bottom waters. B: sediments under anoxic or euxinic bottom waters. C: sediments in low carbon depositional environments (C_{burial} less than 10 $gC/m^2/yr$). D: sediments in high carbon depositional environments (C_{burial} more than 10 $gC/m^2/yr$). Average seawater $\delta^{238}U$ is noted with the dashed line at -0.4 ‰. Data used for this figure are Weyer et al. (2008); Montoya-Pino et al. (2010); Andersen et al. (2014); Hinojosa et al. (2014); Holmden et al. (2015); Noordmann et al. (2015b); Rolison et al. (2017).

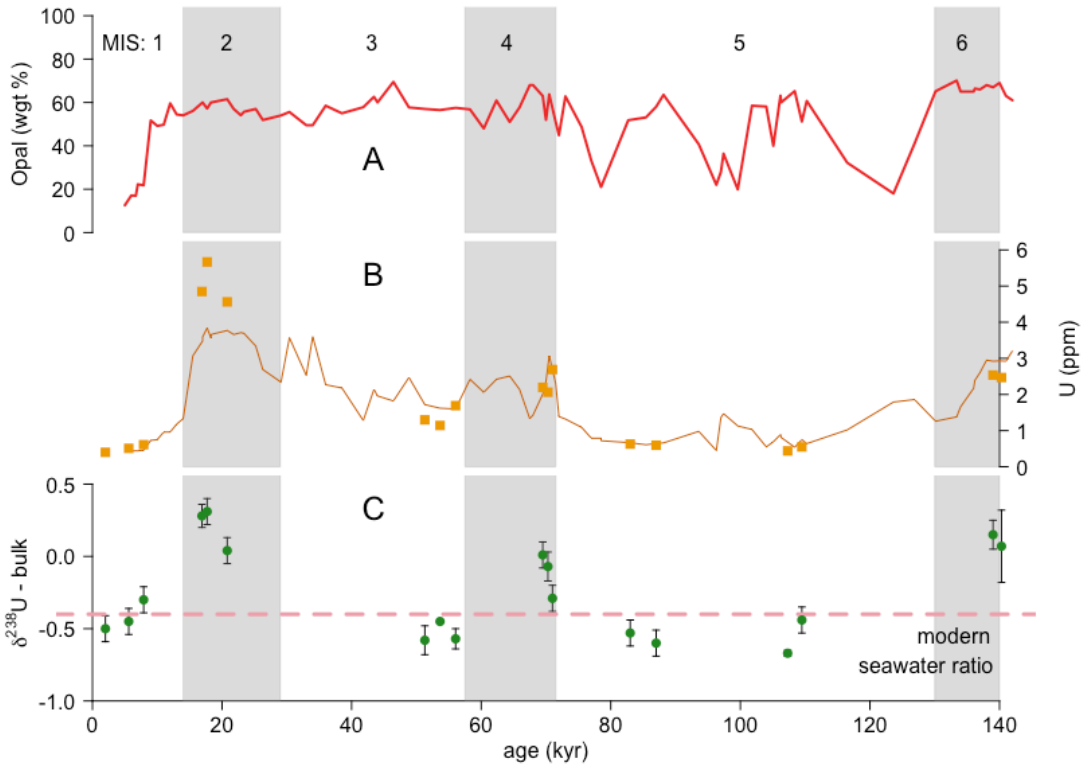

Figure 5: Records from RC13-254 in the Southern Ocean spanning glacial-interglacial cycles from 2-140 kya. A: % opal by weight (from Mortlock et al., 1991 and Kumar et al., 1995). B: U concentration in ppm (squares – this study; solid line from Kumar et al., 1995). C: δ^{238}U in bulk sediment, with the modern seawater ratio noted with a dashed pink line. The δ^{238}U values are given as per mil deviations from CRM112a, with 2SD error bars. In Table 4, information about 2SD, number of analysis per sample, and replicated digestions with separate isotopic measurements are noted. Age model for this site from Charles et al., 1991 with revisions by R.F. Anderson. Glacial stages shaded in grey (MIS based on Lisiecki & Raymo, 2005).

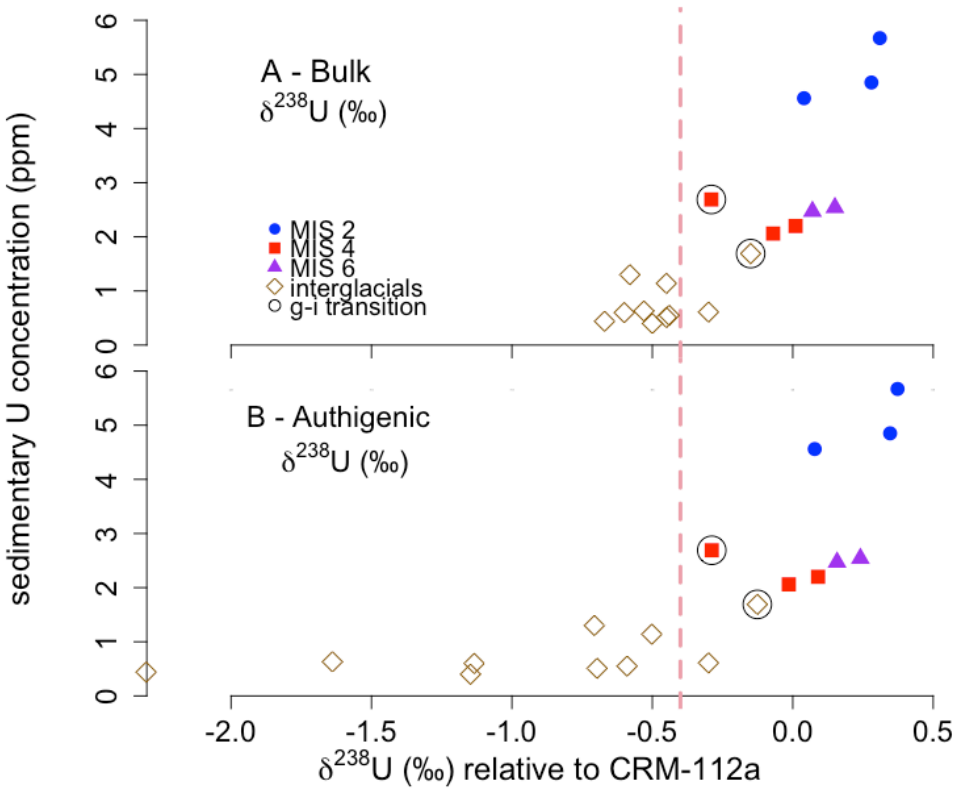

Figure 6: Plots of the $\delta^{238}U$ versus the U concentration within the sediments for A: bulk $\delta^{238}U$ and B: authigenic $\delta^{238}U$. Distinct symbols were used to highlight the different glacial stages: MIS 2 (blue circles), MIS 4 (red squares), MIS 6 (purple triangles), interglacial periods (brown unfilled diamonds), and samples that were near the transitions between glacial-interglacial (outlined in a black circle). A pink dashed line represents the modern seawater $\delta^{238}U$ (Dunk et al., 2002). MIS 4 does not have as tight a correlation with the other glacial stages $\delta^{238}U$, as this was a weaker glacial period, unlike the strong, eccentricity aligned glacial periods at the Last Glacial Maximum (MIS 2) and the Penultimate Glaciation (MIS 6).

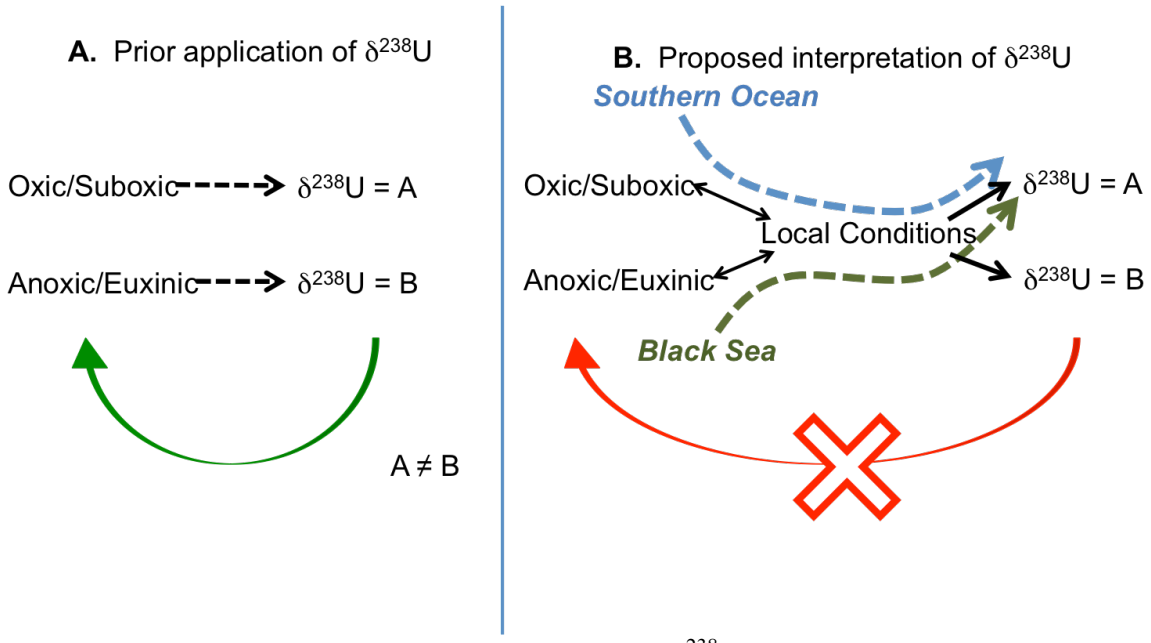

Figure 7: Schematic representation of application of $\delta^{238}U$ proxy A: as previously used and B: my new interpretation. A: In the prior application, the redox conditions of the environment shaped the way the $\delta^{238}U$ was viewed. Based on this, redox conditions of samples were reconstructed based on the $\delta^{238}U$. B: In light of studies of the Black Sea and the Southern Ocean, which result in similar $\delta^{238}U$ values, the disconnect suggests that the prior application is missing a step. By considering local conditions (including C_{burial}) as an intermediary, sites with different redox conditions can result in similar $\delta^{238}U$. Therefore, a $\delta^{238}U$ signal should not be used to reconstruct the original dominant redox pair influencing the bottom water conditions.

Tables

Table 1: RC13-254 Sample information

Name	IGSN	Parent IGSN	depth (m)	age (kyr)#
RC13-254PC_2cm	DSR000EGB	DSR00055H	0.02	2
RC13-254PC_10cm	DSR000EGC	DSR00055H	0.10	5.6
RC13-254PC_18cm	DSR000EGD	DSR00055H	0.18	7.9
RC13-254PC_120cm	DSR000EGE	DSR00055H	1.20	16.9
RC13-254PC_140cm	DSR000EGF	DSR00055H	1.40	17.7
RC13-254PC_200cm	DSR000EGG	DSR00055H	2.00	20.8
RC13-254PC_575cm	DSR000EGH	DSR00055H	5.75	51.3
RC13-254PC_595cm	DSR000EGI	DSR00055H	5.95	53.65
RC13-254PC_615cm	DSR000EGJ	DSR00055H	6.15	56.05
RC13-254PC_745cm	DSR000EGK	DSR00055H	7.45	69.5
RC13-254PC_753cm	DSR000EGL	DSR00055H	7.53	70.3
RC13-254PC_760cm	DSR000EGM	DSR00055H	7.60	71
RC13-254PC_806cm	DSR000EGN	DSR00055H	8.06	83
RC13-254PC_813cm	DSR000EGO	DSR00055H	8.13	87
RC13-254PC_880cm	DSR000EGP	DSR00055H	8.80	107.3
RC13-254PC_890cm	DSR000EGQ	DSR00055H	8.90	109.49
RC13-254PC_990cm	DSR000EGR	DSR00055H	9.91	139
RC13-254PC_1000cm	DSR000EGS	DSR00055H	10.03	140.3

#Age model for this site from Charles et al., 1991 with revisions by R.F. Anderson.

Table 2: RC13-254 auxiliary data

depth (m)	age (kyr)#	Al (mg/g)	Ca (mg/g)	Cr (ng/g)	Mn (μg/g)	Fe (mg/g)	Mo (μg/g)	Ba (μg/g)	Th (μg/g)	U (μg/g)
0.02	2	9.22	245.43	5010.79	202.21	6.38	2.38	726.71	1.29	0.40
0.10	5.6	9.57	229.90	5087.45	364.45	6.94	1.77	1420.87	1.52	0.51
0.18	7.9	10.91	244.97	5602.15	617.75	6.76	2.33	1593.28	1.55	0.61
1.20	16.9	15.08	3.94	11.06	149.54	16.53	2.53	581.29	1.48	4.85
1.40	17.7	16.02	7.69	11.36	226.46	19.45	1.09	618.42	1.60	5.67
2.00	20.8	13.89	3.32	12.52	134.85	19.55	2.32	568.04	1.55	4.56
5.75	51.3	12.18	37.16	7.94	190.24	14.85	1.42	723.28	1.47	1.30
5.95	53.65	8.86	45.26	5.83	141.45	10.48	1.07	601.68	0.99	1.15
6.15	56.05	6.99	46.96	4.22	172.71	6.89	0.92	669.42	0.91	1.69
7.45	69.5	13.61	27.35	12.68	277.75	15.76	4.70	1389.13	1.62	2.20
7.53	70.3	12.18	43.70	6.55	150.95	12.31	0.73	696.26	1.58	2.07
7.60	71	10.85	65.57	7.72	118.19	10.86	0.16	864.78	1.31	2.69
8.06	83	15.71	59.43	10.24	177.63	19.09	0.53	1155.86	1.92	0.63
8.13	87	11.50	53.13	7.25	128.74	11.91	0.53	946.66	1.40	0.60
8.80	107.3	10.80	21.29	25.71	133.29	16.14	0.67	907.71	1.10	0.44
8.90	109.49	8.58	57.62	6.37	111.10	12.48	0.45	1075.14	1.01	0.55
9.91	139	13.05	16.29	9.55	136.61	16.20	1.70	572.60	1.37	2.58
10.03	140.3	14.28	24.70	10.96	160.02	18.03	1.65	418.46	1.49	2.47

Table 3: Authigenic uranium calculations at RC13-254.

depth (m)	age (kyr)#	Al conc. (mg/g)	bulk U conc. (μg/g)	authigenic U conc. (μg/g)**	fraction authigenic U**
0.02	2	9.216	0.40	0.09	0.236
0.10	5.6	9.567	0.51	0.19	0.378
0.18	7.9	10.910	0.61	0.25	0.408
1.20	16.9	15.080	4.85	4.35	0.897
1.40	17.7	16.022	5.67	5.14	0.906
2.00	20.8	13.893	4.56	4.10	0.899
5.75	51.3	12.180	1.30	0.89	0.689
5.95	53.65	8.861	1.14	0.85	0.743
6.15	56.05	6.994	1.69	1.46	0.863
7.45	69.5	13.609	2.20	1.74	0.795
7.53	70.3	12.175	2.06	1.66	0.804
7.60	71	10.848	2.69	2.33	0.866
8.06	83	15.713	0.63	0.11	0.172
8.13	87	11.502	0.60	0.21	0.360
8.80	107.3	10.804	0.44	0.08	0.185
8.90	109.49	8.585	0.55	0.27	0.483
9.91	139	12.846	2.54	2.11	0.832
10.03	140.3	14.280	2.47	2.00	0.808

#Age model for this site from Charles et al., 1991 with revisions by R.F. Anderson.
**Rudnick & Gao (2003) detrital aluminum correction ratio applied.

Table 4: Uranium isotope data at RC13-254.

depth (m)	age (kyr)#	bulk δ238U	2SD^	n	authigenic δ238U	authigenic 2SD
0.02	2	-0.50	0.09^	1	-1.15	
0.10	5.6	-0.45	0.09^	1	-0.70	
0.18	7.9	-0.30	0.09^	1	-0.30	
1.20	16.9	0.28	0.08	3*	0.35	0.08
1.40	17.7	0.31	0.09^	1	0.37	
2.00	20.8	0.04	0.09^	1	0.08	
5.75	51.3	-0.58	0.10	2*	-0.71	0.15
5.95	53.65	-0.45	0.005	2*	-0.50	0.03
6.15	56.05	-0.15	0.07	2	-0.13	
7.45	69.5	0.01	0.09^	1	0.09	
7.53	70.3	-0.07	0.10	2*	-0.01	0.13
7.60	71	-0.29	0.09^	1	-0.29	
8.06	83	-0.53	0.09^	1	-1.64	
8.13	87	-0.60	0.09^	1	-1.13	
8.80	107.3	-0.67	0.02	2	-2.30	
8.90	109.49	-0.44	0.09^	1	-0.59	
9.91	139	0.15	0.10	2*	0.24	0.11
10.03	140.3	0.07	0.25	2*	0.16	0.28

#Age model for this site from Charles et al., 1991 with revisions by R.F. Anderson.
^Based on replicate measurements with CRM129. Average -0.94; 2SD 0.09. n=6.
* replicates represent separate digestions.

Table 5: iCap concentration accuracy
iCap accuracy based on reference materials analyzed with Cretaceous sediments
BCR-2 reference material was analyzed with these samples (similar trends were observed with the other reference standards - SCO-1, MAG-1, SDO-1).
Mn, Cu, Co, Sr, Mo, Ba, Ce, Nd, Th, U met reference standards stated in BCR-2 certificate of analysis.
V were close to the reference standard, but were 10% low. Fe was also close, but was 10% higher than the certified value.
Cr data can be used to understand overarching trends but not for its numbers. For BCR it was 60% of certified value.
Had consistent problems with major ions measuring to have lower than expected concentrations.
Cd was not noted in the certificate
iCap accuracy based on reference materials analyzed with Black and Baltic Sea sediments and Southern Ocean
BCR-2 reference material was analyzed with these samples
Mo, Ba, Ce, Nd, Th, U met reference standards stated in BCR-2 certificate of analysis.
Sr, Co, Fe, Mn for these elements half of the time they met the values stated in the certificate, the other half the time they were 5% lower.
V, Cu were close to the reference standard, but were 10% below certified value.
Cr data can be used to understand overarching trends but not for its numbers. For BCR it was 60% of certified value.
Had consistent problems with major ions measuring to have lower than expected concentrations.
Cd, Ni was not noted in the certificate

Table 6: Neptune isotopic accuracy

Analysis group	solution	average delta value	standard deviation	n	notes
Southern Ocean Sediments	BCR	-0.3		1	
	CRM129	-0.94	0.05	6	
	EPR	-0.24	0.10	7	problems with solution
Cretaceous Sediments	BCR	-0.27	0.06	28	
	CRM129	inconsistent			inconsistent
	EPR	-0.39	0.10	42	
Black and Baltic Seawaters	BCR	-0.32	0.06	10	
	CRM129- day 1-3	-1.46	0.07	6	
	CRM129- day 4-6	-0.93	0.08	4	
	EPR	-0.41	0.09	8	
Black and Baltic Sediments	BCR	-0.32	0.08	14	
	CRM129	inconsistent			inconsistent
	EPR	-0.39	0.06	17	
Typical values within literature			0.04 - 0.05		

Appendices

Appendix 1: Overview

The four subsequent appendices were conceptualized as a way to thoroughly examine uranium isotopes (^{238}U and ^{235}U) in different locations and during different geological periods. Each appendix includes a brief overview of the region, environmental features, and considerations of how this study fits into the overarching discussion on how the $\delta^{238}U$ proxy framework. These studies cover a range of redox environments and variations in primary production and burial rates. A map and sample descriptions are provided. The bulk of this section is devoted to the data tables, which contains a combination of concentration data and $\delta^{238}U$ measurements.

In Appendix 2, is an additional Southern Ocean study using the site ODP 1094. The samples come from the glacial-interglacial transition that occurred around 130kya. This site represents an oxygenated bottom water site.

Dating to the Cretaceous, Appendix 3 studies sediments from multiple sites around the proto-North Atlantic around the Ocean Anoxic Event 2 (OAE 2). This period was marked by regional differences in the extent and duration of anoxia and the amount of organic rich sediments deposited. Six sites were selected for this study from sites around the proto-North Atlantic to answer two main questions. First a comparison of sites within close proximity to each other (ideally with similar redox conditions but different organic carbon burial rates), I expect these will have different isotope ratios due to differences in water column depth. Secondly by analyzing sites around the basin with

known variations in redox conditions but ideally similar organic carbon burial rates, I hope to find locations with similar isotope ratios but differing redox conditions.

In the final two appendices, the Black (Appendix 4) and Baltic (Appendix 5) Seas provided a range of environmental conditions that would allow for completing a modern day calibration of $\delta^{238}U$. The hydrology of the Baltic Sea and Black Sea show similarities in redox ranges, but vary in productivity. The productivity of the Black Sea is similar to rates observed in low productivity environments (Calvert et al., 1991), while the Baltic is one of the most productive systems in the world due to eutrophication (Winogradow and Pempkowiak, 2014). By comparing both basins together and having other environmental conditions available, the goal of this study is to be as comprehensive as possible in understanding the context of where U isotopes fractionate and how the $\delta^{238}U$ proxy works. To fully capture where the fractionation occurs, four types of samples were collected during cruises to these seas, which include sediments and porewaters along with water column and particulate matter. Thus, by investigating U isotopes in various settings in their environmental context I can calibrate the use of the $\delta^{238}U$ proxy.

References

Calvert, S.E., Karlin, R.E., Toolin, L.J., Donahue, D.J., Southon, J.R., and Vogel, J.S., 1991, Low Organic-Carbon Accumulation Rates in Black-Sea Sediments: Nature, v. 350, p. 692-695, doi: 10.1038/350692a0.

Winogradow, A., and Pempkowiak, J., 2014, Organic carbon burial rates in the Baltic Sea sediments: Estuarine Coastal and Shelf Science, v. 138, p. 27-36, doi: 10.1016/j.ecss.2013.12.001.

Appendix 2: Southern Ocean ODP 1094

Appendix 2-1: Overview of Southern Ocean ODP 1094

This project envisioned comparing two sites in the Southern Ocean with different periods of high productivity. The magnitude of productivity in the Southern Ocean depends on the locations of atmospheric fronts. The Antarctic Polar Front (APF) is an important front for non-coastal productivity as it determines the location of upwelling of nutrient-rich waters and therefore the location with greatest productivity (Appendix 2-2) (Kumar et al., 1993; Anderson et al., 2002; Jaccard et al., 2013). The location of the APF moves in response to the extent of sea-ice during glacial and interglacial cycles. Previously, studies noted changes in productivity during glacial-interglacial cycles, i.e. sites north of the APF had high productivity during glacial while southern sites were more productive during interglacial period (Charles et al., 1991; Mortlock et al., 1991; Kumar et al., 1993; Kumar et al., 1995; Rosenthal et al., 1995; Anderson et al., 1998). Additionally, increased productivity has been attributed to increased input of iron from Patagonia (due to stronger winds) to the north APF during glacial periods (Kumar et al., 1995; Latimer and Filippelli, 2001), with glacial productivity being 10-20 times higher than productivity during interglacial times (Latimer and Filippelli, 2001).

Sedimentary U concentration studies in the Southern Ocean show a correlation of U with productivity proxies of Pa/Th particle flux (Kumar et al., 1993) and opal (Charles et al., 1991; Mortlock et al., 1991). Kumar et al (1995) showed a link between concentration of U in the sediments and the productivity, while Rosenthal et al. (1995) demonstrated that a bimodal relationship exists between locations north of and south of the APF for a U concentration over glacial and interglacial cycles. The bimodal

relationship has been related to productivity (Anderson et al., 1998). In addition, variability in U concentration aligned with changes in the Pa/Th particle flux proxy (Kumar et al., 1995). Frank et al. (2000) argued that sediment focusing could be important to explain the observed Southern Ocean U concentration peaks. They state that the slow sedimentation rate there cannot be enough organic carbon present to create a U peak. Studying sites with different depths in the Subantarctic, Chase et al. (2001) discovered similar elevated U concentration during glacial periods that suggested that sediment focusing is not causing the peak in U.

For this study, two sites were selected to compare based on their current proximity to the APF and documented changes in U concentration over glacial-interglacial cycles (Appendix 2-2). The northern site (high productivity during glacials) was RC 13-254, which was discussed in the main body of this thesis; while the southern site, ODP 1094, is included here in the Appendix. Chris Hayes (University of Southern Mississippi) previously worked on these samples and provided them to me. The project envisioned expanding on his previous work using $\delta^{234}U$ ($^{234}U/^{238}U$) (Hayes et al., 2014). The decision to discuss two distinctive narratives, without comparing the two sites, arose from complications within the ODP 1094 data set (not an analytical issue). I found some unexpected data trends, and together with Chris's $\delta^{234}U$ anomaly, I don't have a good explanation. The data, which focused on a narrow time range surrounding the glacial-interglacial transition at 130 kya (MIS 6a – MIS 5e), provided additional challenges that would likely need additional sedimentary examinations to understand the processes influencing that site. Therefore, the two sites are not being compared together.

References

Anderson, R.F., Kumar, N., Mortlock, R.A., Froelich, P.N., Kubik, P., Dittrich-Hannen, B., and Suter, M., 1998, Late-Quarternary changes in productivity of the Southern Ocean: Journal of Marine Systems, v. 17, p. 497-514, doi: 10.1016/S0924-7963(98)00060-8.

Anderson, R.F., Chase, Z., Fleisher, M.Q., and Sachs, J., 2002, The Southern Ocean's biological pump during the Last Glacial Maximum: Deep-Sea Research Part II-Topical Studies in Oceanography, v. 49, p. 1909-1938, Pii S0967-0645(02)00018-8, doi: 10.1016/S0967-0645(02)00018-8.

Charles, C.D., Froelich, P.N., Zibello, M.A., Mortlock, R.A., and Morley, J.J., 1991, Biogenic opal in Southern Ocean sediments over the last 450,000 years: Implications for surface water chemistry and circulation: Paleoceanography, v. 6, p. 697-728, doi: 10.1029/91PA02477.

Chase, Z., Anderson, R.F., and Fleisher, M.Q., 2001, Evidence from authigenic uranium for increased productivity of the glacial Subantarctic Ocean: Paleoceanography, v. 16, p. 468-478, doi 10.1029/2000pa000542.

Frank, M., Gersonde, R., van der Loeff, M.R., Bohrmann, G., Nürnberg, C.C., Kubik, P.W., Suter, M., and Mangini, A., 2000, Similar glacial and interglacial export bioproductivity in the Atlantic Sector of the Southern Ocean: Multiproxy evidence and implications for glacial atmospheric CO_2: Paleoceanography, v. 15, p. 642-658, doi: 10.1029/2000PA000497.

Hayes, C.T., Martínez-García, A., Hasenfratz, A.P., Jaccard, S.L., Hodell, D.A., Sigman, D.M., Haug, G.H., and Anderson, R.F., 2014, A stagnation event in the deep South Atlantic during the last interglacial period: Science, v. 346, p. 1514-1517, 10.1126/science.1256620.

Jaccard, S.L., Hayes, C.T., Martínez-García, A., Hodell, D.A., Anderson, R.F., Sigman, D.M., and Haug, G.H., 2013, Two Modes of Change in Southern Ocean Productivity Over the Past Million Years: Science, v. 339, p. 1419-1423, doi: 10.1126/science.1227545.

Kumar, N., Gwiazda, R., Anderson, R., and Froelich, P., 1993, $^{231}Pa/^{230}Th$ ratios in sediments as a proxy for past changes in Southern Ocean productivity: Nature, v. 362, p. 45-48, doi: 10.1038/362045a0.

Kumar, N., Anderson, R.F., Mortlock, R.A., Froelich, P.N., Kubik, P., Dittrichhannen, B., and Suter, M., 1995, Increased Biological Productivity and Export Production in the Glacial Southern-Ocean: Nature, v. 378, p. 675-680, doi: 10.1038/378675a0.

Latimer, J.C., and Filippelli, G.M., 2001, Terrigenous input and paleoproductivity in the Southern Ocean: Paleoceanography, v. 16, p. 627-643, doi: 10.1029/2000PA000586.

Mortlock, R.A., Charles, C.D., Froelich, P.N., Zibello, M.A., Saltzman, J., Hays, J.D., and Burckle, L.H., 1991, Evidence for lower productivity in the Antarctic Ocean during the last glaciation: Nature, v. 351, p. 220-223, doi: 10.1038/351220a0.

Rosenthal, Y., Boyle, E.A., Labeyrie, L., and Oppo, D., 1995, Glacial enrichments of authigenic Cd and U in Subantarctic sediments: A climatic control on the

elements' oceanic budget?: Paleoceanography, v. 10, p. 395-413, doi: 10.1029/95PA00310.

Appendix 2-2: Map of Southern Ocean sites

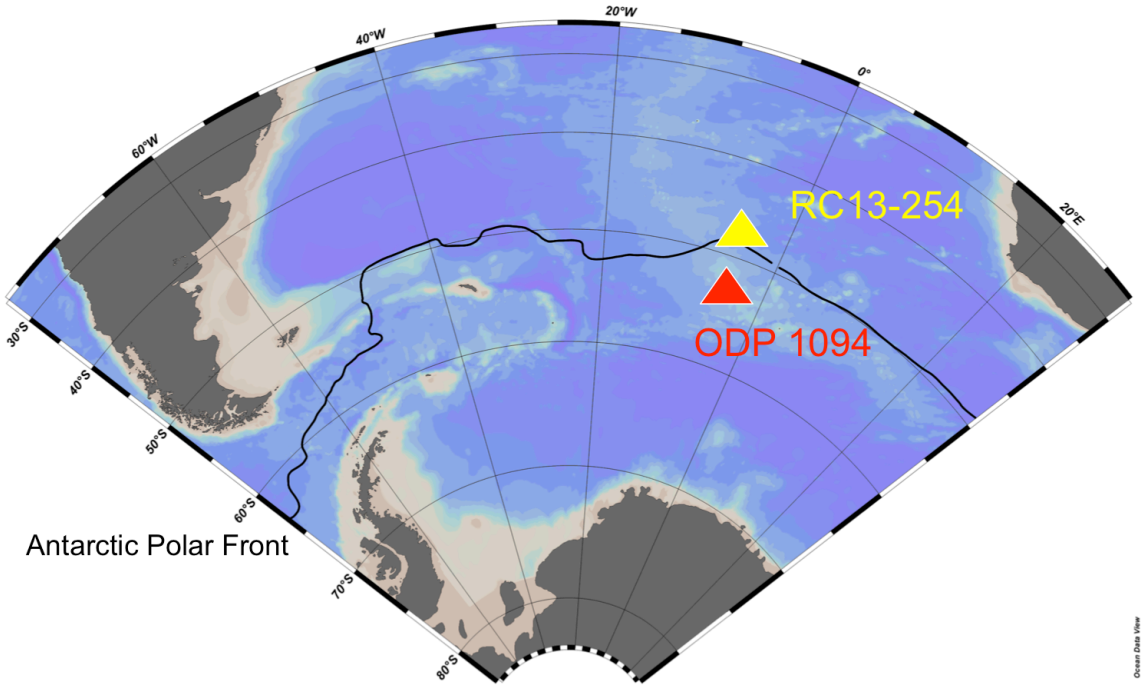

Appendix 2-3: Sample information for ODP 1094.

Exp	Site	Hole	Core	Section	Section Half	Top Interval (cm)	Bottom Interval (cm)	depth (m)	age (kyr)
177	1094	C	3	2	W	111	112	22.77	118.13
177	1094	C	3	2	W	141	142	23.07	119.38
177	1094	C	3	3	A	83	84	23.98	124.54
177	1094	C	3	3	A	103	104	24.18	125.49
177	1094	C	3	3	A	123	124	24.38	126.45
177	1094	C	3	3	A	143	144	24.58	127.71
177	1094	C	3	4	A	3	4	24.68	128.57
177	1094	C	3	4	A	5	6	24.71	128.74
177	1094	C	3	4	A	23	24	24.88	130.77
177	1094	C	3	4	A	35	36	25.01	131.81
177	1094	C	3	4	A	43	44	25.08	132.21
177	1094	C	3	4	A	63	64	25.29	133.03
177	1094	C	3	4	A	123	124	25.89	134.29
177	1094	C	3	5	A	33	34	26.49	135.67
177	1094	C	3	5	A	63	64	26.79	137.51
177	1094	C	3	5	A	93	94	27.09	139.34
177	1094	C	3	5	A	123	124	27.39	141.69

Appendix 2-4: ODP 1094 auxiliary data

depth (m)	age (kyr)#	Al (mg/g)	Ca (mg/g)	Cr (ng/g)	Mn (μg/g)	Fe (mg/g)	Mo (μg/g)	Ba (μg/g)	Th (μg/g)	U (μg/g)
22.77	118.13	2.25	2.50	3.81	52.20	5.22	2.07	574.01	0.22	0.80
23.07	119.38	2.11	2.81	2.83	65.88	4.53	2.47	614.31	0.22	0.79
23.99	124.54	3.57	8.12	3.44	102.13	5.53	1.30	418.36	0.34	0.94
24.19	125.49	1.33	16.74	0.76	167.60	1.89	1.35	420.80	0.23	1.75
24.39	126.45	1.20	23.55	0.23	287.37	1.61	2.07	140.00	0.27	2.59
24.59	127.71	1.36	28.62	0.54	379.34	1.77	1.84	711.29	0.26	2.71
24.69	128.57	1.45	25.09	0.53	285.96	0.99	1.24	480.14	0.29	2.39
24.71	128.74	1.58	27.76	2.27	264.09	1.04	3.94	825.82	0.33	2.43
24.89	130.77	1.49	17.51	0.86	156.43	1.19	0.92	554.84	0.25	1.76
25.01	131.81	1.36	8.83	3.43	61.34	2.15	4.74	425.32	0.25	1.20
25.09	132.21	1.26	3.93	0.96	58.67	2.58	0.68	237.52	0.17	0.98
25.29	133.66	1.46	3.43	2.51	49.72	2.27	0.97	392.31	0.22	0.93
25.89	134.29	1.46	3.96	2.46	65.60	2.63	1.15	383.33	0.17	0.95
26.49	135.67	9.15	7.52	6.89	226.17	18.14	2.33	635.07	0.78	1.74
26.79	137.51	34.18	21.59	13.87	827.78	62.51	2.30	747.07	1.69	2.09
27.09	139.34	27.02	13.69	15.22	803.62	47.19	1.86	758.47	1.97	2.18
27.39	141.69	33.01	16.47	16.43	771.19	58.13	3.28	814.62	2.25	2.11

Appendix 2-5: Authigenic uranium calculations at ODP 1094.

depth (m)	age (kyr)#	Al conc. (mg/g)	bulk U conc. (µg/g)	authigenic U conc. (µg/g)**	fraction authigenic U**
22.77	118.13	2.25	0.8	0.73	0.907
23.07	119.38	2.11	0.79	0.72	0.912
23.99	124.54	3.57	0.94	0.82	0.874
24.19	125.49	1.33	1.75	1.71	0.975
24.39	126.45	1.2	2.59	2.55	0.985
24.59	127.71	1.36	2.71	2.66	0.983
24.69	128.57	1.45	2.39	2.34	0.980
24.71	128.74	1.58	2.43	2.38	0.978
24.89	130.77	1.49	1.76	1.71	0.972
25.01	131.81	1.36	1.2	1.15	0.962
25.09	132.21	1.26	0.98	0.94	0.957
25.29	133.66	1.46	0.93	0.88	0.948
25.89	134.29	1.46	0.95	0.90	0.949
26.49	135.67	9.15	1.74	1.44	0.826
26.79	137.51	34.18	2.09	0.96	0.458
27.09	139.34	27.02	2.18	1.28	0.589
27.39	141.69	33.01	2.11	1.02	0.482

**Rudick & Gao (2003) detrital aluminum correction ratio applied.

Appendix 2-6: Uranium isotope data at ODP 1094.

depth (m)	age (kyr)#	bulk δ238U	2SD^	n	authigenic δ238U	authigenic 2SD
22.77	118.13	-0.35	0.09^	1	-0.36	
23.07	119.38	-0.2	0.09^	1	-0.19	
23.99	124.54	-0.29	0.05	2*	-0.29	0.05
24.19	125.49	-0.74	0.07	3*	-0.75	0.07
24.39	126.45	-0.93	0.03	4*	-0.94	0.03
24.59	127.71	-0.91	0.12	4*	-0.92	0.12
24.69	128.57	-0.68	0.02	3*	-0.69	0.02
24.71	128.74	-0.59	0.01	3*	-0.60	0.01
24.89	130.77	-0.32	0.08	3*	-0.32	0.08
25.01	131.81	-0.32	0.09^	1	-0.32	
25.09	132.21	-0.4	0.02	2*	-0.40	0.02
25.29	133.66	-0.04	0.09^	1	-0.03	
25.89	134.29	-0.06	0.15	2*	-0.05	0.16
26.49	135.67	-0.03	0.01	2*	0.03	0.02
26.79	137.51	0.08	0.09^	1	0.53	
27.09	139.34	0.37	0.09^	1	0.84	
27.39	141.69	0.25	0.09^	1	0.84	

^Based on replicate measurements with CRM129. Average -0.94; 2SD 0.09. n=6.
* replicates represent separate digestions.

Appendix 3: Proto-North Atlantic during Ocean Anoxic Event 2

Appendix 3-1: Overview of proto-North Atlantic during OAE 2

During the mid-Cretaceous (Trabucho Alexandre et al., 2010), temperatures were significantly higher than today. Paleotemperature records reveal that the temperatures exceeded 33°C at low-latitudes, and that Earth was at its warmest (Clarke and Jenkyns, 1999). The global warming then was driven by increased volcanic (Leckie et al., 2002; Brumsack, 2006) and/or methanogenic activity (Meyer and Kump, 2008; Jenkyns, 2010), which increased greenhouse gas concentrations in the atmosphere. These atmospheric changes directly influenced the hydrological cycle, rock weathering, upwelling, and biological productivity (Arthur and Sageman, 1994).

Within the mid-Cretaceous, Ocean Anoxic Event 2 (OAE 2) represented a period of a significant perturbation to the global carbon cycle. The OAE 2, also known as the Bonarelli event (Jenkyns, 2010), occurred at the boundary of the Cenomanian-Turonian at 93.5 Ma (Gradstein et al., 1995), and lasted for 0.5 Myr (Kuhnt et al., 1997). It is preserved in the paleo-record as organic rich sediments (Schlanger and Jenkyns, 1976; Arthur et al., 1987). During this event, deposits of laminated, organic-rich sediments occurred in many locations around the proto-North Atlantic as well as in the closing Tethys Sea (Schlanger and Jenkyns, 1976; Arthur et al., 1988). In addition to high organic-carbon content, a positive δ^{13}C excursion indicates that a significant perturbation to the carbon cycle occurred during the event that allowed for greater burial of organic carbon (Arthur et al., 1987; Arthur et al., 1988; Leckie et al., 2002; Erbacher et al., 2005; Mort et al., 2007). Changes in the carbon cycle were related to changes in the nutrient cycling, including increased recycling of phosphorus due to expansions of reducing

conditions (Mort et al., 2007; Trabucho Alexandre et al., 2010). Other environmental factors that could have impacted carbon cycling include: elevated global sea level (Schlanger and Jenkyns, 1976; Arthur et al., 1987; Arthur et al., 1988; Kuhnt et al., 1997; Leckie et al., 2002), absence of oxygen in the photic zone (Pancost et al., 2004), disruptions to the hydrological cycle and circulation (Schlanger and Jenkyns, 1976; Sarmiento et al., 1988; Leckie et al., 2002; van Helmond et al., 2014), and Milankovitch orbital cycles (Kuhnt et al., 1997; Kuypers et al., 2005).

Previous paleo-reconstructions of the OAE 2 in the proto-North Atlantic suggest that there were regional differences in both productivity and redox conditions. Initial work on the OAE 2 showed that anoxic conditions were widespread in the proto-North Atlantic (Schlanger and Jenkyns, 1976; Pancost et al., 2004). With the advances in analytical techniques, including isotope analysis, variations between different parts of the basins emerged. Paleo-reconstructions show regional differences in surface productivity and local redox conditions (Tissot et al., 1980; Summerhayes, 1981; Trabucho Alexandre et al., 2010). The Southern proto-North Atlantic was marked by strong upwelling and therefore sustained nutrient supply, resulting in high primary production and carbon burial (Trabucho Alexandre et al., 2010). In the Northern proto-North Atlantic, in contrast, the regional hydrography was unlikely to generate upwelling, and surface productivity was expected to be lower (Trabucho Alexandre et al., 2010), with occasional periods of high productivity (Kuypers et al., 2004). Also, Owens et al. (2012) showed that both margins experienced at least periodic anoxia. Thus in the OAE 2, the proto-North Atlantic had regional differences in redox conditions and productivity (Trabucho

Alexandre et al., 2010), which makes it ideal region to compare different burial rates and redox conditions.

In a study at Demerara Rise, Montoya-Pino et al. (2010) applied $\delta^{238}U$ to quantify the extent of anoxia during OAE 2. Located off the coast of Suriname, Demerara Rise contains sediments from the southern proto-North Atlantic. Observed changes of $\delta^{238}U$ in sediments before, during, and after the OAE 2 were interpreted to correspond to global increases in anoxia (Montoya-Pino et al., 2010). This interpretation utilized the observed fractionation in modern-type euxinia in the Black Sea and Peru Margin and applied it to calculate the areal extent of euxinia during OAE 2 using an isotope mass balance. By developing a model on a very preliminary survey of modern sediments, Montoya-Pino et al (2010) did not consider the full breadth of modern-like sedimentary isotope signatures. The study predicted that the areal coverage of anoxic conditions spanned 40% of the proto-North Atlantic, compared to another study using sulfur isotopes suggest the extent of anoxia did not exceed 5% (Owens et al., 2013). One key issue with the Montoya-Pino et al (2010) analysis involved a misclassified point as "before" the OAE 2 instead of "during". In Erbacher et al. (2005), high resolution $\delta^{13}C$ record showed that the onset of OAE 2 at 638.04m, while Montoya-Pino et al (2010) classified a data point at 635.83 as being before the onset. When statistical tests are conducted on the data with the correct classification of the point, there is no statistical difference between "during" and those "before or after" (p-value = 0.14). Therefore, more sites are needed to understand the applicability of $\delta^{238}U$ based reconstructions to studying processes millions of years ago.

References

Arthur, M.A., Dean, W.E., and Pratt, L.M., 1988, Geochemical and climatic effects of increased marine organic carbon burial at the Cenomanian/Turonian boundary: Nature, v. 335, p. 714-717.

Arthur, M.A., and Sageman, B.B., 1994, Marine Black Shales - Depositional Mechanisms and Environments of Ancient-Deposits: Annual Review of Earth and Planetary Sciences, v. 22, p. 499-551, doi: 10.1146/annurev.ea.22.050194.002435.

Arthur, M.A., Schlanger, S.O., and Jenkyns, H.C., 1987, The Cenomanian-Turonian Oceanic Anoxic Event, II. Palaeoceanographic controls on organic-matter production and preservation: Geological Society, London, Special Publications, v. 26, p. 401-420, doi: 10.1144/gsl.sp.1987.026.01.25.

Brumsack, H.J., 2006, The trace metal content of recent organic carbon-rich sediments: Implications for Cretaceous black shale formation: Palaeogeography Palaeoclimatology Palaeoecology, v. 232, p. 344-361, doi: 10.1016/j.palaeo.2005.05.011.

Clarke, L.J., and Jenkyns, H.C., 1999, New oxygen isotope evidence for long-term Cretaceous climatic change in the Southern Hemisphere: Geology, v. 27, p. 699-702, doi: 10.1130/0091-7613(1999)027<0699:NOIEFL>2.3.CO;2.

Erbacher, J., Friedrich, O., Wilson, P.A., Birch, H., and Mutterlose, J., 2005, Stable organic carbon isotope stratigraphy across Oceanic Anoxic Event 2 of Demerara Rise, western tropical Atlantic: Geochemistry, Geophysics, Geosystems, v. 6, doi: 10.1029/2004GC000850.

Gradstein, F.M., Agterberg, F.P., Ogg, J.G., Hardenbol, J., Van Veen, P., Thierry, J., and Huang, Z., 1995, A Triassic, Jurassic and Cretaceous time scale.

Jenkyns, H.C., 2010, Geochemistry of oceanic anoxic events: Geochemistry Geophysics Geosystems, v. 11, Artn Q03004, doi 10.1029/2009gc002788.

Kuhnt, W., Nederbragt, A., and Leine, L., 1997, Cyclicity of Cenomanian-Turonian organic-carbon-rich sediments in the Tarfaya Atlantic coastal basin (Morocco): Cretaceous Research, v. 18, p. 587-601,.

Kuypers, M.M., Lavik, G., Woebken, D., Schmid, M., Fuchs, B.M., Amann, R., Jorgensen, B.B., and Jetten, M.S., 2005, Massive nitrogen loss from the Benguela upwelling system through anaerobic ammonium oxidation: Proc Natl Acad Sci U S A, v. 102, p. 6478-6483, doi: 10.1073/pnas.0502088102.

Kuypers, M.M.M., Lourens, L.J., Rijpstra, W.I.C., Pancost, R.D., Nijenhuis, I.A., and Sinninghe Damsté, J.S., 2004, Orbital forcing of organic carbon burial in the proto-North Atlantic during oceanic anoxic event 2: Earth and Planetary Science Letters, v. 228, p. 465-482, doi: 10.1016/j.epsl.2004.09.037.

Leckie, R.M., Bralower, T.J., and Cashman, R., 2002, Oceanic anoxic events and plankton evolution: Biotic response to tectonic forcing during the mid-Cretaceous: Paleoceanography, v. 17.

Meyer, K.M., and Kump, L.R., 2008, Oceanic euxinia in Earth history: Causes and consequences: Annual Review of Earth and Planetary Sciences, v. 36, p. 251-288, doi: 10.1146/annurev.earth.36.031207.124256.

Montoya-Pino, C., Weyer, S., Anbar, A.D., Pross, J., Oschmann, W., van de Schootbrugge, B., and Arz, H.W., 2010, Global enhancement of ocean anoxia during Oceanic Anoxic Event 2: A quantitative approach using U isotopes: Geology, v. 38, p. 315-318, doi: 10.1130/G30652.1.

Mort, H.P., Adatte, T., Föllmi, K.B., Keller, G., Steinmann, P., Matera, V., Berner, Z., and Stüben, D., 2007, Phosphorus and the roles of productivity and nutrient recycling during oceanic anoxic event 2: Geology, v. 35, p. 483-486.

Owens, J.D., Gill, B.C., Jenkyns, H.C., Bates, S.M., Severmann, S., Kuypers, M.M., Woodfine, R.G., and Lyons, T.W., 2013, Sulfur isotopes track the global extent and dynamics of euxinia during Cretaceous Oceanic Anoxic Event 2: Proceedings of the National Academy of Sciences, v. 110, p. 18407-18412.

Owens, J.D., Lyons, T.W., Li, X.N., Macleod, K.G., Gordon, G., Kuypers, M.M.M., Anbar, A., Kuhnt, W., and Severmann, S., 2012, Iron isotope and trace metal records of iron cycling in the proto-North Atlantic during the Cenomanian-Turonian oceanic anoxic event (OAE-2): Paleoceanography, v. 27, Artn Pa3223, doi: 10.1029/2012pa002328.

Pancost, R.D., Crawford, N., Magness, S., Turner, A., Jenkyns, H.C., and Maxwell, J.R., 2004, Further evidence for the development of photic-zone euxinic conditions during Mesozoic oceanic anoxic events: Journal of the Geological Society, v. 161, p. 353-364, 10.1144/0016764903-059.

Sarmiento, J.L., Herbert, T.D., and Toggweiler, J., 1988, Causes of anoxia in the world ocean: Global Biogeochemical Cycles, v. 2, p. 115-128.

Schlanger, S., and Jenkyns, H., 1976, Cretaceous oceanic anoxic events: causes and consequences: Geologie en Mijnbouw, v. 55, p. 179-184.

Summerhayes, C.P., 1981, Organic facies of middle Cretaceous black shales in deep North Atlantic: AAPG Bulletin, v. 65, p. 2364-2380.

Tissot, B., Demaison, G., Masson, P., Delteil, J., and Combaz, A., 1980, Paleoenvironment and petroleum potential of middle Cretaceous black shales in Atlantic basins: AAPG Bulletin, v. 64, p. 2051-2063.

Trabucho Alexandre, J., Tuenter, E., Henstra, G.A., van der Zwan, K.J., van de Wal, R.S., Dijkstra, H.A., and de Boer, P.L., 2010, The mid-Cretaceous North Atlantic nutrient trap: Black shales and OAEs: Paleoceanography, v. 25.

van Helmond, N.A., Sluijs, A., Reichart, G.-J., Damsté, J.S.S., Slomp, C.P., and Brinkhuis, H., 2014, A perturbed hydrological cycle during Oceanic Anoxic Event 2: Geology, v. 42, p. 123-126.

Appendix 3-2: Map of proto-North Atlantic sites during OAE 2

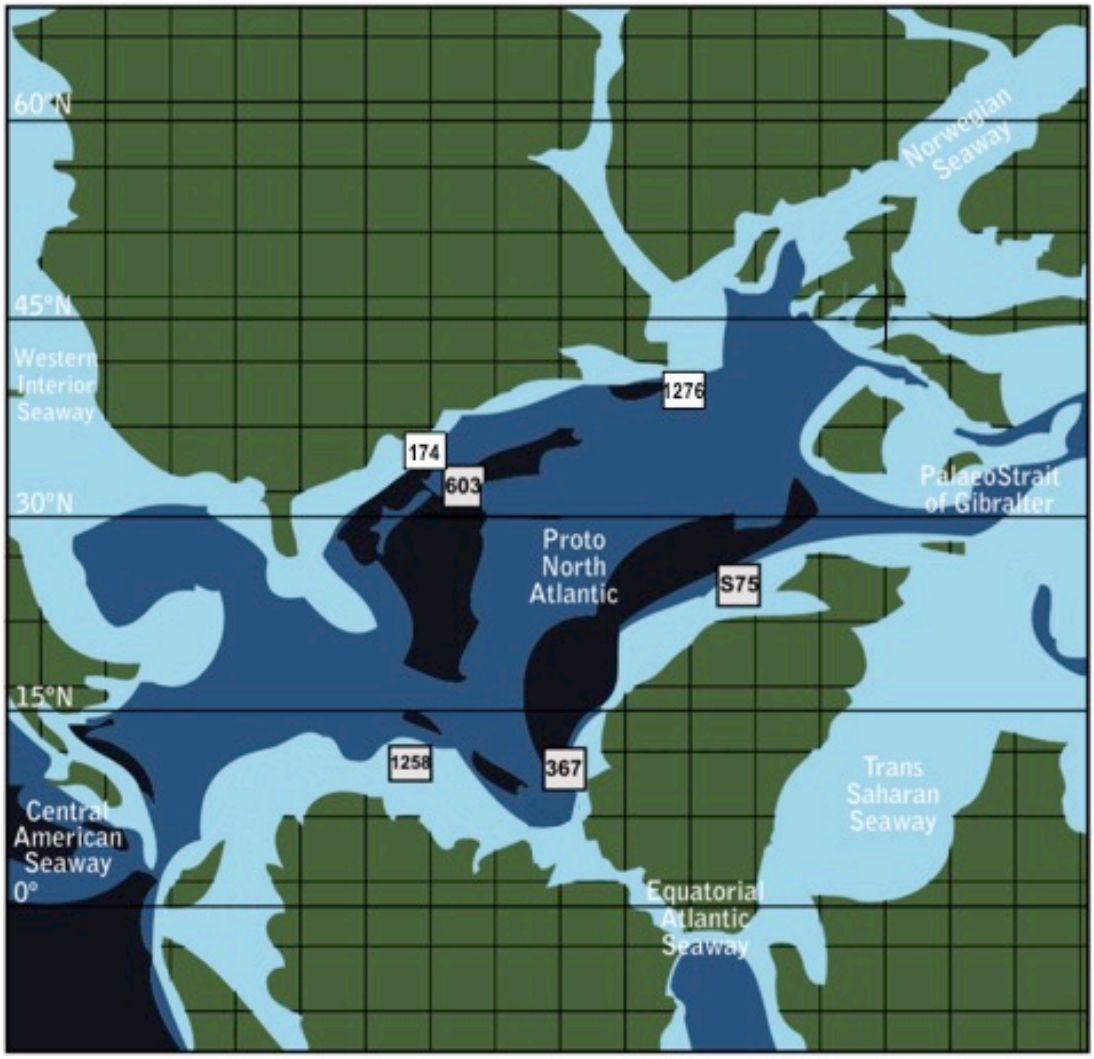

Appendix 3-3: ODP 174AX (Bass River)

Appendix 3-3-1: Sample information for OAE 2 samples ODP 174AX (Bass River)

Exp	Site	Section Half	Top Interval (ft)	Bottom Interval (ft)	depth (ft)	OAE 2?
174AX	BassRiver	W	1868.7	1868.75	1868.7	post
174AX	BassRiver	W	1879.25	1879.3	1879.25	post
174AX	BassRiver	W	1890.65	1890.7	1890.65	post
174AX	BassRiver	W	1900.15	1900.2	1900.15	post
174AX	BassRiver	W	1907.6	1907.65	1907.6	during
174AX	BassRiver	W	1912.1	1912.15	1912.1	during
174AX	BassRiver	W	1917.05	1917.1	1917.05	during
174AX	BassRiver	W	1918.6	1918.65	1918.6	during
174AX	BassRiver	W	1921.6	1921.65	1921.6	during
174AX	BassRiver	W	1925.9	1925.95	1925.9	during
174AX	BassRiver	W	1930.45	1930.5	1930.45	during
174AX	BassRiver	W	1934.1	1934.15	1934.1	during
174AX	BassRiver	W	1938	1938.05	1938	during
174AX	BassRiver	W	1939.4	1939.45	1939.4	during
174AX	BassRiver	W	1939.8	1939.85	1939.8	during
174AX	BassRiver	W	1940.3	1940.35	1940.3	during
174AX	BassRiver	W	1940.65	1940.7	1940.65	during
174AX	BassRiver	W	1942	1942.05	1942	during
174AX	BassRiver	W	1943.95	1944	1943.95	during
174AX	BassRiver	W	1946	1946.05	1946	during
174AX	BassRiver	W	1947.95	1948	1947.95	pre
174AX	BassRiver	W	1949.9	1949.95	1949.9	pre
174AX	BassRiver	W	1952.45	1952.5	1952.45	pre

Appendix 3-3-2: ODP 174AX (Bass River) auxiliary data

depth (ft)	Mg (mg/g)	Al (mg/g)	Ca (mg/g)	Ti (mg/g)	V (μg/g)	Cr (μg/g)	Mn (mg/g)	Fe (mg/g)	Co (μg/g)	U (μg/g)
1868.7	8.63	85.69	16.04	3.13	102.81	80.09	0.28	41.14	19.62	2.46
1879.25	8.92	84.28	19.60	3.21	97.75	75.89	0.29	41.33	14.41	2.16
1890.65	8.44	80.17	15.95	3.47	105.54	85.41	0.30	42.40	15.04	2.12
1900.15	8.27	78.72	31.07	3.26	93.92	76.10	0.26	37.03	12.68	2.18
1907.6	8.68	81.94	31.14	3.51	88.81	81.50	0.21	36.18	11.97	2.11
1912.1	9.15	84.39	24.61	3.28	79.88	73.66	0.21	37.91	11.99	2.11
1917.05	8.82	78.67	31.55	3.23	80.44	74.16	0.21	37.80	12.32	2.06
1918.6	8.26	65.34	58.03	3.32	67.36	69.83	0.19	39.21	9.72	1.73
1921.6	8.83	78.08	44.89	2.93	70.44	70.00	0.19	35.11	10.26	1.55
1925.9	8.31	74.11	60.70	3.26	68.19	71.59	0.20	33.86	9.63	2.23
1930.45	7.93	83.04	41.20	3.89	78.96	87.07	0.20	31.74	10.37	2.80
1934.1	8.18	84.12	39.63	4.02	80.35	86.60	0.21	40.81	12.03	2.53
1938	6.31	55.32	102.13	3.10	57.81	61.57	0.29	30.31	8.47	1.59
1939.4	6.47	57.14	82.16	3.53	59.28	61.71	0.25	31.62	9.29	1.84
1939.8	7.42	72.17	33.71	4.57	72.30	70.65	0.29	36.30	11.28	2.33
1940.3	9.10	73.79	23.96	3.07	73.72	67.18	0.36	46.30	12.70	1.79
1940.65	9.61	88.92	22.67	3.81	89.54	82.48	0.35	55.02	14.08	2.08
1942	8.06	84.63	26.60	3.70	87.09	79.74	0.29	37.45	13.36	2.15
1943.95	8.11	94.48	23.34	4.00	90.52	86.13	0.27	46.02	14.60	2.52
1946	7.06	86.31	31.85	3.45	113.49	82.79	0.22	38.33	13.45	2.19
1947.95	6.62	83.57	28.72	3.69	89.36	77.16	0.20	34.28	10.44	2.31
1949.9	7.11	88.14	45.49	3.88	91.74	78.51	0.21	39.06	11.92	2.27
1952.45	6.75	83.01	29.04	3.52	94.49	78.84	0.24	41.06	11.77	2.60

Appendix 3-3-2 cont.: ODP 174AX (Bass River) auxiliary data

depth (ft)	Ni (μg/g)	Cu (μg/g)	Sr (μg/g)	Mo (μg/g)	Cd (μg/g)	Ba (μg/g)	Ce (μg/g)	Nd (μg/g)	Th (μg/g)	U (μg/g)
1868.7	40.12	21.02	238.76	0.87	0.06	494.71	93.51	38.98	12.97	2.46
1879.25	38.91	20.33	264.06	0.67	0.07	493.10	84.79	36.60	12.25	2.16
1890.65	41.94	20.93	249.08	0.59	0.07	489.87	65.89	28.74	9.96	2.12
1900.15	36.84	17.80	331.70	0.55	0.07	411.81	77.84	33.32	11.89	2.18
1907.6	40.30	17.63	324.41	0.62	0.07	442.03	81.76	34.25	12.25	2.11
1912.1	38.60	18.31	299.58	0.49	0.07	438.29	77.64	31.73	12.34	2.11
1917.05	37.78	18.67	359.92	0.43	0.06	409.52	70.82	28.30	10.86	2.06
1918.6	32.31	16.19	535.49	0.80	0.04	312.24	61.53	24.27	10.49	1.73
1921.6	35.26	16.55	449.76	0.55	0.06	329.17	69.86	27.56	11.44	1.55
1925.9	34.02	15.35	761.19	0.53	0.05	296.83	73.97	29.32	12.36	2.23
1930.45	38.72	16.43	389.15	0.83	0.06	399.24	80.46	32.52	13.74	2.80
1934.1	42.80	21.02	504.28	0.89	0.05	391.88	83.76	33.39	13.88	2.53
1938	25.01	12.68	651.10	0.53	0.05	243.57	55.69	22.08	9.16	1.59
1939.4	26.41	12.94	965.06	0.56	0.07	249.83	80.21	31.12	11.46	1.84
1939.8	31.72	14.67	404.00	0.53	0.07	412.41	83.26	34.71	13.85	2.33
1940.3	34.71	14.17	252.22	0.54	0.05	415.56	71.31	31.22	10.65	1.79
1940.65	42.10	22.46	320.09	0.73	0.06	408.66	81.21	35.02	12.78	2.08
1942	39.62	20.07	392.42	0.40	0.05	453.98	81.61	35.50	12.94	2.15
1943.95	46.88	23.10	317.54	0.56	0.07	428.65	81.77	36.03	13.56	2.52
1946	46.68	19.28	316.78	0.33	0.07	398.23	84.70	35.77	13.00	2.19
1947.95	40.51	19.24	286.84	0.35	0.09	390.64	81.96	34.11	13.63	2.31
1949.9	44.85	20.74	404.32	0.28	0.07	359.11	85.60	35.19	13.79	2.27
1952.45	43.60	19.53	280.53	0.32	0.06	394.28	82.76	35.17	13.07	2.60

Appendix 3-3-3: Uranium isotope data at ODP 174AX (Bass River).

depth (ft)	OAE 2?	bulk δ238U	2SD^	2SE^	n
1868.7	post	-0.27	0.17	0.08	4
1879.25	post	-0.23	0.10	0.07	2
1890.65	post	-0.42	0.08	0.05	2
1900.15	post	-0.56	0.12^	0.12^	1
1907.6	during	-0.51	0.05	0.03	2
1912.1	during	-0.24	0.25	0.14	3
1917.05	during	-0.32	0.38	0.22	3
1918.6	during	-0.33	0.07	0.05	2
1921.6	during	-0.43	0.02	0.02	2
1925.9	during	-0.52	0.07	0.05	2
1930.45	during	-0.54	0.01	0.01	2
1934.1	during	-0.40	0.12^	0.12^	1
1938	during	-0.39	0.13	0.08	3
1939.4	during	-0.10	0.07	0.04	4*
1939.8	during	-0.35	0.14	0.08	3
1940.3	during	-0.29	0.19	0.11	3
1940.65	during	-0.11	0.12^	0.12^	1
1942	during	-0.38	0.21	0.15	2
1943.95	during	-0.28	0.07	0.05	2
1946	during	-0.40	0.05	0.03	3*
1947.95	pre	-0.27	0.12^	0.12^	1
1949.9	pre	-0.32	0.12^	0.12^	1
1952.45	pre	-0.26	0.08	0.06	2

^Based on an average of the standard deviations of the other samples at this site.
* replicates represent separate digestions.

Appendix 3-4: DSDP 603B (Continental Rise)

Appendix 3-4-1: Sample information for OAE 2 samples DSDP 603B (Continental Rise)

Exp	Site	Hole	Core	Section	Top Interval (cm)	Bottom Interval (cm)	depth (m)	OAE 2?
93	603	B	33	1	46	48	1118.96	post?
93	603	B	33	1	136	138	1119.86	post?
93	603	B	33	3	21	23	1121.71	post?
93	603	B	33	3	98	100	1122.48	post?
93	603	B	34	1	42	43	1127.92	during
93	603	B	34	1	105	106	1128.55	during
93	603	B	34	2	67	68.5	1129.67	during
93	603	B	34	2	121	122	1130.21	during
93	603	B	34	3	51	52	1131.01	during
93	603	B	34	3	147	148	1131.97	during
93	603	B	34	4	67	68	1132.67	during
93	603	B	34	4	127	128	1133.27	during
93	603	B	34	6	3	4	1135.03	pre
93	603	B	35	1	72	73	1137.22	pre

Appendix 3-4-2: DSDP 603B (Continental Rise) auxiliary data

depth (m)	Mg (mg/g)	Al (mg/g)	Ca (mg/g)	Ti (mg/g)	V (µg/g)	Cr (µg/g)	Mn (mg/g)	Fe (mg/g)	Co (µg/g)	U (µg/g)
1118.96	5.54	78.96	2.27	3.79	161.21	84.43	2.85	74.75	22.46	0.85
1119.86	11.11	81.65	7.15	3.40	188.01	71.60	14.15	35.72	14.81	2.27
1121.71	9.75	65.30	3.98	2.40	76.80	58.16	0.32	46.58	6.59	0.70
1122.48	8.40	60.58	5.47	2.46	70.05	50.84	0.24	28.09	6.02	1.11
1127.92	5.54	46.56	5.42	2.00	1017.34	97.18	0.09	46.70	10.96	8.04
1128.55	6.66	49.91	4.29	2.12	719.12	83.58	0.13	34.05	18.88	4.96
1129.67	5.16	42.02	3.78	1.78	803.26	109.77	0.07	42.07	10.31	4.85
1130.21	4.88	42.30	4.16	1.68	506.05	71.99	0.07	26.66	12.80	5.82
1131.01	4.76	35.77	3.50	1.74	309.05	54.93	0.35	40.79	17.06	7.28
1131.97	4.94	43.01	5.23	2.02	239.99	54.47	0.15	47.40	24.02	10.42
1132.67	5.39	45.16	3.60	2.18	729.81	92.22	0.10	33.59	18.57	8.69
1133.27	3.94	34.87	4.45	1.54	527.75	66.82	0.02	35.20	12.17	11.84
1135.03	10.89	79.54	7.03	3.34	91.88	74.83	0.25	36.78	18.20	1.27
1137.22	13.69	97.30	1.53	4.22	260.22	104.05	0.28	35.02	16.21	3.30

Appendix 3-4-2 cont.: DSDP 603B (Continental Rise) auxiliary data

depth (m)	Ni (µg/g)	Cu (µg/g)	Sr (µg/g)	Mo (µg/g)	Cd (µg/g)	Ba (µg/g)	Ce (µg/g)	Nd (µg/g)	Th (µg/g)	U (µg/g)
1118.96	72.44	43.21	123.72	3.94	0.12	326.13	16.99	9.42	3.84	0.85
1119.86	49.68	142.39	451.10	1.73	0.00	1184.25	66.96	24.43	8.40	2.27
1121.71	26.42	18.69	237.13	0.50	-0.01	492.73	43.72	20.11	5.86	0.70
1122.48	20.49	53.39	382.55	0.56	-0.02	1080.03	48.96	20.29	6.07	1.11
1127.92	263.79	103.15	375.20	47.71	2.03	1036.49	33.55	16.09	4.97	8.04
1128.55	322.65	136.05	363.66	22.77	2.54	1095.71	25.89	14.73	5.45	4.96
1129.67	172.90	174.57	299.94	17.36	2.21	912.01	25.84	12.95	5.66	4.85
1130.21	188.99	98.61	367.35	14.74	4.70	1054.93	27.21	14.40	3.52	5.82
1131.01	150.98	83.68	277.91	12.51	0.57	819.48	23.68	13.43	3.53	7.28
1131.97	209.97	71.24	371.79	12.63	1.15	1128.28	50.78	25.03	4.51	10.42
1132.67	287.86	127.19	343.76	37.79	15.64	1128.84	37.79	19.50	5.12	8.69
1133.27	319.43	86.38	322.57	24.80	1.55	979.32	45.04	25.26	4.02	11.84
1135.03	60.51	99.05	505.82	0.90	0.00	834.41	68.36	27.68	8.53	1.27
1137.22	87.93	43.91	100.47	3.78	0.96	300.28	67.68	27.99	8.85	3.30

Appendix 3-4-3: Uranium isotope data at DSDP 603B (Continental Rise).

depth (m)	OAE 2?	bulk δ238U	2SD^	2SE^	n
1118.96	post?	-0.46	0.03	0.02	3
1119.86	post?	-0.20	0.15	0.09	3
1121.71	post?	-0.57	0.23	0.13	3
1122.48	post?	-0.56	0.21	0.12	3
1127.92	during	0.23	0.18	0.10	3
1128.55	during	0.39	0.18	0.10	3
1129.67	during	0.02	0.01	0.01	2
1130.21	during	0.19	0.14	0.10	2
1131.01	during	0.09	0.11	0.06	3
1131.97	during	0.24	0.14^	0.14^	1
1132.67	during	0.23	0.09	0.07	2
1133.27	during	0.18	0.14	0.07	4
1135.03	pre	-0.68	0.08	0.06	2
1137.22	pre	0.03	0.29	0.17	3

^Based on an average of the standard deviations of the other samples at this site.

Appendix 3-5: ODP 1276 (Newfoundland)

Appendix 3-5-1: Sample information for OAE 2 samples ODP 1276 (Newfoundland)

Exp	Site	Hole	Core	Section	Section Half	Top Interval (cm)	Bottom Interval (cm)	depth (m)	ID #	OAE 2?
210	1276	A	30	4	W	111	112	1074.74	5039193	post
210	1276	A	30	5	W	64	65	1075.77	5039194	post
210	1276	A	31	1	W	41	42	1079.41	5039195	post
210	1276	A	31	1	W	108	109	1080.08	5039197	post
210	1276	A	31	2	W	28	29	1080.78	5039200	during
210	1276	A	31	2	W	66	67	1081.16	5039201	during
210	1276	A	31	2	W	116	117	1081.66	5039202	during
210	1276	A	31	3	W	3	4	1081.98	5039203	during
210	1276	A	31	3	W	32	33	1082.27	5039204	during
210	1276	A	31	3	W	50	51	1082.45	5039205	during
210	1276	A	31	3	W	67	68	1082.63	5039207	during
210	1276	A	31	3	W	80	81	1082.75	5039208	during
210	1276	A	31	3	W	94	95	1082.89	5039209	during
210	1276	A	31	3	W	139	140	1083.34	5039210	during
210	1276	A	31	4	W	48	49	1083.87	5039217	during
210	1276	A	31	4	W	87	88	1084.26	5039218	during
210	1276	A	31	5	W	4	5	1084.93	5039219	pre
210	1276	A	31	6	W	4	5	1085.97	5039220	pre
210	1276	A	31	6	W	76	77	1086.69	5039221	pre

Appendix 3-5-2: ODP 1276 (Newfoundland) auxiliary data

depth (m)	Mg (mg/g)	Al (mg/g)	Ca (mg/g)	Ti (mg/g)	V (µg/g)	Cr (µg/g)	Mn (mg/g)	Fe (mg/g)	Co (µg/g)	U (µg/g)
1074.74	9.89	63.19	37.00	4.40	115.14	77.56	0.27	28.47	15.03	2.02
1075.77	7.23	48.97	13.60	4.32	155.89	59.87	0.21	22.43	13.36	2.88
1079.41	8.87	53.99	48.26	3.65	102.55	63.99	0.61	27.27	11.03	1.39
1080.08	10.12	61.91	33.66	3.19	90.41	61.26	0.42	42.84	36.05	0.83
1080.78	9.51	56.47	3.34	3.42	209.78	65.81	0.10	27.73	5.82	2.18
1081.16	6.03	40.10	1.91	2.11	251.47	56.38	0.11	53.69	18.42	4.05
1081.66	9.35	58.84	4.09	3.48	519.81	146.19	0.13	23.84	3.88	3.51
1081.98	8.03	47.52	2.11	3.73	229.82	68.66	0.22	28.56	11.43	2.24
1082.27	7.65	47.33	1.58	3.39	92.29	67.90	0.38	42.09	13.07	3.20
1082.45	7.74	47.21	1.96	3.44	144.58	71.69	0.39	43.17	15.03	3.15
1082.63	8.25	45.78	2.42	3.06	200.91	77.10	0.28	51.49	24.86	2.46
1082.75	9.56	51.98	2.38	3.73	105.59	75.69	0.38	40.73	20.53	1.61
1082.89	9.38	52.29	2.03	3.47	148.27	108.20	0.33	44.22	25.07	1.91
1083.34	6.21	39.75	2.62	3.84	64.84	49.93	0.09	20.24	4.00	1.05
1083.87	9.00	54.76	2.77	3.53	482.41	90.28	0.12	32.48	20.80	3.07
1084.26	11.79	70.63	5.08	4.56	199.95	91.85	0.14	33.33	11.03	2.43
1084.93	8.10	49.67	64.55	3.56	93.96	59.51	2.05	26.64	10.37	1.88
1085.97	8.43	49.62	60.14	3.48	87.00	59.31	1.45	24.32	10.77	1.65
1086.69	10.00	58.68	3.82	3.43	97.51	60.22	0.11	31.31	9.10	0.99

Appendix 3-5-2 cont.: ODP 1276 (Newfoundland) auxiliary data

depth (m)	Ni (µg/g)	Cu (µg/g)	Sr (µg/g)	Mo (µg/g)	Cd (µg/g)	Ba (µg/g)	Ce (µg/g)	Nd (µg/g)	Th (µg/g)	U (µg/g)
1074.74	46.12	55.13	361.39	1.08	0.12	583.94	47.77	20.60	7.92	2.02
1075.77	47.83	46.54	186.82	3.54	0.39	505.30	51.96	24.72	7.82	2.88
1079.41	23.46	53.83	385.63	0.79	0.10	872.23	43.76	19.71	7.27	1.39
1080.08	153.91	24.74	285.08	0.56	0.07	437.68	37.87	18.77	7.25	0.83
1080.78	28.64	110.92	177.55	0.60	0.24	408.28	25.85	14.45	5.96	2.18
1081.16	271.01	78.73	113.97	22.78	0.67	241.97	43.90	23.71	6.06	4.05
1081.66	20.42	250.55	199.43	0.93	0.26	399.91	22.84	14.65	5.12	3.51
1081.98	41.36	42.03	140.20	0.97	0.56	319.08	13.92	8.48	4.33	2.24
1082.27	28.20	51.87	125.99	1.97	0.09	275.31	15.95	9.09	3.97	3.20
1082.45	48.93	61.77	125.16	2.03	0.20	272.01	18.40	10.35	4.31	3.15
1082.63	67.76	63.11	161.52	2.08	0.34	241.38	25.94	14.34	4.03	2.46
1082.75	55.80	60.74	154.10	0.69	0.21	276.21	43.74	20.17	6.04	1.61
1082.89	67.88	69.91	173.16	1.10	0.24	268.98	27.56	14.29	4.83	1.91
1083.34	13.33	13.93	125.90	0.36	0.05	240.84	51.44	21.76	6.12	1.05
1083.87	66.10	94.67	152.48	2.09	0.75	315.94	28.93	17.57	4.44	3.07
1084.26	43.06	52.52	235.09	1.27	0.34	407.10	33.19	17.50	8.41	2.43
1084.93	31.95	36.63	423.15	0.63	0.11	305.71	43.15	19.41	7.01	1.88
1085.97	34.60	33.01	423.46	0.47	0.09	300.72	43.67	19.80	6.64	1.65
1086.69	31.99	33.41	181.50	0.28	0.05	345.93	45.51	21.23	7.40	0.99

Appendix 3-5-3: Uranium isotope data at ODP 1276 (Newfoundland).

depth (m)	OAE 2?	bulk δ238U	2SD^	2SE^	n
1074.74	post	-0.41	0.10	0.07	2
1075.77	post	-0.48	0.27	0.12	5
1079.41	post	-0.44	0.14^	0.14^	1
1080.08	post	-0.21	0.14^	0.14^	1
1080.78	during	-0.02	0.16	0.09	3
1081.16	during	0.16	0.27	0.15	3
1081.66	during	0.13	0.03	0.02	2
1081.98	during	-0.34	0.05	0.03	2
1082.27	during	-0.12	0.05	0.03	2
1082.45	during	-0.22	0.04	0.02	3
1082.63	during	-0.28	0.14^	0.14^	1
1082.75	during	-0.39	0.28	0.14	4
1082.89	during	-0.50	0.17	0.10	3
1083.34	during	-0.38	0.21	0.10	4
1083.87	during	0.04	0.16	0.09	3
1084.26	during	-0.16	0.07	0.03	4
1084.93	pre	-0.28	0.20	0.10	4
1085.97	pre	-0.29	0.12	0.07	3
1086.69	pre	-0.38	0.14^	0.14^	1

^Based on an average of the standard deviations of the other samples at this site.

Appendix 3-6: Shell S75 (Tarfaya)

Appendix 3-6-1: Sample information for OAE 2 samples S75 (Tarfaya)

Exp	Site	depth (m)	ID #	OAE 2?
Shell	S75	50.41	S 75 34	post
Shell	S75	52.37	S 75 36	post
Shell	S75	54.05	S 75 40	post
Shell	S75	56.37	S 75 43	post
Shell	S75	58.14	S 75 45	post
Shell	S75	59.00	S 75 46	post
Shell	S75	59.74	S 75 48	post
Shell	S75	64.31	S 75 54	during
Shell	S75	66.36	S 75 59	during
Shell	S75	70.55	S 75 64	during
Shell	S75	72.06	S 75 65 AI	during
Shell	S75	74.00	S 75 65 BE	during
Shell	S75	75.94	S 75 67	during
Shell	S75	79.06	S 75 72	during
Shell	S75	82.18	S 75 76B	during
Shell	S75	87.46	S 75 77U	during
Shell	S75	87.90	S75 77X	during
Shell	S75	88.87	S 75 79	during
Shell	S75	90.60	S 75 81	during
Shell	S75	92.09	S 75 84	pre
Shell	S75	94.33	S75 86	pre

Appendix 3-6-2: S75 (Tarfaya) auxiliary data

depth (m)	Mg (mg/g)	Al (mg/g)	Ca (mg/g)	Ti (mg/g)	V (µg/g)	Cr (µg/g)	Mn (mg/g)	Fe (mg/g)	Co (µg/g)	U (µg/g)
50.41	8.38	5.44	234.58	0.27	135.06	17.71	0.06	6.00	1.33	1.64
52.37	7.11	6.85	234.72	0.38	127.43	19.45	0.08	4.39	1.51	1.67
54.05	7.86	8.41	233.27	0.42	83.72	21.87	0.07	6.21	1.81	1.06
56.37	7.08	19.52	160.60	0.60	210.05	91.55	0.06	11.34	3.89	6.23
58.14	6.46	3.68	234.79	0.21	107.59	14.02	0.07	3.87	0.91	1.05
59	11.26	19.36	102.01	0.60	492.13	78.86	0.08	13.50	4.61	6.69
59.74	9.52	15.75	125.89	0.21	604.95	77.45	0.07	9.92	3.64	10.72
64.31	17.13	27.29	146.72	0.68	330.37	97.66	0.12	16.18	6.01	7.37
66.36	7.78	5.91	240.60	0.27	77.23	23.85	0.07	3.56	1.19	2.53
70.55	2.91	11.05	198.55	0.29	195.68	85.38	0.04	5.79	2.34	11.23
72.06	8.05	15.59	220.22	0.68	109.68	27.09	0.09	10.65	3.80	3.09
74	6.48	17.84	209.89	0.81	173.53	49.97	0.08	15.82	4.06	4.12
75.94	3.87	4.94	286.31	0.17	152.17	17.21	0.07	2.57	1.18	1.43
79.06	1.97	2.27	264.80	0.10	60.41	7.71	0.05	2.13	0.60	1.53
82.18	3.03	7.05	223.88	0.25	146.41	15.38	0.05	5.23	2.22	6.13
87.46	1.65	3.59	239.51	0.11	21.33	11.39	0.04	2.02	0.97	2.18
87.9	2.21	3.14	248.19	0.11	13.92	8.36	0.04	2.09	0.92	1.13
88.87	2.73	18.26	182.59	0.29	290.14	91.02	0.04	9.46	3.79	5.27
90.6	1.93	5.16	237.13	0.09	61.71	26.02	0.04	2.80	1.22	3.31
92.09	2.55	5.13	244.82	0.12	57.57	26.68	0.04	3.05	1.20	2.89
94.33	3.44	7.08	220.32	0.11	144.81	57.95	0.04	6.01	1.61	5.31

Appendix 3-6-2 cont.: S75 (Tarfaya) auxiliary data

depth (m)	Ni (µg/g)	Cu (µg/g)	Sr (µg/g)	Mo (µg/g)	Cd (µg/g)	Ba (µg/g)	Ce (µg/g)	Nd (µg/g)	Th (µg/g)	U (µg/g)
50.41	26.99	14.34	978.73	10.38	1.44	100.70	4.90	2.33	0.73	1.64
52.37	26.66	13.14	895.89	7.43	0.94	70.33	6.80	3.05	0.95	1.67
54.05	20.02	12.22	807.78	5.19	0.94	160.25	6.46	2.96	1.08	1.06
56.37	117.79	51.11	676.83	22.81	5.44	108.87	13.84	6.58	2.08	6.23
58.14	19.89	12.38	887.04	7.49	1.53	71.89	3.93	1.75	0.52	1.05
59	135.34	48.87	482.48	58.99	9.84	107.00	16.49	7.36	2.51	6.69
59.74	242.65	62.35	533.71	85.10	15.74	116.49	18.03	8.83	2.04	10.72
64.31	110.87	58.20	641.98	29.06	3.16	135.37	22.16	10.00	3.19	7.37
66.36	24.82	16.68	903.23	6.01	0.93	145.79	5.71	2.58	0.80	2.53
70.55	133.53	61.13	785.08	15.45	2.90	82.22	12.27	6.44	1.50	11.23
72.06	36.36	30.38	884.91	8.45	0.55	105.79	11.39	5.25	1.99	3.09
74	55.41	52.76	798.17	11.13	1.26	109.28	14.17	6.75	2.42	4.12
75.94	18.76	34.91	1114.25	4.70	0.60	110.39	4.21	2.09	0.59	1.43
79.06	14.89	17.93	1064.28	2.52	0.48	119.42	2.70	1.58	0.35	1.53
82.18	41.90	30.33	994.49	6.80	0.22	83.08	8.03	4.39	1.05	6.13
87.46	21.09	29.38	1098.90	1.17	0.16	50.90	3.31	2.33	0.38	2.18
87.9	53.06	30.69	1096.67	1.77	1.13	186.24	2.86	1.97	0.36	1.13
88.87	106.75	72.49	920.48	14.03	2.61	71.12	14.39	9.00	1.68	5.27
90.6	61.07	44.82	1057.42	4.83	0.75	54.82	4.74	3.73	0.51	3.31
92.09	35.22	30.17	965.58	8.31	0.49	68.22	4.06	2.18	0.56	2.89
94.33	68.57	36.70	990.18	23.82	1.49	69.18	6.62	3.27	0.79	5.31

Appendix 3-6-3: Uranium isotope data at S75 (Tarfaya).

depth (m)	OAE 2?	bulk δ238U	2SD^	2SE^	n
50.41	post	-0.02	0.12	0.08	2
52.37	post	-0.32	0.14^	0.14^	1
54.05	post	-0.32	0.14^	0.14^	1
56.37	post	-0.35	0.20	0.10	4
58.14	post	-0.23	0.14^	0.14^	1
59	post	-0.27	0.14^	0.14^	1
59.74	post	-0.24	0.03	0.02	3
64.31	during	-0.42	0.22	0.12	3
66.36	during	-0.21	0.14^	0.14^	1
70.55	during	-0.39	0.21	0.11	4
72.06	during	-0.33	0.14^	0.14^	1
74	during	-0.26	0.14^	0.14^	1
75.94	during	-0.50	0.12	0.09	2
79.06	during	-0.41	0.03	0.02	2
82.18	during	-0.09	0.18	0.13	2
87.46	during	-0.24	0.19	0.11	3
87.9	during	-0.79	0.12	0.07	3
88.87	during	-0.68	0.13	0.09	2
90.6	during	-0.64	0.14^	0.14^	1
92.09	pre	-0.51	0.15	0.10	2
94.33	pre	-0.19	0.15	0.10	2

^Based on an average of the standard deviations of the other samples at this site.

Appendix 3-7: DSDP 367 (Cape Verde)

Appendix 3-7-1: Sample information for OAE 2 samples DSDP 367 (Cape Verde)

Exp	Site	Hole	Core	Section	Top Interval (cm)	Bottom Interval (cm)	depth (m)	OAE 2?
41	367	A	17	2	102	107	618.52	post
41	367	A	17	3	68	74	619.70	post
41	367	A	17	4	74	80	621.20	post
41	367	A	18	1	120	124	637.20	during
41	367	A	18	2	6	9	637.56	during
41	367	A	18	2	59	62	638.09	during
41	367	A	18	2	121	125	638.71	during
41	367	A	18	3	39	42	639.39	during
41	367	A	18	3	111	114	640.11	during
41	367	A	18	4	40	43	640.90	during
41	367	A	18	4	79	83	641.29	during
41	367	A	18	4	121	125	641.71	during
41	367	A	18	5	24	30	642.24	during
41	367	A	18	5	100	106	643.00	pre
41	367	A	19	1	143	147	645.93	pre
41	367	A	19	2	14	18	646.14	pre
41	367	A	19	3	43	47	647.93	pre
41	367	A	19	4	62	66	649.62	pre

Appendix 3-7-2: DSDP 367 (Cape Verde) auxiliary data

depth (m)	Mg (mg/g)	Al (mg/g)	Ca (mg/g)	Ti (mg/g)	V (µg/g)	Cr (µg/g)	Mn (mg/g)	Fe (mg/g)	Co (µg/g)	U (µg/g)
618.52	14.25	62.83	3.23	2.94	641.31	223.28	0.51	41.96	22.52	5.85
619.7	17.33	65.80	2.59	3.36	421.06	135.43	0.42	39.58	17.65	7.85
621.2	13.53	60.43	4.11	3.10	837.07	195.86	0.42	35.22	20.43	6.84
637.2	3.46	12.90	7.45	0.63	621.33	52.32	0.14	46.81	17.30	49.62
637.56	5.49	25.78	38.55	1.13	807.84	83.63	0.26	36.78	18.59	29.07
638.09	5.07	23.10	14.49	1.07	1401.39	98.81	0.25	47.85	19.78	28.71
638.71	5.99	27.38	31.66	1.39	1441.32	112.74	0.31	28.27	19.22	15.97
639.39	4.07	19.58	3.12	1.17	523.97	86.51	0.14	35.23	12.18	11.27
640.11	4.85	29.15	11.80	1.45	639.00	93.08	0.15	21.90	10.11	23.86
640.9	4.63	20.78	48.85	0.99	1259.22	88.93	0.35	21.14	11.15	47.33
641.29	6.23	31.47	4.01	1.56	1134.05	98.50	0.11	26.99	12.49	20.58
641.71	6.21	29.30	49.22	1.58	974.37	109.73	0.47	21.61	11.04	26.19
642.24	10.66	51.37	10.12	2.73	384.66	136.45	0.13	34.25	9.02	4.10
643	7.76	34.07	54.26	1.57	3074.91	166.97	0.34	20.83	9.09	25.02
645.93	10.31	50.49	4.13	2.23	1865.54	275.39	0.12	25.64	11.12	10.15
646.14	10.97	52.05	14.29	2.42	3632.97	352.60	0.18	25.54	10.05	15.13
647.93	12.06	53.00	6.10	2.48	2536.08	241.76	0.16	29.51	9.87	19.60
649.62	10.32	53.63	6.53	2.40	1873.48	137.39	0.14	26.31	8.54	17.88

Appendix 3-7-2 cont.: DSDP 367 (Cape Verde) auxiliary data

depth (m)	Ni (µg/g)	Cu (µg/g)	Sr (µg/g)	Mo (µg/g)	Cd (µg/g)	Ba (µg/g)	Ce (µg/g)	Nd (µg/g)	Th (µg/g)	U (µg/g)
618.52	205.72	255.68	132.76	33.96	2.69	615.69	62.25	27.91	8.00	5.85
619.7	132.72	136.11	96.85	33.00	3.17	530.13	61.54	25.97	8.37	7.85
621.2	164.95	218.77	141.59	59.07	4.69	566.26	57.72	25.43	7.42	6.84
637.2	331.91	73.10	107.96	55.57	0.85	588.56	22.19	20.98	2.50	49.62
637.56	323.23	89.86	258.04	58.99	1.56	956.42	23.96	18.94	3.21	29.07
638.09	610.35	93.05	199.82	167.14	6.62	344.75	29.55	22.21	3.04	28.71
638.71	369.39	120.98	282.19	102.47	13.27	536.94	20.11	14.48	2.92	15.97
639.39	170.07	117.17	115.95	81.48	3.20	985.21	14.61	8.43	2.26	11.27
640.11	194.70	125.99	290.88	63.49	7.49	3043.03	28.07	17.87	2.94	23.86
640.9	317.61	105.86	208.48	135.62	8.87	300.15	16.31	12.86	2.03	47.33
641.29	249.55	92.23	150.65	88.34	6.02	1129.19	23.42	13.53	3.14	20.58
641.71	266.06	121.65	293.09	156.83	6.86	391.85	23.50	14.98	3.52	26.19
642.24	97.71	137.13	284.97	27.49	3.97	997.41	41.47	19.33	6.96	4.10
643	302.55	140.54	312.65	325.86	20.36	423.18	46.10	24.41	3.90	25.02
645.93	224.18	196.91	239.90	103.66	23.01	1143.11	29.56	14.93	5.75	10.15
646.14	213.85	206.93	191.96	145.81	46.74	813.75	37.48	18.35	5.96	15.13
647.93	175.20	143.85	161.36	91.49	14.19	627.90	44.00	21.80	6.84	19.60
649.62	141.17	52.39	149.38	84.08	5.34	690.39	41.10	19.66	6.16	17.88

Appendix 3-7-3: Uranium isotope data at DSDP 367 (Cape Verde).

depth (m)	OAE 2?	bulk δ238U	2SD^	2SE^	n
618.52	post	0.06	0.12	0.09	2
619.7	post	-0.05	0.11	0.08	2
621.2	post	0.06	0.12	0.09	2
637.2	during	-0.25	0.11	0.06	3
637.56	during	-0.27	0.06	0.04	2
638.09	during	-0.21	0.11^	0.11^	1
638.71	during	-0.19	0.11^	0.11^	1
639.39	during	-0.29	0.01	0.01	2
640.11	during	-0.68	0.11^	0.11^	1
640.9	during	-0.58	0.21	0.10	5
641.29	during	-0.23	0.03	0.02	3
641.71	during	0.03	0.14	0.10	2
642.24	during	-0.24	0.12	0.07	3
643	pre	0.09	0.11^	0.11^	1
645.93	pre	0.11	0.30	0.14	5
646.14	pre	0.14	0.11^	0.11^	1
647.93	pre	0.32	0.01	0.00	2
649.62	pre	0.04	0.11	0.08	2

^Based on an average of the standard deviations of the other samples at this site.

Appendix 3-8: ODP 1258 (Demerara Rise)

Appendix 3-8-1: Sample information for OAE 2 samples ODP 1258 (Demerara Rise)

Exp	Site	Hole	Core	Section	Section Half	Top Interval (cm)	Bottom Interval (cm)	depth (m)	ID #	OAE 2?
207	1258	B	45	1	W	48	49	397.98	5039155	post?
207	1258	B	45	2	W	30	31	398.8	5039157	post?
207	1258	B	45	3	W	30	31	399.65	5039158	post?
207	1258	B	45	3	W	120	121	400.55	5039159	post?
207	1258	B	45	4	W	19	20	400.95	5039160	post?
207	1258	B	45	4	A	40	41	401.16	5039267	post?
207	1258	B	45	4	W	70	71	401.46	5039161	during
207	1258	B	45	4	W	89	90	401.65	5039162	during
207	1258	B	45	4	W	100	101	401.76	5039163	during
207	1258	B	45	4	W	130	131	402.06	5039164	during
207	1258	C	17	1	W	19	20	399.59	5039177	during
207	1258	C	17	1	W	49	50	399.89	5039180	during
207	1258	C	17	1	W	89	90	400.29	5039181	during
207	1258	C	17	2	W	7	8	400.86	5039182	during
207	1258	B	46	2	W	22	23	403.96	5039172	during
207	1258	C	17	2	W	39	40	401.18	5039185	during
207	1258	B	46	3	W	0	1	405.23	5039173	pre
207	1258	B	46	3	W	97	98	406.2	5039174	pre
207	1258	B	46	4	W	99	100	407.21	5039176	pre

Appendix 3-8-2: ODP 1258 (Demerara Rise) auxiliary data

depth (m)	Mg (mg/g)	Al (mg/g)	Ca (mg/g)	Ti (mg/g)	V (µg/g)	Cr (µg/g)	Mn (mg/g)	Fe (mg/g)	Co (µg/g)	U (µg/g)
418.81	9.50	44.96	14.04	2.08	816.55	342.50	0.08	20.55	7.86	5.77
419.63	3.50	18.15	173.25	0.63	484.21	51.19	0.06	10.03	5.51	13.99
420.48	5.99	28.79	92.78	0.74	2403.20	180.31	0.06	11.92	4.89	11.70
421.38	2.87	10.70	229.70	0.39	178.52	19.39	0.11	6.43	4.58	11.30
421.78	5.11	24.80	67.39	0.72	920.63	164.16	0.05	9.23	3.75	33.21
421.99	5.23	23.63	120.53	0.78	813.87	179.42	0.06	10.41	4.11	44.48
422.29	3.50	29.78	48.38	1.17	256.78	57.93	0.08	25.05	13.61	9.71
422.48	3.76	23.93	90.82	0.85	244.52	44.48	0.07	14.47	10.20	13.96
422.59	3.90	29.46	18.75	1.32	594.91	72.08	0.06	17.82	7.50	5.18
422.89	3.53	22.46	27.93	1.02	354.18	59.07	0.10	23.43	13.87	27.76
424.63	4.10	28.17	49.24	1.20	446.84	75.78	0.07	16.14	7.82	38.30
424.93	8.47	31.23	82.98	2.88	201.97	73.20	0.40	39.10	19.83	4.47
425.33	5.74	37.60	26.63	1.96	373.61	96.61	0.26	34.85	21.90	9.84
425.9	3.85	23.09	65.82	1.03	1052.84	67.39	0.07	13.92	5.83	33.80
426.02	3.47	22.75	71.40	0.96	347.32	45.62	0.07	13.21	6.56	18.02
426.23	3.95	19.77	126.60	0.87	1803.57	171.20	0.04	9.25	3.53	7.58
427.29	2.70	2.54	269.85	0.09	129.43	7.44	0.05	1.33	0.56	4.41
428.26	2.44	11.50	20.87	0.40	730.20	135.55	0.03	5.22	2.22	4.69
429.27	4.02	18.82	147.77	0.83	1495.41	95.03	0.05	10.10	3.76	9.10

Appendix 3-8-2 cont.: ODP 1258 (Demerara Rise) auxiliary data

depth (m)	Ni (µg/g)	Cu (µg/g)	Sr (µg/g)	Mo (µg/g)	Cd (µg/g)	Ba (µg/g)	Ce (µg/g)	Nd (µg/g)	Th (µg/g)	U (µg/g)
418.81	199.50	110.33	564.83	85.54	9.14	592.29	14.14	7.99	5.62	5.77
419.63	130.33	27.58	719.05	87.51	1.34	314.62	13.45	6.75	2.03	13.99
420.48	147.84	94.42	658.45	92.15	75.52	414.88	14.56	7.60	3.47	11.70
421.38	51.46	21.55	582.82	65.04	0.21	248.44	10.04	4.90	1.20	11.30
421.78	83.89	53.42	544.62	71.54	6.80	348.03	78.34	43.80	3.21	33.21
421.99	90.11	56.14	871.50	62.97	4.38	465.76	64.73	40.98	3.57	44.48
422.29	125.35	44.21	614.68	35.53	0.51	107.74	17.79	10.84	3.32	9.71
422.48	109.18	42.74	660.78	27.48	0.46	291.68	21.49	12.28	2.77	13.96
422.59	153.13	56.54	440.21	48.44	1.77	304.81	15.97	8.30	3.49	5.18
422.89	225.48	72.10	429.63	58.83	0.53	130.93	45.90	26.23	2.91	27.76
424.63	186.43	47.81	550.48	42.39	1.72	343.22	147.30	91.59	4.34	38.30
424.93	60.95	66.64	315.04	5.80	0.44	175.54	12.81	7.61	0.83	4.47
425.33	162.43	168.09	642.55	43.83	2.18	163.16	34.64	21.54	4.39	9.84
425.9	349.51	69.89	453.08	291.51	5.35	180.35	22.67	11.84	2.83	33.80
426.02	189.32	88.01	476.81	96.67	2.94	180.17	26.27	13.57	2.88	18.02
426.23	150.73	109.62	703.52	81.98	22.20	267.35	8.99	4.75	2.38	7.58
427.29	18.79	6.38	260.81	15.59	0.30	49.12	3.45	1.58	0.31	4.41
428.26	88.77	44.82	141.70	40.32	13.33	81.67	6.98	3.78	1.44	4.69
429.27	166.69	47.80	732.50	128.41	8.19	234.04	11.09	5.27	2.50	9.10

Appendix 3-8-3: Uranium isotope data at ODP 1258 (Demerara Rise).

depth (m)	OAE 2?	bulk δ238U	2SD^	2SE^	n
418.81	post?	-0.04	0.06	0.04	2
419.63	post?	0.03	0.29	0.15	4
420.48	post?	0.03	0.12^	0.12^	1
421.38	post?	0.03	0.10	0.05	5
421.78	post?	-0.05	0.07	0.05	2
421.99	post?	-0.16	0.13	0.09	2
422.29	during	0.06	0.12	0.07	3
422.48	during	0.00	0.09	0.06	2
422.59	during	-0.09	0.18	0.09	4
422.89	during	-0.12	0.03	0.02	2
424.63	during	0.14	0.12^	0.12^	1
424.93	during	-0.27	0.16	0.10	3
425.33	during	0.12	0.08	0.06	2
425.9	during	0.29	0.12^	0.12^	1
426.02	during	-0.18	0.04	0.03	2
426.23	during	0.26	0.12	0.09	2
427.29	pre	-0.02	0.06	0.04	3
428.26	pre	0.04	0.12^	0.12^	1
429.27	pre	0.33	0.22	0.12	3

^Based on an average of the standard deviations of the other samples at this site.

Appendix 4: Modern day comparison – Black Sea

Appendix 4-1: Overview of modern day comparison – Black Sea

The physical features of the Black Sea impact its ability to overturn, creating euxinic conditions for the deep basin (Appendix 4-2; 4-3) (Degens et al., 1977). Well documented, euxinic conditions have dominated the deep waters (Haraldsson and Westerlund, 1988; Buesseler et al., 1991; Murray et al., 1991; Anderson et al., 1994) for the past 7.5 ka (Arthur and Dean, 1998; Eckert et al., 2013). The chemocline of the Black Sea, with low (<5 μM) concentrations of both O_2 and H_2S, is broad, spanning 50m (Haraldsson and Westerlund, 1988; Buesseler et al., 1994), and coincides with the pycnocline. The pycnocline separates the two main water bodies: fresher (salinity 18), warm (25°C) oxygenated waters at the surface that originate from rivers mixing with seawater, and the saltier (salinity 22), cold (8.8^{o}C), anoxic waters (Buesseler et al., 1991). Saltwater enters and exits into the Black Sea from the Mediterranean via the Bosporus Strait. Water moving through the Bosporus is restricted by a shallow sill (60m), and thus inhibits ventilation of the deep waters (Latif et al., 1991). The physical constraints of the Bosporus Strait and the strong density gradient hinder mixing of the two water masses, which enables euxinia to persist (Degens et al., 1977).

The redox conditions of the Black Sea bottom water influences the reactions occurring in the sediments beneath it. A range of bottom water redox conditions exist in the Black Sea along the transect from the shelf to the deep basin. Along the shelf, small changes in the chemocline or redox conditions can greatly impact the geochemistry (Anderson et al., 1994). For example, iron geochemistry responds to these changes: Fe^{3+} precipitates in oxic waters, Fe^{2+} dissolves in anoxic conditions, while $Fe^{2+}S$ and $Fe^{2+}S_2$

(pyrite) form in euxinic conditions. Based on these reactions, as redox conditions change with movement of the chemocline, it will directly impact the speciation of iron (Wijsman et al., 2001). Changes in the redox state impact on sediments can be observed with the Fe shuttle, a mechanism to transport released reactive iron from the shelf to the deep basin where it is precipitated out as pyrite (Canfield et al., 1996; Raiswell and Canfield, 1998; Wijsman et al., 2001; Lyons and Severmann, 2006; Severmann et al., 2008; Eckert et al., 2013). Through a different mechanism, Mo also responds to changes in the bottom water conditions: Mo binds with H_2S to form molybdenum sulfides (Erickson and Helz, 2000; Anbar, 2004; Neubert et al., 2008). Arnold et al. (2012) used sedimentary Mo as a redox proxy showing that the location of the chemocline shoaled and then receded during the Little Ice Age. Thus, different elements are influenced by the redox conditions in the bottom waters, which can be used to decipher changes in oxygenation.

Profiles of U in the Black Sea water column show that U is being depleted from bottom water and enriched in the sediments. The earliest study of U in the Black Sea noted a sedimentary U anomaly, with higher concentrations than anticipated based on comparisons to crustal-rock source material (Degens et al., 1977). Subsequent studies worked to understand the removal mechanism, and results showed that U reduction and removal occurs in the sediments and that diffusion of dissolved U from bottom waters into the porewaters further supplies additional U for bacterial reduction(Anderson et al., 1989; Barnes and Cochran, 1991). The impact of the diffusion decreases the U present in the bottom waters of the water column by approximately 40% (Anderson et al., 1989; Colodner et al., 1995). By applying the observations from the Black Sea, the earliest oceanic U mass balance included U removal via reducing environments (Barnes and

Cochran, 1990). More recently, the U balance was supplemented with $\delta^{238}U$ data (Montoya-Pino et al., 2010; Tissot and Dauphas, 2015), in which the Black Sea data was included as the euxinic sediment endmember (Weyer et al., 2008; Montoya-Pino et al., 2010). Additional studies observed the variations in U isotope ratios within the water column, as a response to bacterial reduction in the sediments and diffusion from the water column (Wall and Krumholz, 2006; Romaniello, 2012; Rolison, 2016).

References

Anbar, A.D., 2004, Molybdenum stable isotopes: Observations, interpretations and directions: Geochemistry of Non-Traditional Stable Isotopes, v. 55, p. 429-454, doi: 10.2138/gsrmg.55.1.429.

Anderson, R.F., Fleisher, M.Q., and Lehuray, A.P., 1989, Concentration, Oxidation-State, and Particulate Flux of Uranium in the Black-Sea: Geochimica Et Cosmochimica Acta, v. 53, p. 2215-2224, doi: 10.1016/0016-7037(89)90345-1.

Anderson, R.F., Lyons, T.W., and Cowie, G.L., 1994, Sedimentary Record of a Shoaling of the Oxic Anoxic Interface in the Black-Sea: Marine Geology, v. 116, p. 373-384, doi: 10.1016/0025-3227(94)90052-3.

Arnold, G.L., Lyons, T.W., Gordon, G.W., and Anbar, A.D., 2012, Extreme change in sulfide concentrations in the Black Sea during the Little Ice Age reconstructed using molybdenum isotopes: Geology, v. 40, p. 595-598, doi: 10.1130/G32932.1.

Arthur, M.A., and Dean, W.E., 1998, Organic-matter production and preservation and evolution of anoxia in the Holocene Black Sea: Paleoceanography, v. 13, p. 395-411, doi: 10.1029/98pa01161.

Barnes, C.E., and Cochran, J.K., 1990, Uranium Removal in Oceanic Sediments and the Oceanic-U Balance: Earth and Planetary Science Letters, v. 97, p. 94-101, doi: 10.1016/0012-821x(90)90101-3.

Barnes, C.E., and Cochran, J.K., 1991, Geochemistry of Uranium in Black-Sea Sediments: Deep-Sea Research Part a-Oceanographic Research Papers, v. 38, p. S1237-S1254, doi: 10.1016/S0198-0149(10)80032-9.

Buesseler, K.O., Livingston, H.D., and Casso, S.A., 1991, Mixing between Oxic and Anoxic Waters of the Black-Sea as Traced by Chernobyl Cesium Isotopes: Deep-Sea Research Part a-Oceanographic Research Papers, v. 38, p. S725-S745, doi: 10.1016/S0198-0149(10)80006-8.

Buesseler, K.O., Livingston, H.D., Ivanov, L., and Romanov, A., 1994, Stability of the oxic-anoxic interface in the Black Sea: Deep Sea Research Part I: Oceanographic Research Papers, v. 41, p. 283-296, doi: 10.1016/0967-0637(94)90004-3.

Canfield, D.E., Lyons, T.W., and Raiswell, R., 1996, A model for iron deposition to euxinic Black Sea sediments: American Journal of Science, v. 296, p. 818-834.

Colodner, D., Edmond, J., and Boyle, E., 1995, Rhenium in the Black-Sea - Comparison with Molybdenum and Uranium: Earth and Planetary Science Letters, v. 131, p. 1-15, doi: 10.1016/0012-821x(95)00010-A.

Degens, E.T., Khoo, F., and Michaelis, W., 1977, Uranium anomaly in Black Sea sediments: Nature, v. 269, p. 566-569.

Eckert, S., Brumsack, H.J., Severmann, S., Schnetger, B., Marz, C., and Frollje, H., 2013, Establishment of euxinic conditions in the Holocene Black Sea: Geology, v. 41, p. 431-434, doi: 10.1130/G33826.1.

Erickson, B.E., and Helz, G.R., 2000, Molybdenum(VI) speciation in sulfidic waters: Stability and lability of thiomolybdates: Geochimica Et Cosmochimica Acta, v. 64, p. 1149-1158, doi: 10.1016/S0016-7037(99)00423-8.

Haraldsson, C., and Westerlund, S., 1988, Trace-Metals in the Water Columns of the Black-Sea and Framvaren Fjord: Marine Chemistry, v. 23, p. 417-424, doi: 10.1016/0304-4203(88)90108-9.

Latif, M.A., Ozsoy, E., Oguz, T., and Unluata, U., 1991, Observations of the Mediterranean Inflow into the Black-Sea: Deep-Sea Research Part a-Oceanographic Research Papers, v. 38, p. S711-S723, doi: 10.1016/S0198-0149(10)80005-6.

Lyons, T.W., and Severmann, S., 2006, A critical look at iron paleoredox proxies: New insights from modern euxinic marine basins: Geochimica Et Cosmochimica Acta, v. 70, p. 5698-5722, doi: 10.1016/j.gca.2006.08.021.

Montoya-Pino, C., Weyer, S., Anbar, A.D., Pross, J., Oschmann, W., van de Schootbrugge, B., and Arz, H.W., 2010, Global enhancement of ocean anoxia during Oceanic Anoxic Event 2: A quantitative approach using U isotopes: Geology, v. 38, p. 315-318, doi: 10.1130/G30652.1.

Murray, J.W., Top, Z., and Ozsoy, E., 1991, Hydrographic Properties and Ventilation of the Black-Sea: Deep-Sea Research Part a-Oceanographic Research Papers, v. 38, p. S663-S689, doi: 10.1016/S0198-0149(10)80003-2.

Neubert, N., Nagler, T.F., and Bottcher, M.E., 2008, Sulfidity controls molybdenum isotope fractionation into euxinic sediments: Evidence from the modern Black Sea: Geology, v. 36, p. 775-778, doi: 10.1130/G24959a.1.

Raiswell, R., and Canfield, D.E., 1998, Sources of iron for pyrite formation in marine sediments: American Journal of Science, v. 298, p. 219-245.

Rolison, J.M., 2016, The biogeochemistry of trace metals and their isotopes in the Mediterranean and Black Seas [PhD: University of Otago].

Romaniello, S.J., 2012, Incorporation and preservation of molybdenum and uranium isotope variations in modern marine sediments [Doctor of Philosophy: Arizona State University, 154 p].

Severmann, S., Lyons, T.W., Anbar, A., McManus, J., and Gordon, G., 2008, Modern iron isotope perspective on the benthic iron shuttle and the redox evolution of ancient oceans: Geology, v. 36, p. 487-490, doi: 10.1130/G24670a.1.

Tissot, F.L.H., and Dauphas, N., 2015, Uranium isotopic compositions of the crust and ocean: Age corrections, U budget and global extent of modern anoxia: Geochimica et Cosmochimica Acta, v. 167, p. 113-143, doi: 10.1016/j.gca.2015.06.034.

Wall, J.D., and Krumholz, L.R., 2006, Uranium reduction: Annu Rev Microbiol, v. 60, p. 149-166, doi: 10.1146/annurev.micro.59.030804.121357.

Weyer, S., Anbar, A.D., Gerdes, A., Gordon, G.W., Algeo, T.J., and Boyle, E.A., 2008, Natural fractionation of $^{238}U/^{235}U$: Geochimica et Cosmochimica Acta, v. 72, p. 345-359, doi: 10.1016/j.gca.2007.11.012.

Wijsman, J.W.M., Middelburg, J.J., and Heip, C.H.R., 2001, Reactive iron in Black Sea Sediments: implications for iron cycling: Marine Geology, v. 172, p. 167-180, doi: 10.1016/S0025-3227(00)00122-5.

Appendix 4-2: Map of Black Sea sites

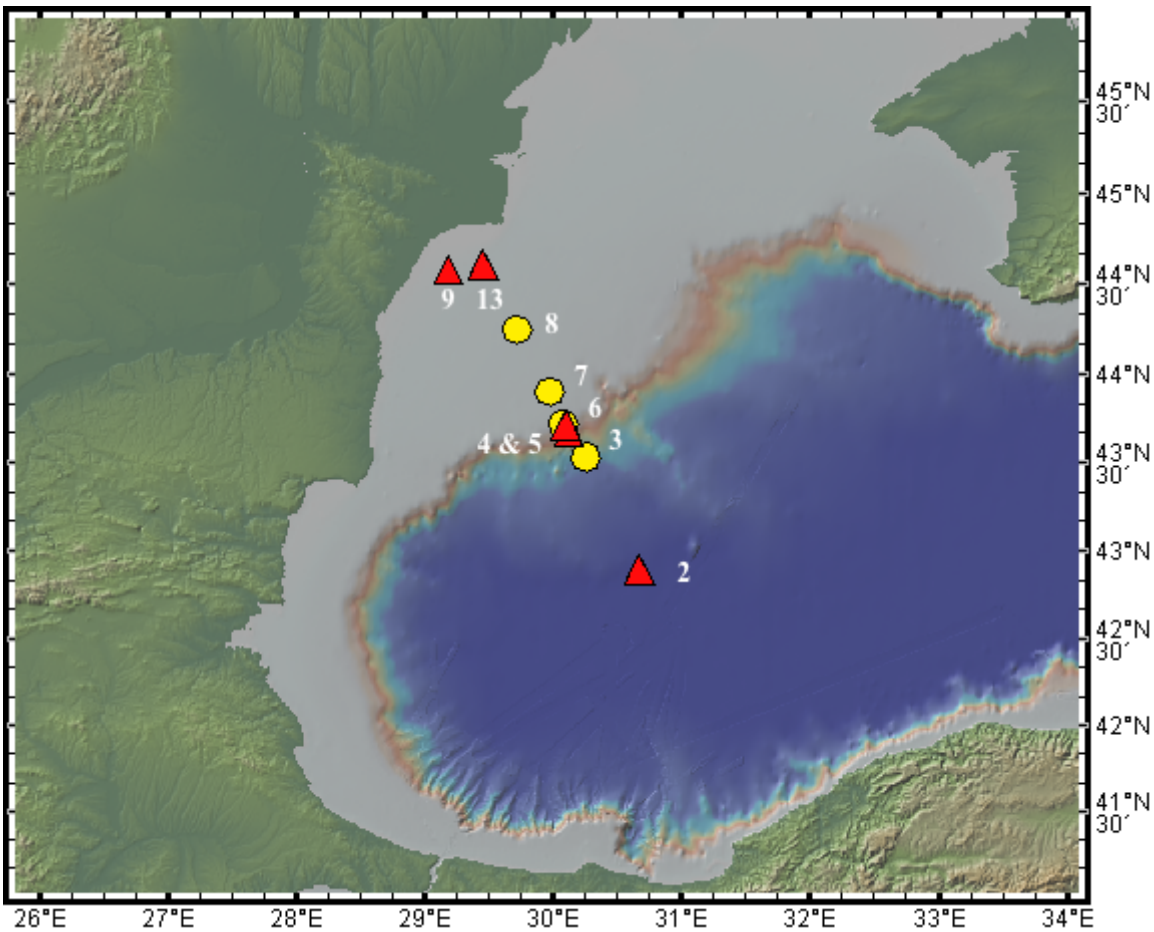

Key stations noted with red triangles. Minor stations are marked with yellow circles.

Appendix 4-3: Black Sea site descriptions by region

St.	depth (m)	BW O_2 (μM/kg)	H_2S (μM/kg)
Coastal Shelf			
St. 9*	27	91.1	
St. 13*	39	206.5	
Mid Shelf			
St. 8	64	188.4	
St. 7	78	152.7	
Shelf Edge			
St. 6	130	26.7	
Shelf Break			
St. 5*	190		11.1
St. 4*	380		126.7
Deep			
St. 3	1100		485.4
St. 2*	2077		437.4

*Key stations that were studied more throughly.

Appendix 4-4-1: Sedimentary Black Shelf (St. 13) auxiliary data

depth (cm)	Mg (mg/g)	Al (mg/g)	Ca (mg/g)	Ti (µg/g)	V (µg/g)	Cr (µg/g)	Mn (mg/g)	Fe (mg/g)	Co (µg/g)	U (µg/g)
0.5	13.93	64.54	38.53	3.59	104.90	99.98	0.62	39.67	12.86	1.98
1.5	15.61	69.60	47.01	3.92	113.07	109.28	0.63	41.07	13.88	2.28
2.5	12.40	54.69	49.43	3.14	87.82	84.79	0.51	31.63	11.24	1.96
3.5	13.82	58.43	46.85	3.20	90.73	83.30	0.59	31.76	12.41	1.91
4.5	14.71	63.00	38.99	3.58	99.48	93.93	0.64	35.20	12.30	1.89
5.5	13.27	59.46	49.52	3.30	93.88	88.27	0.56	32.07	11.70	1.86
6.5	13.31	58.51	50.06	3.23	93.79	85.32	0.58	31.97	11.80	1.93
8.5	14.54	66.75	40.02	3.49	111.24	100.95	0.61	38.04	13.27	2.10
10.5	13.61	63.19	37.77	3.25	104.98	95.62	0.58	36.89	12.51	1.95
12.5	14.22	64.84	39.64	3.46	104.75	97.44	0.60	37.15	12.84	1.93
15.5	13.37	64.77	39.75	3.49	104.54	100.62	0.66	43.48	14.93	1.77
18.5	11.82	54.74	49.32	3.17	84.54	84.31	0.56	36.17	12.70	1.60
21.5	14.83	71.44	31.94	3.65	117.11	107.18	0.64	50.78	16.94	1.96
24.5	15.18	70.80	35.43	3.69	114.02	110.58	0.67	43.25	15.29	2.32
27.5	13.77	65.21	43.12	3.34	105.50	99.38	0.61	43.01	14.08	2.15
30.5	14.77	69.67	35.64	3.64	112.61	107.21	0.79	46.53	16.03	1.93
34.5	13.85	63.37	46.93	3.28	103.56	100.93	0.76	41.73	14.13	1.79
38.5	13.42	64.11	54.35	3.21	102.55	101.84	0.76	41.58	13.86	1.88
42.5	14.59	72.09	32.19	3.50	114.17	112.46	0.77	43.91	15.20	1.96
46.5	13.92	70.99	26.65	3.32	118.28	119.55	0.72	51.08	15.87	2.16

Appendix 4-4-1 cont.: Sedimentary Black Shelf (St. 13) auxiliary data

depth (cm)	Ni (µg/g)	Cu (µg/g)	Sr (µg/g)	Mo (µg/g)	Cd (µg/g)	Ba (µg/g)	Ce (µg/g)	Nd (µg/g)	Th (µg/g)	U (µg/g)
0.5	59.76	44.53	212.08	1.51	0.11	340.77	59.73	25.56	10.56	1.98
1.5	64.32	51.33	254.48	1.52	0.12	392.42	70.89	30.36	12.07	2.28
2.5	51.14	39.22	272.66	1.13	0.09	324.44	53.56	22.87	8.69	1.96
3.5	53.59	37.53	254.64	1.27	0.08	337.98	58.34	24.26	9.08	1.91
4.5	56.01	39.18	200.39	1.16	0.09	337.45	59.24	25.04	9.97	1.89
5.5	52.23	43.78	265.50	1.10	0.11	317.81	54.12	22.67	9.05	1.86
6.5	53.73	44.82	274.69	1.14	0.09	320.51	56.93	24.59	9.37	1.93
8.5	62.73	54.83	224.10	1.20	0.08	338.11	60.34	25.04	10.37	2.10
10.5	59.80	54.44	221.97	1.11	0.09	299.07	57.19	24.45	9.99	1.95
12.5	59.86	52.26	227.54	1.00	0.09	331.86	58.87	25.03	9.96	1.93
15.5	69.64	64.04	276.43	1.14	0.13	338.08	61.57	25.40	9.82	1.77
18.5	56.80	49.61	329.25	0.86	0.12	346.11	54.97	23.23	8.42	1.60
21.5	74.95	63.10	228.93	1.34	0.11	379.00	62.39	25.82	10.36	1.96
24.5	75.61	71.27	253.75	1.23	0.11	412.10	66.90	27.52	10.53	2.32
27.5	69.60	70.08	313.73	2.10	0.10	380.09	62.20	25.68	9.91	2.15
30.5	74.34	77.65	252.39	1.31	0.14	554.89	67.70	28.46	10.51	1.93
34.5	67.23	74.72	348.52	1.41	0.10	387.48	60.00	25.06	9.19	1.79
38.5	70.67	75.52	442.41	1.40	0.10	373.13	61.68	25.80	9.43	1.88
42.5	75.38	103.11	234.97	1.45	0.21	419.69	68.11	28.00	10.21	1.96
46.5	76.97	102.53	234.24	2.70	0.25	477.54	66.82	27.49	9.87	2.16

Appendix 4-4-2: 0.2 μm filtered sea water concentration data at Black Sea Shelf (St. 9)

depth (m)	V (nmol/L)	Cr (nmol/L)	Mn (μmol/L)	Fe (μmol/L)	Co (nmol/L)	Ni (nmol/L)	Cu (nmol/L)	As (nmol/L)	Sr (μmol/L)
10 m	14.88	b.d.l.	3.51	0.21	0.45	11.07	b.d.l.	12.64	47.48

depth (m)	Mo (nmol/L)	Cd (nmol/L)	Sb (nmol/L)	Ba (μmol/L)	Ce (nmol/L)	Nd (nmol/L)	Re (nmol/L)	Tl (nmol/L)	U (nmol/L)
10 m	69.95	0.01	1.55	0.04	2.50	b.d.l.	0.23	0.59	8.72

Appendix 4-4-3: Pore water concentration data at Black Sea Shelf (St. 13 - core 1)

core(s)	depth (cm)	V (nmol/L)	Cr (nmol/L)	Mn (µmol/L)	Fe (µmol/L)	Co (nmol/L)	Ni (nmol/L)	Cu (nmol/L)	As (nmol/L)	Sr (µmol/L)
1	Sed. Surf.	8.29	b.d.l.	3.01	b.d.l.	1.37	14.48	6.25	19.74	49.49
1	1	27.75	b.d.l.	10.37	130.29	18.28	23.72	1.51	186.58	50.43
1	2	22.67	b.d.l.	15.31	229.22	29.64	29.45	b.d.l.	282.87	50.59
1	3	27.59	1.40	17.23	162.04	27.36	24.37	b.d.l.	172.61	49.37
1	4	33.98	1.45	22.20	178.95	35.06	25.86	b.d.l.	178.37	49.64
1	5	61.13	6.07	28.63	142.43	38.59	36.21	0.14	197.55	49.18
1	6	44.02	7.46	31.65	156.27	32.43	24.20	b.d.l.	187.76	49.09
1	8	54.06	6.37	28.29	84.45	18.09	24.86	b.d.l.	182.75	49.31
1	10	52.23	11.51	27.09	50.42	16.32	19.14	b.d.l.	135.71	48.90
1	12	64.51	13.94	24.10	26.20	20.31	27.96	b.d.l.	137.26	49.37
1	15	67.51	21.38	23.46	16.10	23.63	24.96	b.d.l.	88.25	49.03
1	18	75.68	29.93	28.44	59.45	30.81	24.99	b.d.l.	91.35	50.07
1	21	78.62	32.71	27.00	47.58	34.11	18.61	b.d.l.	85.39	49.98
1	24	107.14	44.47	15.58	8.26	29.80	21.76	b.d.l.	44.67	50.26
1	27	97.24	43.70	9.80	5.59	27.00	16.42	b.d.l.	66.43	50.36
1	30	188.22	67.26	7.00	3.39	32.67	31.39	b.d.l.	75.62	53.67
1	34	102.40	74.06	6.04	3.10	37.38	22.66	b.d.l.	35.55	50.55
1	38	193.20	80.48	6.51	2.69	38.37	32.00	b.d.l.	73.50	50.29
1	42	139.98	91.59	8.65	4.01	42.37	22.88	b.d.l.	118.66	50.84
1	46	157.17	78.53	14.20	3.37	47.43	22.75	b.d.l.	115.99	49.46

Appendix 4-4-3 cont.: Pore water concentration data at Black Sea Shelf (St. 13 - core 1)

core(s)	depth (cm)	Mo (nmol/L)	Cd (nmol/L)	Sb (nmol/L)	Ba (µmol/L)	Ce (nmol/L)	Nd (nmol/L)	Re (nmol/L)	Tl (nmol/L)	U (nmol/L)
1	Sed. Surf.	62.54	0.41	2.43	0.16	1.01	0.06	0.19	0.78	8.32
1	1	55.76	0.44	1.88	0.25	2.67	0.22	0.17	0.73	6.65
1	2	49.81	0.30	1.72	0.30	2.52	0.13	0.18	0.73	3.28
1	3	40.69	0.44	1.80	0.28	1.66	0.36	0.15	0.73	4.20
1	4	32.52	0.25	1.88	0.31	11.56	0.39	0.17	0.72	2.79
1	5	33.36	0.38	2.00	0.37	2.68	0.25	0.19	0.72	2.54
1	6	24.93	0.36	1.04	0.42	1.48	0.40	0.17	0.72	1.82
1	8	30.77	0.45	1.63	0.47	2.99	0.22	0.16	0.72	2.95
1	10	25.57	0.24	1.52	0.58	1.08	0.15	0.16	0.73	1.96
1	12	28.69	0.32	1.86	0.76	0.14	0.12	0.16	0.72	4.08
1	15	25.97	0.50	1.16	1.12	1.50	0.21	0.18	0.73	2.67
1	18	19.13	0.39	0.80	1.72	5.04	0.40	0.16	0.72	0.69
1	21	24.52	0.23	0.87	1.92	2.55	0.07	0.17	0.73	1.47
1	24	24.66	0.47	1.18	2.83	6.17	0.29	0.15	0.73	1.22
1	27	29.80	0.28	2.45	3.40	1.43	0.25	0.17	0.73	2.77
1	30	34.07	0.29	3.59	4.60	4.59	0.32	0.17	0.73	0.91
1	34	21.04	0.49	0.84	3.96	2.23	0.14	0.20	0.73	2.95
1	38	34.31	0.43	2.93	3.41	5.41	0.19	0.17	0.73	2.49
1	42	37.54	0.40	5.09	3.37	3.84	0.22	0.17	0.72	2.56
1	46	28.85	0.41	3.90	3.50	1.76	0.28	0.17	0.72	1.72

Appendix 4-4-4: Pore water concentration data at Black Sea Shelf (St. 13 - core 2)

core(s)	depth (cm)	V (nmol/L)	Cr (nmol/L)	Mn (µmol/L)	Fe (µmol/L)	Co (nmol/L)	Ni (nmol/L)	Cu (nmol/L)	As (nmol/L)	Sr (µmol/L)
2	Sed. Surf.	14.28	b.d.l.	28.88	12.37	2.96	1.91	13.80	51.62	47.06
2	1	30.77	1.11	22.02	236.15	15.76	12.93	1.31	268.93	47.25
2	2	37.83	1.90	20.87	337.04	28.50	36.23	0.82	344.60	47.76
2	3	36.38	2.45	22.00	282.00	32.65	42.83	5.20	234.59	47.53
2	4	34.68	0.27	24.34	204.65	28.14	25.51	b.d.l.	198.75	46.54
2	5	52.21	5.85	26.94	152.28	32.75	30.25	4.52	143.20	45.89
2	6	46.94	7.01	27.34	141.83	28.02	21.92	2.63	150.89	46.05
2	8	52.99	11.50	28.08	105.84	20.07	22.59	b.d.l.	147.52	45.30
2	10	70.22	12.72	25.59	46.81	19.50	26.68	b.d.l.	150.08	46.42
2	12	65.54	16.78	24.25	27.62	19.44	25.49	b.d.l.	124.92	46.42
2	15	88.58	25.61	22.94	13.47	24.37	34.21	b.d.l.	142.01	47.27
2	18	108.29	27.68	23.92	9.45	35.89	43.07	1.27	137.87	45.92
2	21	97.19	33.19	24.38	29.39	38.34	27.45	b.d.l.	100.87	44.83
2	24	172.00	33.63	16.77	5.01	23.05	38.72	b.d.l.	88.03	44.77
2	27	118.63	50.98	9.21	1.84	28.90	24.35	0.15	78.09	48.29
2	30	182.38	50.51	7.95	3.95	23.17	32.46	6.45	107.37	46.93
2	34	147.32	55.49	6.58	1.36	21.67	35.06	b.d.l.	79.91	48.31
2	38	141.18	63.58	6.46	1.71	20.24	33.06	b.d.l.	132.55	47.79
2	42	155.31	81.44	7.92	3.59	38.86	52.56	2.43	148.97	52.14
2	46	3.78	1.64	0.29	0.09	0.69	0.85	b.d.l.	13.77	1.25

Appendix 4-4-4 cont.: Pore water concentration data at Black Sea Shelf (St. 13 - core 2)

core(s)	depth (cm)	Mo (nmol/L)	Cd (nmol/L)	Sb (nmol/L)	Ba (µmol/L)	Ce (nmol/L)	Nd (nmol/L)	Re (nmol/L)	Tl (nmol/L)	U (nmol/L)
2	Sed. Surf.	60.21	b.d.l.	2.32	0.26	0.41	0.54	0.27	0.68	8.10
2	1	54.50	b.d.l.	1.81	0.28	0.12	0.64	0.26	0.53	5.73
2	2	49.52	b.d.l.	1.72	0.28	b.d.l.	0.61	0.25	0.53	3.55
2	3	46.34	0.11	1.96	0.29	0.55	0.56	0.26	0.53	3.69
2	4	41.60	0.07	2.20	0.27	b.d.l.	0.49	0.26	0.53	5.65
2	5	39.20	0.06	2.62	0.30	b.d.l.	0.51	0.27	0.52	4.79
2	6	33.48	0.01	2.08	0.34	2.61	0.46	0.26	0.53	3.73
2	8	23.13	b.d.l.	1.25	0.40	b.d.l.	0.42	0.24	0.51	1.57
2	10	34.21	b.d.l.	2.15	0.47	b.d.l.	0.53	0.25	0.52	2.58
2	12	23.21	0.04	1.68	0.58	b.d.l.	0.54	0.26	0.53	1.74
2	15	22.69	b.d.l.	2.35	0.95	b.d.l.	0.54	0.29	0.53	1.49
2	18	22.40	0.10	1.59	1.14	b.d.l.	0.45	0.24	0.51	2.33
2	21	19.32	0.11	0.83	1.52	b.d.l.	0.52	0.24	0.52	0.71
2	24	80.42	b.d.l.	15.65	1.91	b.d.l.	0.52	0.25	0.53	9.35
2	27	51.53	0.08	5.19	3.38	2.50	0.49	0.25	0.51	1.18
2	30	92.42	b.d.l.	8.66	3.59	b.d.l.	0.56	0.24	0.54	2.26
2	34	83.20	0.10	8.54	3.84	b.d.l.	0.51	0.26	0.51	3.18
2	38	121.27	0.14	11.10	3.75	b.d.l.	0.54	0.26	0.53	3.18
2	42	73.54	0.02	9.46	3.56	b.d.l.	0.50	0.27	0.53	3.30
2	46	3.61	b.d.l.	1.05	0.09	0.01	0.00	0.01	0.01	0.19

Appendix 4-4-5: Pore water concentration data at Black Sea Shelf (St. 9)

core(s)	depth (cm)	V (nmol/L)	Cr (nmol/L)	Mn (µmol/L)	Fe (µmol/L)	Co (nmol/L)	Ni (nmol/L)	Cu (nmol/L)	As (nmol/L)	Sr (µmol/L)
1-3	BW	16.94	b.d.l.	3.27	b.d.l.	3.21	19.82	b.d.l.	18.68	46.92
1-3	1	19.68	b.d.l.	13.70	34.75	11.78	24.62	b.d.l.	58.85	47.67
1-3	2	19.18	1.62	18.40	79.58	11.32	14.98	38.48	125.17	47.70
1-3	3	23.43	1.97	16.35	86.46	10.84	17.42	b.d.l.	102.01	48.19
1-3	4	25.27	5.09	19.83	122.71	11.12	16.97	b.d.l.	87.39	47.50
1-2	5	29.39	4.34	23.06	120.99	12.62	23.60	b.d.l.	97.34	48.56
3	5	26.93	0.72	26.90	125.12	9.12	23.43	b.d.l.	71.15	48.84
1-3	6	30.76	3.54	24.76	120.63	10.48	20.84	b.d.l.	86.68	49.44
1-3	8	34.53	2.84	22.45	83.64	5.09	14.40	b.d.l.	58.11	49.69
1-3	10	40.36	5.52	20.45	49.97	7.31	22.69	0.52	52.49	49.11
1-3	12	41.64	5.83	23.70	67.22	4.55	12.89	b.d.l.	40.15	47.89
1-3	14	35.33	10.61	26.66	114.58	2.75	10.25	b.d.l.	47.13	48.23
1-2	17	36.38	10.70	27.61	146.20	4.30	10.11	0.23	36.44	48.33
3	17	30.43	b.d.l.	27.43	132.87	3.54	14.68	b.d.l.	41.20	46.77
1-3	20	59.44	12.88	36.51	153.06	6.97	10.64	b.d.l.	55.02	46.95
1-2	24	69.19	12.65	36.15	98.85	12.02	16.69	b.d.l.	73.62	48.71
3	24	39.45	1.14	31.10	111.34	5.08	15.50	55.02	62.52	48.48
1-3	28	68.50	7.89	38.25	91.13	12.79	18.20	b.d.l.	124.26	47.73
1-3	32	62.43	13.16	38.11	104.52	12.30	12.48	b.d.l.	224.80	45.70
1-2	36	80.38	9.90	40.55	88.44	16.34	14.83	b.d.l.	355.80	43.72
3	36	58.13	5.83	43.48	152.14	14.29	13.74	b.d.l.	205.57	49.22

Appendix 4-4-5 cont.: Pore water concentration data at Black Sea Shelf (St. 9)

core(s)	depth (cm)	Mo (nmol/L)	Cd (nmol/L)	Sb (nmol/L)	Ba (µmol/L)	Ce (nmol/L)	Nd (nmol/L)	Re (nmol/L)	Tl (nmol/L)	U (nmol/L)
1-3	BW	58.19	b.d.l.	2.81	0.16	b.d.l.	0.32	0.17	b.d.l.	8.17
1-3	1	57.70	0.35	3.30	0.23	1.97	0.42	0.19	b.d.l.	8.24
1-3	2	54.09	0.15	1.86	0.26	5.05	0.34	0.15	b.d.l.	5.68
1-3	3	52.65	0.08	2.39	0.28	3.54	0.37	0.16	b.d.l.	5.20
1-3	4	47.74	0.04	2.14	0.35	4.46	0.43	0.14	b.d.l.	3.34
1-2	5	45.05	b.d.l.	1.89	0.37	4.27	0.38	0.15	b.d.l.	3.12
3	5	57.20	0.03	2.40	0.44	0.81	0.38	0.16	b.d.l.	4.23
1-3	6	59.90	0.21	2.45	0.42	3.93	0.42	0.15	b.d.l.	6.00
1-3	8	45.87	0.03	2.19	0.41	7.56	0.66	0.15	b.d.l.	4.11
1-3	10	66.20	0.08	4.03	0.40	25.83	1.44	0.16	b.d.l.	5.92
1-3	12	42.45	b.d.l.	1.85	0.45	16.81	0.78	0.14	b.d.l.	2.56
1-3	14	60.92	0.14	2.14	0.48	7.16	0.90	0.15	b.d.l.	2.62
1-2	17	65.16	0.04	2.16	0.56	16.38	1.30	0.15	b.d.l.	3.00
3	17	48.01	0.05	1.93	0.52	1.43	0.41	0.16	b.d.l.	3.64
1-3	20	51.63	0.06	1.93	0.66	2.79	0.51	0.15	b.d.l.	1.95
1-2	24	39.05	0.08	1.96	0.74	12.55	0.42	0.14	b.d.l.	2.95
3	24	53.53	0.15	2.91	0.61	0.04	0.36	0.15	b.d.l.	5.75
1-3	28	39.45	0.08	2.02	0.76	1.78	0.53	0.14	b.d.l.	1.73
1-3	32	28.45	0.05	1.44	0.81	2.93	0.48	0.14	b.d.l.	1.28
1-2	36	30.55	b.d.l.	1.98	0.81	1.23	0.37	0.14	b.d.l.	1.39
3	36	23.31	0.19	0.71	0.93	b.d.l.	0.25	0.14	b.d.l.	0.65

Appendix 4-4-6: Sedimentary uranium isotope data at Black Sea Shelf (St. 13).

depth (cm)	bulk δ238U	2SD^	2SE^	n
0.5	-0.05	0.24	0.14	3
1.5	-0.05	0.20	0.14	2
2.5	-0.14	0.13^	0.13^	1
3.5	-0.41	0.10	0.06	3
4.5	-0.28	0.13^	0.13^	1
6.5	-0.37	0.13^	0.13^	1
8.5	-0.37	0.09	0.06	2
12.5	-0.50	0.13^	0.13^	1
15.5	-0.37	0.20	0.10	4
18.5	-0.25	0.02	0.01	2

^Based on an average of the standard deviations of the East Pacific Seawater. Average δ = -0.39. 2SD = 0.13. N= 17.

Appendix 4-4-7: Uranium isotope data for water column samples from Black Sea shelf (St. 9).

Station	depth (m)	bottle #	bulk δ238U	2SD	2SE	n
St. 9	10	5	-0.67	0.09	0.06	2

Appendix 4-5-1: Sedimentary Black Shelf Break (St. 5) auxiliary data

depth (cm)	Mg (mg/g)	Al (mg/g)	Ca (mg/g)	Ti (µg/g)	V (µg/g)	Cr (µg/g)	Mn (mg/g)	Fe (mg/g)	Co (µg/g)	U (µg/g)
0.5	8.99	28.99	146.47	1.36	131.01	43.20	0.46	16.66	16.18	9.52
1.5	9.83	33.78	130.84	1.57	124.00	47.10	0.49	17.50	14.59	8.74
2.5	9.18	34.85	129.91	1.68	123.71	49.47	0.49	18.66	14.75	7.84
3.5	9.17	36.95	143.71	1.69	106.49	47.79	0.49	17.98	11.94	7.14
4.5	8.60	36.65	156.17	1.66	103.95	46.80	0.48	18.41	12.76	7.05
5.5	9.04	37.47	157.76	1.63	118.28	48.47	0.47	18.30	12.46	6.83
6.5	8.90	39.31	144.86	1.81	117.90	50.20	0.51	18.79	11.91	7.68
7.5	8.76	36.11	150.25	1.60	118.75	48.00	0.51	18.73	11.23	7.59
8.5	9.72	41.37	143.37	1.80	129.25	53.15	0.50	19.24	11.07	7.22
10.5	9.28	44.62	136.34	1.99	129.78	56.54	0.67	21.94	13.47	7.04
12.5	8.95	41.35	150.01	1.68	124.97	51.93	0.48	19.39	11.61	7.11
14.5	8.20	37.33	167.68	1.59	117.50	47.42	0.46	17.88	10.64	7.54
16.5	8.97	40.59	147.05	1.72	131.45	52.10	0.47	19.97	10.95	7.24
20.5	8.82	34.88	153.03	1.62	99.09	45.92	0.55	15.57	8.78	9.93

Appendix 4-5-1 cont.: Sedimentary Black Shelf Break (St. 5) auxiliary data

depth (cm)	Ni (µg/g)	Cu (µg/g)	Sr (µg/g)	Mo (µg/g)	Cd (µg/g)	Ba (µg/g)	Ce (µg/g)	Nd (µg/g)	Th (µg/g)	U (µg/g)
0.5	69.42	20.50	1067.05	50.28	0.14	272.15	29.10	13.68	4.26	9.52
1.5	64.11	16.52	877.56	33.20	0.14	583.24	32.78	15.10	5.00	8.74
2.5	64.77	22.25	873.22	33.30	0.17	372.15	33.99	16.15	4.94	7.84
3.5	56.62	16.16	913.82	20.44	0.14	489.21	34.74	16.51	5.54	7.14
4.5	54.86	19.62	990.25	19.02	0.14	433.21	32.57	15.63	5.34	7.05
5.5	59.01	18.21	1005.76	25.55	0.17	438.25	33.04	16.12	5.32	6.83
6.5	58.20	24.79	920.29	22.30	0.18	410.99	36.62	17.29	5.87	7.68
7.5	58.29	21.53	951.08	25.56	0.16	399.55	34.77	16.70	5.50	7.59
8.5	57.15	21.41	917.91	22.89	0.12	426.10	36.51	17.28	6.06	7.22
10.5	65.72	42.26	882.75	22.57	0.14	379.39	39.92	18.51	6.53	7.04
12.5	59.48	27.15	950.35	25.48	0.15	348.64	34.72	16.64	5.75	7.11
14.5	54.44	33.89	1068.36	22.57	0.23	344.50	32.24	15.12	5.48	7.54
16.5	63.33	33.19	937.47	26.06	0.12	419.74	36.50	17.36	5.92	7.24
20.5	45.42	25.89	982.18	12.15	0.14	484.06	32.01	15.19	5.08	9.93

Appendix 4-5-2: 0.2 μm filtered sea water concentration data at Black Sea Shelf Break site (St. 4)

bottle #	depth (m)	V (nmol/L)	Mn (μmol/L)	Fe (μmol/L)	Co (nmol/L)	Ni (nmol/L)	Cu (nmol/L)	As (nmol/L)	Sr (μmol/L)
1	360	17.78	9.03	1.57	0.63	12.54	6.87	40.91	56.09
2	298	17.21	9.56	1.56	0.93	12.63	5.80	41.29	56.35
3	250	18.57	9.95	1.67	1.31	12.60	7.02	41.43	57.90
4	200	22.34	10.85	1.83	5.94	14.67	7.13	42.82	56.24
5	180	22.84	9.75	1.64	5.90	15.62	7.32	36.93	56.48
6	160	19.92	5.05	1.56	1.56	14.31	6.51	35.23	54.62
7	140	22.81	3.06	1.52	b.d.l.	13.53	9.01	33.87	53.62
8	130	22.89	3.01	1.52	b.d.l.	13.64	9.94	31.30	53.17
9	120	22.76	3.01	1.52	b.d.l.	13.25	10.33	27.45	52.94
11	110	20.68	3.01	1.51	b.d.l.	14.08	9.46	27.65	51.40
13	100	20.85	3.02	1.52	b.d.l.	11.29	10.23	25.52	51.28
15	90	17.97	3.01	1.52	b.d.l.	11.81	11.53	22.12	50.50
17	80	18.53	3.01	1.78	b.d.l.	13.87	11.83	20.71	50.05
19	60	17.43	3.01	1.53	b.d.l.	13.18	13.97	16.72	49.90
20	50	16.07	3.02	1.53	b.d.l.	12.51	13.82	16.24	49.50
22	40	16.54	3.03	1.55	b.d.l.	12.58	10.83	12.72	49.80
24	10	13.29	3.01	1.52	0.01	13.27	11.82	13.10	48.73

Appendix 4-5-2 cont.: 0.2 μm filtered sea water concentration data at Black Sea Shelf Break site (St. 4)

bottle #	depth (m)	Mo (nmol/L)	Cd (nmol/L)	Sb (nmol/L)	Ba (μmol/L)	Re (nmol/L)	Tl (nmol/L)	U (nmol/L)
1	360	48.55	0.58	2.04	0.50	0.19	b.d.l.	7.64
2	298	49.03	0.44	1.54	0.50	0.20	b.d.l.	7.86
3	250	54.09	0.43	1.53	0.51	0.18	b.d.l.	8.23
4	200	60.13	0.34	1.26	0.48	0.21	b.d.l.	8.63
5	180	61.97	0.53	1.13	0.46	0.19	b.d.l.	8.74
6	160	62.92	0.56	0.49	0.40	0.20	b.d.l.	8.88
7	140	61.32	0.39	0.94	0.32	0.19	b.d.l.	8.76
8	130	62.72	0.54	1.24	0.27	0.20	b.d.l.	8.97
9	120	61.49	0.49	1.22	0.25	0.20	b.d.l.	8.58
11	110	61.06	0.48	1.09	0.21	0.20	b.d.l.	8.92
13	100	60.72	0.85	1.64	0.20	0.22	b.d.l.	9.04
15	90	60.31	0.35	1.56	0.17	0.20	b.d.l.	8.65
17	80	58.58	0.48	1.81	0.16	0.20	b.d.l.	8.77
19	60	62.63	0.46	1.71	0.13	0.19	b.d.l.	8.82
20	50	60.17	0.33	1.70	0.12	0.21	b.d.l.	8.77
22	40	60.75	0.79	1.69	0.11	0.21	b.d.l.	8.75
24	10	61.71	0.51	1.56	0.04	0.21	b.d.l.	8.85

Appendix 4-5-3: Pore water concentration data at Black Sea Shelf Break (St. 5)

core(s)	depth (cm)	V (nmol/L)	Cr (nmol/L)	Mn (μmol/L)	Fe (μmol/L)	Co (nmol/L)	Ni (nmol/L)	Cu (nmol/L)	As (nmol/L)	Sr (μmol/L)
1-3	Sed. Surf.	143.92	b.d.l.	9.42	b.d.l.	3.98	26.11	53.33	95.68	56.85
1-3	1	217.15	0.40	10.12	b.d.l.	4.51	36.76	b.d.l.	146.96	56.72
1-3	2	115.48	1.15	10.59	b.d.l.	2.47	24.50	b.d.l.	117.49	57.40
1-3	3	84.12	2.21	11.44	b.d.l.	1.01	19.13	b.d.l.	108.02	57.52
1-3	4	62.82	3.26	11.31	b.d.l.	1.28	21.20	b.d.l.	117.17	58.51
1-3	5	61.09	1.78	10.75	b.d.l.	1.12	20.35	b.d.l.	110.58	56.98
1-3	6	64.50	4.03	10.67	b.d.l.	0.70	18.58	b.d.l.	114.05	57.25
1-3	7	141.68	2.68	10.13	b.d.l.	1.62	24.86	b.d.l.	116.83	58.83
1-3	8	203.34	4.13	10.25	b.d.l.	0.62	21.08	b.d.l.	116.44	56.77
1-3	10	159.67	3.29	9.94	b.d.l.	0.59	20.45	b.d.l.	107.60	57.12
1-3	12	110.90	4.82	9.53	b.d.l.	0.58	16.81	b.d.l.	109.17	57.14
1-3	14	82.61	3.51	9.43	b.d.l.	0.60	15.75	b.d.l.	100.69	56.59
1-3	16	93.97	3.22	9.34	b.d.l.	0.39	27.35	b.d.l.	116.12	59.23
1-3	18	156.22	3.52	8.93	b.d.l.	0.66	33.99	b.d.l.	154.60	57.50
1-3	20	129.45	3.89	9.06	b.d.l.	0.67	24.61	b.d.l.	134.96	59.81

Appendix 4-5-3 cont.: Pore water concentration data at Black Sea Shelf Break (St. 5)

core(s)	depth (cm)	Mo (nmol/L)	Cd (nmol/L)	Sb (nmol/L)	Ba (µmol/L)	Ce (nmol/L)	Nd (nmol/L)	Re (nmol/L)	Tl (nmol/L)	U (nmol/L)
1-3	Sed. Surf.	174.62	0.16	5.58	0.48	0.81	0.34	0.16	b.d.l.	10.37
1-3	1	254.13	0.18	11.00	0.49	0.94	2.13	0.16	b.d.l.	12.22
1-3	2	171.33	0.12	10.43	0.47	1.05	0.49	0.15	b.d.l.	9.15
1-3	3	101.47	0.27	7.37	0.45	2.25	0.36	0.15	b.d.l.	5.92
1-3	4	87.25	0.23	8.10	0.44	1.67	0.72	0.14	b.d.l.	4.95
1-3	5	118.49	0.22	8.61	0.43	1.27	0.36	0.14	b.d.l.	6.06
1-3	6	156.60	b.d.l.	10.14	0.42	3.26	0.47	0.15	b.d.l.	6.26
1-3	7	155.53	0.01	13.67	0.44	0.81	0.50	0.14	b.d.l.	9.23
1-3	8	112.66	0.05	9.52	0.42	3.16	0.46	0.15	b.d.l.	7.79
1-3	10	86.93	0.16	9.94	0.41	3.20	0.40	0.15	b.d.l.	6.76
1-3	12	88.54	0.02	9.51	0.39	3.10	0.36	0.15	b.d.l.	4.86
1-3	14	63.70	0.05	8.40	0.38	3.72	0.48	0.14	b.d.l.	3.26
1-3	16	78.72	0.10	10.11	0.39	7.61	0.89	0.15	b.d.l.	3.53
1-3	18	195.68	0.03	17.05	0.38	8.21	0.68	0.14	b.d.l.	9.63
1-3	20	104.50	0.03	14.80	0.40	2.30	0.45	0.15	b.d.l.	7.13

Appendix 4-5-4: Pore water concentration data at Black Sea Shelf Break (St. 4)

core(s)	depth (cm)	V (nmol/L)	Cr (nmol/L)	Mn (µmol/L)	Fe (µmol/L)	Co (nmol/L)	Ni (nmol/L)	Cu (nmol/L)	As (nmol/L)	Sr (µmol/L)
1-3	Sed. Surf.	40.05	2.83	7.93	b.d.l.	b.d.l.	10.83	b.d.l.	46.96	55.86
1-3	1	130.91	0.17	7.99	b.d.l.	b.d.l.	12.38	b.d.l.	88.78	59.46
1-3	2	58.78	3.25	7.79	b.d.l.	b.d.l.	10.71	b.d.l.	101.41	56.66
1-3	3	71.25	1.90	7.83	b.d.l.	b.d.l.	12.51	b.d.l.	111.95	57.70
1-3	4	209.95	1.97	7.54	b.d.l.	b.d.l.	11.80	b.d.l.	165.58	57.31
1-3	5	58.12	1.62	7.73	b.d.l.	b.d.l.	10.92	b.d.l.	81.34	57.22
1-3	6	62.06	1.59	7.76	b.d.l.	0.24	10.21	b.d.l.	84.36	57.75
1-3	7	91.60	2.16	7.61	b.d.l.	b.d.l.	9.77	b.d.l.	145.99	57.87
1-3	8	223.86	2.09	7.44	b.d.l.	b.d.l.	9.75	b.d.l.	141.46	58.06
1-3	9	85.85	1.59	7.71	b.d.l.	b.d.l.	11.76	b.d.l.	81.94	58.67
1-3	10	155.16	4.63	7.59	b.d.l.	0.05	10.24	b.d.l.	112.67	59.70
1-3	12	68.65	2.90	7.54	b.d.l.	0.05	9.58	b.d.l.	100.60	58.73
1-3	14	104.39	3.14	7.47	b.d.l.	0.05	11.98	b.d.l.	103.11	60.38
1-3	16	174.96	4.64	7.29	b.d.l.	b.d.l.	15.18	b.d.l.	126.50	58.79
1-3	18	158.58	3.11	7.16	b.d.l.	b.d.l.	13.15	b.d.l.	128.29	57.49
1-3	20	146.27	3.60	7.10	b.d.l.	b.d.l.	12.56	b.d.l.	125.63	57.50

Appendix 4-5-4 cont.: Pore water concentration data at Black Sea Shelf Break (St. 4)

core(s)	depth (cm)	Mo (nmol/L)	Cd (nmol/L)	Sb (nmol/L)	Ba (µmol/L)	Ce (nmol/L)	Nd (nmol/L)	Re (nmol/L)	Tl (nmol/L)	U (nmol/L)
1-3	Sed. Surf.	42.73	b.d.l.	2.51	0.47	2.65	0.44	0.14	b.d.l.	7.83
1-3	1	139.72	0.10	6.17	0.48	0.47	0.29	0.15	b.d.l.	10.56
1-3	2	150.90	0.11	6.07	0.43	4.17	0.50	0.15	b.d.l.	9.92
1-3	3	175.53	0.08	8.06	0.43	1.12	0.54	0.14	b.d.l.	9.35
1-3	4	371.22	0.15	13.24	0.42	7.75	0.45	0.14	b.d.l.	20.18
1-3	5	101.33	0.13	6.58	0.41	4.18	0.43	0.12	b.d.l.	5.94
1-3	6	119.64	b.d.l.	7.92	0.41	2.16	0.38	0.14	b.d.l.	9.06
1-3	7	277.42	0.33	13.07	0.39	1.70	0.54	0.15	b.d.l.	12.31
1-3	8	235.24	0.19	8.44	0.40	3.06	0.47	0.15	b.d.l.	14.85
1-3	9	111.44	b.d.l.	7.35	0.40	2.61	0.29	0.15	b.d.l.	8.02
1-3	10	244.45	0.43	9.89	0.40	11.07	0.51	0.14	b.d.l.	11.70
1-3	12	153.50	0.01	9.19	0.38	4.71	0.42	0.15	b.d.l.	8.94
1-3	14	143.77	b.d.l.	8.91	0.39	1.80	0.43	0.13	b.d.l.	11.40
1-3	16	191.25	0.15	11.57	0.38	3.57	0.41	0.14	b.d.l.	21.07
1-3	18	196.80	0.11	12.06	0.36	2.55	0.31	0.14	b.d.l.	17.36
1-3	20	218.73	0.08	13.33	0.36	1.64	0.51	0.14	b.d.l.	18.30

Appendix 4-5-5: Sedimentary uranium isotope data at Black Sea Shelf Break (St. 5).

depth (cm)	bulk δ238U	2SD^	2SE^	n
0.5	0.11	0.13^	0.13^	1
1.5	0.16	0.17	0.10	3
2.5	-0.02	0.13^	0.13^	1
3.5	-0.11	0.13^	0.13^	1
4.5	-0.04	0.07	0.04	3
5.5	-0.10	0.13^	0.13^	1
7.5	0.15	0.08	0.05	2
10.5	0.05	0.13^	0.13^	1
12.5	0.09	0.01	0.01	2

^Based on an average of the standard deviations of the East Pacific Seawater. Average δ = -0.39. 2SD = 0.13. N= 17.

Appendix 4-5-6: Uranium isotope data for water column samples from Black Sea shelf break (St. 4).

Station	depth (m)	bottle #	bulk δ238U	2SD	2SE	n
St. 4	180	5	-0.52	0.04	0.03	2

Appendix 4-6-1: Sedimentary Black Deep (St. 2) auxiliary data

depth (cm)	Mg (mg/g)	Al (mg/g)	Ca (mg/g)	Ti (µg/g)	V (µg/g)	Cr (µg/g)	Mn (mg/g)	Fe (mg/g)	Co (µg/g)	U (µg/g)
0.5	9.33	16.13	155.08	0.81	85.54	23.32	0.35	18.68	20.97	7.30
1.5	8.31	22.27	145.06	1.09	90.25	35.26	0.44	23.75	25.74	8.52
2.5	9.17	26.34	151.76	1.31	75.97	38.03	0.48	26.58	25.82	9.95
3.5	7.60	22.30	196.91	1.08	59.35	29.81	0.45	22.79	21.63	12.03
4.5	8.03	26.24	171.69	1.23	76.39	34.30	0.52	28.19	26.17	15.88
5.5	7.91	25.87	163.25	1.16	89.11	32.87	0.53	29.17	26.61	18.40
6.5	7.94	22.13	194.83	0.98	74.86	29.33	0.48	24.99	22.95	18.01
7.5	6.50	17.75	222.45	0.79	61.89	23.76	0.44	20.99	19.62	18.19
8.5	8.60	21.71	184.52	0.95	82.05	29.29	0.49	26.25	25.96	17.90
9.5	8.09	21.93	173.44	0.98	83.61	29.97	0.50	27.19	27.80	18.65
14.5	4.54	8.62	283.21	0.39	45.05	11.44	0.32	11.30	12.00	13.51
18.5	5.29	12.67	235.37	0.62	67.91	17.72	0.34	14.50	17.78	19.13
22.5	5.52	13.52	241.39	0.63	68.67	19.74	0.34	14.95	24.99	17.93
26.5	4.80	10.69	257.40	0.51	79.68	15.13	0.30	11.89	15.70	15.64
29.5	8.68	30.50	147.55	1.41	114.47	43.76	0.45	31.70	45.01	16.10
30.5	10.32	38.02	104.53	1.87	146.78	53.75	0.50	38.09	40.37	14.05
31.5	12.38	46.21	53.13	2.32	211.91	65.21	0.52	48.62	51.18	14.08
32.5	7.92	24.58	157.63	1.14	151.57	34.61	0.30	30.50	42.92	28.36
34.5	12.80	41.30	47.02	2.05	265.44	55.44	0.25	23.82	17.08	16.32
36.5	13.16	41.93	42.07	2.10	264.66	56.48	0.26	24.72	17.03	20.88
38.5	12.02	38.80	39.51	1.90	255.54	60.86	0.36	24.84	22.15	17.27
40.5	12.78	42.73	47.43	2.07	312.48	66.16	0.50	25.33	17.00	25.78

Appendix 4-6-1 cont.: Sedimentary Black Deep (St. 2) auxiliary data

depth (cm)	Ni (μg/g)	Cu (μg/g)	Sr (μg/g)	Mo (μg/g)	Cd (μg/g)	Ba (μg/g)	Ce (μg/g)	Nd (μg/g)	Th (μg/g)	U (μg/g)
0.5	53.37	19.30	1139.70	27.43	0.13	293.93	25.99	11.54	2.72	7.30
1.5	67.24	20.92	1107.32	34.98	0.16	324.44	29.84	13.19	3.33	8.52
2.5	63.94	14.22	1036.24	28.88	0.13	313.21	32.06	14.35	4.16	9.95
3.5	51.98	21.34	1334.12	24.28	0.18	324.49	31.12	14.24	3.70	12.03
4.5	63.81	26.57	1178.52	30.31	0.16	340.27	33.43	15.00	4.17	15.88
5.5	63.59	32.72	1123.45	31.84	0.15	363.25	32.98	15.06	4.06	18.40
6.5	55.80	27.17	1344.62	30.07	0.15	265.46	27.72	12.62	3.54	18.01
7.5	49.99	45.41	1584.56	26.12	0.73	284.86	25.48	11.74	3.01	18.19
8.5	64.72	21.39	1275.59	37.05	0.12	280.15	28.34	12.83	3.57	17.90
9.5	69.19	35.44	1195.36	38.59	0.14	315.69	27.58	12.51	3.76	18.65
14.5	32.20	28.39	1995.58	18.47	0.54	264.60	12.98	6.17	1.50	13.51
18.5	43.70	34.81	1530.69	25.82	0.71	301.36	21.54	9.82	2.54	19.13
22.5	53.19	36.08	1566.96	34.00	0.76	313.49	21.03	9.17	2.33	17.93
26.5	44.13	35.62	1713.04	33.62	0.68	277.99	18.10	8.49	2.11	15.64
29.5	97.49	44.03	934.67	65.74	0.31	280.22	38.47	16.35	4.73	16.10
30.5	99.42	44.47	690.37	80.43	0.31	175.48	45.28	18.93	5.97	14.05
31.5	118.79	63.27	388.08	88.98	0.22	177.46	50.79	21.57	7.40	14.08
32.5	90.27	51.61	979.11	69.43	0.72	342.52	33.43	14.99	4.12	28.36
34.5	117.63	48.11	355.84	99.43	0.18	172.37	39.02	17.72	6.54	16.32
36.5	119.19	32.77	318.82	107.01	0.18	174.29	37.74	17.77	6.74	20.88
38.5	137.32	32.94	286.95	128.80	0.16	209.22	33.59	15.43	6.05	17.27
40.5	137.24	41.44	339.48	137.71	0.21	249.95	38.91	18.53	6.54	25.78

Appendix 4-6-2: 0.2 μm filtered sea water concentration data at Black Sea Deep site (St. 2)

bottle #	depth (m)	V (nmol/L)	Mn (μmol/L)	Fe (μmol/L)	Co (nmol/L)	Ni (nmol/L)	Cu (nmol/L)	As (nmol/L)	Sr (μmol/L)
1	2077	8.89	7.26	3.04	1.38	15.90	7.16	35.78	58.02
2	1500	8.34	7.21	3.02	1.24	16.47	5.32	41.87	56.88
3	1000	10.22	7.52	3.11	1.53	16.74	5.33	40.50	57.44
4	750	10.74	7.79	3.03	1.29	14.85	5.09	42.09	56.64
5	500	11.99	8.35	3.04	1.44	14.53	6.86	45.32	56.86
6	250	16.85	9.84	3.09	2.16	14.21	5.85	46.28	56.49
7	187	19.47	10.52	3.34	4.51	13.67	5.05	39.76	55.37
8	170	19.20	10.60	3.39	5.88	14.78	5.40	49.28	55.17
9	150	19.17	10.60	3.32	6.61	16.49	5.53	47.65	55.32
10	140	20.19	10.77	3.26	7.05	16.72	6.96	51.40	56.06
11	130	19.62	10.13	3.15	6.92	15.31	6.97	44.09	54.93
12	120	19.30	8.77	3.08	6.21	16.81	7.09	46.40	55.62
13	120	20.32	8.57	3.09	5.31	14.34	8.06	44.92	56.16
14	115	18.13	7.67	3.06	5.42	16.73	5.79	48.46	54.83
15	110	19.26	6.62	3.05	4.20	15.27	6.70	46.15	55.30
16	105	17.81	5.67	3.03	3.34	14.86	5.17	39.06	54.77
17	100	18.34	4.58	3.03	2.22	15.63	6.05	37.86	55.05
18	95	21.08	4.14	3.04	1.89	17.02	7.08	43.76	55.40
19	90	18.94	3.44	3.02	1.18	15.52	8.18	38.82	54.79
20	85	21.10	3.34	3.03	0.91	15.55	8.55	37.47	55.55
21	80	20.32	3.34	3.05	0.99	14.75	9.74	35.55	55.07
22	60	21.82	3.33	3.04	0.98	15.91	10.37	26.37	50.83
23	30	12.95	3.34	3.03	1.12	14.33	12.06	17.56	48.42
24	10	14.58	3.34	3.11	1.23	15.30	11.25	14.40	46.77

Appendix 4-6-2 cont.: 0.2 μm filtered sea water concentration data at Black Sea Deep site (St. 2)

bottle #	depth (m)	Mo (nmol/L)	Cd (nmol/L)	Sb (nmol/L)	Ba (μmol/L)	Re (nmol/L)	Tl (nmol/L)	U (nmol/L)
1	2077	29.13	0.64	0.75	0.46	b.d.l.	0.01	5.74
2	1500	28.45	0.43	1.08	0.45	b.d.l.	0.00	5.89
3	1000	30.19	0.22	1.02	0.46	b.d.l.	0.02	6.05
4	750	33.83	0.56	1.14	0.45	b.d.l.	0.01	6.49
5	500	41.08	0.54	0.93	0.47	b.d.l.	0.01	7.24
6	250	52.66	0.65	1.69	0.49	b.d.l.	0.02	8.12
7	187	54.53	0.33	1.50	0.49	b.d.l.	0.02	8.57
8	170	57.50	0.28	1.87	0.48	b.d.l.	0.01	8.45
9	150	57.94	0.20	1.59	0.47	b.d.l.	0.02	8.52
10	140	57.24	0.25	1.44	0.47	b.d.l.	0.02	8.86
11	130	59.59	0.23	1.42	0.45	b.d.l.	0.01	8.53
12	120	63.21	0.37	1.04	0.45	b.d.l.	0.00	8.89
13	120	60.49	0.35	1.29	0.45	b.d.l.	0.02	8.90
14	115	60.47	0.11	1.01	0.42	b.d.l.	0.01	9.00
15	110	62.35	0.62	0.99	0.43	b.d.l.	0.03	8.83
16	105	61.61	0.68	0.90	0.41	b.d.l.	0.04	8.52
17	100	64.70	0.68	0.83	0.38	b.d.l.	0.03	8.47
18	95	63.55	0.49	0.79	0.39	b.d.l.	0.03	8.57
19	90	60.61	0.28	0.76	0.36	b.d.l.	0.03	8.52
20	85	64.65	0.55	1.06	0.36	b.d.l.	0.04	8.63
21	80	64.92	0.55	1.12	0.33	b.d.l.	0.03	8.65
22	60	63.60	0.37	1.69	0.21	b.d.l.	0.05	8.36
23	30	61.11	0.56	2.06	0.09	b.d.l.	0.06	8.40
24	10	61.81	0.30	2.01	0.01	b.d.l.	0.05	8.31

Appendix 4-6-3: Pore water concentration data at Black Sea Deep (St. 2 - cores 1-2)

core(s)	depth (cm)	V (nmol/L)	Cr (nmol/L)	Mn (µmol/L)	Fe (µmol/L)	Co (nmol/L)	Ni (nmol/L)	Cu (nmol/L)	As (nmol/L)	Sr (µmol/L)
1	BW - 1	28.72	7.17	6.30	0.55	b.d.l.	19.81	0.18	33.89	56.61
1	BW - 2	44.20	0.57	6.22	0.46	b.d.l.	22.74	b.d.l.	41.10	55.23
1	Sed. Surf. 1	69.41	0.92	6.28	0.42	b.d.l.	27.00	b.d.l.	41.68	55.31
1	Sed. Surf 2	98.50	1.01	6.30	0.41	b.d.l.	26.00	b.d.l.	53.86	56.90
1-2	1	49.93	9.04	6.20	0.47	b.d.l.	24.48	3.44	60.96	52.04
1-2	2	55.58	3.99	6.21	0.41	b.d.l.	12.19	b.d.l.	60.96	55.41
1-2	3	78.12	9.94	6.02	0.47	b.d.l.	16.17	0.75	72.08	61.47
1-2	4	30.09	2.28	6.08	0.43	b.d.l.	7.01	b.d.l.	58.22	62.11
1-2	5	49.91	12.37	6.07	0.59	b.d.l.	8.36	b.d.l.	62.22	61.51
1-2	6	62.86	7.80	6.02	0.47	b.d.l.	8.62	2.77	65.66	61.76
1-2	7	81.08	4.08	6.07	0.44	b.d.l.	10.81	b.d.l.	71.70	61.33
1-2	8	80.56	2.90	5.93	0.40	b.d.l.	9.92	b.d.l.	69.22	58.90
1-2	9	275.29	6.25	5.45	0.46	b.d.l.	6.67	b.d.l.	149.90	58.49
1-2	10	592.88	4.37	5.50	0.49	0.08	32.70	8.34	199.66	59.59
1-2	14	105.65	9.53	5.67	0.50	b.d.l.	10.94	1.06	141.48	58.45
1	18	102.96	8.57	5.80	0.47	b.d.l.	12.07	4.24	125.32	58.46
1-2	22	27.87	3.50	5.95	0.56	0.07	15.14	1.86	70.87	56.77
1-2	26	55.32	1.15	6.02	0.80	0.30	58.60	8.35	94.21	55.54
1-2	30	46.47	8.78	5.93	0.47	b.d.l.	13.56	b.d.l.	92.90	58.13
1-2	32	98.68	7.20	5.97	1.21	1.09	31.46	6.67	86.53	57.85
1-2	34	27.01	2.54	6.08	0.44	b.d.l.	11.01	b.d.l.	79.61	57.70
1-2	36	69.99	2.32	6.19	0.40	b.d.l.	7.94	b.d.l.	84.48	58.50
1-2	38	99.20	7.58	5.96	0.43	b.d.l.	13.22	b.d.l.	81.34	57.31
1-2	40	64.05	6.66	6.00	0.44	b.d.l.	7.65	9.70	76.41	56.57

Appendix 4-6-3 cont.: Pore water concentration data at Black Sea Deep (St. 2 - cores 1-2)

core(s)	depth (cm)	Mo (nmol/L)	Cd (nmol/L)	Sb (nmol/L)	Ba (µmol/L)	Ce (nmol/L)	Nd (nmol/L)	Re (nmol/L)	Tl (nmol/L)	U (nmol/L)
1	BW - 1	29.68	b.d.l.	4.50	0.46	3.28	0.80	0.23	0.53	6.28
1	BW - 2	29.94	0.01	3.88	0.44	0.34	0.56	0.25	0.55	6.24
1	Sed. Surf. 1	30.41	0.11	3.21	0.46	b.d.l.	0.54	0.25	0.53	6.92
1	Sed. Surf 2	38.35	b.d.l.	3.07	0.45	b.d.l.	0.48	0.25	0.53	7.12
1-2	1	33.23	b.d.l.	3.56	0.43	6.26	0.67	0.25	0.52	6.88
1-2	2	32.44	0.10	3.26	0.39	3.30	0.64	0.25	0.55	4.68
1-2	3	60.23	0.10	4.81	0.40	4.15	0.66	0.27	0.52	11.40
1-2	4	34.02	b.d.l.	4.50	0.40	2.88	0.68	0.24	0.52	9.37
1-2	5	42.17	0.04	6.42	0.40	12.52	1.04	0.24	0.53	15.60
1-2	6	46.90	b.d.l.	7.96	0.40	6.51	0.82	0.24	0.53	10.47
1-2	7	53.75	b.d.l.	6.09	0.40	4.64	0.71	0.25	0.53	15.56
1-2	8	47.93	0.05	4.42	0.40	3.79	0.66	0.24	0.52	13.32
1-2	9	229.89	b.d.l.	16.19	0.40	5.94	0.75	0.24	0.53	36.32
1-2	10	335.21	0.20	19.44	0.39	4.43	0.46	0.24	0.52	78.36
1-2	14	214.73	0.27	17.04	0.39	6.34	0.73	0.25	0.52	32.34
1	18	106.88	0.15	10.44	0.37	4.77	0.69	0.26	0.52	35.12
1-2	22	39.27	0.27	4.57	0.35	4.03	0.60	0.25	0.53	11.09
1-2	26	145.16	0.12	8.32	0.34	5.17	0.65	0.25	0.52	10.20
1-2	30	62.16	0.10	7.00	0.35	5.50	0.89	0.25	0.53	9.41
1-2	32	76.70	0.07	7.17	0.36	6.35	0.96	0.23	0.52	10.80
1-2	34	44.98	0.23	6.16	0.36	4.71	0.74	0.23	0.53	9.39
1-2	36	52.15	0.01	6.32	0.37	2.35	0.63	0.25	0.53	10.60
1-2	38	54.52	0.09	6.14	0.36	4.76	0.71	0.26	0.52	9.52
1-2	40	51.55	b.d.l.	6.69	0.35	4.00	0.71	0.25	0.53	10.08

Appendix 4-6-4: Pore water concentration data at Black Sea Deep (St. 2 - cores 2-3)

core(s)	depth (cm)	V (nmol/L)	Cr (nmol/L)	Mn (µmol/L)	Fe (µmol/L)	Co (nmol/L)	Ni (nmol/L)	Cu (nmol/L)	As (nmol/L)	Sr (µmol/L)
2-3	1	78.51	0.96	6.19	0.60	b.d.l.	14.92	12.11	61.79	58.18
2-3	2	77.23	0.59	6.15	0.37	b.d.l.	11.82	b.d.l.	54.23	54.73
2-3	3	44.08	0.67	6.17	0.36	b.d.l.	10.52	b.d.l.	58.30	62.61
2-3	4	43.19	0.40	6.20	0.38	b.d.l.	11.27	b.d.l.	61.53	62.81
2-3	5	40.91	b.d.l.	6.14	0.36	b.d.l.	9.13	b.d.l.	63.41	63.56
2-3	6	49.72	0.47	6.07	0.37	b.d.l.	7.83	b.d.l.	60.98	60.44
2-3	7	50.87	0.79	6.18	0.37	b.d.l.	14.91	b.d.l.	63.36	60.45
2-3	8	76.98	b.d.l.	6.16	0.38	b.d.l.	12.04	b.d.l.	70.88	59.46
2-3	9	55.52	1.28	6.08	0.74	0.20	212.20	229.13	71.39	59.83
2-3	10	22.10	b.d.l.	6.09	0.61	b.d.l.	34.15	15.53	59.18	58.11
2-3	14	43.34	b.d.l.	5.99	0.37	b.d.l.	17.12	b.d.l.	77.53	58.05
3	18	21.73	b.d.l.	5.99	0.37	b.d.l.	5.25	b.d.l.	87.28	56.96
2	22	23.63	0.70	6.07	0.78	1.01	35.54	1.03	68.59	56.57
2-3	26	40.87	6.99	5.91	0.62	0.08	46.73	12.93	95.99	55.16
2-3	30	60.29	b.d.l.	6.02	0.38	b.d.l.	14.95	b.d.l.	90.28	58.14
2-3	32	52.87	b.d.l.	5.91	0.37	b.d.l.	8.75	b.d.l.	88.31	57.33
2-3	34	74.17	b.d.l.	6.00	0.38	b.d.l.	10.34	b.d.l.	112.05	56.44
2-3	36	30.18	1.01	6.05	0.38	0.04	6.39	b.d.l.	93.00	55.80
2-3	38	93.20	1.32	6.05	0.37	b.d.l.	19.78	b.d.l.	104.28	58.37
3	40	93.66	b.d.l.	6.19	0.34	b.d.l.	5.21	b.d.l.	83.84	59.25

Appendix 4-6-4 cont.: Pore water concentration data at Black Sea Deep (St. 2 - cores 2-3)

core(s)	depth (cm)	Mo (nmol/L)	Cd (nmol/L)	Sb (nmol/L)	Ba (µmol/L)	Ce (nmol/L)	Nd (nmol/L)	Re (nmol/L)	Tl (nmol/L)	U (nmol/L)
2-3	1	39.60	b.d.l.	4.78	0.46	8.09	0.85	0.26	0.52	7.41
2-3	2	32.98	b.d.l.	2.57	0.40	b.d.l.	0.45	0.24	0.52	4.70
2-3	3	36.07	b.d.l.	3.74	0.39	b.d.l.	0.45	0.26	0.53	4.82
2-3	4	41.91	b.d.l.	4.69	0.39	b.d.l.	0.50	0.24	0.53	6.50
2-3	5	36.59	0.01	3.99	0.40	b.d.l.	0.48	0.24	0.53	6.26
2-3	6	44.56	0.01	5.45	0.39	b.d.l.	0.49	0.23	0.52	7.49
2-3	7	37.82	b.d.l.	5.51	0.40	b.d.l.	0.50	0.24	0.52	8.23
2-3	8	47.04	b.d.l.	4.55	0.40	b.d.l.	0.51	0.24	0.52	12.48
2-3	9	45.52	b.d.l.	9.16	0.39	4.13	0.60	0.24	0.52	11.16
2-3	10	32.26	0.14	4.83	0.39	b.d.l.	0.55	0.25	0.53	5.41
2-3	14	51.44	b.d.l.	5.64	0.38	b.d.l.	0.51	0.24	0.52	10.58
3	18	50.74	0.09	4.58	0.36	0.20	0.52	0.23	0.52	6.21
2	22	40.60	0.05	5.80	0.36	1.57	0.41	0.25	0.54	15.15
2-3	26	74.95	b.d.l.	6.88	0.34	6.84	0.87	0.26	0.52	14.81
2-3	30	70.19	b.d.l.	7.46	0.34	b.d.l.	0.38	0.25	0.52	9.50
2-3	32	64.84	b.d.l.	6.29	0.33	b.d.l.	0.59	0.24	0.54	7.80
2-3	34	109.42	0.03	5.77	0.34	b.d.l.	0.68	0.24	0.52	12.20
2-3	36	72.07	b.d.l.	6.04	0.36	b.d.l.	0.43	0.27	0.53	5.72
2-3	38	69.39	0.04	6.76	0.37	b.d.l.	0.52	0.25	0.54	10.00
3	40	70.52	0.08	6.67	0.36	b.d.l.	0.45	0.27	0.52	9.42

Appendix 4-6-5: Particulate matter concentration data at Black Sea Deep per L (St. 2)

depth (m)	sub-sample	Mg (µg/L)	Al (µg/L)	Ti (ng/L)	V (ng/L)	Cr (ng/L)	Mn (µg/L)	Fe (µg/L)	Co (ng/L)	Ni (ng/L)	Cu (ng/L)
105	A	41.25	0.27	6.51	4.98	6.06	0.12	0.60	1.85	9.70	185.92
105	B	28.51	0.36	9.81	3.90	6.92	0.06	1.14	2.73	8.80	126.79
170	A	39.77	0.34	16.04	12.23	8.60	0.05	0.82	13.51	43.73	92.93
170	B	17.37	0.44	6.27	10.27	9.75	0.05	0.85	13.65	34.86	97.04
250	A	31.98	0.16	5.75	9.85	5.40	0.08	5.85	19.04	39.03	60.29
250	B	8.51	0.22	4.57	7.18	5.23	0.08	6.28	18.39	25.90	59.43
1000	A	31.95	0.15	7.32	7.23	9.28	0.08	2.62	2.11	14.02	10.24
1000	B	30.97	0.25	10.64	8.23	9.69	0.09	3.11	2.53	15.24	11.19

.

depth (m)	sub-sample	As (ng/L)	Sr (ng/L)	Mo (ng/L)	Cd (ng/L)	Sb (ng/L)	Cs (ng/L)	Ba (ng/L)	Tl (ng/L)	U (ng/L)
105	A	6.34	297.95	11.00	3.49	10.12	0.12	420.30	0.04	0.04
105	B	4.46	234.27	9.91	2.49	7.57	0.14	386.02	0.03	0.00
170	A	26.24	252.87	47.70	3.17	21.24	0.13	64.08	0.31	0.08
170	B	25.45	141.38	42.20	3.28	18.67	0.11	68.32	0.32	0.02
250	A	12.30	181.06	16.45	1.24	2.30	0.08	17.78	0.21	0.26
250	B	8.75	56.69	12.40	1.19	1.74	0.10	14.71	0.22	0.10
1000	A	3.82	208.79	8.52	0.55	0.75	0.08	85.32	0.07	0.97
1000	B	3.93	218.53	8.64	0.66	0.80	0.12	81.93	0.08	1.04

Appendix 4-6-6: Particulate matter concentration data at Black Sea Deep per square cm (St. 2)

depth (m)	sub-sample	Mg (µg/cm^2)	Al (µg/cm^2)	Ti (ng/cm^2)	V (ng/cm^2)	Cr (ng/cm^2)	Mn (µg/cm^2)	Fe (µg/cm^2)	Co (ng/cm^2)	Ni (ng/cm^2)	Cu (ng/cm^2)
105	A	62.74	0.42	9.91	7.57	9.22	0.18	0.91	2.82	14.76	282.79
105	B	43.37	0.55	14.92	5.94	10.53	0.08	1.74	4.16	13.39	192.86
170	A	38.65	0.33	15.58	11.88	8.36	0.04	0.80	13.13	42.50	90.31
170	B	16.88	0.43	6.09	9.98	9.48	0.04	0.82	13.27	33.88	94.31
250	A	38.73	0.20	6.97	11.93	6.54	0.10	7.09	23.06	47.27	73.02
250	B	10.30	0.26	5.54	8.69	6.33	0.10	7.60	22.28	31.37	71.98
1000	A	25.42	0.12	5.83	5.75	7.38	0.06	2.08	1.68	11.15	8.15
1000	B	24.64	0.20	8.46	6.55	7.71	0.07	2.48	2.01	12.12	8.90

.

depth (m)	sub-sample	As (ng/cm^2)	Sr (ng/cm^2)	Mo (ng/cm^2)	Cd (ng/cm^2)	Sb (ng/cm^2)	Cs (ng/cm^2)	Ba (ng/cm^2)	Tl (ng/cm^2)	U (ng/cm^2)
105	A	9.65	453.20	16.72	5.32	15.39	0.18	639.30	0.06	0.05
105	B	6.79	356.34	15.07	3.79	11.51	0.21	587.16	0.05	0.00
170	A	25.50	245.73	46.36	3.08	20.64	0.12	62.27	0.30	0.08
170	B	24.73	137.39	41.00	3.19	18.14	0.11	66.39	0.31	0.02
250	A	14.89	219.30	19.93	1.51	2.79	0.10	21.53	0.25	0.32
250	B	10.60	68.67	15.02	1.44	2.11	0.12	17.81	0.27	0.12
1000	A	3.04	166.14	6.78	0.44	0.60	0.06	67.89	0.06	0.77
1000	B	3.13	173.90	6.87	0.53	0.63	0.09	65.19	0.07	0.83

Appendix 4-6-7: Sedimentary uranium isotope data at Black Sea Deep (St. 2).

depth (cm)	bulk δ238U	2SD^	2SE^	n
0.5	0.34	0.13^	0.13^	1
1.5	-0.08	0.19	0.11	3
2.5	0.31	0.13^	0.13^	1
3.5	0.21	0.13^	0.13^	1
4.5	0.19	0.13^	0.13^	1
5.5	-0.17	0.13^	0.13^	1
7.5	-0.15	0.17	0.08	4
8.5	-0.06	0.13^	0.13^	1
18.5	0.03	0.13^	0.13^	1
26.5	-0.07	0.03	0.02	2
36.50	0.41	0.13^	0.13^	1
40.50	0.28	0.16	0.09	3

^Based on an average of the standard deviations of the East Pacific Seawater. Average δ = -0.39. 2SD = 0.13. N= 17.

Appendix 4-6-8: Water column uranium isotope data at Black Deep (St. 2).

depth (m)	bottle #	bulk δ238U	2SD^	2SE^	n
2077	1	-0.76	0.06	0.05	2
1500	2	-0.85	0.12^	0.12^	1
1000	3	-0.70	0.01	0.01	2
750	4	-0.71	0.12^	0.12^	1
500	5	-0.72	0.13	0.09	2
250	6	-0.47	0.12^	0.12^	1
187	7	-0.45	0.46	0.33	2
170	8	-0.45	0.06	0.04	2
150	9	-0.43	0.12	0.06	4
140	10	-0.37	0.15	0.10	2
130	11	-0.36	0.10	0.06	3
120	12/13	-0.39	0.06	0.04	3
115	14	-0.39	0.12^	0.12^	1
110	15	-0.49	0.08	0.06	2
105	16	-0.41	0.04	0.03	2
100	17	-0.46	0.05	0.03	2
95	18	-0.61	0.06	0.04	2
90	19	-0.53	0.12^	0.12^	1
85	20	-0.39	0.12^	0.12^	1
80	21	-0.50	0.14	0.10	2
60	22	-0.40	0.12^	0.12^	1
30	23	-0.36	0.03	0.02	2
10	24	-0.43	0.09	0.06	2

^Based on an average of the standard deviations of BCR.
Average δ = -0.32. 2SD = 0.12. N=10.

Appendix 4-7-1-1: 0.2 μm filtered sea water concentration data at Black Sea (St. 8)

bottle #	depth (m)	V (nmol/L)	Mn (μmol/L)	Fe (μmol/L)	Co (nmol/L)	Ni (nmol/L)	Cu (nmol/L)	As (nmol/L)	Sr (μmol/L)
1	55	16.09	3.06	1.55	0.17	14.89	12.40	17.21	50.80
2	50	14.44	3.03	1.52	0.19	14.45	12.17	16.58	48.78
3	45	15.23	3.03	1.53	0.05	15.01	11.61	15.70	48.42
4	39	13.80	3.02	1.54	b.d.l.	15.41	12.05	14.37	48.54
5	37	14.86	3.02	1.52	0.06	15.46	11.30	15.44	48.16
6	35	16.03	3.03	2.16	0.36	16.16	21.04	10.57	48.32
7	30	13.36	3.01	1.50	b.d.l.	12.90	11.02	11.67	47.97
8	25	13.17	3.01	1.53	0.03	14.01	12.63	13.42	47.68
9	20	13.67	3.01	1.59	b.d.l.	14.93	12.18	10.66	47.76
10	15	12.68	3.01	1.52	b.d.l.	13.53	12.52	10.18	47.88
11	10	13.53	3.01	1.52	0.16	15.70	12.75	12.25	47.16
12	5	14.89	3.02	1.53	0.05	12.81	14.38	12.75	46.64

Appendix 4-7-1-1 cont.: 0.2 μm filtered sea water concentration data at Black Sea (St. 8)

bottle #	depth (m)	Mo (nmol/L)	Cd (nmol/L)	Sb (nmol/L)	Ba (μmol/L)	Re (nmol/L)	Tl (nmol/L)	U (nmol/L)
1	55	61.75	0.33	1.66	0.19	0.22	b.d.l.	8.66
2	50	62.78	0.37	1.66	0.16	0.19	b.d.l.	8.29
3	45	60.63	0.47	1.38	0.13	0.20	b.d.l.	8.57
4	39	60.96	0.47	1.86	0.14	0.19	b.d.l.	8.19
5	37	59.10	0.63	1.60	0.13	0.20	b.d.l.	8.22
6	35	60.57	0.77	1.80	0.12	0.21	b.d.l.	8.10
7	30	60.50	0.22	1.73	0.09	0.22	b.d.l.	8.41
8	25	61.81	0.38	1.94	0.09	0.20	b.d.l.	8.28
9	20	60.73	0.66	1.94	0.04	0.19	b.d.l.	8.39
10	15	61.17	0.42	1.80	0.04	0.22	b.d.l.	8.62
11	10	61.64	0.48	1.43	0.05	0.21	b.d.l.	8.47
12	5	59.93	0.24	1.86	0.05	0.20	b.d.l.	8.35

Appendix 4-7-1-2: Pore water concentration data at Black Sea (St. 8)

core(s)	depth (cm)	V (nmol/L)	Cr (nmol/L)	Mn (μmol/L)	Fe (μmol/L)	Co (nmol/L)	Ni (nmol/L)	Cu (nmol/L)	As (nmol/L)	Sr (μmol/L)
1-3	BW	18.60	b.d.l.	3.57	0.30	0.93	14.44	4.13	19.85	48.52
1-3	1	31.33	b.d.l.	10.01	9.18	23.85	35.66	0.91	37.69	48.02
1-3	2	44.31	1.48	7.30	3.76	15.62	32.38	4.47	46.22	50.36
1-3	3	67.07	b.d.l.	8.44	2.70	12.16	30.38	0.37	65.49	49.81
1-3	4	47.93	0.14	8.02	3.03	6.14	24.00	b.d.l.	71.45	46.15
1-3	5	53.41	b.d.l.	10.57	1.80	5.05	24.84	b.d.l.	82.05	49.64
1-3	6	48.03	1.07	12.98	1.70	3.18	20.79	b.d.l.	62.88	48.37
1-3	8	295.31	5.80	14.79	0.78	7.44	31.14	b.d.l.	372.21	48.24
1-3	10	639.31	5.03	12.38	0.36	19.68	55.60	b.d.l.	2524.81	48.27
1-3	12	737.74	5.46	9.62	0.34	14.07	38.49	0.05	2807.04	48.66
1-3	14	351.15	2.68	12.96	0.29	3.00	13.74	b.d.l.	1291.51	48.99
1-3	16	281.00	0.18	12.79	0.35	2.40	12.34	b.d.l.	1175.04	48.78
1-3	18	201.69	b.d.l.	11.88	0.22	1.92	9.15	b.d.l.	742.07	49.16

Appendix 4-7-1-2 cont.: Pore water concentration data at Black Sea (St. 8)

core(s)	depth (cm)	Mo (nmol/L)	Cd (nmol/L)	Sb (nmol/L)	Ba (µmol/L)	Ce (nmol/L)	Nd (nmol/L)	Re (nmol/L)	Tl (nmol/L)	U (nmol/L)
1-3	BW	59.03	0.12	1.71	0.17	0.75	b.d.l.	0.20	0.59	8.56
1-3	1	62.53	b.d.l.	5.36	0.23	b.d.l.	0.21	0.21	0.63	8.67
1-3	2	63.25	0.16	12.90	0.23	1.88	0.07	0.21	0.67	10.34
1-3	3	68.50	b.d.l.	20.59	0.26	b.d.l.	b.d.l.	0.21	0.66	15.23
1-3	4	65.45	b.d.l.	12.93	0.24	1.91	0.01	0.21	0.64	11.17
1-3	5	69.06	b.d.l.	12.46	0.28	6.41	0.14	0.21	0.62	10.97
1-3	6	66.00	b.d.l.	8.55	0.29	1.98	0.10	0.22	0.60	8.57
1-3	8	128.22	b.d.l.	100.49	0.40	11.03	0.43	0.26	0.69	77.77
1-3	10	555.77	0.26	193.21	0.44	7.04	0.26	0.54	0.60	180.92
1-3	12	1183.79	0.57	166.72	0.43	5.34	0.21	0.48	0.59	175.61
1-3	14	925.27	0.50	70.24	0.42	2.83	0.10	0.30	0.56	69.06
1-3	16	486.98	0.13	58.60	0.38	0.88	0.16	0.23	0.57	68.67
1-3	18	533.49	b.d.l.	49.82	0.38	b.d.l.	0.08	0.23	0.56	60.43

Appendix 4-7-1-3: Pore water concentration data at Black Sea Shelf Break (St. 7)

core(s)	depth (cm)	V (nmol/L)	Cr (nmol/L)	Mn (µmol/L)	Fe (µmol/L)	Co (nmol/L)	Ni (nmol/L)	Cu (nmol/L)	As (nmol/L)	Sr (µmol/L)
1	2	55.32	b.d.l.	4.56	1.26	10.74	47.22	4.07	32.13	48.27
1	4	59.92	b.d.l.	12.73	3.20	8.93	41.87	4.03	72.47	47.72
1	6	20.41	b.d.l.	18.77	0.64	2.02	15.97	b.d.l.	34.28	47.54
1	8	58.67	b.d.l.	16.99	b.d.l.	4.26	40.95	b.d.l.	899.92	47.31
1	10	58.04	b.d.l.	8.13	b.d.l.	5.60	42.58	b.d.l.	360.02	47.21
1	12	33.89	b.d.l.	19.17	b.d.l.	0.86	10.42	b.d.l.	360.58	48.16
1	14	237.42	b.d.l.	14.27	b.d.l.	3.82	24.39	b.d.l.	1707.39	47.91
1	16	123.41	b.d.l.	15.10	b.d.l.	0.63	23.74	1.49	1224.34	47.90
1	18	340.80	b.d.l.	12.39	b.d.l.	1.07	8.07	b.d.l.	972.65	49.90
1	20	55.41	b.d.l.	13.64	b.d.l.	b.d.l.	3.90	b.d.l.	136.24	49.92

core(s)	depth (cm)	Mo (nmol/L)	Cd (nmol/L)	Sb (nmol/L)	Ba (µmol/L)	Ce (nmol/L)	Nd (nmol/L)	Re (nmol/L)	Tl (nmol/L)	U (nmol/L)
1	2	63.52	0.41	9.59	0.22	3.53	0.15	0.19	1.04	9.59
1	4	71.62	0.41	9.53	0.28	9.16	0.65	0.19	0.79	7.17
1	6	56.09	0.50	3.33	0.30	1.07	0.14	0.17	0.74	3.35
1	8	163.77	0.61	56.33	0.31	0.87	0.24	0.21	0.85	22.79
1	10	93.74	0.47	16.42	0.24	0.18	0.03	0.21	0.81	14.38
1	12	173.75	0.40	11.50	0.34	13.65	0.17	0.19	0.73	12.25
1	14	1072.61	0.57	68.78	0.35	0.78	0.11	0.23	0.75	70.11
1	16	1043.81	0.51	70.48	0.34	1.02	0.18	0.18	0.74	48.81
1	18	1205.09	1.05	42.75	0.34	0.97	0.14	0.17	0.72	34.33
1	20	245.79	0.50	5.49	0.30	2.46	0.33	0.17	0.73	8.84

Appendix 4-7-2-1: 0.2 μm filtered sea water concentration data at Black Sea Shelf Break site (St. 6)

bottle #	depth (m)	V (nmol/L)	Mn (μmol/L)	Fe (μmol/L)	Co (nmol/L)	Ni (nmol/L)	Cu (nmol/L)	As (nmol/L)	Sr (μmol/L)
2	122	19.34	3.34	3.04	1.24	16.13	7.26	34.92	53.54
3	119	20.34	3.34	3.03	0.98	15.08	8.14	31.89	53.57
4	115	19.31	3.34	3.04	1.02	16.29	8.47	27.41	53.05
5	110	20.21	3.34	3.03	1.01	16.16	8.58	36.36	53.23
6	105	19.70	3.33	3.04	1.12	17.32	10.23	30.57	52.59
7	100	18.99	3.33	3.02	1.00	17.94	9.53	31.93	52.02
8	95	20.32	3.35	3.06	1.47	26.55	80.71	33.57	51.89
9	90	18.73	3.35	3.06	1.12	16.60	10.47	33.19	51.28
10	85	17.72	3.33	3.05	1.06	15.52	10.75	24.02	51.18
11	80	16.39	3.34	3.04	1.10	15.83	10.80	22.55	50.45
12	75	16.52	3.34	3.05	1.17	15.79	10.70	21.86	49.80
13	70	15.98	3.33	3.04	1.04	15.16	10.58	20.94	50.15
14	65	15.43	3.34	3.05	1.09	16.00	11.90	18.77	50.25
15	60	13.81	3.33	3.03	1.04	16.61	10.68	17.35	50.09
16	55	13.39	3.33	3.04	1.19	15.41	11.58	17.31	50.03
17	50	13.82	3.33	3.04	1.15	15.73	10.62	20.78	50.52
18	45	14.69	3.33	3.03	1.11	16.35	10.65	13.33	50.41
19	40	9.78	3.33	3.04	1.10	14.16	9.55	9.80	40.17
20	35	13.81	3.33	3.06	1.08	16.23	12.05	16.87	51.38
21	30	12.04	3.34	3.06	1.23	14.73	10.58	12.70	50.05
22	25	12.63	3.34	3.05	1.25	15.61	12.37	14.17	49.97
23	20	11.90	3.34	3.02	1.21	17.02	11.55	15.91	50.45
24	10	12.72	3.34	3.04	1.25	16.41	11.86	14.14	50.88

Appendix 4-7-2-1 cont.: 0.2 µm filtered sea water concentration data at Black Sea Shelf Break site (St. 6)

bottle #	depth (m)	Mo (nmol/L)	Cd (nmol/L)	Sb (nmol/L)	Ba (µmol/L)	Re (nmol/L)	Tl (nmol/L)	U (nmol/L)
2	122	61.84	0.58	1.35	0.30	b.d.l.	0.03	8.47
3	119	61.63	0.64	1.23	0.30	b.d.l.	0.04	8.57
4	115	61.97	0.62	1.41	0.28	b.d.l.	0.05	8.55
5	110	62.62	0.69	1.48	0.28	b.d.l.	0.04	8.69
6	105	59.41	0.47	1.58	0.25	b.d.l.	0.05	8.57
7	100	62.90	0.62	1.69	0.24	b.d.l.	0.05	8.59
8	95	62.82	0.86	1.61	0.24	b.d.l.	0.04	8.39
9	90	61.80	0.59	1.51	0.23	b.d.l.	0.03	8.42
10	85	60.37	0.33	1.50	0.18	b.d.l.	0.04	8.65
11	80	61.74	0.69	1.82	0.16	b.d.l.	0.04	8.54
12	75	59.41	0.54	1.97	0.14	b.d.l.	0.04	8.54
13	70	61.40	0.54	1.98	0.13	b.d.l.	0.05	8.75
14	65	60.07	0.48	1.70	0.12	b.d.l.	0.04	8.65
15	60	63.07	0.43	1.84	0.12	b.d.l.	0.04	8.67
16	55	60.05	0.49	1.90	0.11	b.d.l.	0.04	8.66
17	50	59.70	0.61	1.91	0.11	b.d.l.	0.04	8.57
18	45	58.13	0.37	2.02	0.11	b.d.l.	0.04	8.47
19	40	48.90	0.43	1.36	0.08	b.d.l.	0.04	6.48
20	35	59.03	0.33	1.71	0.10	b.d.l.	0.05	8.82
21	30	59.17	0.41	2.15	0.10	b.d.l.	0.06	8.97
22	25	58.16	0.56	2.09	0.09	b.d.l.	0.05	8.72
23	20	58.21	0.23	1.95	0.10	b.d.l.	0.05	8.43
24	10	58.97	0.55	2.36	0.03	b.d.l.	0.06	8.67

Appendix 4-7-3-1: Pore water concentration data at Black Sea (St. 3 - cores 1-2)

core(s)	depth (cm)	V (nmol/L)	Cr (nmol/L)	Mn (µmol/L)	Fe (µmol/L)	Co (nmol/L)	Ni (nmol/L)	Cu (nmol/L)	As (nmol/L)	Sr (µmol/L)
1-2	Sed. Surf.	29.61	4.56	3.55	0.36	1.24	20.80	3.33	29.77	53.26
1	1	46.48	7.12	5.56	0.51	2.74	34.01	1.31	46.31	51.99
1	2	133.89	10.27	6.48	0.57	6.85	57.19	b.d.l.	209.42	53.00
1-2	3	109.90	5.73	13.01	0.56	11.65	79.21	b.d.l.	726.44	53.42
1-2	4	471.13	9.84	13.94	0.37	25.73	126.39	b.d.l.	1875.45	53.63
1-2	5	137.47	1.94	12.41	0.31	9.74	48.10	b.d.l.	598.68	53.53
1-2	6	168.72	7.62	12.57	0.42	8.61	42.71	b.d.l.	540.93	53.97
1-2	8	110.06	6.22	17.01	0.32	4.23	24.36	b.d.l.	536.05	52.63
1-2	10	70.63	5.00	15.30	0.33	3.28	22.09	b.d.l.	270.37	52.22
1-2	12	32.85	4.99	21.33	0.33	2.73	13.19	b.d.l.	232.73	52.59
1-2	14	81.66	15.46	20.20	0.57	2.18	10.81	1.46	390.68	53.72
1-2	16	121.39	4.16	20.23	0.32	1.37	7.71	b.d.l.	118.70	53.43
1-2	18	132.84	5.84	18.79	0.32	1.60	7.56	b.d.l.	165.59	54.08
1-2	20	173.92	6.26	18.54	0.30	2.20	11.71	b.d.l.	105.39	52.99

Appendix 4-7-3-1 cont.: Pore water concentration data at Black Sea (St. 3 - cores 1-2)

core(s)	depth (cm)	Mo (nmol/L)	Cd (nmol/L)	Sb (nmol/L)	Ba (µmol/L)	Ce (nmol/L)	Nd (nmol/L)	Re (nmol/L)	Tl (nmol/L)	U (nmol/L)
1-2	Sed. Surf.	63.22	b.d.l.	2.44	0.32	3.23	0.20	0.21	0.60	8.93
1	1	65.63	0.21	5.51	0.34	3.69	0.18	0.22	0.61	8.70
1	2	85.26	b.d.l.	18.85	0.37	5.31	0.41	0.21	0.64	12.91
1-2	3	324.55	0.12	65.43	0.40	5.68	0.23	0.24	0.63	26.82
1-2	4	1140.57	0.81	153.33	0.45	8.71	0.48	0.27	0.62	94.94
1-2	5	351.33	0.10	35.01	0.38	3.91	0.19	0.20	0.60	26.54
1-2	6	339.58	0.07	31.40	0.40	13.79	0.47	0.24	0.58	27.72
1-2	8	373.38	0.09	34.43	0.41	4.88	0.29	0.21	0.57	22.75
1-2	10	190.17	b.d.l.	16.53	0.40	5.89	0.32	0.21	0.56	14.81
1-2	12	158.25	0.01	12.69	0.40	9.25	0.37	0.20	0.56	11.71
1-2	14	298.91	0.01	21.43	0.42	26.99	0.99	0.20	0.57	35.68
1-2	16	86.83	b.d.l.	5.33	0.41	6.31	0.39	0.18	0.55	25.41
1-2	18	145.50	b.d.l.	6.69	0.41	7.13	0.34	0.19	0.56	37.57
1-2	20	143.64	0.17	5.96	0.43	5.09	0.39	0.18	0.56	76.94

Appendix 4-7-3-2: Pore water concentration data at Black Sea (St. 3 - cores 2-3)

core(s)	depth (cm)	V (nmol/L)	Cr (nmol/L)	Mn (µmol/L)	Fe (µmol/L)	Co (nmol/L)	Ni (nmol/L)	Cu (nmol/L)	As (nmol/L)	Sr (µmol/L)
2-3	Sed. Surf.	39.80	b.d.l.	3.69	0.29	0.97	20.21	0.19	31.54	52.76
2-3	1	45.33	b.d.l.	8.79	1.67	4.95	36.65	b.d.l.	40.27	52.76
2	2	53.33	b.d.l.	5.26	0.42	2.28	30.93	3.54	69.30	52.98
3	2	180.88	b.d.l.	10.39	0.92	7.19	75.95	b.d.l.	322.34	54.45
2-3	3	110.67	b.d.l.	10.50	0.56	10.45	102.89	b.d.l.	504.85	53.69
2	4	75.76	b.d.l.	5.90	0.33	3.22	40.00	5.63	273.02	53.31
2-3	4	105.02	b.d.l.	11.99	0.46	7.77	77.55	b.d.l.	545.68	53.45
2-3	5	71.10	b.d.l.	17.00	0.33	6.94	44.56	b.d.l.	436.38	54.43
2-3	6	58.80	b.d.l.	17.45	0.31	5.70	34.82	b.d.l.	263.44	53.03
2-3	8	769.21	b.d.l.	16.15	0.25	22.66	69.68	b.d.l.	1539.03	52.75
2-3	10	81.37	b.d.l.	20.13	0.28	3.74	16.48	b.d.l.	366.85	53.68
2-3	12	560.20	b.d.l.	17.52	0.27	21.14	69.48	b.d.l.	1740.09	52.63
2-3	14	222.37	b.d.l.	19.45	0.25	4.25	21.39	b.d.l.	710.54	53.71
2-3	16	125.85	b.d.l.	20.41	0.25	2.40	13.75	b.d.l.	367.69	53.75
2-3	18	177.25	b.d.l.	18.57	0.25	1.53	9.68	b.d.l.	198.56	53.67
2-3	20	232.62	b.d.l.	17.76	0.26	2.62	14.15	b.d.l.	311.92	53.16

Appendix 4-7-3-2 cont.: Pore water concentration data at Black Sea (St. 3 - cores 2-3)

core(s)	depth (cm)	Mo (nmol/L)	Cd (nmol/L)	Sb (nmol/L)	Ba (µmol/L)	Ce (nmol/L)	Nd (nmol/L)	Re (nmol/L)	Tl (nmol/L)	U (nmol/L)
2-3	Sed. Surf.	63.83	0.21	4.26	0.31	b.d.l.	0.03	0.21	0.62	9.21
2-3	1	65.54	b.d.l.	14.82	0.36	b.d.l.	b.d.l.	0.21	0.62	11.00
2	2	68.94	0.09	12.02	0.34	b.d.l.	b.d.l.	0.20	0.63	9.89
3	2	108.61	0.07	91.58	0.38	1.16	b.d.l.	0.22	1.03	22.49
2-3	3	123.45	0.01	60.42	0.39	b.d.l.	b.d.l.	0.21	0.74	17.40
2	4	131.10	0.34	18.82	0.33	b.d.l.	0.03	0.21	0.60	12.60
2-3	4	143.91	0.03	57.96	0.39	b.d.l.	b.d.l.	0.21	0.65	20.24
2-3	5	195.13	b.d.l.	31.71	0.40	b.d.l.	0.01	0.20	0.57	16.77
2-3	6	131.17	b.d.l.	18.90	0.40	b.d.l.	0.29	0.21	0.58	9.27
2-3	8	1186.80	0.71	145.84	0.42	b.d.l.	b.d.l.	0.26	0.58	96.83
2-3	10	466.28	0.10	25.97	0.41	b.d.l.	0.01	0.20	0.56	23.48
2-3	12	2283.67	1.32	185.43	0.44	b.d.l.	b.d.l.	0.51	0.60	153.38
2-3	14	779.01	0.61	52.54	0.41	b.d.l.	0.09	0.27	0.56	66.97
2-3	16	145.45	b.d.l.	9.86	0.41	b.d.l.	b.d.l.	0.20	0.57	35.29
2-3	18	145.85	b.d.l.	7.98	0.41	b.d.l.	0.93	0.19	0.55	47.51
2-3	20	322.25	b.d.l.	13.48	0.41	0.44	0.01	0.18	0.56	92.41

Appendix 5: Modern day comparison – Baltic Sea

Appendix 5-1: Overview of modern day comparison – Baltic Sea

Hypoxia and euxinia occurs periodically in some of the basins in the Baltic Sea (Appendix 5-2; 5-3) (Fonselius, 1963; Zillén et al., 2008; Conley et al., 2009a). The Baltic Sea is composed of a series of sub-basins with shallow sills separating them (Omstedt, 1990). The sub-basins receive waters from the rivers in the surrounding river catchment systems (Bergstrom, 1994), and also seawater from the North Sea during inflow events (Kõuts and Omstedt, 1993), and consequently have brackish salinity (range 5-18). The inflow events play an important role to changing the salinity and oxygenation levels in the bottom waters of many of the sub-basins (Fonselius, 1981; Matthäus and Franck, 1992; Kõuts and Omstedt, 1993). Occurring at least once a decade (along with many minor events), major inflow events occur under prolonged meteorological conditions (Schinke and Matthäus, 1998) with strong easterly winds that cause a drop in sea level in Baltic Proper (Matthäus and Franck, 1992; Wieczorek, 2012; Lehmann and Post, 2015). The sea level change allows water from the North Sea to propagate as new bottom water, progressively mixing with the existing water (Conley et al., 2002); therefore reducing the residence time of deep waters (Meier, 2005). The result of the inflows temporarily deliver oxygen to the bottom waters, but once depleted, conditions become anoxic within months until the next inflow for deeper sites (Schinke and Matthäus, 1998), or strong wind mixing in shallow sites can break the stratification related to the salinity gradient (Fonselius, 1981; Meier, 2005).

Over the past century, the extent of hypoxia in the Baltic expanded 10-times to cover 60,000 km^2 (Carstensen et al., 2014). Driven by eutrophication, the hypoxia

expansion impacts the entire ecosystem and sediment geochemistry (Conley et al., 2009b). Observed sedimentary changes include accelerated recycling of phosphorus (Conley et al., 2002; Mort et al., 2010) and a shift from denitification to anammox (Hannig et al., 2007). Additionally, the sediments in the deep euxinic basins show that iron and manganese shuttles exist, similar to the Black Sea (Jilbert and Slomp, 2013).

Uranium studies in the Baltic Sea show many similar trends to those observed in other restricted basins. In oxygenated waters, U concentration has a strong correlation with salinity (Prange and Kremling, 1985; Lofvendahl, 1987). In the water column, non-conservative behavior occurs in anoxic sub-basins (Lofvendahl, 1987). The depletion of U can be up to 48%, which is more than any other euxinic basin (Andersson et al., 1995). The cause for the depletion is due to U diffusion into the sediments (Skwarzec et al., 2002; Noordmann et al., 2015). Knowledge of $\delta^{238}U$ in the Baltic sediments and water column is limited to one study at Landsort Deep, the deepest part of the Baltic and persistently euxinic, which reports delta values with a range of -0.13 to -0.39 ‰, with an average value of -0.30 in the top 15 cm of sediments (Noordmann et al., 2015). By studying additional sites, a more complete picture of the controls and dynamics of $\delta^{238}U$ will be clearer.

References:

Andersson, P.S., Wasserburg, G.J., Chen, J.H., Papanastassiou, D.A., and Ingri, J., 1995, ^{238}U-^{234}U and ^{232}Th-^{230}Th in the Baltic Sea and in River Water: Earth and Planetary Science Letters, v. 130, p. 217-234, doi: 10.1016/0012-821x(94)00262-W.

Bergstrom, S., 1994, River runoff to the Baltic Sea: 1950-1990: Ambio, v. 23, p. 280-287.

Carstensen, J., Andersen, J.H., Gustafsson, B.G., and Conley, D.J., 2014, Deoxygenation of the Baltic Sea during the last century: Proc Natl Acad Sci U S A, v. 111, p. 5628-5633, doi: 10.1073/pnas.1323156111.

Conley, D.J., Bjorck, S., Bonsdorff, E., Carstensen, J., Destouni, G., Gustafsson, B.G., Hietanen, S., Kortekaas, M., Kuosa, H., Meier, H.E., Muller-Karulis, B., Nordberg, K., Norkko, A., Nurnberg, G., Pitkanen, H., Rabalais, N.N., Rosenberg, R., Savchuk, O.P., Slomp, C.P., Voss, M., Wulff, F., and Zillen, L., 2009a, Hypoxia-related processes in the Baltic Sea: Environ Sci Technol, v. 43, p. 3412-3420.

Conley, D.J., Carstensen, J., Vaquer-Sunyer, R., and Duarte, C.M., 2009b, Ecosystem thresholds with hypoxia: Hydrobiologia, v. 629, p. 21-29, doi: 10.1007/s10750-009-9764-2.

Conley, D.J., Humborg, C., Rahm, L., Savchuk, O.P., and Wulff, F., 2002, Hypoxia in the Baltic Sea and basin-scale changes in phosphorus biogeochemistry: Environ Sci Technol, v. 36, p. 5315-5320.

Fonselius, S., 1981, Oxygen and hydrogen sulphide conditions in the Baltic Sea: Marine Pollution Bulletin, v. 12, p. 187-194.

Fonselius, S.H., 1963, Hydrogen sulfide basins and a stagnant period in the Baltic Sea: Journal of Geophysical Research, v. 68, p. 4009-4016.

Hannig, M., Lavik, G., Kuypers, M.M.M., Woebken, D., Martens-Habbena, W., and Jurgens, K., 2007, Shift from denitrification to anammox after inflow events in the central Baltic Sea: Limnology and Oceanography, v. 52, p. 1336-1345, doi: 10.4319/lo.2007.52.4.1336.

Jilbert, T., and Slomp, C.P., 2013, Iron and manganese shuttles control the formation of authigenic phosphorus minerals in the euxinic basins of the Baltic Sea: Geochimica et Cosmochimica Acta, v. 107, p. 155-169, doi: 10.1016/j.gca.2013.01.005.

Kõuts, T., and Omstedt, A., 1993, Deep water exchange in the Baltic Proper: Tellus A, v. 45, p. 311-324.

Lehmann, A., and Post, P., 2015, Variability of atmospheric circulation patterns associated with large volume changes of the Baltic Sea: Advances in Science and Research, v. 12, p. 219-225.

Lofvendahl, R., 1987, Dissolved Uranium in the Baltic Sea: Marine Chemistry, v. 21, p. 213-227, doi: 10.1016/0304-4203(87)90060-0.

Matthäus, W., and Franck, H., 1992, Characteristics of major Baltic inflows—a statistical analysis: Continental Shelf Research, v. 12, p. 1375-1400.

Meier, H.E.M., 2005, Modeling the age of Baltic Seawater masses: Quantification and steady state sensitivity experiments: Journal of Geophysical Research: Oceans, v. 110, doi: 10.1029/2004JC002607.

Mort, H.P., Slomp, C.P., Gustafsson, B.G., and Andersen, T.J., 2010, Phosphorus recycling and burial in Baltic Sea sediments with contrasting redox conditions: Geochimica et Cosmochimica Acta, v. 74, p. 1350-1362.

Noordmann, J., Weyer, S., Montoya-Pino, C., Dellwig, O., Neubert, N., Eckert, S., Paetzel, M., and Böttcher, M.E., 2015, Uranium and molybdenum isotope systematics in modern euxinic basins: Case studies from the central Baltic Sea

and the Kyllaren fjord (Norway): Chemical Geology, v. 396, p. 182-195, doi: 10.1016/j.chemgeo.2014.12.012.

Omstedt, A., 1990, Modelling the Baltic Sea as thirteen sub-basins with vertical resolution: Tellus A, v. 42, p. 286-301, doi: 10.1034/j.1600-0870.1990.00006.x.

Prange, A., and Kremling, K., 1985, Distribution of Dissolved Molybdenum, Uranium and Vanadium in Baltic Sea Waters: Marine Chemistry, v. 16, p. 259-274, doi: 10.1016/0304-4203(85)90066-0.

Schinke, H., and Matthäus, W., 1998, On the causes of major Baltic inflows —an analysis of long time series: Continental Shelf Research, v. 18, p. 67-97, doi: 10.1016/S0278-4343(97)00071-X.

Skwarzec, B., Borylo, A., and Struminska, D., 2002, ^{234}U and ^{238}U isotopes in water and sediments of the southern Baltic: J Environ Radioact, v. 61, p. 345-363.

Wieczorek, G., 2012, Spatiotemporal scales of the deep circulation in the Eastern Gotland Basin, Baltic Sea [PhD: Leibniz-Insitut fur Osteeforschung].

Zillén, L., Conley, D.J., Andrén, T., Andrén, E., and Björck, S., 2008, Past occurrences of hypoxia in the Baltic Sea and the role of climate variability, environmental change and human impact: Earth-Science Reviews, v. 91, p. 77-92, doi: 10.1016/j.earscirev.2008.10.001.

Appendix 5-2: Map of Baltic Sea sites

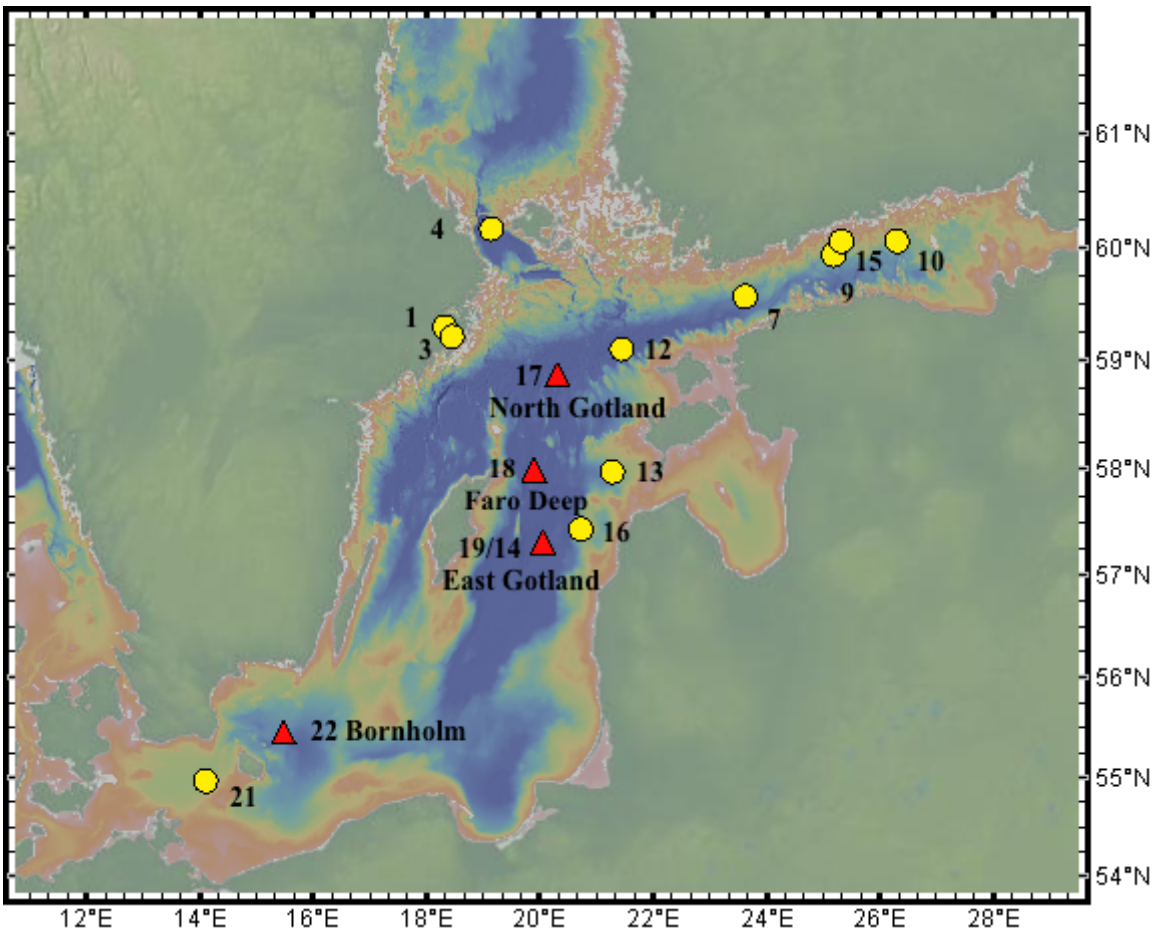

Key stations noted with red triangles and basin name. Minor stations are marked with yellow circles.

Appendix 5-3: Baltic Sea site descriptions by region

St.	depth (m)	BW O_2 (μM/kg)	H_2S (μM/kg)
East Gotland			
St. 14/St. 19*	237	10.3	
St. 13	67	154.7	
St. 16	65	16.3	
North Gotland			
St. 17*	173		6.32
St. 12	135		15.64
Stockholm Archipelago			
St. 1	40	205.9	
St. 3	37	310.4	
Gulf of Finland			
St. 7	80		17.94
St. 9	65	15.4	
St. 10	60	21.8	
St. 15	55	109.4	
Faro Deep			
St. 18*	294		6.0^
Bornholm Basin			
St. 22*	87	49.8	
Arkona Basin			
St. 21	47	238.5	
Aland-Bothnian exchange			
St. 4	290	325.5	

*Key stations that were studied more throughly.
^This concentration is from the multi core sample as the water column bottom water sample had time to degas before measurement.

Appendix 5-4-1: Sedimentary Baltic North Gotland (St. 17) auxiliary data

depth (cm)	Mg (mg/g)	Al (mg/g)	Ca (mg/g)	Ti (µg/g)	V (µg/g)	Cr (µg/g)	Mn (mg/g)	Fe (mg/g)	Co (µg/g)	U (µg/g)
0.5	12.25	46.61	6.56	2.51	72.50	53.49	0.28	31.82	10.85	31.60
1.5	12.66	50.55	6.56	2.74	90.05	58.77	0.34	38.48	14.15	50.86
2.5	13.84	60.18	7.10	3.06	154.71	69.35	0.63	55.57	35.08	24.92
3.5	15.14	63.43	8.10	3.14	166.12	73.31	0.73	49.47	34.87	15.91
4.5	14.46	58.64	7.92	3.04	137.18	75.71	0.93	59.41	29.92	18.67
5.5	12.85	57.13	6.70	2.73	134.43	71.79	1.63	77.52	39.70	17.21
6.5	14.42	68.43	6.63	3.34	117.62	76.20	5.24	76.06	44.75	8.09
8.5	16.73	78.48	6.88	4.01	120.99	83.56	1.08	52.26	21.82	6.01
10.5	16.12	76.67	6.46	4.08	118.68	86.98	0.85	53.74	20.28	5.57
12.5	12.59	55.86	5.67	4.27	121.26	89.04	0.82	55.28	19.62	5.44
15.5	13.06	56.39	5.71	4.32	122.04	91.21	0.92	57.11	20.26	4.09
18.5	16.03	75.70	6.18	3.98	113.31	83.03	0.88	57.36	19.49	5.55
21.5	16.98	78.47	6.37	4.22	119.14	89.25	0.98	57.47	19.03	5.72
24.5	16.05	76.46	6.16	4.03	115.15	86.51	1.03	56.05	18.83	5.80
26.5	15.67	70.81	6.10	4.13	118.04	86.82	1.03	54.34	19.74	5.27
28.5	14.90	68.16	6.18	4.11	118.62	88.44	1.00	55.93	18.93	5.82
30.5	15.91	72.72	6.37	3.94	114.45	86.21	1.00	55.17	19.42	5.08
32.5	16.62	78.89	6.54	4.26	121.74	89.01	0.95	50.61	17.96	5.87
34.5	17.16	83.32	6.70	4.14	116.59	86.15	0.84	52.10	19.62	5.22
36.5	17.86	85.24	6.83	4.28	121.61	89.01	0.88	50.28	16.28	5.08

Appendix 5-4-1 cont.: Sedimentary Baltic North Gotland (St. 17) auxiliary data

depth (cm)	Ni (µg/g)	Cu (µg/g)	Sr (µg/g)	Mo (µg/g)	Cd (µg/g)	Ba (µg/g)	Ce (µg/g)	Nd (µg/g)	Th (µg/g)	U (µg/g)
0.5	56.37	94.83	110.96	110.09	0.47	413.13	61.54	25.82	9.33	31.60
1.5	78.23	140.46	114.04	174.74	1.55	580.23	74.13	30.09	10.50	50.86
2.5	120.50	89.13	123.78	181.40	4.74	632.69	103.23	39.88	13.74	24.92
3.5	111.37	84.62	109.28	174.04	4.18	564.19	82.46	34.57	11.67	15.91
4.5	101.73	119.22	122.98	169.73	7.04	575.67	104.62	40.67	13.78	18.67
5.5	101.19	125.16	116.39	151.58	11.70	598.36	96.22	38.83	12.15	17.21
6.5	60.15	47.76	126.36	26.11	2.72	617.02	119.43	46.67	16.96	8.09
8.5	50.02	41.63	121.80	8.33	1.39	591.41	99.58	40.76	15.31	6.01
10.5	48.09	42.37	132.18	8.15	0.92	623.88	121.64	46.74	17.33	5.57
12.5	52.01	38.64	114.38	8.50	0.80	523.12	31.84	18.19	6.00	5.44
15.5	51.31	38.10	111.30	4.68	0.59	510.41	40.41	21.63	6.77	4.09
18.5	47.36	38.21	134.63	5.25	0.72	608.68	127.89	48.46	18.93	5.55
21.5	49.56	41.05	133.91	4.30	0.74	600.47	118.85	46.34	18.14	5.72
24.5	49.28	37.44	134.61	7.05	0.75	635.77	123.74	48.50	18.72	5.80
26.5	50.73	38.36	128.06	10.90	0.56	587.60	73.02	34.01	12.86	5.27
28.5	50.27	38.41	133.56	8.89	0.46	618.82	65.08	30.43	10.96	5.82
30.5	50.00	36.08	137.35	8.77	0.35	647.26	97.13	41.79	14.57	5.08
32.5	48.46	38.41	122.97	9.91	0.57	623.81	104.37	42.14	16.49	5.87
34.5	47.08	56.31	128.86	6.46	0.47	650.29	103.67	41.77	19.06	5.22
36.5	45.98	46.94	125.36	5.99	0.45	630.35	108.41	44.20	17.06	5.08

Appendix 5-4-2: 0.2 μm filtered sea water concentration data at North Gotland, Baltic Sea (St. 17)

bottle #	depth (m)	V (nmol/L)	Cr (nmol/L)	Mn (μmol/L)	Fe (μmol/L)	Co (nmol/L)	Ni (nmol/L)	Cu (nmol/L)
1	161	4.94	15.82	2.69	0.37	1.71	19.55	2.41
2	151	5.45	19.47	2.48	0.38	1.83	19.94	2.32
3	141	4.84	19.47	2.31	0.36	1.75	20.35	2.31
4	131	4.87	18.18	2.27	0.37	1.84	20.10	2.20
5	121	4.64	18.64	2.65	0.51	1.77	19.70	2.25
7	111	4.69	19.05	2.36	0.39	1.77	19.86	2.45
8	101	4.76	18.89	2.57	0.45	1.80	21.19	2.25
9	91	4.51	19.00	2.60	0.34	1.88	21.22	2.26
11	81	4.61	19.10	3.02	0.17	1.85	20.23	2.18
13	75	4.02	18.82	1.42	0.12	1.58	21.31	2.32
14	70	3.74	19.43	0.63	0.12	1.41	23.38	3.41
17	41	4.39	20.66	0.03	0.12	1.43	21.22	6.36
20	20	4.17	20.25	0.02	0.11	1.33	21.02	6.73
22	10	4.09	20.70	0.01	0.11	1.39	21.89	7.23

Appendix 5-4-2 cont.: 0.2 μm filtered sea water concentration data at North Gotland, Baltic Sea (St. 17)

bottle #	depth (m)	As (nmol/L)	Sr (μmol/L)	Mo (nmol/)L	Sb (nmol/L)	Ba (nmol/L)	U (nmol/L)
1	161	8.29	31.48	22.15	0.77	80.74	4.01
2	151	8.40	32.06	22.45	0.83	80.19	4.01
3	141	8.01	31.88	22.11	0.73	78.19	3.91
4	131	8.15	31.52	21.93	0.89	80.91	3.95
5	121	8.32	30.56	20.72	0.72	80.15	3.73
7	111	7.88	30.56	20.33	0.77	79.66	3.74
8	101	7.89	29.94	20.43	0.81	79.08	3.74
9	91	8.13	29.56	19.93	0.76	79.52	3.70
11	81	8.27	28.69	18.81	0.74	80.58	3.30
13	75	7.83	27.85	18.13	0.69	76.13	3.15
14	70	7.97	27.21	17.63	0.67	78.38	3.18
17	41	7.41	19.24	16.70	0.82	81.95	2.87
20	20	7.25	18.20	16.05	0.74	77.46	2.62
22	10	7.37	17.53	15.94	0.81	78.15	2.53

Appendix 5-4-3: Pore water concentration data at North Gotland, Baltic Sea (St. 17 - core A & >18cm)

core (s)	depth (cm)	V (nmol/L)	Cr (nmol/L)	Mn (µmol/L)	Fe (µmol/L)	Co (nmol/L)	Ni (nmol/L)	Cu (nmol/L)	As (nmol/L)	Sr (µmol/L)
A	1	6.08	2.40	5.59	1.18	5.52	22.07	b.d.l.	13.77	27.86
A	2	7.65	2.42	5.19	1.25	4.70	18.54	5.95	13.25	26.96
A	3	28.79	2.93	9.34	2.03	2.77	16.75	b.d.l.	50.43	26.97
A	4	75.45	4.74	15.35	1.73	3.30	15.44	3.11	47.72	26.64
A	5	56.49	4.35	20.33	1.54	2.77	11.55	b.d.l.	33.66	27.00
A	6	50.10	4.07	23.31	1.28	2.60	7.38	b.d.l.	29.80	26.41
A	8	41.34	4.62	29.36	1.11	2.23	5.93	b.d.l.	24.77	26.80
A	10	48.14	7.29	41.66	1.02	3.30	12.92	21.82	19.13	27.09
A	12	39.86	5.56	47.94	0.71	2.56	7.17	b.d.l.	19.70	26.94
A	15	37.97	7.80	64.86	0.68	3.43	11.97	51.15	15.05	26.81
ABC	18	54.87	8.10	76.83	0.70	4.48	9.33	b.d.l.	14.58	26.21
ABC	24	69.14	11.56	106.25	0.71	7.49	12.54	2.33	10.42	26.63
ABC	28	63.48	11.96	111.40	0.70	7.22	10.10	b.d.l.	9.14	26.12
ABC	32	68.38	12.06	111.10	0.64	6.75	8.82	b.d.l.	9.00	25.77
ABC	36	65.43	14.10	108.46	0.68	7.06	10.24	b.d.l.	12.30	24.59

Appendix 5-4-3 cont.: Pore water concentration data at North Gotland, Baltic Sea (St. 17 - core A & >18cm)

core (s)	depth (cm)	Mo (nmol/L)	Cd (nmol/L)	Sb (nmol/L)	Ba (µmol/L)	Ce (nmol/L)	Nd (nmol/L)	Re (nmol/L)	Tl (nmol/L)	U (nmol/L)
A	1	69.23	0.04	0.80	0.15	0.05	b.d.l.	0.18	b.d.l.	5.77
A	2	65.70	b.d.l.	0.58	0.15	0.21	b.d.l.	0.19	b.d.l.	6.22
A	3	509.30	0.46	4.67	0.17	2.08	0.23	0.17	b.d.l.	23.24
A	4	704.69	0.57	5.27	0.20	4.35	0.29	0.16	b.d.l.	16.05
A	5	498.82	0.10	5.08	0.22	6.51	0.30	0.17	b.d.l.	14.58
A	6	437.31	0.31	4.22	0.23	1.38	0.21	0.14	b.d.l.	9.91
A	8	265.07	b.d.l.	2.24	0.26	0.63	0.08	0.15	b.d.l.	8.70
A	10	436.87	0.07	4.22	0.29	b.d.l.	0.21	0.14	b.d.l.	8.03
A	12	405.47	0.27	3.76	0.31	b.d.l.	0.05	0.16	b.d.l.	6.99
A	15	260.37	b.d.l.	3.70	0.36	b.d.l.	b.d.l.	0.15	b.d.l.	4.89
ABC	18	334.23	0.28	6.74	0.37	b.d.l.	0.01	0.16	b.d.l.	15.38
ABC	24	138.29	0.12	6.07	0.40	2.35	0.07	0.15	b.d.l.	10.36
ABC	28	41.34	0.02	5.93	0.38	0.82	0.10	0.15	b.d.l.	3.39
ABC	32	65.12	0.04	5.46	0.38	b.d.l.	b.d.l.	0.15	b.d.l.	4.14
ABC	36	49.62	b.d.l.	6.37	0.35	b.d.l.	0.10	0.14	b.d.l.	3.04

Appendix 5-4-4: Pore water concentration data at North Gotland, Baltic Sea (St. 17 - cores B&C)

core (s)	depth (cm)	V (nmol/L)	Cr (nmol/L)	Mn (µmol/L)	Fe (µmol/L)	Co (nmol/L)	Ni (nmol/L)	Cu (nmol/L)	As (nmol/L)	Sr (µmol/L)
B	1	5.51	1.24	7.46	1.17	2.67	17.62	b.d.l.	26.32	26.53
B	2	5.31	1.81	5.97	1.39	3.33	17.37	b.d.l.	18.06	27.13
B	3	27.04	3.13	12.19	1.47	1.86	12.36	b.d.l.	34.06	27.15
B	4	71.84	3.64	13.08	2.29	3.64	20.85	b.d.l.	57.43	26.91
B	5	66.67	4.58	20.71	1.24	2.99	10.65	b.d.l.	31.45	26.97
B	6	52.79	4.91	21.74	1.66	3.03	11.12	b.d.l.	28.93	26.75
B	8	42.20	4.99	31.74	0.83	2.43	6.73	b.d.l.	17.59	27.62
B	10	87.39	4.62	35.95	1.18	2.56	8.29	b.d.l.	20.24	27.56
B	12-1	39.50	5.08	54.08	0.71	2.89	6.80	b.d.l.	16.71	27.07
B	12-2	41.67	5.45	47.45	0.78	2.62	6.98	b.d.l.	20.75	27.05
B	15	41.51	6.52	68.49	0.69	3.03	5.89	b.d.l.	10.99	26.67
C	1	8.18	2.14	7.03	1.41	1.71	16.76	b.d.l.	19.82	26.51
C	2	13.56	2.91	10.63	1.36	1.38	10.73	b.d.l.	35.35	26.64
C	3	43.11	3.40	18.30	1.31	2.02	11.48	b.d.l.	31.64	27.01
C	4	49.03	4.44	22.62	1.83	2.26	11.45	b.d.l.	38.24	26.79
C	5	42.68	3.87	21.76	1.95	2.69	14.33	b.d.l.	40.39	26.87
C	6	43.75	4.87	30.51	1.95	3.09	10.47	b.d.l.	26.33	26.51
C	8	48.27	3.28	34.61	1.11	2.61	6.76	9.81	22.60	26.66
C	10	41.84	5.54	47.85	0.79	2.74	7.13	b.d.l.	14.16	26.30
C	15	90.47	8.03	75.13	0.74	3.82	7.75	b.d.l.	17.94	26.52

Appendix 5-4-4 cont.: Pore water concentration data at North Gotland, Baltic Sea (St. 17 - cores B&C)

core (s)	depth (cm)	Mo (nmol/L)	Cd (nmol/L)	Sb (nmol/L)	Ba (µmol/L)	Ce (nmol/L)	Nd (nmol/L)	Re (nmol/L)	Tl (nmol/L)	U (nmol/L)
B	1	128.19	b.d.l.	1.42	0.16	0.34	b.d.l.	0.18	b.d.l.	11.26
B	2	125.30	b.d.l.	0.93	0.16	3.64	0.04	0.18	b.d.l.	10.42
B	3	240.94	0.02	2.90	0.18	0.15	0.19	0.18	b.d.l.	16.00
B	4	1109.57	0.78	10.53	0.19	b.d.l.	0.13	0.17	b.d.l.	36.77
B	5	799.10	0.38	5.30	0.23	2.02	0.24	0.17	b.d.l.	18.05
B	6	1275.43	1.25	8.75	0.24	199.05	14.11	0.16	b.d.l.	26.14
B	8	665.29	0.68	6.82	0.28	b.d.l.	b.d.l.	0.15	b.d.l.	19.52
B	10	546.74	0.37	7.47	0.31	b.d.l.	b.d.l.	0.17	b.d.l.	23.52
B	12-1	606.31	0.85	7.07	0.32	b.d.l.	b.d.l.	0.15	b.d.l.	15.15
B	12-2	588.72	0.31	6.35	0.33	b.d.l.	b.d.l.	0.16	b.d.l.	13.47
B	15	457.09	0.07	5.33	0.37	b.d.l.	0.57	0.15	b.d.l.	5.93
C	1	120.98	0.28	0.79	0.15	1.29	0.00	0.18	b.d.l.	9.90
C	2	251.15	b.d.l.	1.61	0.17	b.d.l.	0.01	0.18	b.d.l.	14.78
C	3	407.37	b.d.l.	3.41	0.19	1.41	0.14	0.17	b.d.l.	19.81
C	4	1550.02	0.71	13.05	0.21	2.59	0.26	0.18	b.d.l.	37.75
C	5	1915.24	1.01	13.69	0.21	b.d.l.	0.04	0.16	b.d.l.	44.54
C	6	985.97	0.23	10.08	0.23	0.44	0.09	0.14	b.d.l.	35.47
C	8	960.56	0.27	10.31	0.28	1.78	0.03	0.16	b.d.l.	39.08
C	10	604.72	0.28	5.80	0.30	b.d.l.	0.03	0.14	b.d.l.	15.31
C	15	349.51	0.17	11.73	0.39	2.62	0.13	0.15	b.d.l.	29.37

Appendix 5-4-5: Sedimentary uranium isotope data at Baltic North Gotland (St. 17).

depth (cm)	bulk δ238U	2SD^	2SE^	n
0.5	0.13	0.08	0.06	2
1.5	0.02	0.05	0.03	4
2.5	-0.23	0.06	0.04	2
3.5	0.03	0.03	0.02	2
4.5	-0.22	0.10	0.07	2
5.5	-0.20	0.10	0.06	3
6.5	-0.25	0.01	0.01	2
8.5	-0.37	0.17	0.10	3
10.5	-0.34	0.06	0.03	3
17.5	-0.25	0.13^	0.13^	1
28.5	-0.29	0.13^	0.13^	1
36.5	-0.25	0.11	0.08	2

^Based on an average of the standard deviations of the East Pacific Seawater. Average δ = -0.39. 2SD = 0.13. N= 17.

Appendix 5-4-6: Uranium isotope data for water column samples from North Gotland, Baltic Sea (St. 17).

Station	depth (m)	bottle #	bulk δ238U	2SD^	2SE^	n
St. 17	161	1	-0.37	0.12^	0.12^	1

^Based on an average of the standard deviations of BCR. Average δ = -0.32. 2SD = 0.12. N=10

Appendix 5-5-1: Sedimentary Baltic Faro Deep (St. 18) auxiliary data

depth (cm)	Mg (mg/g)	Al (mg/g)	Ca (mg/g)	Ti (µg/g)	V (µg/g)	Cr (µg/g)	Mn (mg/g)	Fe (mg/g)	Co (µg/g)	U (µg/g)
0.5	11.61	37.82	6.67	1.98	69.27	44.01	0.34	29.15	12.99	57.41
1.5	13.64	47.78	7.74	2.44	85.44	50.16	0.40	32.59	15.91	61.84
2.5	11.88	42.53	7.10	2.25	81.56	46.85	0.41	32.71	15.07	49.12
3.5	15.43	52.60	9.03	2.72	115.23	58.86	0.55	45.06	21.63	55.22
4.5	12.01	42.65	6.99	2.20	95.50	47.80	0.43	36.38	16.81	45.93
5.5	17.61	64.05	10.05	3.21	140.03	68.62	0.65	47.95	28.98	56.95
7.5	12.68	50.16	6.63	2.56	90.72	52.93	0.52	35.89	17.09	46.37
9.5	12.37	47.73	6.89	2.65	104.06	58.35	0.95	44.78	26.16	34.69
11.5	12.68	49.69	6.98	2.49	88.19	57.65	0.66	39.15	17.38	41.73
14.5	12.67	46.87	10.19	2.39	113.36	60.73	18.72	47.85	26.06	32.90
16.5	12.73	45.58	7.30	2.26	105.90	104.91	0.92	60.04	31.84	22.55
18.5	12.56	50.00	6.67	2.53	112.44	64.65	1.24	58.49	28.74	17.99
20.5	12.67	49.80	6.80	2.42	109.28	60.42	2.96	80.02	32.33	12.06
22.5	13.45	54.10	21.85	2.66	98.31	55.33	65.37	54.28	42.46	6.88
24.5	14.26	63.84	11.93	3.25	102.43	66.93	25.15	63.06	40.84	5.04

Appendix 5-5-1 cont.: Sedimentary Baltic Faro Deep (St. 18) auxiliary data

depth (cm)	Ni (µg/g)	Cu (µg/g)	Sr (µg/g)	Mo (µg/g)	Cd (µg/g)	Ba (µg/g)	Ce (µg/g)	Nd (µg/g)	Th (µg/g)	U (µg/g)
0.5	82.37	157.37	98.62	199.62	0.65	178.96	48.58	21.56	7.24	57.41
1.5	89.47	189.07	103.61	216.27	0.77	618.15	58.84	24.82	9.09	61.84
2.5	91.14	172.88	102.83	186.87	0.90	261.73	53.39	23.02	8.24	49.12
3.5	129.25	264.80	158.90	247.05	0.75	3465.64	77.04	29.28	12.68	55.22
4.5	99.82	235.08	108.56	200.29	1.17	209.59	52.84	23.00	7.67	45.93
5.5	126.12	240.95	141.62	265.32	1.98	961.59	79.12	33.36	11.72	56.95
7.5	83.70	173.21	100.91	173.44	3.33	586.38	62.62	26.28	9.76	46.37
9.5	98.06	175.37	107.79	215.50	3.15	616.13	51.25	23.48	6.28	34.69
11.5	94.66	177.30	106.62	215.34	3.61	578.60	62.12	26.41	9.33	41.73
14.5	100.72	138.34	126.22	160.18	4.66	510.84	59.44	25.61	8.51	32.90
16.5	123.99	191.65	110.61	137.32	2.65	436.99	55.22	23.48	8.13	22.55
18.5	84.10	162.98	109.71	99.31	7.01	612.14	64.12	27.12	9.07	17.99
20.5	84.02	158.82	115.78	136.89	13.14	654.67	60.51	25.02	9.14	12.06
22.5	56.45	53.08	179.66	36.36	0.76	281.92	68.16	27.36	10.26	6.88
24.5	53.32	40.23	141.34	42.98	1.31	422.16	67.63	28.21	10.24	5.04

Appendix 5-5-2: 0.2 μm filtered sea water concentration data at Faro Deep, Baltic Sea (St. 18)

bottle #	depth (m)	V (nmol/L)	Cr (nmol/L)	Mn (μmol/L)	Fe (μmol/L)	Co (nmol/L)	Ni (nmol/L)	Cu (nmol/L)
1	186	4.57	12.47	3.26	0.18	1.48	17.37	2.77
2	176	4.55	12.50	3.32	0.24	1.45	16.43	2.70
3	166	4.44	12.25	3.07	0.18	1.40	18.18	2.48
4	151	4.78	12.57	3.02	0.25	1.41	17.50	3.41
5	141	4.68	12.05	3.01	0.27	1.39	18.26	2.52
6	131	5.16	12.51	2.96	0.40	1.59	17.96	2.57
7	120	5.28	12.27	3.24	0.28	1.56	17.84	2.42
8	111	4.66	11.96	0.96	0.09	1.31	18.17	2.98
9	101	4.74	12.14	0.02	0.08	1.10	17.07	3.52
11	91	4.41	13.02	0.45	0.10	1.18	18.06	3.82
13	81	4.02	13.34	0.07	0.09	1.09	17.96	4.29
14	76	4.41	13.13	0.02	0.09	1.06	17.77	5.14
15	71	4.48	12.99	0.05	0.10	1.19	17.73	5.27
16	66	4.53	13.42	0.03	0.09	1.17	17.81	6.01
17	60	5.85	14.42	0.05	0.11	1.14	17.94	6.55
19	50	4.45	13.19	0.02	0.09	1.09	17.21	6.01
20	40	4.26	13.08	0.02	0.09	1.07	18.37	6.75
23	20	4.24	13.35	0.02	0.08	1.05	17.29	6.63

Appendix 5-5-2 cont.: 0.2 µm filtered sea water concentration data at Faro Deep, Baltic Sea (St. 18)

bottle #	depth (m)	As (nmol/L)	Sr (µmol/L)	Mo (nmol/)L	Sb (nmol/L)	Ba (nmol/L)	U (nmol/L)
1	186	8.53	33.60	25.26	0.75	77.37	4.62
2	176	8.77	34.07	25.50	0.78	77.74	4.58
3	166	8.61	33.90	24.96	0.74	78.19	4.82
4	151	8.56	33.62	24.48	0.78	78.98	4.48
5	141	8.50	33.61	24.19	0.81	79.31	4.43
6	131	8.57	33.26	24.36	0.71	79.58	4.31
7	120	8.31	33.09	23.67	0.79	77.91	4.37
8	111	8.48	32.50	23.18	0.75	74.61	4.24
9	101	8.59	30.58	21.32	0.76	75.77	3.93
11	91	7.94	29.26	19.46	0.77	78.17	3.57
13	81	7.74	26.95	17.73	0.70	77.45	3.16
14	76	8.08	25.95	18.02	0.77	77.41	3.25
15	71	7.55	23.49	17.70	0.75	76.76	3.06
16	66	7.43	20.34	17.10	0.76	77.66	3.03
17	60	7.26	19.95	16.99	0.80	79.85	2.95
19	50	7.13	19.77	16.68	0.79	78.97	2.85
20	40	7.26	19.70	16.64	0.82	78.44	2.86
23	20	7.30	18.86	16.21	0.77	79.68	2.83

Appendix 5-5-3: Pore water concentration data at Faro Deep, Baltic Sea (St. 18)

core (s)	depth (cm)	V (nmol/L)	Cr (nmol/L)	Mn (µmol/L)	Fe (µmol/L)	Co (nmol/L)	Ni (nmol/L)	Cu (nmol/L)	As (nmol/L)	Sr (µmol/L)
A	0	16.10	2.35	6.98	2.14	b.d.l.	15.41	b.d.l.	17.58	31.71
A	1	8.78	2.01	7.12	1.60	b.d.l.	11.59	0.21	14.17	31.69
A	2	9.55	3.07	12.85	1.73	0.17	10.27	b.d.l.	42.27	32.08
A	3	22.27	2.35	16.39	2.60	0.35	14.90	b.d.l.	59.81	32.23
A	4	31.17	4.19	23.30	2.53	1.11	17.48	b.d.l.	79.17	32.38
A	5	81.94	3.86	17.89	4.86	0.75	25.31	b.d.l.	128.85	32.02
A	6	35.95	7.97	39.70	1.43	2.63	113.16	b.d.l.	90.24	32.26
A	8	46.94	12.76	58.26	1.31	4.05	23.74	b.d.l.	114.54	31.52
A	10-1	52.26	19.71	68.76	1.13	5.34	31.80	b.d.l.	121.85	30.00
A	10-2	52.62	17.95	75.11	0.76	5.43	23.93	b.d.l.	136.26	30.90
A	12	79.63	22.28	97.59	1.13	6.06	23.72	b.d.l.	157.94	28.75
A	15	95.20	23.06	117.66	1.16	7.32	23.79	b.d.l.	170.72	29.05
A	19	121.99	24.64	152.81	1.13	8.63	21.00	b.d.l.	172.46	29.74
A	23	152.51	27.03	202.58	1.30	11.67	24.99	b.d.l.	205.30	30.03

Appendix 5-5-3 cont.: Pore water concentration data at Faro Deep, Baltic Sea (St. 18)

core (s)	depth (cm)	Mo (nmol/L)	Cd (nmol/L)	Sb (nmol/L)	Ba (µmol/L)	Ce (nmol/L)	Nd (nmol/L)	Re (nmol/L)	Tl (nmol/L)	U (nmol/L)
A	0	121.43	0.35	1.38	0.15	2.44	0.13	0.14	b.d.l.	12.74
A	1	56.16	0.25	0.98	0.15	2.90	0.24	0.13	b.d.l.	5.87
A	2	189.95	0.55	1.75	0.20	5.74	0.17	0.14	b.d.l.	14.81
A	3	505.69	0.57	4.70	0.23	2.02	0.23	0.13	b.d.l.	37.12
A	4	1240.79	1.07	10.64	0.27	2.95	0.15	0.15	b.d.l.	75.80
A	5	2069.59	1.39	20.18	0.24	2.12	0.10	0.13	b.d.l.	165.38
A	6	364.05	0.46	3.90	0.39	5.67	0.12	0.10	b.d.l.	23.64
A	8	319.81	0.32	6.82	0.50	4.45	0.35	0.11	b.d.l.	26.37
A	10-1	113.86	0.49	7.39	0.57	2.25	0.25	0.13	b.d.l.	15.84
A	10-2	98.60	b.d.l.	7.27	0.62	3.89	0.22	0.20	0.39	18.13
A	12	50.69	b.d.l.	9.04	0.71	10.36	0.24	0.11	b.d.l.	14.83
A	15	61.14	0.32	12.89	0.83	3.70	0.35	0.11	b.d.l.	13.46
A	19	49.27	0.02	17.03	1.03	3.83	0.41	0.13	b.d.l.	8.97
A	23	44.66	0.34	20.21	1.24	7.57	0.28	0.11	b.d.l.	3.99

Appendix 5-5-4: Particulate matter concentration data at Faro Deep, Baltic Sea per L (St. 18)

depth (m)	sub-sample	Mg (µg/L)	Al (µg/L)	Ti (ng/L)	V (ng/L)	Cr (ng/L)	Mn (µg/L)	Fe (µg/L)	Co (ng/L)	Ni (ng/L)	Cu (ng/L)
50	A	6.94	0.31	10.76	0.79	1.74	0.21	0.23	0.39	4.82	4.21
50	B	7.74	0.28	10.30	0.73	1.18	0.15	0.20	0.33	4.92	3.88
100	A	5.69	0.14	6.33	4.94	1.33	9.19	0.74	2.06	8.68	5.22
100	B	5.86	0.11	4.99	5.06	0.98	9.70	0.76	2.14	9.11	4.88
150	A	11.14	0.05	2.57	2.19	0.86	0.02	0.13	0.61	4.33	109.38
150	B	7.47	0.06	2.94	2.01	1.70	0.01	0.13	0.58	4.33	100.64
175	FH1-A	15.13	0.63	21.90	4.77	6.48	0.04	1.26	1.25	9.32	216.32
175	FH1-B	13.58	0.50	13.19	4.46	6.50	0.06	1.11	1.17	8.62	192.48
175	FH2-A	12.67	0.17	5.51	4.02	6.18	0.05	0.89	1.15	8.52	195.81
175	FH2-B	15.44	0.10	4.26	3.97	5.49	0.05	0.84	1.16	8.10	201.05

depth (m)	sub-sample	As (ng/L)	Sr (ng/L)	Mo (ng/L)	Cd (ng/L)	Sb (ng/L)	Cs (ng/L)	Ba (ng/L)	Tl (ng/L)	U (ng/L)
50	A	1.68	89.76	0.66	1.34	0.18	0.06	142.84	0.02	0.31
50	B	1.60	87.57	0.58	1.19	0.17	0.06	125.52	0.02	0.29
100	A	4.21	61.21	8.86	0.31	0.53	0.03	93.10	0.02	0.92
100	B	4.54	66.10	9.05	0.33	0.47	0.03	101.64	0.02	0.97
150	A	5.71	50.66	31.73	5.21	0.81	0.02	29.82	0.38	2.70
150	B	5.09	40.34	30.98	4.20	0.65	0.02	26.09	0.33	2.59
175	FH1-A	10.29	100.18	38.07	2.54	0.55	0.09	250.62	0.33	3.39
175	FH1-B	9.66	84.44	35.70	2.52	0.55	0.07	195.88	0.30	3.08
175	FH2-A	9.25	80.28	35.78	2.80	0.44	0.05	137.79	0.32	2.96
175	FH2-B	9.54	92.73	37.18	2.50	0.71	0.04	112.37	0.31	3.07

Appendix 5-5-5: Particulate matter concentration data at Faro Deep, Baltic Sea per square cm (St. 18)

depth (m)	sub-sample	Mg (µg/cm^2)	Al (µg/cm^2)	Ti (ng/cm^2)	V (ng/cm^2)	Cr (ng/cm^2)	Mn (µg/cm^2)	Fe (µg/cm^2)	Co (ng/cm^2)	Ni (ng/cm^2)	Cu (ng/cm^2)
50	A	34.97	1.55	54.16	4.00	8.77	1.07	1.14	1.97	24.28	21.19
50	B	38.99	1.43	51.88	3.67	5.95	0.75	1.01	1.66	24.77	19.54
100	A	38.36	0.93	42.67	33.31	8.95	62.01	4.96	13.91	58.54	35.21
100	B	39.51	0.73	33.66	34.12	6.63	65.42	5.13	14.41	61.43	32.90
150	A	57.99	0.27	13.38	11.42	4.47	0.10	0.66	3.19	22.51	569.22
150	B	38.87	0.33	15.30	10.46	8.85	0.05	0.66	3.02	22.51	523.73
175	FH1-A	40.60	1.68	58.76	12.80	17.39	0.11	3.38	3.36	25.01	580.37
175	FH1-B	36.43	1.34	35.38	11.96	17.44	0.16	2.99	3.14	23.13	516.42
175	FH2-A	31.86	0.43	13.84	10.10	15.54	0.12	2.24	2.89	21.41	492.25
175	FH2-B	38.83	0.25	10.71	9.99	13.80	0.12	2.12	2.93	20.37	505.43

depth (m)	sub-sample	As (ng/cm^2)	Sr (ng/cm^2)	Mo (ng/cm^2)	Cd (ng/cm^2)	Sb (ng/cm^2)	Cs (ng/cm^2)	Ba (ng/cm^2)	Tl (ng/cm^2)	U (ng/cm^2)
50	A	8.46	451.95	3.30	6.77	0.90	0.29	719.19	0.10	1.55
50	B	8.05	440.94	2.93	5.98	0.87	0.29	632.00	0.09	1.47
100	A	28.37	412.91	59.79	2.11	3.60	0.21	628.06	0.13	6.23
100	B	30.61	445.89	61.04	2.21	3.17	0.22	685.66	0.13	6.54
150	A	29.70	263.64	165.13	27.10	4.21	0.12	155.17	1.96	14.05
150	B	26.50	209.95	161.22	21.84	3.40	0.11	135.77	1.71	13.50
175	FH1-A	27.60	268.77	102.15	6.82	1.49	0.25	672.41	0.89	9.08
175	FH1-B	25.91	226.56	95.78	6.77	1.49	0.19	525.54	0.80	8.27
175	FH2-A	23.26	201.82	89.94	7.04	1.10	0.13	346.40	0.79	7.45
175	FH2-B	23.97	233.12	93.46	6.29	1.80	0.09	282.49	0.77	7.72

Appendix 5-5-6: Uranium isotope data for water column samples from Faro Deep, Baltic Sea (St. 18).

Station	depth (m)	bottle #	bulk δ238U	2SD^	2SE^	n
St. 18	176	2	-0.41	0.01	0.01	2
St. 18	101	9	-0.48	0.12^	0.12^	1

^Based on an average of the standard deviations of BCR. Average δ = -0.32. 2SD = 0.12. N=10

Appendix 5-6-1: Sedimentary Baltic East Gotland (St. 14) auxiliary data

depth (cm)	Mg (mg/g)	Al (mg/g)	Ca (mg/g)	Ti (µg/g)	V (µg/g)	Cr (µg/g)	Mn (mg/g)	Fe (mg/g)	Co (µg/g)	U (µg/g)
0.5	11.94	32.45	9.09	1.76	121.61	41.99	29.15	30.86	16.71	22.35
1.5	12.20	39.31	7.74	2.13	94.20	49.29	10.00	33.00	16.37	39.01
2.5	12.28	41.06	7.07	2.20	101.51	51.76	7.61	38.37	17.71	37.85
3.5	13.44	53.05	6.23	2.63	133.21	63.31	5.35	47.31	25.54	32.62
4.5	12.74	53.19	5.44	2.63	133.69	65.57	3.23	58.09	44.31	30.44
5.5	12.48	55.00	4.87	2.90	121.75	71.81	2.58	47.17	23.90	45.03
7.5	12.22	58.73	4.31	2.80	144.76	74.40	1.78	57.93	42.46	25.94
9.5	15.06	77.63	4.81	3.32	118.81	77.34	0.69	45.54	18.09	9.61
11.5	13.01	68.79	4.28	3.52	122.47	80.79	0.61	46.33	20.77	7.15
13.5	12.59	64.65	4.07	3.60	120.66	83.16	0.56	46.98	18.25	7.38
15.5	14.90	75.38	4.66	3.68	119.10	84.56	0.55	49.66	14.83	9.23
17.5	13.52	67.44	4.30	3.84	122.98	86.12	0.53	47.51	16.31	8.59
19.5	13.73	69.24	4.37	3.59	117.03	83.45	0.56	47.73	15.79	8.31
21.5	14.19	71.83	4.53	3.85	122.40	85.39	0.51	46.60	15.25	8.67
23.5	14.06	70.44	4.39	3.65	117.13	83.69	0.49	47.41	17.14	8.27
24.5	12.61	63.03	4.07	3.65	116.11	81.12	0.48	51.38	18.95	8.06
26.5	12.73	62.40	4.30	3.63	119.38	82.24	0.50	53.79	18.16	8.68
29.5	14.68	72.58	4.59	3.53	119.63	79.88	0.53	53.04	20.63	8.52

Appendix 5-6-1 cont.: Sedimentary Baltic East Gotland (St. 14) auxiliary data

depth (cm)	Ni (µg/g)	Cu (µg/g)	Sr (µg/g)	Mo (µg/g)	Cd (µg/g)	Ba (µg/g)	Ce (µg/g)	Nd (µg/g)	Th (µg/g)	U (µg/g)
0.5	67.44	97.21	181.39	106.39	0.60	238.12	42.43	19.15	5.93	22.35
1.5	72.26	121.06	132.16	191.71	0.49	512.13	51.73	22.83	7.63	39.01
2.5	81.43	136.54	121.33	189.80	0.70	424.58	57.00	24.29	7.94	37.85
3.5	94.82	139.76	115.88	209.79	2.50	726.23	79.81	33.56	10.69	32.62
4.5	111.19	146.60	111.81	199.61	4.68	645.47	82.37	32.82	11.01	30.44
5.5	87.32	123.92	108.57	173.99	3.95	561.85	71.46	31.03	10.13	45.03
7.5	94.88	112.96	114.19	141.54	7.34	622.26	100.28	38.44	12.84	25.94
9.5	49.60	56.05	122.04	20.50	2.15	615.05	139.59	53.92	19.12	9.61
11.5	54.25	55.01	105.99	11.03	1.73	549.43	60.70	28.50	9.96	7.15
13.5	52.66	52.69	105.04	11.40	1.34	552.12	69.46	29.42	11.02	7.38
15.5	48.45	49.27	121.62	9.81	0.89	633.54	129.67	47.66	17.39	9.23
17.5	54.13	51.27	110.51	11.78	0.59	602.80	60.99	28.93	10.74	8.59
19.5	49.29	47.58	114.11	10.37	0.55	599.09	89.38	35.90	13.05	8.31
21.5	48.91	50.33	115.47	10.21	0.52	623.90	80.05	35.06	12.81	8.67
23.5	48.95	47.32	116.54	9.83	0.48	632.02	101.94	41.46	14.31	8.27
24.5	50.69	47.49	105.09	12.51	0.50	587.37	50.56	24.66	9.06	8.06
26.5	51.05	51.56	105.18	15.16	0.58	609.61	63.13	27.75	9.75	8.68
29.5	52.08	52.52	120.84	16.49	0.68	663.63	124.23	47.61	17.21	8.52

Appendix 5-6-2: 0.2 μm filtered sea water concentration data at East Gotland, Baltic Sea (St. 19)

bottle #	depth (m)	V (nmol/L)	Cr (nmol/L)	Mn (μmol/L)	Fe (μmol/L)	Co (nmol/L)	Ni (nmol/L)	Cu (nmol/L)
1	230	3.85	1.78	0.32	0.03	0.69	12.30	4.43
3	201	4.29	1.84	0.01	0.02	0.62	11.00	4.63
4	176	4.53	1.83	0.01	0.02	0.68	12.19	4.82
5	151	4.53	12.29	0.01	0.08	1.20	16.71	4.81
7	111	4.36	1.70	0.26	0.02	0.54	11.94	3.08
9	101	4.65	1.71	0.05	0.02	0.60	12.50	3.67
11	91	4.40	1.72	0.03	0.02	0.60	12.23	3.70
13	80	4.05	1.65	0.12	0.03	0.55	12.46	3.42
15	70	4.12	1.76	0.06	0.04	0.60	13.41	4.85
16	65	4.19	1.60	0.03	0.03	0.55	12.03	4.66
17	60	4.19	1.69	0.02	0.02	0.55	11.75	5.65
19	50	4.63	1.70	0.01	0.02	0.57	12.26	6.11
21	40	4.32	17.56	0.02	0.10	0.98	17.75	6.08
23	20	4.37	3.26	0.02	0.03	0.66	12.79	6.21

Appendix 5-6-2 cont.: 0.2 µm filtered sea water concentration data at East Gotland, Baltic Sea (St. 19)

bottle #	depth (m)	As (nmol/L)	Sr (µmol/L)	Mo (nmol/)L	Sb (nmol/L)	Ba (nmol/L)	U (nmol/L)
1	230	9.10	36.79	36.37	0.71	79.49	6.01
3	201	8.47	36.92	30.70	0.72	76.93	5.87
4	176	9.04	35.96	28.95	0.82	77.75	5.74
5	151	8.42	34.90	28.09	0.78	78.05	5.64
7	111	8.50	33.21	23.82	0.74	77.75	4.65
9	101	8.52	31.98	22.72	0.71	76.39	4.50
11	91	8.14	30.75	21.93	0.74	77.96	4.22
13	80	8.35	28.94	19.40	0.71	77.14	3.73
15	70	8.50	27.68	19.55	0.76	79.20	3.74
16	65	7.94	24.18	18.09	0.83	75.57	3.39
17	60	8.12	21.21	17.43	0.74	77.90	3.23
19	50	7.82	19.63	16.82	0.76	77.88	3.23
21	40	7.59	19.77	16.99	0.72	78.78	3.01
23	20	7.68	18.84	16.93	0.80	80.08	3.13

Appendix 5-6-3: Pore water concentration data at East Gotland, Baltic Sea (St. 14)

core (s)	depth (cm)	V (nmol/L)	Cr (nmol/L)	Mn (µmol/L)	Fe (µmol/L)	Co (nmol/L)	Ni (nmol/L)	Cu (nmol/L)	As (nmol/L)	Sr (µmol/L)
A	OLW	44.97	1.77	53.27	1.33	4.68	25.00	3.53	27.55	34.61
A	1	16.41	2.49	131.96	1.13	2.21	20.05	1.72	26.78	33.05
A	2	87.73	1.11	260.63	1.17	5.11	22.60	0.33	77.34	34.53
A	3	38.04	28.89	377.64	2.09	3.61	20.85	2.32	99.24	33.89
A	4	53.48	5.30	323.16	1.20	1.47	12.98	0.98	59.67	33.68
A	5	52.01	7.44	276.56	1.16	1.70	11.58	b.d.l.	52.51	33.97
A	6	57.40	6.76	241.53	1.24	1.56	10.03	0.65	57.65	33.57
A	8	39.99	4.12	214.50	1.16	0.50	9.50	b.d.l.	76.37	33.04
A	10	48.56	6.38	147.93	1.22	1.13	9.02	b.d.l.	62.17	32.94
A	15	62.89	8.61	89.52	1.19	1.48	7.15	b.d.l.	76.49	33.09
A	20	67.09	10.33	91.06	1.18	1.90	9.10	b.d.l.	114.27	32.37
A	25	57.35	10.26	106.21	1.18	2.00	7.10	b.d.l.	139.84	32.26

Appendix 5-6-3 cont.: Pore water concentration data at East Gotland, Baltic Sea (St. 14)

core (s)	depth (cm)	Mo (nmol/L)	Cd (nmol/L)	Sb (nmol/L)	Ba (µmol/L)	Ce (nmol/L)	Nd (nmol/L)	Re (nmol/L)	Tl (nmol/L)	U (nmol/L)
A	OLW	92.41	0.36	1.42	0.21	3.45	0.18	0.15	b.d.l.	6.79
A	1	211.05	0.53	1.28	0.18	1.25	0.21	0.11	b.d.l.	8.98
A	2	394.77	0.45	4.66	0.36	1.21	0.07	0.13	b.d.l.	24.35
A	3	424.25	0.54	7.86	0.38	2.18	0.12	0.13	b.d.l.	41.37
A	4	399.56	0.46	3.45	0.31	3.38	0.29	0.12	b.d.l.	38.58
A	5	425.30	0.65	2.97	0.27	3.78	0.33	0.14	b.d.l.	33.69
A	6	302.94	0.65	3.21	0.26	5.90	0.43	0.13	b.d.l.	26.10
A	8	378.27	0.85	4.75	0.23	3.53	0.35	0.12	b.d.l.	22.07
A	10	227.06	0.44	3.45	0.25	5.38	0.37	0.12	b.d.l.	10.50
A	15	146.68	0.03	3.25	0.29	3.22	0.26	0.10	b.d.l.	5.13
A	20	31.10	0.19	4.78	0.30	4.09	0.46	0.10	b.d.l.	3.13
A	25	58.33	0.29	5.35	0.30	3.54	0.48	0.11	b.d.l.	2.64

Appendix 5-6-4: Sedimentary uranium isotope data at Baltic East Gotland (St. 14).

depth (cm)	bulk δ238U	2SD^	2SE^	n
0.5	0.28	0.14	0.10	2
1.5	0.00	0.02	0.01	2
2.5	-0.04	0.01	0.01	2
3.5	0.03	0.13	0.07	3
4.5	-0.12	0.07	0.05	2
5.5	-0.16	0.00	0.00	2
7.5	-0.16	0.39	0.28	2
9.5	-0.08	0.01	0.00	2
11.5	-0.24	0.13^	0.13^	1
13.5	-0.16	0.13^	0.13^	1
15.5	-0.21	0.00	0.00	2
19.5	-0.30	0.16	0.08	4
24.5	-0.35	0.13^	0.13^	1

^Based on an average of the standard deviations of the East Pacific Seawater. Average δ = -0.39. 2SD = 0.13. N= 17.

Appendix 5-6-5: Uranium isotope data for water column samples from East Gotland, Baltic Sea (St. 19).

Station	depth (m)	bottle #	bulk δ238U	2SD^	2SE^	n
St. 19	230	1	-0.47	0.12^	0.12^	1

^Based on an average of the standard deviations of BCR. Average δ = -0.32. 2SD = 0.12. N=10

Appendix 5-7-1: Sedimentary Baltic Bornhom Basin (St. 22) auxiliary data

depth (cm)	Mg (mg/g)	Al (mg/g)	Ca (mg/g)	Ti (µg/g)	V (µg/g)	Cr (µg/g)	Mn (mg/g)	Fe (mg/g)	Co (µg/g)	U (µg/g)
0.5	14.35	64.37	5.29	3.39	117.56	71.45	4.88	43.03	19.59	6.02
1.5	14.28	67.04	4.78	3.47	118.69	74.18	0.72	43.33	19.30	6.26
2.5	14.08	66.78	4.77	3.43	114.25	71.87	0.60	44.30	18.77	5.41
3.5	14.66	67.63	4.98	3.60	115.59	73.16	0.61	46.01	19.26	5.41
4.5	15.07	73.96	5.23	3.46	111.17	72.53	0.56	43.37	17.85	5.59
5.5	15.39	72.32	5.47	3.52	112.44	70.95	0.55	41.81	17.15	5.09
7.5	15.34	71.85	5.46	3.47	114.42	71.07	0.60	44.24	18.68	6.27
9.5	16.45	81.25	5.71	3.66	106.22	71.28	0.62	45.67	16.83	6.10
12.5	13.79	67.66	5.25	3.67	104.00	70.78	0.62	43.66	15.03	6.17
15.5	14.04	66.91	5.39	3.76	108.31	72.28	0.56	41.79	13.93	5.93

Appendix 5-7-1 cont.: Sedimentary Baltic Bornhom Basin (St. 22) auxiliary data

depth (cm)	Ni (µg/g)	Cu (µg/g)	Sr (µg/g)	Mo (µg/g)	Cd (µg/g)	Ba (µg/g)	Ce (µg/g)	Nd (µg/g)	Th (µg/g)	U (µg/g)
0.5	46.40	53.79	119.09	13.31	0.44	450.72	86.84	36.01	12.85	6.02
1.5	47.99	51.55	108.13	10.23	0.74	466.44	101.14	39.46	13.75	6.26
2.5	46.23	49.18	107.40	9.61	0.69	468.31	114.30	42.13	15.30	5.41
3.5	47.85	49.20	110.26	11.30	0.51	458.93	106.85	40.70	14.43	5.41
4.5	44.12	47.53	117.46	11.08	0.77	526.31	164.23	58.45	20.82	5.59
5.5	46.16	51.25	116.90	7.23	0.58	473.69	138.40	50.17	19.99	5.09
7.5	49.55	56.00	115.89	18.58	0.96	514.48	139.35	51.96	18.42	6.27
9.5	43.12	38.92	123.48	17.65	0.55	542.18	182.52	63.77	23.37	6.10
12.5	41.90	37.91	105.43	15.10	0.44	491.55	106.18	40.17	14.64	6.17
15.5	42.24	38.26	105.87	7.79	0.32	480.22	76.59	33.30	11.90	5.93

Appendix 5-7-2: 0.2 μm filtered sea water concentration data at Bornholm Basin, Baltic Sea (St. 22)

bottle #	depth (m)	V (nmol/L)	Cr (nmol/L)	Mn (μmol/L)	Fe (μmol/L)	Co (nmol/L)	Ni (nmol/L)	Cu (nmol/L)
3	76	6.73	2.43	0.15	0.03	0.70	13.88	6.16
7	66	9.73	7.61	0.02	0.06	1.09	15.50	6.29
10	56	9.82	2.19	0.02	0.02	0.72	11.39	6.61
12	45	6.23	1.81	0.02	0.02	0.58	11.60	6.02
14	35	4.82	2.36	0.02	0.02	0.55	11.18	6.45
16	25	4.52	22.22	0.02	0.13	1.40	20.32	6.13

bottle #	depth (m)	As (nmol/L)	Sr (μmol/L)	Mo (nmol/L)	Sb (nmol/L)	Ba (nmol/L)	U (nmol/L)
3	76	8.67	46.72	39.35	0.98	69.52	8.21
7	66	8.30	44.20	37.49	0.95	69.31	7.45
10	56	7.83	38.59	33.28	0.93	69.88	6.19
12	45	7.66	26.57	21.95	0.79	75.48	3.87
14	35	7.77	19.72	17.77	0.75	77.45	3.09
16	25	7.33	19.04	17.50	0.73	76.60	3.06

Appendix 5-7-3: Pore water concentration data at Bornholm Basin, Baltic Sea (St. 22)

core (s)	depth (cm)	V (nmol/L)	Cr (nmol/L)	Mn (µmol/L)	Fe (µmol/L)	Co (nmol/L)	Ni (nmol/L)	Cu (nmol/L)	As (nmol/L)	Sr (µmol/L)
A	1	24.59	4.52	27.77	26.60	16.09	17.45	2.01	33.79	45.39
A	2	34.79	5.27	36.63	14.92	2.93	11.67	b.d.l.	38.14	45.82
A	3	36.91	5.41	32.72	2.10	0.89	10.77	b.d.l.	33.55	46.30
A	4	38.77	4.74	37.16	1.43	0.67	7.94	b.d.l.	32.53	46.22
A	5	37.73	5.21	22.43	1.46	0.25	8.12	b.d.l.	45.45	45.30
A	6	32.75	4.01	22.80	3.03	0.14	8.57	b.d.l.	51.76	45.58
A	8	47.99	10.22	44.72	1.21	1.43	7.85	b.d.l.	32.75	45.95
A	10	64.36	12.12	56.36	1.18	2.57	10.67	b.d.l.	29.68	45.27
A	13	64.56	15.59	66.11	1.16	3.61	10.79	b.d.l.	27.22	46.01
A	16	66.77	17.66	68.44	1.16	4.50	11.90	b.d.l.	24.60	44.43

core (s)	depth (cm)	Mo (nmol/L)	Cd (nmol/L)	Sb (nmol/L)	Ba (µmol/L)	Ce (nmol/L)	Nd (nmol/L)	Re (nmol/L)	Tl (nmol/L)	U (nmol/L)
A	1	73.82	0.03	1.40	0.15	5.67	0.06	0.14	b.d.l.	8.75
A	2	54.36	0.12	2.02	0.18	3.99	0.12	0.12	b.d.l.	6.45
A	3	41.59	0.20	1.95	0.18	3.51	0.71	0.11	b.d.l.	5.65
A	4	35.47	0.21	1.57	0.20	2.77	0.21	0.12	b.d.l.	5.37
A	5	97.34	0.14	2.36	0.19	3.12	0.23	0.11	b.d.l.	7.08
A	6	153.03	0.15	3.41	0.20	0.83	0.14	0.13	b.d.l.	9.93
A	8	29.65	0.24	1.37	0.32	2.45	0.23	0.11	b.d.l.	6.89
A	10	25.04	0.13	2.79	0.41	3.57	0.51	0.11	b.d.l.	6.14
A	13	24.02	0.43	3.09	0.54	2.36	0.25	0.10	b.d.l.	3.04
A	16	14.32	0.42	3.47	0.63	3.71	0.41	0.11	b.d.l.	2.00

Appendix 5-7-4: Particulate matter concentration data at Bornholmn Basin, Baltic Sea per L (St. 22)

depth (m)	sub-sample	Mg (µg/L)	Al (µg/L)	Ti (ng/L)	V (ng/L)	Cr (ng/L)	Mn (µg/L)	Fe (µg/L)	Co (ng/L)	Ni (ng/L)	Cu (ng/L)
45	A	14.83	4.08	83.68	12.48	7.43	6.58	4.88	6.56	13.18	13.84
45	B	12.56	4.35	95.53	12.86	7.92	6.39	4.98	6.60	14.09	14.96
55	A	13.32	4.35	104.70	21.95	8.72	6.98	6.83	12.61	15.37	17.11
55	B	11.60	4.05	95.54	21.29	8.80	6.47	6.43	11.89	14.56	16.01
65	A	30.58	2.66	67.40	56.63	7.43	52.49	14.73	26.63	19.87	18.16
65	B	16.55	2.17	61.69	57.85	6.07	55.04	15.07	27.70	18.04	18.06
75	FH1-A	61.25	8.58	176.15	183.55	41.14	237.98	129.20	112.67	45.80	37.26
75	FH1-B	85.85	8.53	183.22	175.24	35.74	225.86	122.66	108.04	41.41	36.42
75	FH2-A	68.39	8.56	171.49	183.39	30.31	237.64	128.67	113.85	41.28	37.11
75	FH2-B	116.77	7.95	167.14	178.88	34.72	229.44	124.34	110.28	41.86	35.78

depth (m)	sub-sample	As (ng/L)	Sr (ng/L)	Mo (ng/L)	Cd (ng/L)	Sb (ng/L)	Cs (ng/L)	Ba (ng/L)	Tl (ng/L)	U (ng/L)
45	A	4.72	131.10	3.26	1.29	0.33	0.68	171.18	0.07	0.72
45	B	4.82	109.17	2.80	1.33	0.36	0.68	171.97	0.07	0.76
55	A	6.39	106.43	5.00	0.62	0.37	0.93	111.18	0.09	0.68
55	B	5.88	96.33	4.64	0.63	0.30	0.89	105.69	0.09	0.67
65	A	29.94	249.44	58.65	0.73	2.07	0.49	136.39	0.07	1.53
65	B	31.00	195.22	58.78	0.75	2.48	0.49	139.29	0.08	1.45
75	FH1-A	249.25	1076.22	236.30	1.83	9.47	1.06	571.78	0.20	7.64
75	FH1-B	234.12	1170.19	229.92	1.78	9.86	1.04	570.30	0.18	7.57
75	FH2-A	245.34	1106.62	238.92	1.84	10.28	1.05	557.66	0.18	7.78
75	FH2-B	235.94	1323.91	236.37	1.84	9.86	1.14	559.86	0.17	8.05

Appendix 5-7-5: Particulate matter concentration data at Bornholm Basin, Baltic Sea per square cm (St. 22)

depth (m)	sub-sample	Mg (µg/cm^2)	Al (µg/cm^2)	Ti (ng/cm^2)	V (ng/cm^2)	Cr (ng/cm^2)	Mn (µg/cm^2)	Fe (µg/cm^2)	Co (ng/cm^2)	Ni (ng/cm^2)	Cu (ng/cm^2)
45	A	63.93	17.57	360.64	53.77	32.00	28.35	21.02	28.28	56.81	59.65
45	B	54.11	18.73	411.68	55.44	34.15	27.52	21.46	28.46	60.74	64.45
55	A	68.67	22.44	539.69	113.12	44.95	36.00	35.21	65.01	79.23	88.18
55	B	59.80	20.87	492.46	109.75	45.34	33.35	33.15	61.28	75.04	82.52
65	A	83.11	7.22	183.22	153.94	20.19	142.69	40.04	72.38	54.02	49.37
65	B	45.00	5.90	167.69	157.23	16.50	149.62	40.97	75.28	49.04	49.09
75	FH1-A	44.85	6.28	129.00	134.43	30.13	174.29	94.62	82.51	33.54	27.28
75	FH1-B	62.87	6.24	134.18	128.34	26.17	165.41	89.83	79.12	30.33	26.67
75	FH2-A	47.68	5.97	119.55	127.85	21.13	165.67	89.70	79.37	28.78	25.87
75	FH2-B	81.41	5.54	116.52	124.71	24.21	159.96	86.68	76.88	29.18	24.94

depth (m)	sub-sample	As (ng/cm^2)	Sr (ng/cm^2)	Mo (ng/cm^2)	Cd (ng/cm^2)	Sb (ng/cm^2)	Cs (ng/cm^2)	Ba (ng/cm^2)	Tl (ng/cm^2)	U (ng/cm^2)
45	A	20.34	564.98	14.04	5.55	1.42	2.94	737.72	0.31	3.08
45	B	20.77	470.50	12.07	5.73	1.56	2.94	741.14	0.31	3.27
55	A	32.96	548.59	25.77	3.21	1.89	4.77	573.11	0.49	3.48
55	B	30.30	496.55	23.93	3.23	1.52	4.60	544.78	0.48	3.46
65	A	81.38	678.02	159.41	1.99	5.61	1.34	370.73	0.20	4.15
65	B	84.26	530.65	159.79	2.03	6.75	1.33	378.63	0.21	3.95
75	FH1-A	182.54	788.18	173.06	1.34	6.94	0.78	418.75	0.15	5.59
75	FH1-B	171.46	857.00	168.39	1.30	7.22	0.76	417.67	0.13	5.54
75	FH2-A	171.04	771.48	166.56	1.28	7.16	0.73	388.77	0.13	5.42
75	FH2-B	164.48	922.96	164.78	1.29	6.88	0.80	390.31	0.12	5.61

Appendix 5-7-6: Sedimentary uranium isotope data at Baltic Bornholm Basin (St. 22).

depth (cm)	bulk δ238U	2SD^	2SE^	n
0.5	-0.18	0.13^	0.13^	1
1.5	-0.35	0.09	0.05	3
2.5	-0.25	0.13^	0.13^	1
3.5	-0.17	0.13^	0.13^	1
4.5	-0.24	0.13	0.08	3
5.5	-0.07	0.24	0.14	3
7.5	-0.02	0.09	0.05	3
9.5	-0.24	0.04	0.03	2
15.5	-0.27	0.13^	0.13^	1

^Based on an average of the standard deviations of the East Pacific Seawater. Average δ = -0.39. 2SD = 0.13. N= 17.

Appendix 5-7-7: Uranium isotope data for water column samples from Bornholm Basin, Baltic Sea (St. 22).

Station	depth (m)	bottle #	bulk δ238U	2SD^	2SE^	n
St. 22	76	3	-0.43	0.12^	0.12^	1
St. 22	66	7	-0.41	0.12^	0.12^	1
St. 22	56	10	-0.35	0.04	0.03	2
St. 22	45	12	-0.38	0.12^	0.12^	1

^Based on an average of the standard deviations of BCR. Average δ = -0.32. 2SD = 0.12. N=10

Appendix 5-8-1: Aland-Bothnian exchange, Baltic Sea (St. 4)

Appendix 5-8-1-1: 0.2 µm filtered sea water concentration data at Aland-Bothnian exchange, Baltic Sea (St. 4)

bottle #	depth (m)	V (nmol/L)	Cr (nmol/L)	Mn (µmol/L)	Fe (µmol/L)	Co (nmol/L)	Ni (nmol/L)	Cu (nmol/L)
13	61	3.96	14.41	0.02	0.09	1.11	16.98	6.92
15	50	3.95	14.34	0.02	0.09	1.15	17.78	7.41
17	40	3.95	1.85	0.01	0.02	0.59	12.32	7.10
19	30	3.84	1.78	0.02	0.02	0.55	12.79	7.75
21	20	3.24	1.86	0.02	0.02	0.59	13.59	8.19
23	10	3.43	1.88	0.02	0.02	0.56	13.92	8.61

bottle #	depth (m)	As (nmol/L)	Sr (µmol/L)	Mo (nmol/)L	Sb (nmol/L)	Ba (nmol/L)	U (nmol/L)
13	61	7.43	17.82	15.54	0.72	75.92	2.59
15	50	7.63	17.85	15.65	0.80	77.07	2.69
17	40	7.23	17.78	15.18	0.70	76.73	2.60
19	30	7.42	16.91	15.18	0.71	71.78	2.50
21	20	7.52	15.72	14.65	0.69	68.57	2.20
23	10	7.22	15.55	14.46	0.70	68.59	2.20

Appendix 5-8-1-2: Pore water concentration data at Aland-Bothnian exchange, Baltic Sea (St. 4)

core (s)	depth (cm)	V (nmol/L)	Cr (nmol/L)	Mn (μmol/L)	Fe (μmol/L)	Co (nmol/L)	Ni (nmol/L)	Cu (nmol/L)	As (nmol/L)	Sr (μmol/L)
	2-4	31.64	15.19	238.19	9.12	9.46	50.28	10.88	122.57	16.47
nodule-A	0-2	99.99	66.10	180.74	38.03	29.26	83.87	34.94	32.82	16.37
nodule-B	0-2	14.93	28.32	61.37	2.12	10.50	116.69	20.13	18.46	17.01
nodule-C	0-2	22.65	34.25	50.50	8.30	20.57	53.13	23.17	16.98	17.21

core (s)	depth (cm)	Mo (nmol/L)	Cd (nmol/L)	Sb (nmol/L)	Ba (μmol/L)	Ce (nmol/L)	Nd (nmol/L)	Re (nmol/L)	Tl (nmol/L)	U (nmol/L)
	2-4	254.55	0.17	6.69	0.45	62.38	2.10	0.19	0.55	2.87
nodule-A	0-2	238.26	0.32	3.36	2.09	310.10	12.51	0.19	0.75	7.05
nodule-B	0-2	77.12	0.34	1.68	0.23	44.07	1.33	0.22	0.57	1.18
nodule-C	0-2	69.43	0.49	1.88	0.22	72.51	3.06	0.20	0.61	1.51

Appendix 5-8-2-1: 0.2 μm filtered sea water concentration data at North Gotland, Baltic Sea (St. 12)

bottle #	depth (m)	V (nmol/L)	Cr (nmol/L)	Mn (μmol/L)	Fe (μmol/L)	Co (nmol/L)	Ni (nmol/L)	Cu (nmol/L)
1	130	5.46	1.87	4.51	0.38	1.36	11.05	1.87
3	110	5.09	1.85	4.00	0.61	1.31	11.62	2.15
7	91	5.10	1.81	4.41	0.74	1.47	11.90	1.73
10	76	5.43	1.86	5.27	0.42	1.57	11.62	1.73
13	60	3.81	1.71	0.18	0.03	0.61	11.67	4.81
17	40	4.38	1.76	0.02	0.02	0.56	11.40	6.46

bottle #	depth (m)	As (nmol/L)	Sr (μmol/L)	Mo (nmol/)L	Sb (nmol/L)	Ba (nmol/L)	U (nmol/L)
1	130	8.01	30.98	20.85	0.77	83.77	3.99
3	110	8.17	30.55	19.96	0.74	82.57	3.78
7	91	8.34	30.53	19.84	0.70	84.55	3.77
10	76	8.01	29.30	19.36	0.72	83.72	3.74
13	60	7.31	24.65	16.94	0.68	80.93	3.20
17	40	7.43	19.55	16.37	0.74	85.21	3.12

Appendix 5-8-3-1: 0.2 µm filtered sea water concentration data at Gulf of Finland Sites, Baltic Sea (St. 7, 9, 10)

Station	bottle #	depth (m)	V (nmol/L)	Cr (nmol/L)	Mn (µmol/L)	Fe (µmol/L)	Co (nmol/L)	Ni (nmol/L)	Cu (nmol/L)
7	1	73	5.95	1.80	11.27	1.41	2.66	11.87	2.32
9	1	60	2.33	18.40	7.03	0.15	2.04	20.08	3.84
9	5	50	4.26	23.36	0.06	0.14	1.62	21.00	6.30
9	9	40	4.49	19.40	0.06	0.12	1.40	19.22	7.31
9	13	30	4.34	23.35	0.03	0.14	1.58	20.50	8.34
9	17	20	4.24	22.79	0.01	0.14	1.64	19.95	8.93
9	21	10	3.96	17.34	0.01	0.11	1.35	17.33	9.24
10	2	57	2.48	1.70	8.67	0.08	1.27	11.74	3.71

Station	bottle #	depth (m)	As (nmol/L)	Sr (µmol/L)	Mo (nmol/)L	Sb (nmol/L)	Ba (nmol/L)	U (nmol/L)
7	1	73	8.75	29.88	20.52	0.83	91.51	3.56
9	1	60	8.02	24.92	17.99	0.57	81.28	3.26
9	5	50	7.36	18.92	16.66	0.65	78.38	2.94
9	9	40	7.60	17.66	15.97	0.72	80.25	2.78
9	13	30	7.26	16.14	15.22	0.69	85.16	2.60
9	17	20	6.80	14.38	13.95	0.69	84.81	2.33
9	21	10	6.55	14.00	13.62	0.70	81.87	2.29
10	2	57	8.27	24.75	17.24	0.63	84.73	3.13

Appendix 5-8-3-2: Pore water concentration data at Gulf of Finland, Baltic Sea (St. 9)

core (s)	depth (cm)	V (nmol/L)	Cr (nmol/L)	Mn (μmol/L)	Fe (μmol/L)	Co (nmol/L)	Ni (nmol/L)	Cu (nmol/L)	As (nmol/L)	Sr (μmol/L)
Split 1	1	5.71	1.35	109.26	18.34	15.47	29.09	0.86	17.56	23.02
Split 1	2	24.91	3.56	160.05	18.79	2.88	11.35	b.d.l.	22.48	22.35
Split 1	3	27.84	5.01	132.99	13.19	1.65	11.59	b.d.l.	26.95	21.84
Split 1	4	24.83	5.88	116.88	10.95	2.37	10.25	b.d.l.	22.22	22.12
Split 1	5	30.60	7.72	97.13	4.49	2.64	10.52	1.50	23.22	21.96
Split 1	6	37.76	14.06	72.90	3.33	1.97	7.84	b.d.l.	25.26	21.38
Split 2	1	5.15	2.65	111.06	18.53	15.77	35.44	b.d.l.	19.02	22.94
Split 2	2	26.73	4.47	159.75	19.12	2.69	11.34	b.d.l.	23.63	22.11
Split 2	3	30.82	4.95	134.70	13.41	1.72	11.78	b.d.l.	23.12	22.06
Split 2	4	26.01	5.48	117.31	10.98	2.11	9.78	b.d.l.	21.58	21.92
Split 2	5	34.42	9.92	97.13	4.71	4.41	54.66	22.16	23.26	21.88
Split 2	6	39.77	15.56	72.34	3.35	1.86	9.50	b.d.l.	27.26	21.62

Appendix 5-8-3-2 cont.: Pore water concentration data at Gulf of Finland, Baltic Sea (St. 9)

core (s)	depth (cm)	Mo (nmol/L)	Cd (nmol/L)	Sb (nmol/L)	Ba (µmol/L)	Ce (nmol/L)	Nd (nmol/L)	Re (nmol/L)	Tl (nmol/L)	U (nmol/L)
Split 1	1	38.64	0.39	0.85	0.28	2.28	0.13	0.15	b.d.l.	3.64
Split 1	2	31.95	0.23	0.65	0.33	18.88	1.15	0.11	b.d.l.	1.54
Split 1	3	21.23	0.32	0.66	0.34	14.24	0.82	0.14	b.d.l.	0.88
Split 1	4	17.90	0.24	0.50	0.37	12.08	0.85	0.13	b.d.l.	1.06
Split 1	5	15.86	0.51	0.55	0.41	12.59	0.63	0.13	b.d.l.	0.55
Split 1	6	13.20	0.36	0.61	0.47	7.82	0.64	0.12	b.d.l.	0.46
Split 2	1	36.57	0.32	0.87	0.28	2.68	0.21	0.15	b.d.l.	3.55
Split 2	2	29.86	0.40	0.65	0.32	14.62	0.98	0.14	b.d.l.	1.58
Split 2	3	21.59	0.17	0.51	0.34	14.65	0.95	0.12	b.d.l.	1.00
Split 2	4	17.29	0.54	0.82	0.37	13.99	0.89	0.13	b.d.l.	1.13
Split 2	5	16.46	0.52	0.67	0.41	9.95	0.79	0.14	b.d.l.	0.62
Split 2	6	13.61	0.18	0.89	0.48	11.13	0.75	0.11	b.d.l.	0.45

Appendix 5-8-3-3: Pore water concentration data at Gulf of Finland, Baltic Sea (St. 10)

core (s)	depth (cm)	V (nmol/L)	Cr (nmol/L)	Mn (µmol/L)	Fe (µmol/L)	Co (nmol/L)	Ni (nmol/L)	Cu (nmol/L)	As (nmol/L)	Sr (µmol/L)
0.02µm filt	1	41.62	11.05	233.40	3.83	1.89	17.55	b.d.l.	44.20	22.23
0.02µm filt	2	49.15	9.49	261.19	1.96	1.89	13.72	b.d.l.	57.72	21.64
0.02µm filt	3	42.87	13.61	181.44	1.84	3.09	11.84	b.d.l.	54.53	21.17
0.02µm filt	4	49.59	18.65	168.20	1.32	3.93	13.09	1.02	59.19	20.54
0.02µm filt	6	69.64	29.69	142.73	1.20	6.17	15.35	b.d.l.	57.15	20.38
0.2µm filt	1	30.64	4.44	155.38	17.59	7.28	12.85	5.53	56.18	22.23
0.2µm filt	1 - Split 2	30.27	3.29	151.52	17.13	7.09	14.67	b.d.l.	49.09	21.80
0.2µm filt	2	59.85	13.12	272.19	2.31	2.58	13.56	b.d.l.	56.40	23.00
0.2µm filt	3	53.64	15.80	180.66	1.94	3.11	13.06	b.d.l.	49.18	21.15
0.2µm filt	4	63.26	22.47	165.54	1.30	4.13	15.04	b.d.l.	72.47	20.70
0.2µm filt	6	84.01	35.33	144.84	1.22	6.18	16.16	b.d.l.	80.95	20.20

Appendix 5-8-3-3 cont.: Pore water concentration data at Gulf of Finland, Baltic Sea (St. 10)

core (s)	depth (cm)	Mo (nmol/L)	Cd (nmol/L)	Sb (nmol/L)	Ba (µmol/L)	Ce (nmol/L)	Nd (nmol/L)	Re (nmol/L)	Tl (nmol/L)	U (nmol/L)
0.02µm filt	1	29.35	0.25	1.27	0.60	11.52	0.69	0.12	b.d.l.	1.28
0.02µm filt	2	25.30	0.29	1.42	0.50	10.56	0.85	0.14	b.d.l.	1.80
0.02µm filt	3	16.09	0.09	1.80	0.49	8.08	0.78	0.13	b.d.l.	1.57
0.02µm filt	4	17.25	0.36	1.66	0.60	10.22	0.82	0.10	b.d.l.	1.28
0.02µm filt	6	15.65	0.06	2.32	0.71	14.03	0.78	0.10	b.d.l.	1.56
0.2µm filt	1	49.38	0.46	2.85	0.57	15.50	0.64	0.14	b.d.l.	4.84
0.2µm filt	1 - Split 2	51.14	0.67	2.99	0.55	10.74	0.63	0.14	b.d.l.	4.69
0.2µm filt	2	27.81	0.37	0.94	0.57	26.40	1.86	0.13	b.d.l.	2.12
0.2µm filt	3	15.99	0.33	0.94	0.49	17.46	1.10	0.13	b.d.l.	1.43
0.2µm filt	4	17.28	0.17	2.15	0.61	17.18	1.37	0.12	b.d.l.	1.26
0.2µm filt	6	15.76	0.29	2.46	0.73	15.36	1.13	0.11	b.d.l.	1.83

Appendix 5-8-3-4: Pore water concentration data at Gulf of Finland, Baltic Sea (St. 15)

core (s)	depth (cm)	V (nmol/L)	Cr (nmol/L)	Mn (μmol/L)	Fe (μmol/L)	Co (nmol/L)	Ni (nmol/L)	Cu (nmol/L)	As (nmol/L)	Sr (μmol/L)
Split 1	1	40.76	4.01	91.20	137.41	16.95	17.66	2.00	83.63	19.73
Split 1	2	72.78	9.24	164.73	228.33	30.82	22.06	1.06	144.55	20.13
Split 1	3	61.80	9.18	102.71	116.72	10.58	13.77	2.60	86.63	20.15
Split 1	4	59.26	13.40	96.14	3.33	2.45	17.76	0.10	90.91	19.23
Split 1	5	41.68	12.13	69.50	1.32	1.77	10.55	b.d.l.	56.77	19.11
Split 1	6	33.31	8.92	55.22	3.15	1.16	12.60	b.d.l.	81.87	18.92
Split 1	8	31.83	9.74	48.40	1.32	1.27	12.81	b.d.l.	52.76	19.00
Split 1	10	59.78	27.23	61.59	2.16	3.97	21.97	b.d.l.	74.47	18.26
Split 2	1	41.52	3.40	92.99	136.98	15.93	18.35	4.51	75.52	19.65
Split 2	2	75.67	7.80	165.55	228.21	30.03	21.97	0.18	134.00	19.97
Split 2	3	63.05	8.31	102.19	114.27	11.03	14.30	1.34	72.74	19.81
Split 2	4	62.17	11.45	94.49	3.28	2.30	16.38	0.71	79.51	18.88
Split 2	5	41.07	9.99	70.40	1.31	1.98	10.37	b.d.l.	43.63	18.88
Split 2	6	33.23	7.26	57.17	3.24	1.20	13.80	b.d.l.	73.02	18.76
Split 2	8	33.63	10.11	48.86	1.33	1.51	12.38	b.d.l.	46.96	19.28
Split 2	10	59.82	24.85	62.23	2.19	4.17	24.27	b.d.l.	41.46	18.66

Appendix 5-8-3-4 cont.: Pore water concentration data at Gulf of Finland, Baltic Sea (St. 15)

core (s)	depth (cm)	Mo (nmol/L)	Cd (nmol/L)	Sb (nmol/L)	Ba (µmol/L)	Ce (nmol/L)	Nd (nmol/L)	Re (nmol/L)	Tl (nmol/L)	U (nmol/L)
Split 1	1	36.47	0.99	0.98	0.33	4.21	0.52	0.13	b.d.l.	2.63
Split 1	2	35.78	0.34	0.89	0.42	12.48	0.85	0.12	b.d.l.	2.05
Split 1	3	32.93	0.05	0.69	0.51	26.39	1.57	0.12	b.d.l.	1.35
Split 1	4	15.92	0.53	0.87	0.41	38.76	2.23	0.10	b.d.l.	0.92
Split 1	5	15.14	0.21	0.59	0.36	22.24	1.40	0.11	b.d.l.	0.81
Split 1	6	33.32	0.29	1.82	0.37	13.78	1.07	0.12	b.d.l.	4.12
Split 1	8	20.99	0.34	0.79	0.43	10.53	0.68	0.13	b.d.l.	2.77
Split 1	10	12.74	0.38	1.02	0.57	23.32	0.92	0.11	b.d.l.	1.17
Split 2	1	35.84	0.14	0.83	0.34	4.36	0.40	0.14	b.d.l.	2.62
Split 2	2	37.65	0.24	1.00	0.41	12.55	0.69	0.12	b.d.l.	1.96
Split 2	3	30.76	0.14	0.67	0.50	23.92	1.69	0.12	b.d.l.	1.32
Split 2	4	16.21	0.25	0.76	0.41	34.62	2.24	0.12	b.d.l.	0.92
Split 2	5	16.83	0.29	0.72	0.36	25.82	1.29	0.11	b.d.l.	0.72
Split 2	6	36.40	0.33	2.17	0.38	12.98	1.00	0.11	b.d.l.	4.11
Split 2	8	25.58	0.24	1.07	0.44	12.48	0.53	0.13	b.d.l.	2.76
Split 2	10	13.09	0.44	0.62	0.58	15.95	1.12	0.11	b.d.l.	1.21

Appendix 5-8-4-1: 0.2 µm filtered sea water concentration data at Baggensfjarden, Stockholm Archipelago, Baltic Sea (St. 1)

bottle #	depth (m)	V (nmol/L)	Cr (nmol/L)	Mn (µmol/L)	Fe (µmol/L)	Co (nmol/L)	Ni (nmol/L)	Cu (nmol/L)
1	35	2.83	1.72	0.58	0.07	0.68	14.73	7.93
5	30	3.06	1.76	1.05	0.08	0.85	14.99	8.20
8	25	3.20	1.75	0.93	0.08	0.83	15.33	8.47
13	20	3.39	1.80	0.25	0.05	0.59	15.90	9.30
15	15	3.71	2.08	0.18	0.12	0.66	18.79	9.57
21	5	3.84	1.75	0.02	0.04	0.69	16.11	10.36

bottle #	depth (m)	As (nmol/L)	Sr (µmol/L)	Mo (nmol/)L	Sb (nmol/L)	Ba (nmol/L)	U (nmol/L)
1	35	7.40	17.56	15.00	0.76	70.77	2.77
5	30	7.44	17.35	15.13	0.68	70.51	2.78
8	25	7.59	17.28	15.41	0.70	71.21	2.78
13	20	7.59	16.82	15.17	0.72	72.10	2.79
15	15	7.25	16.60	15.04	0.75	73.00	2.86
21	5	7.07	15.51	14.72	0.71	67.19	2.99

Appendix 5-8-4-2: Pore water concentration data at Stockholm Archipelago, Baltic Sea (St. 3)

core (s)	depth (cm)	V (nmol/L)	Cr (nmol/L)	Mn (μmol/L)	Fe (μmol/L)	Co (nmol/L)	Ni (nmol/L)	Cu (nmol/L)	As (nmol/L)	Sr (μmol/L)
A	1	3.03	1.24	97.14	5.79	38.06	32.32	14.86	24.07	15.50
A	2	2.63	0.85	188.74	28.97	95.64	44.64	8.56	58.55	15.97
A	3	12.31	3.79	96.47	230.50	62.73	49.18	4.36	156.46	15.99
A	4	16.46	6.71	71.74	149.64	49.19	39.77	1.32	98.80	15.80
A	5	11.49	9.26	66.05	56.22	33.19	21.34	1.93	103.00	15.78
A	6	18.10	6.73	44.21	1.56	1.85	13.69	b.d.l.	100.50	16.03
A	8	14.94	6.91	44.16	1.41	1.07	13.94	b.d.l.	137.23	15.94
A	11	31.18	19.08	54.58	1.37	2.30	18.94	b.d.l.	126.52	16.20
A	15	54.11	30.30	67.81	1.67	4.46	37.44	b.d.l.	135.49	16.69
A	20	50.64	29.83	73.11	1.55	4.61	38.96	b.d.l.	114.79	16.66
A	24	57.34	34.88	83.78	1.30	6.48	40.99	b.d.l.	87.24	16.48
A	28	66.88	36.17	114.65	1.50	7.21	41.48	b.d.l.	91.39	17.18
A	32	77.53	34.14	131.98	1.47	8.28	41.35	b.d.l.	70.26	17.29
A	36	95.43	33.18	143.33	1.71	9.34	43.22	1.29	52.39	17.94
A	40	110.10	28.83	155.93	1.51	9.44	34.64	b.d.l.	63.58	16.91
A	44	120.23	33.43	174.66	2.03	10.64	41.07	0.42	89.28	18.10

Appendix 5-8-4-2 cont.: Pore water concentration data at Stockholm Archipelago, Baltic Sea (St. 3)

core (s)	depth (cm)	Mo (nmol/L)	Cd (nmol/L)	Sb (nmol/L)	Ba (µmol/L)	Ce (nmol/L)	Nd (nmol/L)	Re (nmol/L)	Tl (nmol/L)	U (nmol/L)
A	1	49.00	0.44	0.88	0.15	2.84	0.17	0.13	b.d.l.	4.03
A	2	62.77	0.51	1.38	0.19	1.91	0.09	0.09	b.d.l.	5.14
A	3	48.82	0.15	0.76	0.24	4.55	0.31	0.11	b.d.l.	2.55
A	4	40.10	0.51	0.48	0.26	10.46	0.80	0.11	b.d.l.	1.18
A	5	44.99	0.16	1.35	0.27	6.41	0.53	0.11	b.d.l.	3.08
A	6	33.80	0.19	0.83	0.24	10.80	0.84	0.11	b.d.l.	1.43
A	8	40.78	b.d.l.	0.67	0.23	9.22	0.75	0.12	b.d.l.	1.67
A	11	21.17	0.33	0.93	0.32	13.13	0.94	0.11	b.d.l.	1.32
A	15	12.82	0.43	1.90	0.41	16.15	1.26	0.10	b.d.l.	1.21
A	20	19.07	0.21	1.69	0.48	15.40	1.41	0.11	b.d.l.	2.14
A	24	14.93	0.49	1.92	0.51	16.33	1.46	0.10	b.d.l.	1.35
A	28	15.35	0.23	2.32	0.53	17.73	1.42	0.10	b.d.l.	1.32
A	32	15.42	0.22	2.39	0.51	16.91	1.46	0.09	b.d.l.	1.91
A	36	15.49	0.47	3.17	0.49	12.97	1.35	0.11	b.d.l.	2.21
A	40	15.06	0.32	3.39	0.45	12.57	1.41	0.10	b.d.l.	2.77
A	44	20.44	0.47	4.11	0.50	14.35	1.44	0.11	b.d.l.	4.19

Appendix 5-8-5-1: 0.2 µm filtered sea water concentration data at East Gotland, Baltic Sea (St. 16)

bottle #	depth (m)	V (nmol/L)	Cr (nmol/L)	Mn (µmol/L)	Fe (µmol/L)	Co (nmol/L)	Ni (nmol/L)	Cu (nmol/L)
1	60	4.15	1.84	0.20	0.24	0.65	11.27	3.17
5	51	4.50	1.77	0.04	0.05	0.54	11.40	6.10
9	40	4.42	1.82	0.03	0.03	0.58	11.73	6.88
13	30	4.23	1.75	0.03	0.02	0.58	11.35	6.18

bottle #	depth (m)	As (nmol/L)	Sr (µmol/L)	Mo (nmol/)L	Sb (nmol/L)	Ba (nmol/L)	U (nmol/L)
1	60	7.79	28.46	18.57	0.70	80.89	3.64
5	51	7.05	20.49	16.81	0.76	82.35	3.20
9	40	7.38	19.65	16.43	0.73	82.90	3.13
13	30	7.38	19.66	16.30	0.76	84.80	3.10

Appendix 5-8-5-2: Pore water concentration data at East Gotland, Baltic Sea (St. 16 - core A)

core (s)	depth (cm)	V (nmol/L)	Cr (nmol/L)	Mn (µmol/L)	Fe (µmol/L)	Co (nmol/L)	Ni (nmol/L)	Cu (nmol/L)	As (nmol/L)	Sr (µmol/L)
A	1	8.65	2.73	5.64	106.06	5.04	18.22	b.d.l.	25.33	24.08
A	2	11.53	2.70	8.33	73.03	2.80	11.41	b.d.l.	36.88	23.82
A	3	34.87	0.91	11.75	39.62	4.34	13.34	b.d.l.	173.27	22.90
A	4	36.22	3.08	10.13	30.04	3.88	12.85	3.81	161.53	23.65
A	6	9.90	3.14	17.27	107.91	2.47	2.41	b.d.l.	32.88	21.75
A	8	9.52	0.93	17.30	93.83	2.65	1.95	b.d.l.	55.71	21.44
A	10	8.29	2.49	18.07	102.28	2.35	2.66	b.d.l.	48.50	21.40
A	13	8.61	1.80	19.66	116.52	3.06	1.28	b.d.l.	7.61	21.24
A	16	6.46	1.60	21.36	128.80	2.70	1.18	b.d.l.	3.05	21.00
A	20	5.66	0.33	23.67	139.25	2.70	b.d.l.	b.d.l.	1.46	21.23
A	24	4.12	0.26	26.15	143.99	3.96	1.66	b.d.l.	1.65	21.24
A	28	5.13	0.11	27.36	142.54	3.21	1.69	b.d.l.	0.86	21.53

Appendix 5-8-5-2 cont.: Pore water concentration data at East Gotland, Baltic Sea (St. 16 - core A)

core (s)	depth (cm)	Mo (nmol/L)	Cd (nmol/L)	Sb (nmol/L)	Ba (µmol/L)	Ce (nmol/L)	Nd (nmol/L)	Re (nmol/L)	Tl (nmol/L)	U (nmol/L)
A	1	28.03	b.d.l.	0.55	0.19	6.08	0.36	0.04	b.d.l.	1.46
A	2	26.88	0.04	0.88	0.22	5.28	0.32	0.05	b.d.l.	1.24
A	3	77.82	0.03	5.26	0.25	9.57	1.01	0.06	b.d.l.	3.49
A	4	71.20	0.13	4.34	0.24	4.19	0.35	0.07	b.d.l.	3.74
A	6	36.85	0.13	0.79	0.23	1.29	0.19	0.03	b.d.l.	0.29
A	8	82.26	b.d.l.	3.09	0.24	4.90	0.33	0.02	b.d.l.	1.22
A	10	80.38	b.d.l.	1.22	0.24	0.09	0.13	0.04	b.d.l.	0.39
A	13	76.62	b.d.l.	0.81	0.26	0.79	0.16	0.03	b.d.l.	0.62
A	16	65.97	0.01	0.67	0.26	14.82	0.57	0.02	b.d.l.	0.38
A	20	42.60	b.d.l.	0.51	0.27	2.71	0.93	0.04	b.d.l.	0.23
A	24	46.87	b.d.l.	0.50	0.28	2.59	0.13	0.04	b.d.l.	0.54
A	28	27.72	b.d.l.	0.21	0.30	0.16	0.21	0.03	b.d.l.	0.62

Appendix 5-8-5-3: Pore water concentration data at East Gotland, Baltic Sea (St. 16 - core B)

core (s)	depth (cm)	V (nmol/L)	Cr (nmol/L)	Mn (µmol/L)	Fe (µmol/L)	Co (nmol/L)	Ni (nmol/L)	Cu (nmol/L)	As (nmol/L)	Sr (µmol/L)
B	1	10.18	2.60	8.55	123.32	4.43	16.20	b.d.l.	14.40	23.67
B	2	8.62	3.55	9.91	135.92	4.26	15.08	b.d.l.	22.76	24.12
B	3	10.72	2.73	10.91	73.52	2.61	7.72	b.d.l.	54.71	23.15
B	4	15.72	4.15	13.72	84.26	3.13	6.63	b.d.l.	53.74	22.25
B	6	10.98	1.90	15.65	96.02	2.95	4.37	b.d.l.	109.90	22.33
B	8	27.17	2.55	17.28	68.31	4.02	5.32	b.d.l.	68.49	22.05
B	10	7.27	1.50	18.35	104.64	2.31	b.d.l.	b.d.l.	18.05	21.91
B	13	6.81	2.00	18.26	96.72	2.48	2.30	b.d.l.	25.93	21.91
B	16	7.11	1.84	21.06	105.27	4.96	8.43	b.d.l.	15.61	21.54
B	20	4.18	3.04	23.17	120.75	2.79	2.13	b.d.l.	9.76	21.09
B	24	4.30	1.87	25.41	134.59	3.37	1.67	b.d.l.	2.47	21.37
B	28	9.37	2.75	27.34	128.25	7.89	13.48	b.d.l.	9.77	21.77

Appendix 5-8-5-3 cont.: Pore water concentration data at East Gotland, Baltic Sea (St. 16 - core B)

core (s)	depth (cm)	Mo (nmol/L)	Cd (nmol/L)	Sb (nmol/L)	Ba (µmol/L)	Ce (nmol/L)	Nd (nmol/L)	Re (nmol/L)	Tl (nmol/L)	U (nmol/L)
B	1	22.44	b.d.l.	0.35	0.21	6.81	0.51	0.06	b.d.l.	0.83
B	2	21.38	b.d.l.	0.33	0.22	15.93	0.95	0.07	b.d.l.	0.56
B	3	29.34	b.d.l.	0.84	0.22	6.68	0.74	0.05	b.d.l.	1.31
B	4	29.19	b.d.l.	0.94	0.23	7.16	0.32	0.06	b.d.l.	0.61
B	6	61.08	b.d.l.	2.05	0.24	2.32	0.31	0.05	b.d.l.	1.14
B	8	111.79	b.d.l.	4.51	0.26	4.33	0.12	0.04	b.d.l.	2.25
B	10	67.22	0.26	1.04	0.25	2.36	0.32	0.05	b.d.l.	0.42
B	13	67.26	0.23	1.76	0.25	2.85	0.11	0.03	b.d.l.	1.17
B	16	131.75	0.14	1.63	0.26	3.54	0.31	0.04	b.d.l.	0.85
B	20	64.55	b.d.l.	0.62	0.27	2.33	0.38	0.03	b.d.l.	0.30
B	24	29.84	b.d.l.	0.40	0.29	2.28	0.20	0.04	b.d.l.	0.09
B	28	27.93	b.d.l.	0.41	0.31	1.93	0.06	0.03	b.d.l.	0.25

Appendix 5-8-5-4: Pore water concentration data at East Gotland, Baltic Sea (St. 16 - core C)

core (s)	depth (cm)	V (nmol/L)	Cr (nmol/L)	Mn (µmol/L)	Fe (µmol/L)	Co (nmol/L)	Ni (nmol/L)	Cu (nmol/L)	As (nmol/L)	Sr (µmol/L)
C	1	7.44	3.71	8.20	143.09	6.63	22.14	b.d.l.	24.72	24.28
C	2	10.31	6.69	10.43	115.76	2.78	13.35	b.d.l.	12.02	22.75
C	3	10.71	3.49	11.97	92.48	2.41	11.51	b.d.l.	41.73	23.00
C	4	13.05	4.07	15.25	75.93	3.51	9.78	b.d.l.	66.81	22.17
C	6	12.48	3.03	17.10	79.98	3.36	5.84	b.d.l.	175.77	21.56
C	8	9.60	2.54	18.78	80.96	2.88	3.76	b.d.l.	98.25	21.65
C	10	5.53	2.50	19.16	92.59	2.39	4.06	b.d.l.	126.59	22.16
C	13	3.62	0.84	18.98	103.31	2.87	5.83	6.70	124.50	21.66
C	16	1.83	1.62	21.32	129.42	2.80	3.70	b.d.l.	51.97	21.19
C	20	3.73	1.89	24.31	136.62	3.54	4.50	b.d.l.	5.62	21.38
C	24	3.84	1.15	25.83	138.16	4.45	5.58	b.d.l.	7.08	21.18
C	28	4.12	2.31	27.79	143.91	4.19	6.75	b.d.l.	5.30	21.00

Appendix 5-8-5-4 cont.: Pore water concentration data at East Gotland, Baltic Sea (St. 16 - core C)

core (s)	depth (cm)	Mo (nmol/L)	Cd (nmol/L)	Sb (nmol/L)	Ba (µmol/L)	Ce (nmol/L)	Nd (nmol/L)	Re (nmol/L)	Tl (nmol/L)	U (nmol/L)
C	1	24.17	b.d.l.	0.33	0.20	4.77	0.51	0.06	b.d.l.	1.10
C	2	17.14	b.d.l.	0.04	0.21	8.71	0.63	0.05	b.d.l.	0.37
C	3	21.37	b.d.l.	0.48	0.22	6.12	0.44	0.06	b.d.l.	0.70
C	4	26.26	b.d.l.	0.84	0.24	8.46	0.46	0.04	b.d.l.	1.24
C	6	40.16	b.d.l.	1.30	0.23	2.73	0.22	0.04	b.d.l.	0.57
C	8	84.89	b.d.l.	0.39	0.23	3.13	0.39	0.04	b.d.l.	0.78
C	10	49.79	b.d.l.	0.84	0.24	2.08	0.28	0.05	b.d.l.	0.37
C	13	102.15	b.d.l.	3.24	0.26	5.78	0.17	0.05	b.d.l.	1.39
C	16	48.25	b.d.l.	0.68	0.25	2.14	0.24	0.05	b.d.l.	0.15
C	20	30.65	b.d.l.	b.d.l.	0.26	1.09	0.26	0.03	b.d.l.	1.67
C	24	39.11	b.d.l.	1.08	0.29	3.89	0.13	0.03	b.d.l.	2.82
C	28	25.85	b.d.l.	0.11	0.28	3.35	0.19	0.03	b.d.l.	0.37

Appendix 5-8-5-5: Pore water concentration data at East Gotland, Baltic Sea (St. 16 - core D)

core (s)	depth (cm)	V (nmol/L)	Cr (nmol/L)	Mn (µmol/L)	Fe (µmol/L)	Co (nmol/L)	Ni (nmol/L)	Cu (nmol/L)	As (nmol/L)	Sr (µmol/L)
D	OLW	2.86	1.48	2.73	5.86	1.42	13.54	1.48	11.70	25.57
D	1	9.48	4.66	7.98	88.89	2.96	14.44	1.54	19.95	24.08
D	2	12.77	4.75	11.84	105.20	2.46	9.97	b.d.l.	32.68	23.62
D	3	8.80	4.53	10.21	59.93	1.93	9.57	b.d.l.	29.39	23.71
D	4	13.92	6.04	14.72	60.73	2.57	5.65	b.d.l.	83.67	22.21
D	6	25.15	4.51	17.31	44.33	3.25	6.59	0.11	89.06	21.97
D	8	13.94	3.00	17.51	55.85	3.52	2.36	b.d.l.	271.86	21.53
D	10	10.16	4.50	19.14	75.68	2.84	0.52	b.d.l.	17.88	21.25
D	13	7.30	3.61	19.64	83.36	2.63	1.72	b.d.l.	32.23	22.09
D	16	7.38	3.35	21.77	96.13	4.00	4.52	b.d.l.	15.83	20.92
D	20	4.92	2.84	23.59	106.61	9.00	15.50	b.d.l.	10.02	21.99
D	24	5.96	1.88	23.00	97.04	6.27	8.73	b.d.l.	13.18	22.72
D	28	4.62	2.00	26.54	112.44	8.19	14.54	b.d.l.	12.54	21.65

Appendix 5-8-5-5 cont.: Pore water concentration data at East Gotland, Baltic Sea (St. 16 - core D)

core (s)	depth (cm)	Mo (nmol/L)	Cd (nmol/L)	Sb (nmol/L)	Ba (µmol/L)	Ce (nmol/L)	Nd (nmol/L)	Re (nmol/L)	Tl (nmol/L)	U (nmol/L)
D	OLW	35.52	b.d.l.	0.24	0.14	6.26	0.43	0.06	b.d.l.	3.77
D	1	25.62	b.d.l.	0.59	0.20	4.20	0.43	0.09	b.d.l.	1.74
D	2	24.24	b.d.l.	0.63	0.21	3.79	0.36	0.05	b.d.l.	1.09
D	3	25.14	b.d.l.	0.64	0.19	3.43	0.47	0.07	b.d.l.	1.63
D	4	30.78	b.d.l.	0.98	0.23	2.93	0.41	0.06	b.d.l.	0.93
D	6	42.64	b.d.l.	2.60	0.23	2.64	0.28	0.05	b.d.l.	1.51
D	8	192.77	b.d.l.	7.63	0.25	1.89	0.24	0.05	b.d.l.	2.46
D	10	84.81	b.d.l.	2.05	0.24	1.16	0.24	0.03	b.d.l.	1.02
D	13	56.12	b.d.l.	1.45	0.25	9.26	0.06	0.04	b.d.l.	0.72
D	16	61.94	b.d.l.	1.00	0.26	b.d.l.	0.24	0.03	b.d.l.	0.56
D	20	43.28	0.04	0.83	0.29	2.43	0.18	0.03	b.d.l.	0.63
D	24	51.58	b.d.l.	0.90	0.31	0.83	0.36	0.03	b.d.l.	1.03
D	28	63.55	b.d.l.	0.85	0.31	b.d.l.	0.09	0.04	b.d.l.	0.85

Appendix 5-8-5-6: Pore water concentration data at East Gotland, Baltic Sea (St. 16 - core E)

core (s)	depth (cm)	V (nmol/L)	Cr (nmol/L)	Mn (µmol/L)	Fe (µmol/L)	Co (nmol/L)	Ni (nmol/L)	Cu (nmol/L)	As (nmol/L)	Sr (µmol/L)
E	1	12.21	3.98	8.42	169.27	5.42	20.41	b.d.l.	36.92	25.06
E	2	17.84	5.30	13.24	146.50	2.44	10.19	b.d.l.	23.95	23.51
E	3	11.70	4.11	11.67	78.31	2.15	8.25	b.d.l.	61.52	23.56
E	4	19.21	4.63	14.80	56.93	2.59	9.46	b.d.l.	109.43	22.14
E	6	8.16	4.30	16.61	102.72	2.42	3.83	b.d.l.	39.10	22.48
E	8	9.31	2.66	16.09	95.37	3.51	6.48	b.d.l.	22.08	21.76
E	10	9.09	2.97	16.70	102.90	4.38	5.16	b.d.l.	24.03	22.28
E	13	6.13	0.91	16.75	111.89	5.02	8.83	b.d.l.	23.49	21.64
E	16	7.44	2.86	19.30	129.98	4.21	5.86	b.d.l.	22.61	21.34
E	20	6.85	8.63	22.28	147.87	3.92	3.72	b.d.l.	3.93	20.58
E	24	5.85	1.63	24.42	161.26	3.01	3.26	b.d.l.	1.09	21.02
E	28	4.64	2.01	26.02	161.16	4.27	3.86	b.d.l.	2.27	21.05

Appendix 5-8-5-6 cont.: Pore water concentration data at East Gotland, Baltic Sea (St. 16 - core E)

core (s)	depth (cm)	Mo (nmol/L)	Cd (nmol/L)	Sb (nmol/L)	Ba (µmol/L)	Ce (nmol/L)	Nd (nmol/L)	Re (nmol/L)	Tl (nmol/L)	U (nmol/L)
E	1	27.95	b.d.l.	0.49	0.23	6.34	0.80	0.05	b.d.l.	1.28
E	2	18.58	b.d.l.	0.44	0.22	6.97	0.79	0.08	b.d.l.	0.63
E	3	27.41	b.d.l.	0.90	0.21	3.90	0.27	0.04	b.d.l.	1.48
E	4	46.64	b.d.l.	1.81	0.24	5.50	0.65	0.06	b.d.l.	1.41
E	6	60.63	b.d.l.	0.44	0.26	5.86	0.18	0.05	b.d.l.	0.29
E	8	89.48	b.d.l.	0.27	0.25	2.02	0.19	0.05	b.d.l.	0.42
E	10	45.00	b.d.l.	0.29	0.26	8.52	0.30	0.04	b.d.l.	0.53
E	13	99.95	b.d.l.	0.59	0.27	0.09	0.11	0.05	b.d.l.	0.73
E	16	50.69	b.d.l.	0.69	0.27	1.12	0.23	0.05	b.d.l.	0.46
E	20	41.07	b.d.l.	0.38	0.28	0.30	0.18	0.04	b.d.l.	0.45
E	24	24.96	b.d.l.	b.d.l.	0.30	b.d.l.	0.32	0.03	b.d.l.	0.17
E	28	21.56	b.d.l.	0.12	0.31	b.d.l.	0.13	0.03	b.d.l.	0.30

Appendix 5-8-5-7: Pore water concentration data at East Gotland, Baltic Sea (St. 13 - cores A&B)

core (s)	depth (cm)	V (nmol/L)	Cr (nmol/L)	Mn (µmol/L)	Fe (µmol/L)	Co (nmol/L)	Ni (nmol/L)	Cu (nmol/L)	As (nmol/L)	Sr (µmol/L)
A	1	16.04	2.64	8.49	150.56	11.31	30.92	2.66	40.23	21.79
A	2	11.54	1.77	9.72	85.76	5.65	19.50	1.45	51.08	21.95
A	3	12.26	3.94	9.78	48.79	2.97	13.94	1.13	55.71	21.22
A	4	13.63	5.76	13.29	62.86	2.39	13.77	0.26	70.10	21.19
A	6	24.36	5.01	13.93	31.83	2.92	11.84	0.30	106.02	21.33
A	8	40.08	5.85	14.15	11.59	3.22	12.54	b.d.l.	115.04	20.80
A	10	65.41	6.72	13.68	5.33	3.62	10.70	b.d.l.	108.88	20.99
A	12	37.63	8.22	13.49	3.28	4.58	10.75	b.d.l.	283.67	20.72
A	15	19.66	8.16	13.65	2.17	4.70	8.83	0.53	753.10	20.26
A	18	18.16	8.38	14.56	1.05	3.83	7.08	b.d.l.	79.47	20.72
A	21	20.61	8.63	14.61	0.94	4.12	5.83	b.d.l.	23.72	20.60
B	1	9.62	3.94	6.32	89.90	7.02	24.53	1.23	22.02	22.37
B	2	12.90	3.93	6.62	50.27	4.91	23.61	8.48	56.30	22.49
B	3	18.89	7.71	15.26	101.03	4.88	18.75	0.09	42.04	21.54
B	4	26.95	8.50	14.25	66.89	9.62	31.65	b.d.l.	91.09	21.57
B	6	26.22	8.56	15.04	46.26	2.59	9.62	b.d.l.	77.23	21.32
B	8	30.56	7.97	14.03	24.27	5.33	15.11	b.d.l.	74.56	21.80
B	10	31.98	7.01	11.08	5.23	2.79	11.91	0.78	82.45	21.77
B	12	31.52	8.60	12.69	4.77	5.00	15.17	b.d.l.	173.03	21.42
B	15	28.38	7.08	12.13	3.97	4.22	10.82	b.d.l.	271.15	21.17
B	18	32.50	7.63	12.88	1.11	5.79	13.35	b.d.l.	330.52	21.04
B	21	33.55	9.42	14.55	0.94	4.65	10.25	b.d.l.	96.65	21.26

Appendix 5-8-5-7 cont.: Pore water concentration data at East Gotland, Baltic Sea (St. 13 - cores A&B)

core (s)	depth (cm)	Mo (nmol/L)	Cd (nmol/L)	Sb (nmol/L)	Ba (µmol/L)	Ce (nmol/L)	Nd (nmol/L)	Re (nmol/L)	Tl (nmol/L)	U (nmol/L)
A	1	32.03	b.d.l.	0.73	0.21	6.35	0.18	0.20	0.55	2.31
A	2	29.05	0.14	1.15	0.21	3.14	0.19	0.21	0.55	2.22
A	3	33.47	0.21	1.41	0.19	1.81	0.06	0.20	0.54	2.08
A	4	33.14	b.d.l.	2.00	0.21	5.78	0.22	0.19	0.54	1.30
A	6	62.85	0.17	3.21	0.25	1.75	b.d.l.	0.19	0.57	2.75
A	8	117.52	b.d.l.	4.84	0.27	2.56	b.d.l.	0.18	0.55	4.91
A	10	64.41	b.d.l.	3.19	0.30	3.37	0.12	0.18	0.55	8.48
A	12	66.58	b.d.l.	3.37	0.32	1.76	0.16	0.18	0.53	3.43
A	15	309.56	0.00	2.49	0.34	8.77	0.27	0.18	0.55	1.12
A	18	25.79	0.10	0.93	0.38	2.50	0.11	0.17	0.54	0.21
A	21	20.63	b.d.l.	0.80	0.42	6.06	0.14	0.17	0.54	0.37
B	1	27.19	0.27	0.97	0.19	3.10	b.d.l.	0.21	0.55	1.90
B	2	28.41	0.89	0.79	0.19	1.48	0.10	0.19	0.54	2.63
B	3	24.56	0.19	1.33	0.24	5.91	0.05	0.19	0.54	0.99
B	4	41.31	0.09	2.62	0.24	2.05	0.14	0.20	0.56	2.75
B	6	76.15	0.08	3.50	0.27	0.88	0.20	0.17	0.54	3.54
B	8	65.34	0.58	3.14	0.26	1.67	b.d.l.	0.18	0.56	3.88
B	10	52.89	b.d.l.	2.76	0.27	0.55	b.d.l.	0.21	0.54	4.40
B	12	46.65	0.18	1.79	0.31	1.34	b.d.l.	0.19	0.55	3.19
B	15	80.42	b.d.l.	1.95	0.30	4.86	0.04	0.19	0.54	1.84
B	18	98.14	b.d.l.	2.01	0.35	1.06	0.02	0.19	0.56	2.64
B	21	52.25	0.25	1.13	0.41	0.33	b.d.l.	0.17	0.54	1.52

Appendix 5-8-5-8: Pore water concentration data at East Gotland, Baltic Sea (St. 13 - cores C&D)

core (s)	depth (cm)	V (nmol/L)	Cr (nmol/L)	Mn (µmol/L)	Fe (µmol/L)	Co (nmol/L)	Ni (nmol/L)	Cu (nmol/L)	As (nmol/L)	Sr (µmol/L)
C	1	9.15	4.34	5.59	88.45	5.21	20.30	0.00	30.87	22.43
C	2	12.63	4.06	8.50	115.27	7.30	22.97	b.d.l.	28.73	22.33
C	3	11.67	6.43	11.99	111.26	4.17	17.24	6.22	29.02	21.93
C	4	14.56	4.88	12.30	86.74	2.30	12.59	3.63	44.92	21.82
C	6	24.46	4.93	11.52	45.58	2.80	13.66	b.d.l.	44.41	21.72
C	8	27.40	10.47	12.39	27.31	3.79	16.89	0.87	46.45	22.15
C	10	27.97	6.23	12.31	16.39	3.78	12.62	0.48	25.92	21.54
C	12	20.91	8.26	13.79	14.12	3.14	9.48	1.87	52.75	21.45
C	15	22.25	9.21	12.99	3.67	3.34	8.05	b.d.l.	168.73	21.51
C	18	24.61	7.21	13.89	1.11	3.13	6.41	b.d.l.	845.80	21.80
C	21	23.29	8.39	14.54	0.89	3.61	6.72	b.d.l.	41.54	21.97
D	1	8.11	2.24	4.37	38.23	3.51	17.18	0.68	15.08	22.17
D	2	16.71	6.00	14.15	165.92	5.63	21.23	2.17	48.28	21.68
D	3	15.06	4.91	13.99	154.09	4.21	16.05	0.35	65.24	21.75
D	4	20.48	6.36	15.73	114.47	2.71	11.02	b.d.l.	95.08	21.47
D	6	24.15	4.81	14.72	54.80	3.08	11.47	b.d.l.	79.41	21.71
D	8	38.61	5.64	10.40	13.29	3.40	15.87	1.06	104.76	21.99
D	10	32.80	6.00	13.87	15.06	2.97	8.96	b.d.l.	99.31	21.44
D	12	27.94	7.93	13.96	7.15	4.49	13.38	b.d.l.	181.55	21.52
D	15	19.35	7.20	13.86	1.75	3.69	7.79	b.d.l.	156.42	21.55
D	18	18.04	7.67	15.32	0.98	3.46	4.67	b.d.l.	58.54	21.11
D	21	27.26	7.76	14.54	0.93	3.67	7.15	b.d.l.	38.25	21.00

Appendix 5-8-5-8 cont.: Pore water concentration data at East Gotland, Baltic Sea (St. 13 - cores C&D)

core (s)	depth (cm)	Mo (nmol/L)	Cd (nmol/L)	Sb (nmol/L)	Ba (µmol/L)	Ce (nmol/L)	Nd (nmol/L)	Re (nmol/L)	Tl (nmol/L)	U (nmol/L)
C	1	26.48	b.d.l.	0.54	0.20	2.62	0.02	0.22	0.57	1.69
C	2	25.11	b.d.l.	0.62	0.20	5.33	0.27	0.22	0.54	1.76
C	3	22.81	b.d.l.	0.81	0.20	7.35	0.19	0.20	0.54	1.05
C	4	25.65	0.12	1.10	0.22	4.49	b.d.l.	0.20	0.54	1.22
C	6	41.67	0.16	1.82	0.21	1.07	b.d.l.	0.21	0.54	2.62
C	8	43.96	0.02	1.33	0.23	1.39	b.d.l.	0.19	0.54	2.52
C	10	27.45	0.02	1.06	0.26	1.25	0.02	0.18	0.55	2.28
C	12	24.72	0.20	0.76	0.29	2.37	b.d.l.	0.19	0.54	1.04
C	15	49.01	b.d.l.	1.52	0.32	0.32	b.d.l.	0.18	0.54	1.32
C	18	248.38	0.25	3.31	0.38	1.26	0.10	0.18	0.53	2.27
C	21	29.80	0.04	0.68	0.40	1.25	0.04	0.18	0.54	0.66
D	1	29.61	0.24	0.40	0.17	1.00	b.d.l.	0.20	0.56	2.89
D	2	27.18	b.d.l.	0.77	0.22	4.53	0.30	0.20	0.54	1.41
D	3	26.76	b.d.l.	1.05	0.22	4.62	0.02	0.19	0.56	1.14
D	4	34.70	b.d.l.	1.70	0.23	1.43	0.04	0.19	0.54	1.25
D	6	43.19	0.10	1.70	0.25	3.52	b.d.l.	0.18	0.54	1.89
D	8	63.52	b.d.l.	2.51	0.24	1.27	0.11	0.18	0.55	3.96
D	10	55.92	b.d.l.	2.54	0.29	0.52	0.04	0.20	0.52	3.28
D	12	47.72	b.d.l.	2.41	0.32	1.80	b.d.l.	0.18	0.57	2.25
D	15	33.40	b.d.l.	0.80	0.35	1.60	b.d.l.	0.17	0.55	0.67
D	18	33.11	0.09	0.44	0.39	1.07	b.d.l.	0.20	0.54	0.41
D	21	30.74	b.d.l.	0.70	0.41	0.44	0.45	0.18	0.53	0.92

Appendix 5-8-6-1: Pore water concentration data at Arkona Basin, Baltic Sea (St. 21 - core A)

core (s)	depth (cm)	V (nmol/L)	Cr (nmol/L)	Mn (µmol/L)	Fe (µmol/L)	Co (nmol/L)	Ni (nmol/L)	Cu (nmol/L)	As (nmol/L)	Sr (µmol/L)
A	1	8.57	2.40	4.04	19.15	7.26	14.02	b.d.l.	29.89	41.52
A	2	11.19	3.60	9.04	90.04	19.09	17.22	b.d.l.	61.29	42.28
A	3	10.34	2.60	6.36	103.54	9.89	12.31	b.d.l.	71.64	41.95
A	4	7.32	4.64	8.96	138.42	12.12	13.59	b.d.l.	118.75	42.62
A	5	9.97	3.85	6.67	75.07	3.27	11.94	b.d.l.	59.80	42.72
A	6	12.61	4.90	8.10	60.22	2.50	10.41	b.d.l.	73.35	43.38
A	8	30.21	6.54	7.60	13.72	2.26	10.34	b.d.l.	90.17	43.37
A	10	28.26	8.65	7.91	1.31	2.05	6.58	b.d.l.	112.35	44.04
A	12	35.21	12.84	8.49	0.74	3.21	5.78	b.d.l.	47.11	44.91
A	14	54.53	13.35	8.73	0.80	4.07	9.27	6.10	59.29	45.77
A	18	61.07	14.52	10.72	0.71	4.03	8.13	b.d.l.	64.67	44.18
A	22	41.34	13.00	13.26	0.64	4.32	6.86	b.d.l.	86.32	44.37
A	26	30.09	14.40	15.81	0.66	4.48	6.49	b.d.l.	33.64	43.89

Appendix 5-8-6-1 cont.: Pore water concentration data at Arkona Basin, Baltic Sea (St. 21 - core A)

core (s)	depth (cm)	Mo (nmol/L)	Cd (nmol/L)	Sb (nmol/L)	Ba (µmol/L)	Ce (nmol/L)	Nd (nmol/L)	Re (nmol/L)	Tl (nmol/L)	U (nmol/L)
A	1	67.68	0.47	0.52	0.12	b.d.l.	b.d.l.	0.18	b.d.l.	6.40
A	2	77.05	0.18	1.59	0.15	b.d.l.	b.d.l.	0.19	b.d.l.	5.70
A	3	67.03	0.11	0.50	0.14	b.d.l.	b.d.l.	0.16	b.d.l.	2.75
A	4	69.86	0.04	1.31	0.16	b.d.l.	b.d.l.	0.16	b.d.l.	3.76
A	5	73.26	0.09	1.28	0.16	1.88	b.d.l.	0.17	b.d.l.	4.61
A	6	73.10	0.25	2.53	0.17	b.d.l.	0.13	0.15	b.d.l.	6.61
A	8	71.99	b.d.l.	3.17	0.17	2.74	0.32	0.16	b.d.l.	9.20
A	10	73.38	b.d.l.	4.11	0.18	b.d.l.	0.19	0.15	b.d.l.	7.81
A	12	86.60	0.04	3.34	0.20	b.d.l.	0.21	0.14	b.d.l.	4.47
A	14	96.95	0.15	3.95	0.21	b.d.l.	0.26	0.15	b.d.l.	9.05
A	18	59.28	0.08	2.00	0.21	b.d.l.	0.15	0.14	b.d.l.	6.34
A	22	37.20	b.d.l.	0.88	0.20	b.d.l.	0.12	0.14	b.d.l.	3.41
A	26	15.89	b.d.l.	0.34	0.20	3.54	0.15	0.14	b.d.l.	0.75

Appendix 5-8-6-2: Pore water concentration data at Arkona Basin, Baltic Sea (St. 21 - core B)

core (s)	depth (cm)	V (nmol/L)	Cr (nmol/L)	Mn (µmol/L)	Fe (µmol/L)	Co (nmol/L)	Ni (nmol/L)	Cu (nmol/L)	As (nmol/L)	Sr (µmol/L)
B	1	14.83	2.83	11.09	27.52	20.45	15.94	b.d.l.	33.03	41.75
B	2	18.46	2.52	5.08	43.52	4.59	12.79	b.d.l.	44.16	41.42
B	3	21.31	5.34	9.87	174.31	13.48	16.51	b.d.l.	97.15	42.05
B	4	25.22	4.31	8.83	161.31	10.89	18.84	15.45	107.57	43.75
B	5	18.92	5.19	7.86	117.05	4.35	10.86	b.d.l.	87.37	42.86
B	6	18.02	4.37	7.16	83.66	2.40	10.81	b.d.l.	63.48	42.78
B	8	28.53	6.96	7.92	66.68	1.12	8.56	b.d.l.	51.49	44.14
B	10	41.54	11.51	8.90	36.62	2.11	10.13	b.d.l.	25.83	42.70
B	12	48.70	13.30	8.82	7.68	1.89	10.05	b.d.l.	14.94	43.70
B	14	57.83	16.46	9.36	1.14	3.15	10.08	b.d.l.	18.58	44.82
B	18	59.11	19.31	11.65	0.91	3.81	8.69	b.d.l.	21.69	45.18
B	22	52.82	16.07	13.65	0.77	3.76	6.04	b.d.l.	36.21	43.27
B	26	41.89	14.66	15.35	0.79	3.31	5.32	b.d.l.	28.05	44.01

Appendix 5-8-6-2 cont.: Pore water concentration data at Arkona Basin, Baltic Sea (St. 21 - core B)

core (s)	depth (cm)	Mo (nmol/L)	Cd (nmol/L)	Sb (nmol/L)	Ba (µmol/L)	Ce (nmol/L)	Nd (nmol/L)	Re (nmol/L)	Tl (nmol/L)	U (nmol/L)
B	1	62.97	0.22	0.85	0.13	1.00	b.d.l.	0.22	0.42	5.62
B	2	64.89	0.18	0.76	0.13	1.68	0.14	0.20	0.43	5.88
B	3	63.75	b.d.l.	0.92	0.17	5.12	0.23	0.23	0.36	0.92
B	4	60.67	b.d.l.	1.15	0.18	4.50	0.16	0.20	0.38	2.16
B	5	60.86	b.d.l.	1.02	0.17	2.96	0.12	0.21	0.39	2.82
B	6	64.45	b.d.l.	1.97	0.17	2.41	0.19	0.20	0.39	7.89
B	8	53.82	0.09	1.76	0.19	9.97	0.32	0.19	0.39	4.72
B	10	28.80	b.d.l.	0.82	0.20	13.75	0.55	0.20	0.38	2.23
B	12	28.76	b.d.l.	1.19	0.21	9.38	0.39	0.18	0.37	2.77
B	14	21.01	b.d.l.	0.60	0.22	8.68	0.67	0.18	0.38	2.92
B	18	16.03	b.d.l.	1.00	0.22	6.13	0.45	0.19	0.37	1.72
B	22	14.91	0.21	0.41	0.21	5.03	0.33	0.19	0.37	1.29
B	26	13.47	b.d.l.	0.55	0.20	3.72	0.41	0.19	0.37	0.81

Appendix 5-8-6-3: Pore water concentration data at Arkona Basin, Baltic Sea (St. 21 - core C)

core (s)	depth (cm)	V (nmol/L)	Cr (nmol/L)	Mn (µmol/L)	Fe (µmol/L)	Co (nmol/L)	Ni (nmol/L)	Cu (nmol/L)	As (nmol/L)	Sr (µmol/L)
C	1	13.93	2.82	7.63	32.03	15.78	17.59	b.d.l.	33.67	41.36
C	2	19.23	2.86	10.21	88.07	16.92	15.84	b.d.l.	55.96	42.53
C	3	22.20	4.66	7.62	110.56	6.94	12.23	b.d.l.	88.88	43.31
C	4	18.70	3.81	7.51	115.49	6.06	11.51	b.d.l.	80.72	43.20
C	5	18.81	6.03	7.79	99.15	3.22	10.84	b.d.l.	66.20	42.87
C	6	27.10	7.89	8.20	81.63	2.75	10.98	b.d.l.	61.16	43.81
C	8	37.20	8.63	8.61	51.61	1.87	11.79	b.d.l.	39.26	44.62
C	10	47.90	9.18	7.34	11.32	1.38	10.76	b.d.l.	29.53	43.90
C	12	48.96	14.07	9.16	1.47	1.58	10.19	b.d.l.	27.59	46.24
C	14	47.13	14.06	9.49	0.98	2.22	9.04	b.d.l.	50.98	45.09
C	18	68.09	15.64	11.54	0.83	2.84	7.15	b.d.l.	65.28	44.62
C	22	46.01	14.73	14.44	0.97	3.13	7.23	b.d.l.	41.05	45.23
C	26	45.02	13.92	15.73	0.88	2.87	6.78	b.d.l.	62.75	44.18

Appendix 5-8-6-3 cont.: Pore water concentration data at Arkona Basin, Baltic Sea (St. 21 - core C)

core (s)	depth (cm)	Mo (nmol/L)	Cd (nmol/L)	Sb (nmol/L)	Ba (µmol/L)	Ce (nmol/L)	Nd (nmol/L)	Re (nmol/L)	Tl (nmol/L)	U (nmol/L)
C	1	60.22	0.44	0.98	0.14	1.27	b.d.l.	0.20	0.41	4.30
C	2	62.48	0.14	1.93	0.15	3.50	0.17	0.22	0.40	3.28
C	3	65.58	0.16	0.97	0.17	3.56	0.28	0.21	0.38	1.62
C	4	61.76	0.07	0.53	0.17	3.35	0.09	0.19	0.38	1.53
C	5	56.09	b.d.l.	0.24	0.18	4.03	0.24	0.19	0.38	1.57
C	6	55.14	0.25	0.77	0.18	4.12	0.12	0.20	0.37	3.80
C	8	47.13	0.14	0.73	0.19	3.52	0.22	0.18	0.39	3.02
C	10	58.46	0.17	3.31	0.19	4.90	0.28	0.19	0.38	9.17
C	12	27.60	b.d.l.	0.97	0.22	5.38	0.42	0.19	0.37	2.98
C	14	40.27	b.d.l.	1.43	0.22	4.53	0.29	0.20	0.37	4.05
C	18	44.25	b.d.l.	2.00	0.22	4.68	0.27	0.18	0.37	6.84
C	22	18.09	0.04	0.74	0.21	4.37	0.46	0.19	0.38	1.96
C	26	27.02	b.d.l.	0.72	0.21	4.07	0.30	0.18	0.36	1.93

Appendix 5-8-6-4: Pore water concentration data at Arkona Basin, Baltic Sea (St. 21 - core D)

core (s)	depth (cm)	V (nmol/L)	Cr (nmol/L)	Mn (µmol/L)	Fe (µmol/L)	Co (nmol/L)	Ni (nmol/L)	Cu (nmol/L)	As (nmol/L)	Sr (µmol/L)
D	1	16.81	2.45	14.52	88.14	44.65	27.50	b.d.l.	76.93	41.58
D	2	23.19	6.12	15.33	204.00	32.23	28.35	b.d.l.	167.52	42.45
D	3	19.33	5.27	12.14	174.78	20.83	19.89	b.d.l.	140.37	42.00
D	4	20.62	6.54	11.01	168.10	9.24	12.94	b.d.l.	163.44	42.26
D	5	22.49	7.09	10.13	150.74	5.37	10.68	b.d.l.	146.42	43.45
D	6	27.62	8.30	10.56	94.83	2.75	11.29	b.d.l.	100.79	42.21
D	8	37.46	10.62	11.23	54.01	2.84	11.62	b.d.l.	53.06	43.31
D	10	34.87	9.45	10.57	27.03	1.85	10.12	b.d.l.	34.64	43.41
D	12	54.50	14.96	12.96	15.37	2.55	12.51	b.d.l.	34.26	43.50
D	14	75.67	19.03	14.52	11.53	3.19	16.27	b.d.l.	45.04	46.68
D	18	70.88	20.59	14.83	1.24	4.72	12.46	b.d.l.	29.84	41.18
D	22	61.04	20.53	16.40	0.95	5.09	10.21	b.d.l.	29.11	43.87
D	26	48.37	17.11	16.87	0.89	4.41	7.94	b.d.l.	28.72	44.19

Appendix 5-8-6-4 cont.: Pore water concentration data at Arkona Basin, Baltic Sea (St. 21 - core D)

core (s)	depth (cm)	Mo (nmol/L)	Cd (nmol/L)	Sb (nmol/L)	Ba (µmol/L)	Ce (nmol/L)	Nd (nmol/L)	Re (nmol/L)	Tl (nmol/L)	U (nmol/L)
D	1	61.40	0.40	0.89	0.15	3.02	b.d.l.	0.20	0.40	5.59
D	2	63.70	0.06	0.95	0.17	2.99	0.03	0.21	0.38	3.83
D	3	61.16	b.d.l.	0.93	0.17	3.90	0.23	0.21	0.39	3.17
D	4	58.24	0.00	0.60	0.18	5.07	0.40	0.20	0.37	1.42
D	5	59.09	b.d.l.	0.56	0.19	3.48	0.11	0.19	0.37	2.50
D	6	47.23	b.d.l.	0.56	0.20	3.27	0.28	0.19	0.38	3.09
D	8	33.61	b.d.l.	0.34	0.22	4.34	0.26	0.19	0.37	1.52
D	10	39.17	b.d.l.	0.98	0.23	4.33	0.22	0.19	0.37	4.55
D	12	23.43	b.d.l.	0.57	0.25	6.72	0.34	0.18	0.36	2.77
D	14	24.82	b.d.l.	1.19	0.27	8.96	0.47	0.19	0.37	4.32
D	18	14.56	b.d.l.	0.81	0.26	6.72	0.24	0.17	0.37	1.92
D	22	15.40	b.d.l.	0.81	0.27	5.90	0.35	0.17	0.37	2.20
D	26	13.97	b.d.l.	0.63	0.24	5.34	0.32	0.18	0.36	1.23

Appendix 6: Additional Methods

Sediment samples composed the bulk of the samples analyzed within the main text and within the appendices (2, 3, 4, and 5). The details of how individual sediment samples were digested, measured, and analyzed was discussed within the Methods section of the thesis.

Within Appendix 4 and 5, additional materials were examined for concentration (water column seawater, porewaters, and particulate material), and U isotopes were measured for the water column seawater. Within the following sections, lab procedures used and considerations for these samples will be discussed. Although the data is separated by basin in Appendix 4 and 5, the methods of treatment were the same and will be discussed together.

Sample Procurement

For this Black and Baltic Seas comparison, samples were collected during two cruises on board the *R/V Pelagia*. In August/September 2015, the *Pelagia* traversed the western part of the Black Sea, near the Romanian shelf. In May/June 2016, the cruise travelled around the Baltic Sea. For both cruises, similar sampling plans were used to collect water, particulate material, sediments and porewaters. The sites of the samples used for this study are shown in the maps (Appendix 4-2 and Appendix 5-2).

Water samples were collected using Titan, an ultra-clean conductivity-temperature depth (CTD) rosette made by the Royal Netherlands Institute for Sea Research (NIOZ). Titan's structure contains an arrangement of 24 polyvinylidene

fluoride (PVDF) plastic sample bottles (24L volume) arranged in two rows and built on a titanium frame. Sampling was conducted in a clean air container (HEPA-filtered air) where all surfaces were thoroughly rinsed off prior to sampling to reduce the chance of contamination from particles from the transit across the deck of the ship (such as smoke, grease or paint chips). Inside the clean container, the sample bottles were connected to a nitrogen gas line, which served several purposes- 1) it provided pressure to move the water through the filters, 2) it maintained anoxic conditions within the sample bottle, and 3) it avoided reoxidation of the remaining waters within the sample bottle. Two bottles were collected for each selected depth – 1L of 0.2 μm filtered seawater and 0.5L unfiltered seawater. Once the samples returned to the US, they were acidified with 6M HCl (two time distilled ACS grade, equivalent to optimum grade) and were then stored at room temperature and away from light until analysis 11 months later.

Particulate samples from the water column were collected using *in situ* pumps (three McClane WTS-LF and one WTS-LV-dual filter pumps). During a deployment, each pump contained a 55 μm prefilter and a 0.8 μm filter (142 mm) to collect the particles. In the Black Sea, Supor® filters (Pall Corp.) were used, while quartz microfiber filters (Whatman) were used in the Baltic Sea. After the deployment, the volume of filtered water was recorded and the filters were then transferred into petri dishes and were stored at -20°C. The WTS-LV-dual filter pump allowed for collecting anoxic samples, which were processed under nitrogen gas after recovery and were stored anoxically. Since U is prone to release on

oxidation, this special anoxic treatment reduced the amount of U reoxidation (e.g. Duff et al., 1999).

Multicoring allowed for the recovery of both the sediments and the porewater samples, while keeping the sediment-water interface intact. Using 10 cm diameter cores on an Oktopus multicorer, sediments were collected and then brought on board; typically a core contained between 30-60 cm of sediment. On deck, the core was brought into a temperature-controlled container with a temperature matching the bottom water (4-7°C). In this container, the porewaters were extracted anoxically using Rhizon samplers (pore size 0.12-0.18 μm, Rhizosphere) and acid-cleaned syringes. The porewaters were then acidified while in the syringe to redissolve any oxides that precipitated after its filtration through the Rhizon membrane and were then bottled and stored at room temperature. The remaining core was then sliced oxically in 1 cm sections, with 1 cm resolution in the top 6 cm, and 2-3 cm resolution for the remainder of the core. The sediment slices were stored in 50 ml centrifuge tubes that were then frozen (-20°C). Upon arrival at Rutgers, the samples were stored in the freezer. The frozen sediments were partially thawed and subsampled. The subsamples were set in an oven at 60°C to dry. These samples were then ground with a mortar and pestle, and were then ashed following the procedures stated in the main methods section.

Water column & porewaters

For the aqueous samples, the first step involved measuring the concentration of uranium along with other major and minor elements. To do this, concentration

measurements were conducted on diluted samples (40x; 5x was used for the Baltic porewaters) using an inductively coupled plasma mass spectrophotometer (ICP-MS; iCap, ThermoFisher). Since the samples had a salt matrix, each analysis involved two sets of standards – a freshwater standard and a salinity matched Bermuda seawater standard. Multiple analysis runs were necessary as the sample and skimmer cones needed to be cleaned of salt residues built up from the matrix.

Particulate matter

Before treating to separate U for isotope analysis, subsampling of filters was conducted to check the amount of U present. Two subsamples (12 mm diameter circles) of each filter were transferred into a Savillex vial and treated to a leaching with 1 ml 6N HNO_3 at 100°C overnight. The subsamples were then dried down to approximately 20 μl so that the dissolved samples were not cooked back into the filters, which were still present in the vial. An aliquot was analyzed and calculations were completed to know the concentration of U present for the particulate, along with other conservative elements in order to make a salt correction, including magnesium (Mg), strontium (Sr), and cesium (Cs). The concentration of the particulate material was defined in two different units, one based on the filter area (ng/cm^2), and the other based on the volume that went through the filter (ng/L).

Water column isotopes

Uranium concentration measurements were used to calculate the amount of sample needed for U-isotope measurements. Sample aliquots were then spiked with

IRMM 3636a, a certified ^{233}U and ^{236}U double spike mixture, with a spiking ratio of ^{235}U:^{236}U ~2:3, and the aliquots aimed to contain 55 ng of U (some sample drydown was necessary to achieve the appropriate amount of U within the aliquot). After spiking the seawater samples, the samples were then heated at 60°C for 24 hours. Afterwards they were dried down. The samples were redissolved into 3N HNO_3 to a total of 5 ml, which were then U purified. The U purification procedure of reagents was similar to that of the sediments. Some slight differences included that a separate batch of resin (no prior exposure to sedimentary U) was used. For the initial sample loading, alternating between 1 ml portions of sample and 3N HNO_3 was done to avoid density driven issues in getting solutions to pass through the column as the seawater samples were denser than the acid. Additionally, seawater samples and Pacific seawater (in house standard) were passed through the resin columns twice, unlike the sediments single pass. After both resin treatments, the sample was dried down and then redissolved into 0.5 ml in ~2% HNO_3. Similar to the sediments, the concentration was measured on the iCap, the vial was microcentrifuged for 10 minutes, and the sample was diluted to 18 ppb solution prior to Neptune analysis.

Before running any seawater samples on the Neptune, a thorough cleaning of the Aridus was completed. For regular upkeep, the membrane was cleaned using 2% HNO_3 following the procedure in the manual, however, the membrane cleaned up effectively with 1% TMAH following the same steps as used for the acid cleaning treatment (cleaning with TMAH should only be as a last resort and should be thoroughly rinsed with water and dried out afterwards).

At the beginning of an analysis run, a blank acid was analyzed followed by CRM112a as bracketing standard (New Brunswick Laboratory, US DOE) and CRM 129, as a certified uranium oxide isotope standard (New Brunswick Laboratory, US DOE). After this, samples and in-house standard materials (BCR-2 Hawaii basalt, East Pacific Rise seawater) were analyzed with two sample measurements in between the bracketing CRM 112a. In a standard block, 10 samples/reference materials with bracketing were analyzed and then a CRM 112a, and a blank finished the block. The data was processed similar to that of the sedimentary data sets.